1994

Part I 2+2 Photocycloaddition Reactions Of Cyclic Enones With Alkenes Part Ii Photochemical Reactions In Supercritical Fluids

David Andrew

PART I
2+2 PHOTOCYCLOADDITION REACTIONS OF CYCLIC ENONES WITH ALKENES

PART II
PHOTOCHEMICAL REACTIONS IN SUPERCRITICAL FLUIDS

by

David Andrew

Department of Chemistry

Submitted in partial fulfilment
of the requirements for the degree of
Doctor of Philosophy

Faculty of Graduate Studies
The University of Western Ontario
London, Ontario, Canada

June 1994

ISBN 0-315-93193-0

ABSTRACT

PART I

The irradiation of 2-cyclopentenone with ultraviolet light in the presence of alkenes results in the formation of 2+2 cycloadducts which contain cyclobutane rings. According to the Corey-de Mayo mechanism, the regiochemistry of the cyclobutane products is controlled by the relative orientation of the alkene and the cyclic enone in an exciplex intermediate which precedes the formation 1,4-biradicals along the reaction pathway.

The biradicals formed in the photocycloaddition reactions of 2-cyclopentenone, 2-methyl-2-cyclopentenone and 3-methyl-2-cyclopentenone with various alkenes were trapped as stable compounds by H_2Se. By determining the structures and relative yields of the trapped products, the structures and relative rates of formation of the biradical intermediates from which the trapped products originated were deduced. These studies indicate that the regiochemistry of the cycloadduct products is not controlled by the relative rates of formation of the isomeric biradical intermediates; rather, the regiochemistry is a result of the way each biradical partitions between closure to form products and reversion to form starting materials. This conclusion is in disagreement with the Corey-de Mayo exciplex mechanism. Therefore, the factors which control the way each biradical partitions between closure and reversion were investigated in detail.

PART II

The Photo-Fries reaction of 1-naphthyl acetate was investigated in supercritical carbon dioxide. This photolysis proceeds via a solvent-caged singlet radical pair to result

in the formation of 2-acetyl-1-naphthol, 4-acetyl-1-naphthol, and 1-naphthol. In supercritical CO_2 the relative ratios of these products are sensitive to pressure variations in the near-critical region. The relative yield of 1-naphthol decreases dramatically as the pressure is decreased in the region near the critical pressure. Since formation of this product is the result of escape from the solvent cage by the naphthoxyl radical, this observation was interpreted in terms of an increase in the strength of the solvent cage near the critical point. Comparison of the pressure dependence of the relative product ratios with the pressure dependence of the partial molar volume of solute molecules in supercritical CO_2 provided strong evidence for the unusual phenomenon of "solvent clustering" near the critical point.

Dedicated to my loving wife Jodi

ACKNOWLEDGEMENTS

Without exaggeration, none of the work described in this thesis could have been completed without the support and encouragement of Professor Alan Weedon. The four years that I spent in Professor Weedon's laboratory were not only rewarding from an academic standpoint, but also very enjoyable. His guidance and direction are greatly appreciated.

I would also like to thank my fellow graduate students for their support and friendship. Specifically, I thank the following people: Dr. David Wong, Dr. David Hastings, Dr. David Oldroyd, Dr. Andreas Rudolph, Dr. Boke Zhang, Dr. Darryl Klassen, Dr. David Muir, Biswajit Choudhury, Brian Des Islet, David Maradyn, Paul Krug, Wendy Holden, Tracy Quevillon, Sumit Faha, Steve Barlow. I am very lucky to have gained a number of valued friendships from the ever expanding Weedon Group.

A special thank-you goes to Professor A. Margaritis of the department of Bio-engineering at the University of Western Ontario. He graciously allowed me to conduct experiments with his Supercritical Fluid Extraction system before we began designing our own SCF reactor.

I would like to convey my deepest appreciation to all the members of the chemistry department faculty and staff who assisted me in the completion of this work. I am especially grateful for the assistance that Cheryl O'Meare provided.

During my graduate studies I received generous support from the National Science and Engineering Research Council of Canada. I consider myself extremely fortunate to live in a country which actively encourages students in all levels of education. I hope

that my future endeavours will allow me to perpetuate the investment that has been made in my education.

Lastly, I would like to thank my wife Jodi Bradford for all the love and support she has given me during my studies. She too has been on board the roller coaster for the last four years--encouraging me during those times when results were not forthcoming and keeping me focused when things were going well. In addition, I would like to thank the rest of my family for their love, encouragement and support: my parents, Gordon and Carole; my sister, Kay; and my parents-in-law, Bill and Jeanne. Together, all these people have been my pillar of strength throughout both the good and difficult times. Thank-you.

TABLE OF CONTENTS

LIST OF TABLES

LIST OF FIGURES

PART :

2+2 PHOTOCYCLOADDITION REACTIONS OF CYCLIC ENONES WITH ALKENES

CHAPTER 1

INTRODUCTION

1.1 General Introduction

The first example of an enone-alkene (2+2) photocycloaddition was published in 1908 by Ciamician and Silber who described the conversion of carvone to carvone-camphor upon exposure to sunlight.[1] Thereafter, the potential application of photochemistry to organic synthesis attracted little attention until the early 1960's when a form of scientific renaissance began to occur in the area. This new-found interest in photochemistry was sparked by the recognition that photochemical transformations might be of great synthetic value for developing strategies to various functional group combinations present in target molecules. One of the photochemical transformations that received considerable attention during the 1960's was the intermolecular photocycloaddition reaction of cyclic α,β-unsaturated ketones with functionalised alkenes.[2] In this reaction, the alkene moiety formally adds across the carbon-carbon double bond of the triplet excited state enone to form α-keto cyclobutane adducts. A generic example of the photocycloaddition reaction between 2-cyclopentenone and a mono-substituted alkene is shown in Scheme 1.

Scheme 1

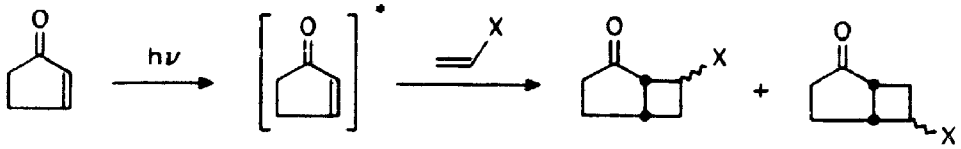

Due to the obvious value of the carbon-carbon bondmaking characteristics of the enone-alkene 2+2 photocycloaddition, the reaction has become one of the most widely used photochemical transformations in organic synthesis. Many comprehensive reviews have appeared in the literature regarding the synthetic usefulness of the reaction.[1] Corey first demonstrated the usefulness of the cyclic enone plus alkene photocycloaddition reaction in natural product synthesis by applying the reaction to the synthesis of caryophyllene (1) and isocaryophllene (2).[2c] This synthesis is summarised in Scheme 2. Other early adaptations of this 2+2 photocycloaddition to natural product synthesis include the use of a photocycloaddition of 2-cyclopentenone to 3-isopropyl-1-methylcyclopentene in the synthesis of the sesquiterpenes α- and β-bourbonene.[4] Since the publication of these first synthetic adaptations of the photocycloaddition reaction many other applications have also appeared in the literature. The purpose of this introduction is not to attempt to describe all aspects of the synthetic utility of the enone-alkene photocycloaddition, but rather to survey the literature from a mechanistic stand-point. Therefore, the remainder of this introductory chapter will outline the mechanistic evidence that has been presented in the literature over the last 30 years. It will also attempt to show the impact that this evidence has had on the development of an accurate mechanism for the reaction in general.

1.2 The Nature of the Enone Excited State

Before introducing the development of a mechanism which describes the various aspects of enone-alkene photocycloaddition reactions, it is appropriate first to comment on the specific nature of the excited state involved in the reaction. All of the

Scheme 2

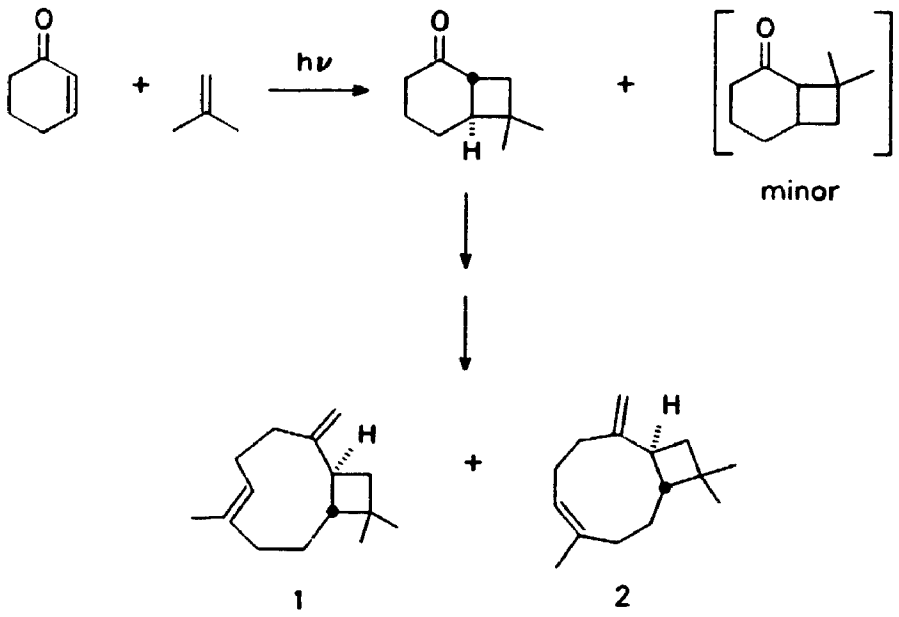

photocycloaddition reactions that will be discussed in this chapter are initiated by irradiating the longest wavelength electronic absorption band of the cyclic enone with light in the near ultra-violet region of the electromagnetic spectrum, specifically at wavelengths between 300 and 350 nm. Upon absorbing such a photon of light, the cyclic enone is excited into the first excited singlet state, from which rapid intersystem crossing to the triplet excited state occurs. All of the photocycloaddition reactions of cyclic enones with alkenes that have appeared in the literature have either been explicitly shown or are assumed to proceed via the triplet state of the enone. The multiplicity of the excited state of the cyclic enone involved in 2+2 photocycloaddition reactions with alkenes was proven to be representative of a triplet in early investigations involving classical sensitisation and quenching studies.[5] However, the specific triplet excited state involved, either n-π^* or π-π^*, was difficult to determine since most triplet excited cyclic enones do not exhibit phosphorescent emission. The reason for this is that most triplet

excited cyclic enones undergo rapid relaxation to the ground state by twisting about the carbon-carbon double bond before phosphorescence can occur.[6] In the case of acyclic enones, decay of the triplet excited state by twisting about the double bond is so fast that these compounds do not undergo cycloaddition reactions with alkenes; rather, these systems exhibit other intramolecular transformations.[7] Flexible cyclic enones such as 2-cycloheptenone and 2-cyclooctenone also exhibit rapid triplet decay by twisting about the carbon-carbon double bond. Irradiation of 2-cycloheptenone or 2-cyclooctenone results in the *cis-trans* isomerisation from the triplet state.[8,9] Therefore, the photocycloaddition reaction of enones to alkenes is generally confined to compounds which contain either the 2-cyclopentenone moiety, the 2-cyclohexenone moiety, or some other enone moiety which is constrained about the carbon-carbon double bond so that relaxation to the ground state is slowed to the point that intermolecular cycloaddition with alkenes can compete.

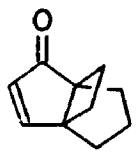

3

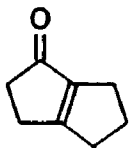

4

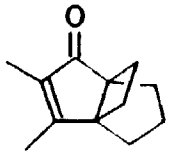

5

Phosphorescence emission has been observed from highly constrained cyclopentenone species. For example, Cargill and co-workers[10] demonstrated that compounds 3 and 4 exhibit phosphorescence in a methylcyclohexane matrix at 77 K. The closeness of the n-π^* and π-π^* triplet states of these molecules is evident from the phosphorescence studies. The triplet energy of compound 3 was estimated to be 71 kcal/mol based on the position of the 0-0 band with the n-π^* state slightly lower in

energy than the π-π^* state. Alkyl-substitution at the 3- and 4-positions of compound **3** results in lowering the energy of the π-π^* state and raising the energy of the n-π^* state so that in a methylcyclohexane matrix at 77 K the lowest triplet state for compound **5** is π-π^* in nature. The $^1S \leftarrow {}^0S$ absorption spectra of these rigid cyclopentenone systems also indicate that the lowest excited singlet state is an n-π^* state and that this state is very close in energy to the two possible triplet states. Work by Kearns, Marsh and Schaffner[11] on the phosphorescence emission from steroidal enones (**6**) at 77K established that the lowest enone triplet in these cases is actually an π-π^* triplet with the lowest n-π^* state only a few kcal/mol higher in energy. In solution at room temperature, however, it is highly probable that the relative order of the π-π^* and n-π^* triplet states of many enone systems changes due to partial rotation about the carbon-carbon double bond.

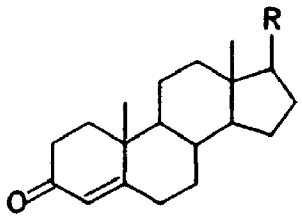

6

The difference in photochemical reactivity of the π-π^* and n-π^* triplet excited states of some cyclic enones has been demonstrated. Schuster and co-workers concluded that the rearrangement of 4,4-dimethyl-2-cyclohexenone (**7**) in the formation of lumiketone (**8**) proceeds via a π-π^* triplet state (see Scheme 3).[12,13] Irradiation of **7** in the presence of tetramethylethylene results in the formation of cycloadducts **9** and **10** and lumiketone. As the concentration of the alkene is increased the relative yield of the cycloadduct products increases at the expense of the relative yield of lumiketone.[13a] In

neat tetramethylethylene the irradiation of **7** also results in the formation of the oxetane addition product **11** as well as compounds **9**, **10**, and **8**.[14] It was demonstrated that the Stern-Volmer slope for quenching the formation of **11** by the addition of naphthalene is significantly different from the Stern-Volmer slope for the quenching of the formation of **8**, **9**, and **10**.[12] Based on these observations it was concluded that **9** and **10** are formed as a result of a reaction between the alkene and the same triplet state of **7** which is responsible for the formation of lumiketone **8**, namely the π-π^* state. The n-π^* triplet state was implicated in the formation of the oxetane product **11**. Therefore, this system indicates that enone-alkene photocycloaddition reactions probably proceed via the π-π^* triplet state of the cyclic enone.

Scheme 3

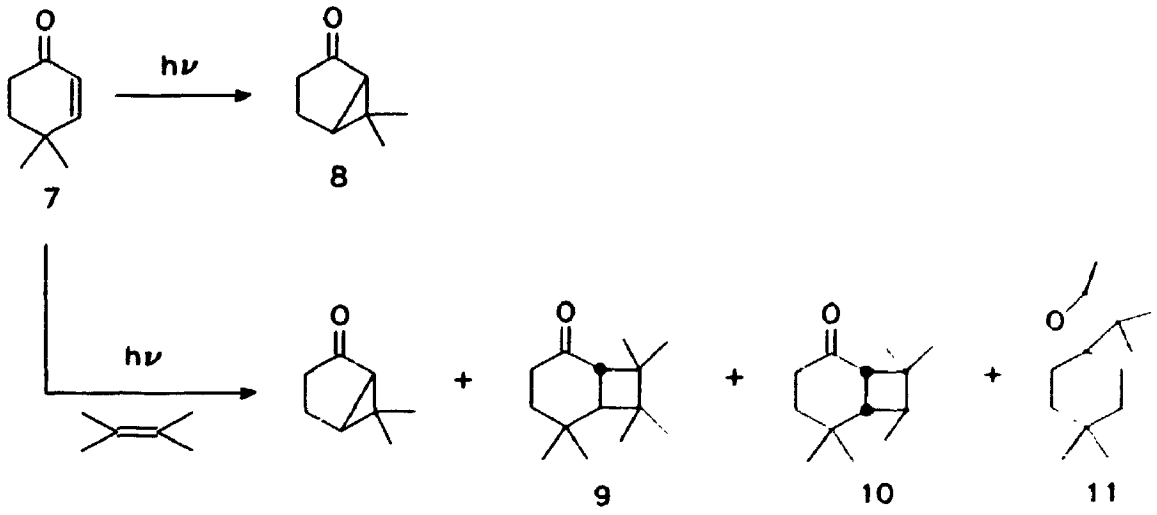

The triplet lifetimes of some simple cyclic enones have been studied recently by laser flash photolysis.[15,16,17] In these investigations the triplet lifetimes of 2-cycloheptenone[17], 2-cyclohexenone[15] and 2-cyclopentenone[15,16] in cyclohexane were found

to be 11 ns, 25 ns, and 185 ns respectively. The triplet lifetimes of the two former enones were not dependent on the concentration of the enone; however, in the case of 2-cyclopentenone the triplet lifetime decreased significantly as the concentration of the enone was increased. The dependence on enone concentration exhibited by the triplet lifetime of 2-cyclopentenone was attributed to a rapid self-quenching process.[16] The rate constants for this self-quenching process was found to be 5.9×10^8 and 2.7×10^8 M^{-1} s^{-1} in cyclohexane and acetonitrile, respectively. Therefore, the lifetime of 185 ns quoted for the 2-cyclopentenone triplet in cyclohexane was calculated by extrapolating the triplet lifetime observed by laser flash photolysis to infinite dilution according equation 1:

$$(\tau_{obs})^{-1} = k_d + k_{sq}[\text{enone}] \qquad (1)$$

In this equation, $1/k_d$ is the triplet lifetime of the cyclic enone extrapolated to infinite dilution and k_{sq} is the rate constant for self quenching.

The self-quenching process of triplet 2-cyclopentenone is responsible for the formation of the dimers **12** and **13** shown in Scheme 4.[18] The dimerisation of 2-cyclopentenone was studied from a mechanistic standpoint by Wagner and Bucheck some time ago.[19] In this classic study, the quantum yields of formation of **12** and **13** upon irradiation of 2-cyclopentenone were studied in different solvents at different enone concentrations. In addition, Wagner and Bucheck also obtained rate constants for the unimolecular decay of triplet 2-cyclopenenone and the bimolecular reaction between triplet 2-cyclopentenone and ground state enone. These rate constants were obtained by observing the decrease in the quantum yield of dimer formation in the presence of increasing concentrations of dienes, such as 1,3-pentadiene and 1,3-cyclohexadiene,

which act as triplet quenchers. The rate of triplet quenching by the dienes was assumed to be diffusion controlled ($1x10^{10}$ M^{-1} sec^{-1}). Later, Schuster and co-workers[15] used laser flash photolysis to demonstrate that the rate constant for quenching of the triplet excited state of 2-cyclopentenone by dienes is one to two orders of magnitude below that assumed by Wagner. When this discrepancy is taken into account, the rates for unimolecular triplet decay and bimolecular self quenching measured by Wagner are comparable to the rates measured by flash photolysis.

Scheme 4

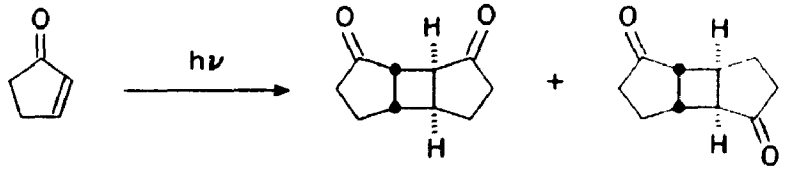

12 13

1.3 The Corey-de Mayo Mechanism

The first proposed reaction mechanism for cyclic enone plus alkene photocycloaddition reactions was published by Corey and co-workers.[2d] The mechanism was proposed in order to rationalise the relative product yields of the various regio- and stereochemical isomers shown in Scheme 1. The reaction mechanism, which is shown in Scheme 5, involves an "oriented π-complex" which forms upon reaction of the excited enone with a ground state alkene molecule. Corey suggested that this complex collapses to form a 1,4-biradical intermediate which then closes to generate the cyclobutane adducts.

Scheme 5

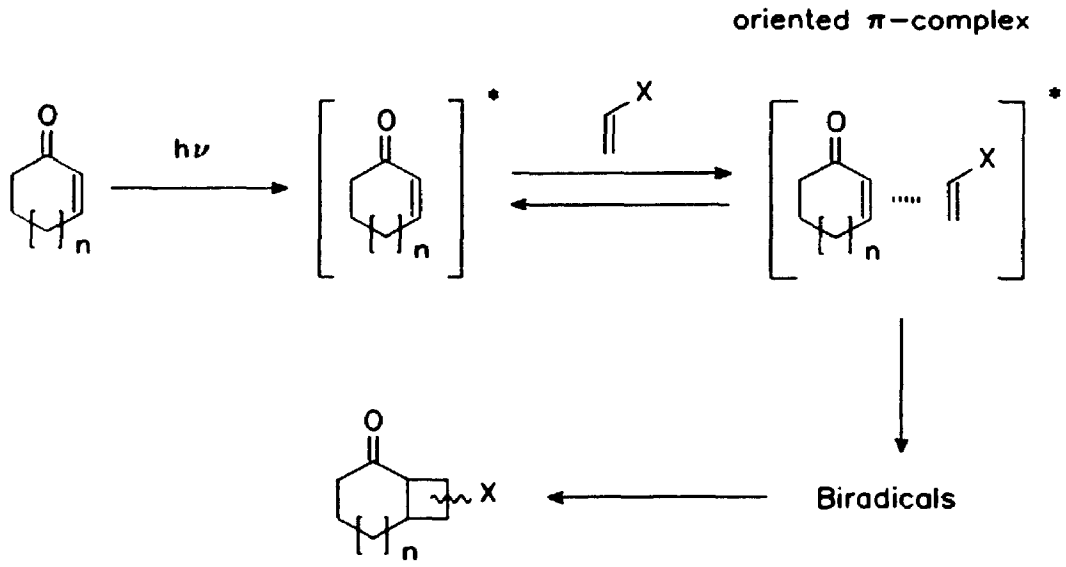

The speculation that an oriented excited π-complex might be involved in the reaction was based on the regiochemistry of the cyclobutane products that are obtained when polar alkenes are added to excited enones. For instance, Corey and co-workers[2d] observed that when the alkene is substituted at one terminus with electron donating groups, such as an alkoxy group, the reaction is directed towards the formation of cyclobutane products that exhibit a head-to-tail regiochemistry[§]. Conversely, it was also observed that when the alkene is substituted at o e terminus with electron withdrawing groups, such as a nitrile functionality, the reaction is directed towards the formation of cyclobutane products that exhibit a head-to-head regiochemistry. These trends in the product distribution were rationalised in terms of a minimum energy alignment of the

---

§ The terms "head-to-head" and "head-to-tail" refer to the relative orientation of the ketone functionality in the enone component of the cycloadduct and the alkene substituent. In a head-to-head cycloadduct the regiochemistry is such that the ketone and alkene substituent are on the same side of the molecule.

molecular dipole moments in a complex involving an excited state cyclic enone and an alkene possessing a polar functional group. Based on simple molecular orbital calculations,[20.2d] the dipole of n-π^* excited state cyclic enone was expected to be oriented so that a partial negative charge resided on the β-carbon of the enone double bond and a partial positive charge resided on the α-carbon. Given the hypothesised polarisatior of the excited enone, the minimum energy alignment of the excited enone and polar alkene in the oriented π-complex is shown in Scheme 6. The oriented π-complexes shown in Scheme 6 demonstrate that, according to the Corey mechanism, the regiochemistry of the cycloadducts is controlled by the relative orientation of the enone and alkene in this complex.

Scheme 6

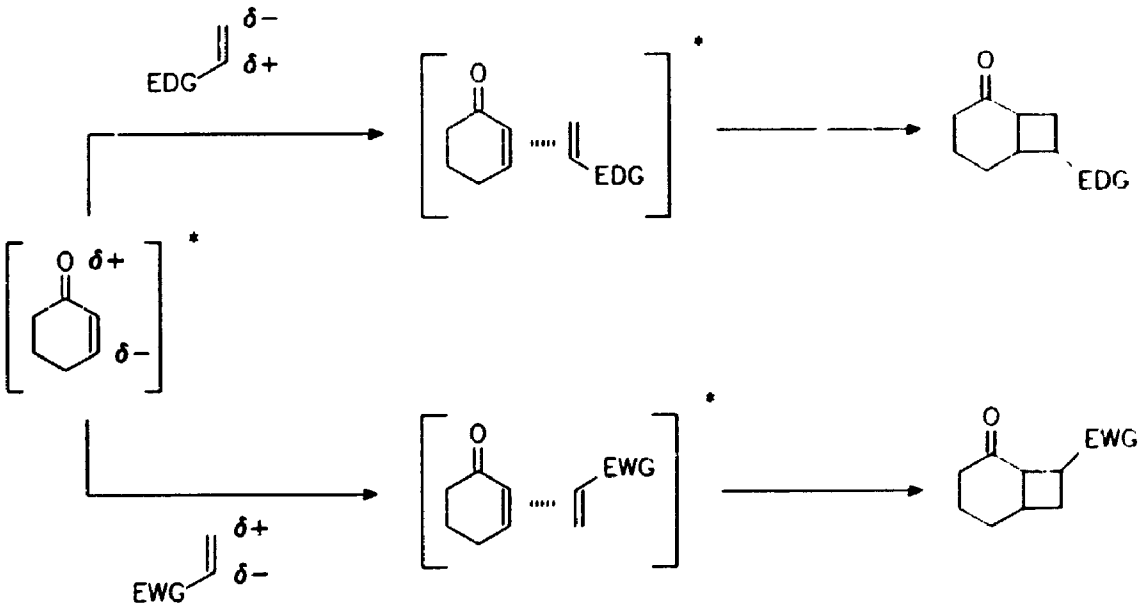

One of the problems with the excited state complex originally proposed by Corey is that the actual triplet excited state of the cyclic enone involved in the cycloaddition is

probably a π-π^* state and not an n-π^* state. Unless the π-π^* state is also polarised in the reverse direction to the ground state, the orientation of the excited state complexes proposed by Corey may not be correct. In fact, based on the expected charge distribution in the π-π^* state, the dipole of this state is probably similar to that of the ground state.

Corey and co-workers[2d] also measured "relative rates of addition" of different alkenes to photochemically excited 2-cyclohexenone. For example, the relative rate of addition of 1,1-dimethoxyethylene (4.66), methyl vinyl ether (1.57), cyclopentene (1.00), isobutylene (0.53), acrylonitrile ("very slow") and allene (0.23) to 2-cyclohexenone were measured by irradiating the enone in the presence of both cyclopentene and the alkene under investigation. These "relative rates" were used by Corey as evidence for a π-complex which involves an electrophilic excited state enone. He argued that in a complex where the excited enone is the acceptor and the alkene is the donor, electron rich alkenes should react quicker than electron poor alkenes in forming the π-complex. The faster rate observed in the addition for 1,1-dimethoxyethylene and methyl vinyl ether to 2-cyclopentenone relative to the rate observed for the addition of acrylonitrile was used as evidence for this argument. Later, de Mayo[21] pointed out that Corey's "relative rates" were not rates at all, but rather relative quantum yields of product formation for each addition (*vide infra*).

The biradical intermediates that appear in Scheme 5 were proposed initially by Corey and co-workers[2d] in order to explain the formation of compounds **17** and **18** which are observed in the photocycloaddition of 2-cyclohexenone to isobutene (see Scheme 7). It was suggested that these compounds are the result of the disproportionation of

intermediate 1,4-biradicals **19** and **20**. Corey also noted that identical mixtures of cycloadducts were obtained from the photoaddition of 2-cyclohexenone to either *cis*- or *trans*-2-butene, indicating that the stereochemistry of the alkene was lost during the reaction. The most reasonable explanation for the apparent loss of stereochemistry of the alkene during the cycloaddition was that 1,4-biradicals intermediates are formed and that these intermediates achieve conformational equilibrium before closure to form cycloadducts can occur.

Scheme 7

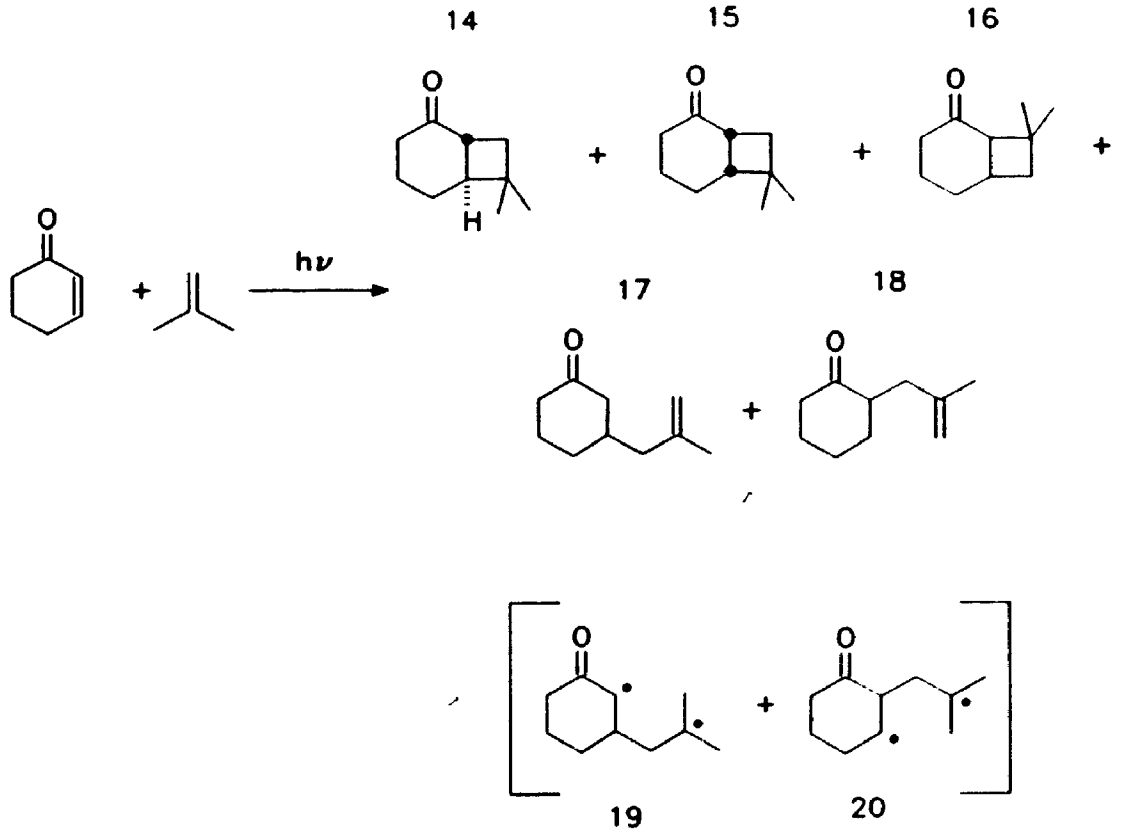

Other investigators have observed the lack of stereochemical specificity exhibited by the cycloadducts obtained from the addition of *cis* and *trans* alkene geometrical

isomers to cyclic enones. Dilling and Tabor[22] demonstrated that the addition of *cis*- and *trans*-1,2-dichloroethene to 2-cyclopentenone results in similar mixtures of products. The products resulting from these photocycloaddition reactions are shown in Scheme 8. The cycloaddition of *cis*- and *trans*-2-butene to bicyclo[4.3.0]non-6-en-2-one also results in similar mixtures of cycloadducts (see Scheme 9).[23] It should be noted that even though photocycloaddition reactions which involve alkene geometrical isomers result in "similar" mixtures of cycloadduct products, the relative ratio of the cycloadducts obtained from the addition of each geometrical isomer of the alkene are slightly different. It can be concluded that, due to biradical involvement, the enone-alkene photocycloaddition is not stereospecific; however, the stereochemistry of the alkene does have a noticeable impact on the relative cycloadduct product distribution.

Scheme 8

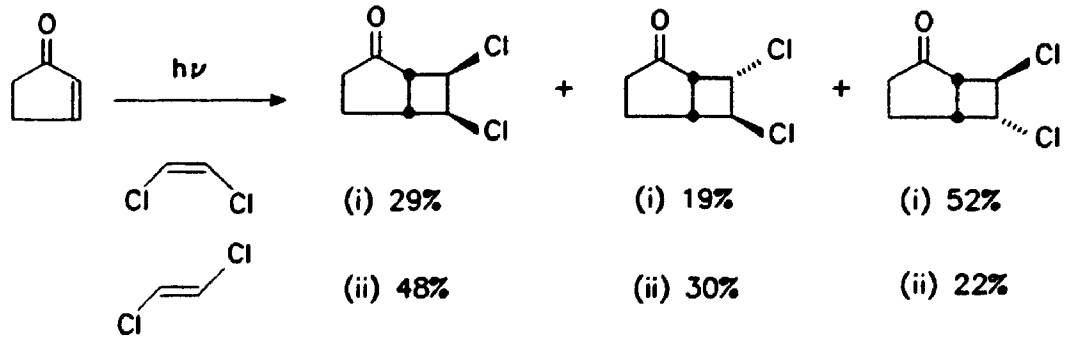

The significance of the biradical intermediates was expanded upon by de Mayo[21] in his 1971 review and later by Loutfy and de Mayo[24] in a landmark paper on the mechanism of the enone photocycloaddition. De Mayo proposed that the 1,4-biradical

Scheme 9

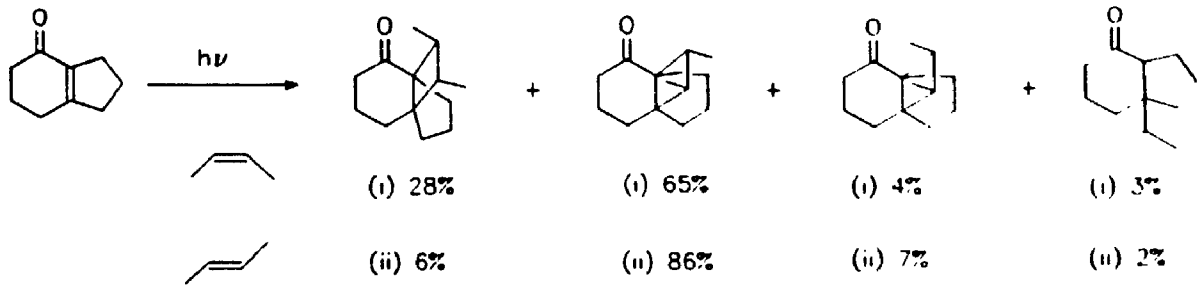

intermediates could fragment and regenerate ground state starting materials in addition to undergoing closure and forming cycloadducts. This process effectively decreases the efficiency of the photocycloaddition, thereby lowering the maximum quantum yield of cycloadduct formation. The maximum quantum yield of cycloadduct formation that was observed by Loutfy and de Mayo[24] in their study of various enone-alkene systems was approximately 0.5 for the addition of cyclohexene to 2-cyclopentenone. Since the quantum yield of triplet excited state formation for 2-cyclopentenone was shown by Wagner and Bucheck[19] to be 1.0, the fact that the quantum yields of cycloadduct formation, extrapolated to infinite alkene concentration, were less than unity indicated that inefficiencies other than intersystem crossing must exist in the reaction mechanism. In addition to biradical reversion, de Mayo suggested that the excited state complex postulated by Corey could also decay to ground state starting materials and thereby contribute to the inefficiency of the photocycloaddition. Therefore, de Mayo proposed a revised reaction mechanism which explicitly included the possibility of biradical reversion as well as the possibility of exciplex decay to the ground state. The revised mechanism also included the self quenching process of cyclic enone triplets which results

in dimer formation at low alkene concentrations. This revised mechanism, shown in Scheme 10, is referred to as the Corey-de Mayo mechanism in the literature.

Scheme 10

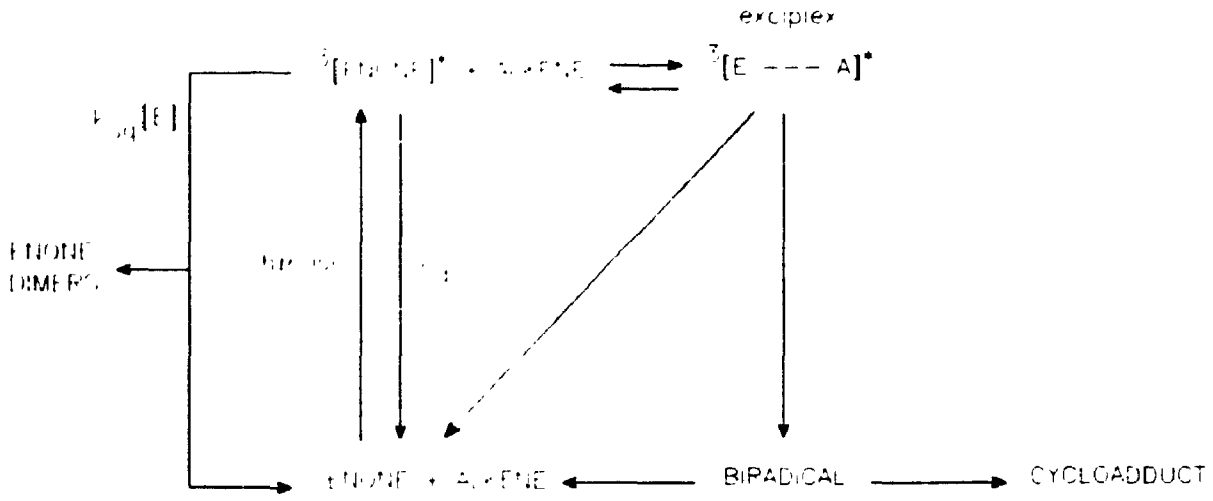

1.4 General problems with the Corey-de Mayo Mechanism.

The Corey-de Mayo mechanism has dominated the literature since its conception in 1964. The mechanism is cited widely in the literature as a means of predicting the regiochemistry of the cycloadducts expected from photocycloaddition reactions of cyclic enones and unsymmetrically substituted polar alkenes. In general, the mechanism's predictive power is very good for those examples which involve the photoaddition of an alkene substituted with electron donating groups, such as an alkoxy group, to a cyclic enone. In these cases, the major products are almost invariably representative of cycloadducts possessing a head-to-tail regiochemistry.[3a,d] There is, however, an

increasing number of examples of photocycloaddition reactions between cyclic enones and alkenes substituted with electron withdrawing groups that do not give the predicted head-to-head cycloadducts as major products. The following examples suggest that the predictive power of the Corey-de Mayo mechanism is significantly inferior to that which one might expect of a reliable reaction mechanism.

The regiochemistry of the cycloadducts obtained from the addition of acrylonitrile to 2-cyclopentenone and 4,4-dimethyl-2-cyclohexenone (7) has been shown to disagree with the regiochemistry predicted by the Corey-de Mayo mechanism. Rao and co-workers demonstrated that major cycloadduct obtained from the photocycloaddition of acrylonitrile to 7 is head-to-tail.[25] Weedon and co-workers found that the head-to-head to head-to-tail regiochemical ratio for the cycloadducts obtained from the photoaddition of acrylonitrile to 2-cyclopentenone was 3:4.8.[26] In other studies, Tada and co-workers[27] and Lange and co-workers[28] demonstrated that the regiochemistry of the products obtained from the addition of some methyl 1-cycloalkene-1-carboxylates to 3-substituted 2-cyclohexenones was highly dependent on the ring size of the cycloalkene (see Scheme 11). As the size of the cycloalkene ring decreases, the yield of the head-to-head cycloadduct products increases relative to the yield of the head-to-tail products. In the case where methyl 1-cyclohexene-1-carboxylate is added to the 3-substituted 2-cyclohexenones the regiochemical ratio of the cycloadducts is the reverse of that predicted by the Corey-de Mayo mechanism. Therefore, these studies indicate that the "oriented π-complexes" proposed by Corey do not explain the regiochemistry of the cycloadducts obtained in a significant number of enone 2+2 photocycloaddition reactions.

Scheme 11

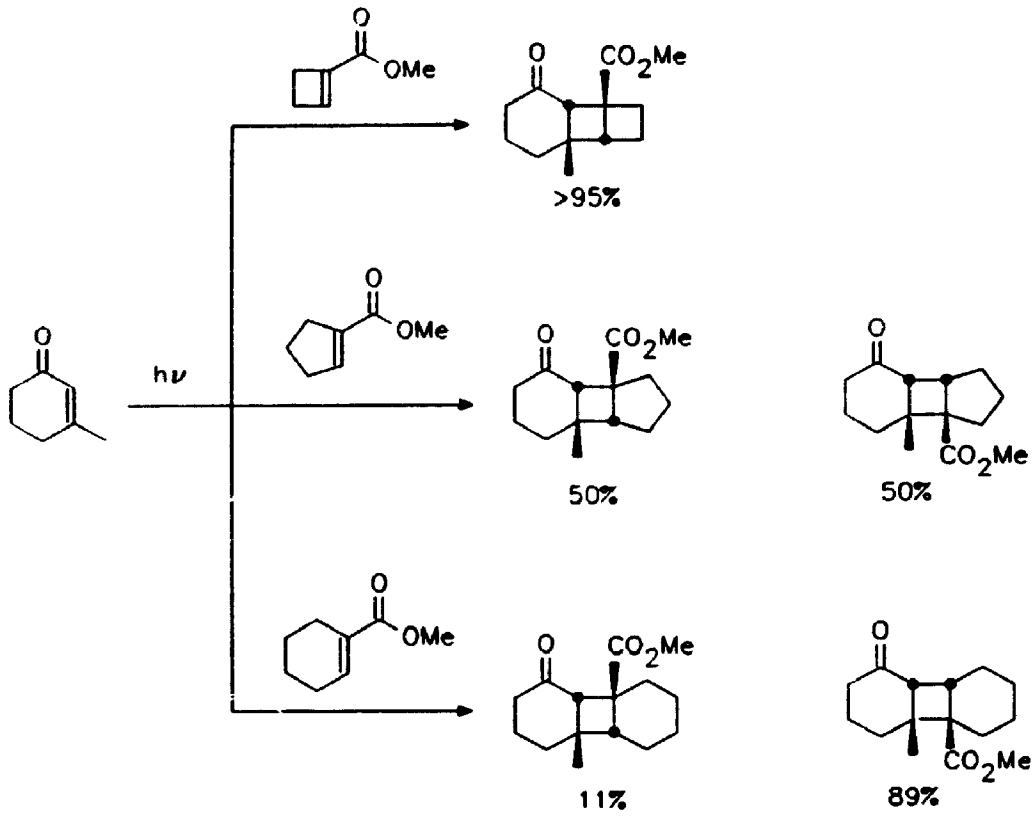

The "relative rate factors" published by Corey[2d] were re-analyzed by de Mayo[21], and more recently by Schuster,[12,29] in the context of the revised Corey-de Mayo mechanism. Both de Mayo and Schuster indicated that in a multi-step mechanism, such as the Corey-de Mayo mechanism, the relative product yields depend on the overall quantum efficiency of the reaction and not on the rate of a specific step. For example, it is possible for the rate of reaction of an alkene with a triplet enone to be very fast, perhaps even approaching the rate of diffusion, and yet the overall quantum yield of

product formation still be very low due to the fact that most of the reactive intermediates decay to starting materials instead of forming products. Therefore, the "relative rate factors" described by Corey offer no insight into the specific mechanistic step which, according to the Corey-de Mayo mechanism, involves the formation of a triplet exciplex. The relative rate factors are actually relative quantum yields of product formation. The trend observed by Corey simply indicates that the cycloadduct quantum yield resulting from the addition of electron poor alkenes to cyclic enones is general lower than the cycloadduct quantum yield resulting from the addition of electron rich alkenes. However, de Mayo[21] also pointed out an interesting inconsistency in this trend. It was noted by de Mayo that the dimerisation of cyclopentenone, which in the strictest sense represents addition to a deactivated double bond, has a limiting quantum yield of cycloadduct formation (0.36 in acetonitrile)[19] similar to systems which involve the addition of an electron rich alkene to a triplet cyclic enone. Therefore, the generality of the trend observed by Corey is questionable.

The rate of quenching of triplet cyclic enones by simple alkenes has been studied by Schuster and co-workers.[15,29] Some of the results obtained in these studies are summarised in Table 1. These data indicate the absence of any correlation between the rate of reaction between the enone triplet and the alkene (k_q) and the quantum yield of cycloadduct formation (Φ_{adduct}). The quantum yield of product formation must therefore be dependent on the mechanistic steps which occur after the initial reaction of the enone triplet with an alkene.

Table 1: Rate constants for quenching enone triplets by alkenes and quantum yields for adduct formation at 0.5 M alkene concentration.

Enone	Alkene	$k_q \times 10^{-7}$ M sec		Φ_{adduct}[a]	
		CH_3CN	C_6H_{12}	CH_3CN	C_6H_{12}
2-cyclopentenone	$H_2C=CCl(CN)$	200	520	0.04	0.05
	acrylonitrile	63	180	0.08	0.03
	fumaronitrile	160	460	0.00	
	cyclohexene	33	42	0.64	0.42
	$Cl_2C=CCl_2$	65		0.00	0.00
	cyclopentene	15	40	0.56	0.26
	$(CH_3)_2C=C(CH_3)_2$		99	0.71	0.29
3-methyl-2-cyclohexenone	$H_2C=CCl(CN)$	46	35	0.10	0.07
	acrylonitrile	15	11	0.14	0.08
	fumaronitrile		67	0.20	
	cyclohexene	5.2	0.5	0.16	0.07
	cyclopentene	<0.1	0.5	0.21	0.10
	$(CH_3)_2C=C(CH_3)_2$	<0.1		0.08	0.03
6 (R=AcO)	acrylonitrile	24			
	cyclopentene	6			

[a]Measured at an alkene concentration of 0.5 M.

One aspect of the data presented in Table 1 that has not yet been discussed concerns the very large values obtained for k_q when the alkene is substituted with an nitrile group. For example, in the case of the reaction between 1-chloroacrylonitrile the and 2-cyclopentenone triplet, enone quenching occurs at a rate approaching that of a diffusion controlled process. This surprisingly fast rate becomes more reasonable if the

triplet energies of some cyano-substituted alkenes are compared to the triplet energy of 2-cyclopentenone. The triplet energies of acrylonitrile and fumaronitrile are 58 ± 4 and 48 ± 3 kcal mol^{-1} respectively according to photoaccoustic work,[30] and the triplet energy of 2-cyclopentenone[5b] is approximately 72 kcal mol^{-1}. Given that triplet energy transfer in these systems should be exergonic by more than 20 kcal mol^{-1}, it is not unreasonable to postulate that at least part of the reason for the observed fast rate of quenching in these systems is due to triplet-triplet energy transfer. The complicating possibility of triplet energy transfer in enone-alkene photocycloaddition reactions involving cyano-substituted alkenes encouraged us to investigate these systems more closely. The results of our investigations are discussed in detail in Chapter 6.

1.5 Trapping of the 1,4-Biradical Intermediates

In the last several years considerable attention has been focused on the importance of the 1,4-biradical intermediates involved in enone-alkene 2+2 photocycloaddition reactions. In fact, Bauslaugh[3d] was the first to propose that the regiochemistry of the cycloadducts obtained from enone-alkene photocycloaddition reactions could be rationalised without invoking the formation of oriented exciplex intermediates. He suggested that the relative ratio of the regiochemical isomers could be explained by considering that each of the possible 1,4-biradicals formed in a photocycloaddition has a different rate of closure relative to fragmentation. That is, the major cycloadducts resulting from the reaction originate from 1,4-biradical intermediates which close more efficiently relative to reversion to starting materials, while the minor cycloadducts are the result of 1,4-biradicals which undergo reversion more efficiently than closure. At

the time Bauslaugh proposed this hypothesis, some 24 years ago, it was equally as valid as the exciplex based explanation; however, there was no mechanistic evidence available that directly supported Bauslaugh's claims.

Recently, Weedon and Hastings proposed a method for investigating the structures of the 1,4-biradicals formed in the photocycloaddition reaction of triplet cyclic enones with alkenes.[31] They demonstrated that hydrogen selenide can be used to trap chemically the 1,4-biradicals formed in the photocycloaddition reactions between ethyl vinyl ether and 2-cyclopentenone, and between cyclopentene and 2-cyclopentenone (see Scheme 12). Hydrogen selenide was chosen as the biradical trap because of previously published reports which indicated that the 1,4-biradicals formed in the Norrish Type II of aryl ketones could be trapped by hydrogen selenide.[32]

When benzene solutions containing 2-cyclopentenone, ethyl vinyl ether, and 0.3 M hydrogen selenide were irradiated with ultra-violet light, the formation of cycloadducts was completely suppressed and 4 new products, **23**, **24**, **25** and **26**, were formed in the ratio 3.2:3.5:5.7:1.0, respectively.[31] Scheme 12 demonstrates which biradicals are responsible for the formation of each of these products. For example, compounds **23** and **25** were formed as a result of complete reduction of the two radical sites in biradicals **27** and **30**, whereas compounds **24** and **26** were formed as a result of a disproportionation reaction between the hydrogen selenyl radical and partially reduced forms of the same two biradicals. No products were detected in the biradical trapping studies that could have originated from biradicals **28** or **29**. Based on the product ratios of the trapped products, the ratio of the relative rates of formation of biradicals **27** and **30** was found to be 1.0:1.0. However, in the absence of hydrogen selenide the regiochemical ratio of

Scheme 12

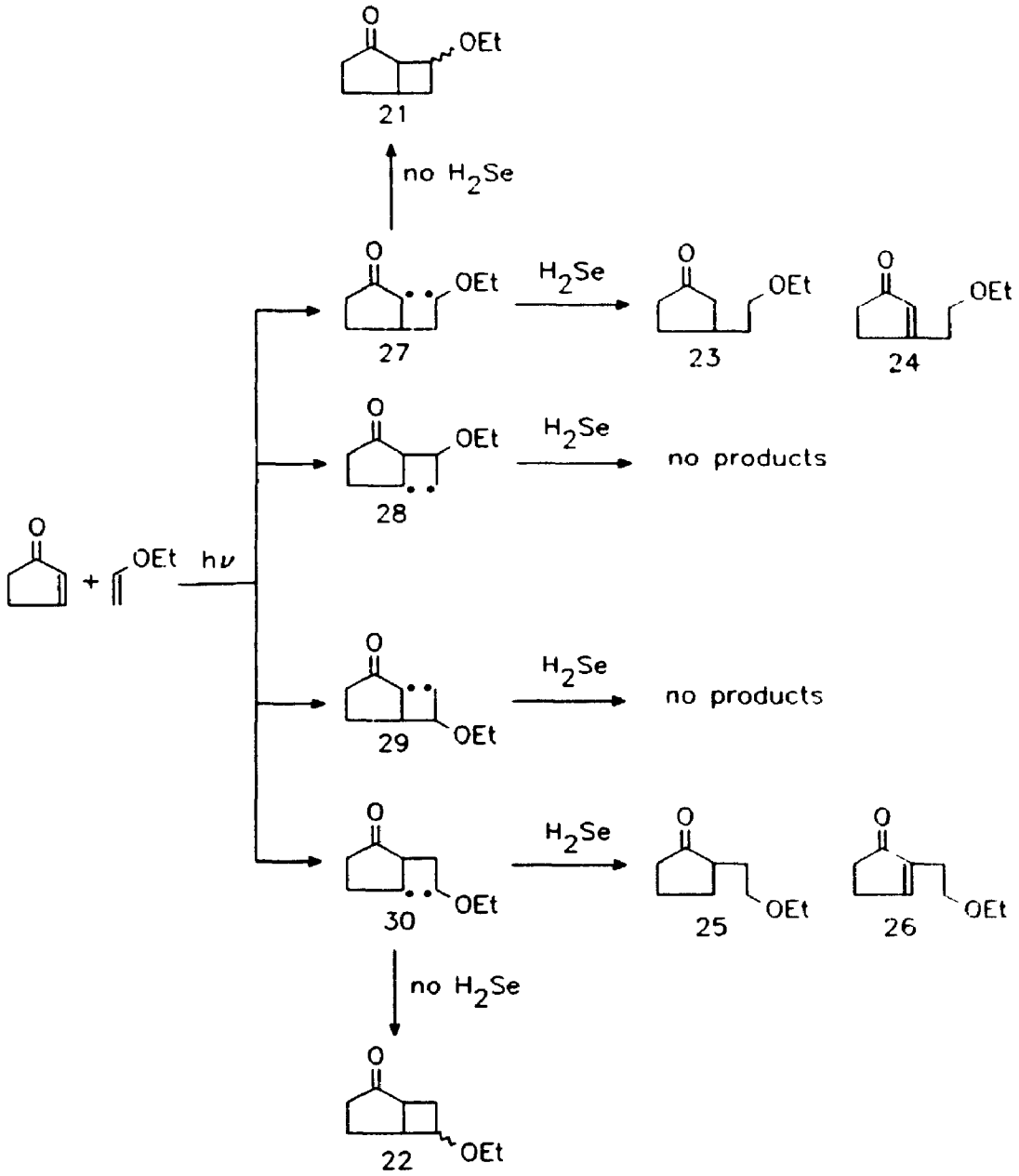

22:21 resulting from the photocycloaddition reaction between 2-cyclopentenone and ethyl vinyl ether is 4:1.[33] The large difference between this ratio and the ratio of the regioisomers obtained in the photocycloaddition indicates that the rate of biradical

formation does not control the relative product distribution of the regioisomeric cycloadducts. In this particular case, the regiochemistry of the cycloaddition is determined by the rate at which each biradical closes to form cyclobutane adducts relative to the rate at which the biradical reverts to form ground state starting materials. This finding disagrees with the Corey-de Mayo Mechanism which suggests that the regiochemistry of a photocycloaddition reaction is controlled by the relative rates of formation of the biradicals.

1.6 The Purpose of the Studies in Part I of this Thesis

The general purpose of the work described in Chapters 2, 3, and 4 of this thesis was to confirm and generalise the conclusions drawn by Hastings and Weedon from the H_2Se trapping of the biradicals involved in the 2-cyclopentenone plus ethyl vinyl ether photocycloaddition reaction. The enones studied included 2- and 3-substituted 2-cyclopentenones as well as 2-cyclopentenone itself. Product studies as well as kinetic analyses were performed on photocycloaddition reactions involving these cyclic enones and a variety of alkenes.

A large proportion of the work described in the following chapters involved the use of hydrogen selenide as a 1,4-biradical trap. By applying this compound to each photocycloaddition reaction it was possible to isolate and characterise stable products revealing the structures of the biradical intermediates. The relative ratios of the trapped products obtained from the photolyses carried out in the presence of hydrogen selenide were also used to determine the relative rates of formation of each of the 1,4-biradicals. In addition to trapping the 1,4-biradicals, steady state kinetic experiments were also

carried out for each enone-alkene system by measuring the quantum yield of cycloadduct formation at different alkene concentrations. The data obtained from these kinetic experiments were used in conjunction with the relative rates of biradical formation obtained in the trapping experiments to determine the fates of the biradicals. That is to say, the partitioning ratio between closure to form cycloadducts and reversion to form starting materials was determined for all of the biradicals involved in each enone-alkene system that was studied. By comparing the structures of biradicals that exhibited drastically different closure to reversion ratios, mechanistic generalisations regarding the regio- and stereochemical control of enone-alkene photocycloadditions were made.

1.7 References

1. Ciamician, G.; Silber, P. *Chem. Ber.* **1908**, *41*, 1928.

2. (a) de Mayo, P.; Takeshita, H.; Satter, A. B. M. A. *Proc. Chem. Soc.* **1962**, 119. (b) Corey, E. J.; Nozoe, S. *J. Am. Chem. Soc.* **1964**, *86*, 1652. (c) Corey, E. J.; Mitra, R. B.; Uda, H. *Ibid.* **1964**, *86*, 485. (d) Corey, E. J.; Bass, J. D.; LeMahieu, R.; Mitra, R. B. *Ibid.* **1964**, *86*, 5570. (e) Eaton, P. E. *Ibid.* **1962**, *84*, 2454.

3. (a) Weedon, A. C. In *Synthetic Organic Photochemistry*; Horspool, W. M., Ed.; Plenum Press: New York, 1984; Chapter 2. (b) Carless, H. A. J. In *Photochemistry in Organic Synthesis*; Coyle, J. D. Ed.; Royal Soc. Chem.; London, 1986; pp 95-117. (c) Baldwin, S. W. In *Organic Chemistry*; Padwa, A., Ed.; Marcel Dekker: New York, 1981; Vol. 5, pp 123-225. (d) Bauslaugh, P. G. *Synthesis* **1970**, 287. (e) Oppolzer, W. *Acc. Chem. Res.* **1982**, *15*, 135.

4. (a) White, J. D.; Gupta, D. N. *J. Am. Chem. Soc.* **1966**, *88*, 5364. (b) White, J. D.; Gupta, D. N. *J. Am. Chem. Soc.* **1968**, *90*, 6171.

5. (a) Eaton, P. E.; Hurt, W. S. *J. Am. Chem. Soc.* **1966**, *88*, 5038. (b) de Mayo, P.; Pete, J-P.; Tchir, M. F. *Can. J. Chem.* **1968**, *46*, 2535. (c) de Mayo, P.; Nicholson, A. A.; Tchir, M. F. *Ibid.* **1970**, *48*, 225. (d) Ruhlen, J. L.; Leermakers, P. A. *J. Am. Chem. Soc.* **1966**, *88*, 5671. (e) Ruhlen, J. L.; Leermakers, P. A. *J. Am. Chem. Soc.* **1967**, *89*, 4944.

6. (a) McCullough, J. J.; Ohorodnyk, H.; Santry, D. P. *Chem. Commun.* **1969**, 570. (b) Yamauchi, S.; Hirota, N.; Higuchi, J. *J. Phys. Chem.* **1988**, *92*, 2129.

7. (a) Yang, N. C.; Jorgenson, M. J. *Tetrahedron Lett.* **1964**, 1203. (b) Graf, J. F.; Lillya, C. P. *Mol. Photochem.* **1979**, *9*, 227. (c) Ricard, R.; Sauvage, P.; Wan, C. S. K.; Weedon, A. C.; Wong, D. F. *J. Org. Chem.* **1986**, *51*, 62. (d) Duhaime, R. M.; Weedon, A. C. *Can. J. Chem.* **1987**, *65*, 1867. (e) Duhaime, R. M.; Weedon, A. C. *J. Am. Chem. Soc.* **1987**, *109*, 2479.

8. (a) Eaton, P. E.; Lin, K. *J. Am. Chem. Soc.* **1964**, *86*, 2087. (b) Corey, E. J.; Tada, R.; LeMahieu, R.; Libit, L. *J. Am. Chem. Soc.* **1965**, *87*, 2051. (c) Eaton, P. E.; Lin, K. *J. Am. Chem. Soc.* **1965**, *87*, 2052.

9. The formation of *trans*-2-cycloheptenone upon irradiation of 2-cycloheptenone was confirmed by laser flash techniques. See: Bonneau, R.; Fornier de Violet, P.; Joussot-Dubien, J. *Nouv. J. Chim.* **1977**, *1*, 31 and Bonneau, R. *J. Am. Chem. Soc.* **1980**, *102*, 3816.

10. (a) Cargill, R. L.; Miller, A. C.; Pond, D. M.; de Mayo, P.; Tchir, M. F.; Neuberger, K. R.; Sitiel, J. *Mol. Photochem.* **1969**, *1*, 301. (b) Cargill, R. L.; Bundy, W. A.; Pond, D. M.; Sears, A. B.; Saltiel, J.; Winterle, J. *Mol. Photochem.* **1971**, *3*, 123.

11. (a) Kearns, D. R.; Marsh, G.; Schaffner, K. *J. Chem. Phys.* **1968**, *49*, 3316. (b) Marsh, G.; Kearns, D. R.; Schaffner, K. *Helv. Chim. Acta* **1968**, *51*, 1890.

12. Schuster, D. I. In *The Chemistry of Enones*; Patai, S., Rappoport, Z., Eds.; John Wiley and Sons, Ltd.: Chichester, U.K., 1989; pp 623-756.

13. (a) Schuster, D. I.; Greenberg, M. M.; Nunez, I. M.; Tucker, P. C. *J. Org. Chem.* **1983**, *48*, 2615. (b) Chan, A. C.; Schuster, D. I. *J. Am. Chem. Soc.* **1986**, *108*, 4561.

14. Nelson, P. J.; Ostrem, D.; Lassila, J.; Chapman, O. L. *J. Org. Chem.* **1969**, *34*, 811.

15. Schuster, D. I.; Dunn, D. A.; Heibel, G. E.; Brown, P. A.; Rao, J. M.; Woning, J.; Bonneau, R. *J. Am. Chem. Soc.* **1991**, *113*, 6245.

16. Caldwell, R. A.; Tang, W.; Schuster, D. I. Heibel, G. E. *Photochem. Photobiol.* **1991**, *53*, 159.

17. Bonneau, R *J. Am. Chem. Soc.* **1980**, *102*, 3816.

18. The dimerisation of 2-cyclopentenone was first reported by Eaton. See: Eaton, P. E. *J. Am. Chem. Soc.* **1962**, *84*, 2454.

19. Wagner, P. J.; Bucheck, D. J. *J. Am. Chem. Soc.* **1969**, *91*, 5090.

20. Zimmerman, H. E.; Swenton, J. S. *J. Am. Chem. Soc.* **1964**, *86*, 1436.

21. de Mayo, P. *Acc. Chem. Res.* **1971**, *4*, 41.

22. Dilling, W. L.; Tabor, T. E. *J. Am. Chem. Soc.* **1970**, *92*, 1399.

23. Peet, N. P.; Cargill, R. L. Bushey, D. F. *J. Org. Chem.* **1973**, *38*, 1218.

24. Loutfy, R. O.; de Mayo, P. *J. Am. Chem. Soc.* **1977**, *99*, 3559.

25. Swanpa, G. V. T.; Lakshmi, A. B.; Rao, J. M.; Kunwar, A. C. *Tetrahedron* **1989**, *45*, 1777.

26. Krug, P.; Rudolph, A.; Weedon, A. C. *Tetrahedron Lett.* **1993**, *34*, 7221.

27. Tada, M.; Nieda, Y. *Bull. Chem. Soc. Jpn.* **1988**, *61*, 1416.

28. Lange, G. L.; Organ, M. G.; Lee, M. *Tetrahedron Lett.* **1990**, *31*, 4689.

29. Schuster, D. I.; Heibel, G. E.; Brown, P. A.; Turro, N. J.; Kumar, C. V. *J. Am. Chem. Soc.* **1988**, *110*, 8261.

30. Lavilla, J. A.; Goodman, J. L. *Chem. Phys. Lett.* **1987**, *141*, 149.

31. Hastings, D. J.; Weedon, A. C. *J. Am. Chem. Soc.* **1991**, *113*, 8525.

32. Kambe, N.; Masawaki, T.; Kondo, K.; Miyoshi, N.; Ogawa, A.; Sonoda, N. *Chem. Lett.* **1987**, 1907.

33. (a) Termont, D.; De Keukeleire, D.; Vandewalle, M. *J. Chem. Soc., Perkin Trans. 1* **1977**, 2349. (b) Griesbeck, A. G.; Stadtmuller, S.; Busse, H.; Bringmann, G.; Buddrus, J. *Chem. Ber.* **1992**, *125*, 933.

CHAPTER 2

2+2 PHOTOCYCLOADDITION REACTIONS OF 2-CYCLOPENTENONE AND POLAR ALKENES

2.1 Introduction

When this work began the Corey-de Mayo mechanism for the photoaddition of excited cyclic enones to alkenes was well accepted in the literature. As described in Chapter 1, the Corey-de Mayo mechanism was initially proposed in order to explain the apparent regioselectivity that the photocycloaddition reaction exhibits when polarised alkenes are added to cyclic enones.[1] That is, alkenes which are substituted at one terminus with electron donating groups photoadd to cyclic enones to give major products exhibiting a head-to-tail regiochemistry. Conversely, alkenes which are substituted with electron withdrawing groups photoadd to cyclic enones to generate major adducts that exhibit a relative head-to-head regiochemistry. The Corey-de Mayo mechanism rationalised this observation in terms of an oriented excited state complex which is formed when the triplet excited enone reacts directly with the alkene. It was suggested that the rate of formation of this exciplex was the factor which controlled the regiochemistry of the cycloadducts. In fact, a major reason for the existence of the Corey-de Mayo exciplex mechanism was to explain the apparent regioselectivity exhibited by photocycloadditions involving cyclic enones and polarised alkenes.

Recently, Hastings and Weedon demonstrated that the relative rates of formation of the biradicals generated in the photoaddition of triplet 2-cyclopentenone to ethyl vinyl ether do not control the regiochemistry of the cycloadducts.[2] It was shown that in this

reaction all of the biradicals are formed at the same rate; however, the regiochemical ratio of the cycloadducts is weighted in favour of the head-to-tail products. This work, which is explained in more detail in Chapter 1, demonstrated that rates of formation of any reactive intermediates existing prior to biradical formation do not affect the regiochemistry of the products obtained from photocycloadditions involving cyclic enones and electron rich alkenes. This is inconsistent with the idea that an oriented exciplex controls the reaction regiochemistry as suggested by the Corey-de Mayo mechanism; such an exciplex would necessarily favour the formation of biradicals responsible for the formation of the major regioisomer.

The purpose of the studies described in this chapter was to explore the photocycloaddition of 2-cyclopentenone to alkenes which are substituted with electron withdrawing groups using similar techniques to those utilised by Hastings and Weedon. Specifically, the attempt was made to trap the biradical intermediates which are formed in photocycloadditions involving 2-cyclopentenone and electron deficient alkenes by performing the reactions in the presence of hydrogen selenide. Hydrogen selenide, being an excellent hydrogen atom donor, is potentially capable of reducing the radical sites present in a biradical in two sequential hydrogen atom additions, thereby transforming the biradical intermediate into an isolable compound. The prerequisite to success in studies which attempt to trap biradicals with hydrogen selenide is that the rate of reaction between H_2Se and each biradical must be much greater than the inverse lifetime of the biradical. In the case of Hastings and Weedon's investigation of the reaction between 2-cyclopentenone and ethyl vinyl ether, this condition seems to have been obtained.

The systems that will be discussed in this chapter include the photocycloadditions

of 2-cyclopentenone to methyl acrylate and 1,1-difluoroethene. The photocycloaddition of 2-cyclopentenone to acrylonitrile, which is also an electron depleted alkene, will be discussed in Chapter 6. Methyl acrylate and 1,1-difluoroethene were selected for study because of the undisputable electron withdrawing properties of the substituents on these alkenes. The cycloadducts resulting from the photoaddition of 2-cyclopentenone to methyl acrylate or 1,1-difluoroethene have not been reported before. Therefore, it was necessary to characterise and quantify these cycloadducts before pursuing any mechanistic studies involving biradical trapping.

2.2 Results for the 2-cyclopentenone plus 1,1-difluoroethene system

2.2.1 Photocycloaddition products

The irradiation of a solution of 2-cyclopentenone (0.040 mole/L) and 1,1-difluoroethene (0.15 mole/L) in methanol with water and Pyrex filtered light from a 450 watt Hanovia medium pressure mercury lamp resulted in the formation of cycloadducts **31** and **32** as well as two enone dimers (see Scheme 13). After seven hours of irradiation the ratio of 2-cyclopentenone:**31**:**32**:**13**:**12** was found to be 17:13:4.7:43:22. The formation of the enone dimers could not be avoided by raising the concentration of the 1,1-difluoroethene because the saturation point of the gas in methanol at 25°C was only 0.15 mole/L. The identification of the enone dimers was accomplished by comparing the g.c. retention times of the products resulting from the irradiation of a solution of 2-cyclopentenone (0.1 mole/L) in benzene with the g.c retention times of the products in the reaction mixture described above. The identity of the head-to-tail dimer and head-to-head dimer in the irradiated solution containing 2-cyclopentenone in benzene was

confirmed by comparing the relative product yields with the head-to-head:head-to-tail ratio of 0.20 observed by Wagner et al.[3]

Scheme 13

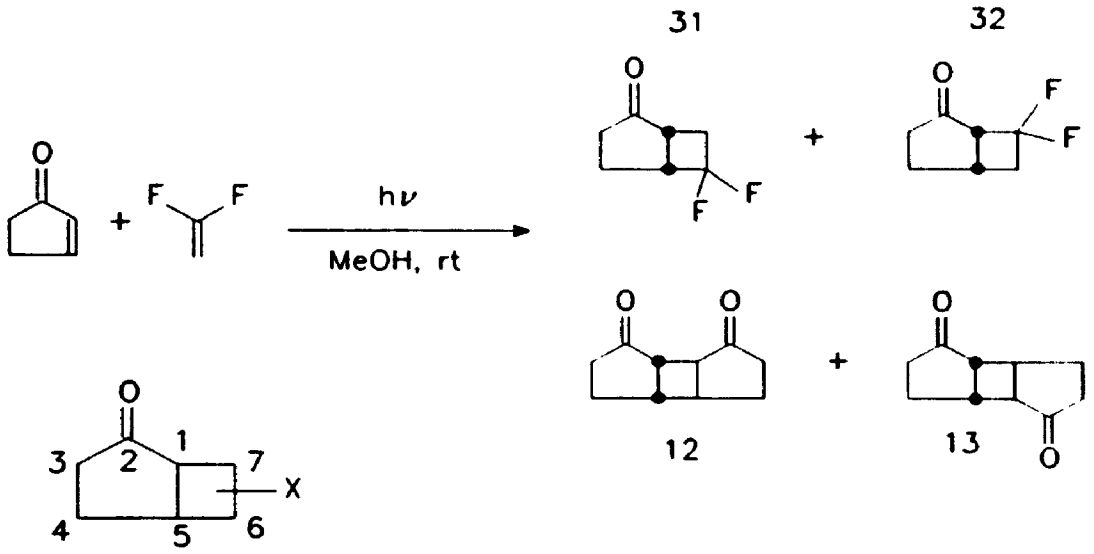

Identification of 31 and 32.

Compounds **31** and **32** were separated from each other and from the other components of the reaction mixture by chromatography. The ^{1}H nmr spectra of compounds **31** and **32** were complicated by the presence of ^{1}H-^{19}F J-coupling. The identity of these compounds could not be determined by simply analyzing the coupling patterns observed in the ^{1}H spectra. Therefore, the results obtained from ^{13}C-^{1}H heteronuclear correlation (HETCOR) experiments were used in conjunction with the chemical shift of each ^{13}C nmr resonance to determine the regiochemistry of cycloadducts **31** and **32**.

It has been observed that fluorine substituents cause down-field shifts for carbons positioned α or β with respect to the substituent and up-field shifts for carbons positioned γ with respect to the substituent.[4,5c,d] This generalisation is consistent with the ^{13}C nmr chemical shift assignments listed in Table 2. In addition to chemical shift data, the magnitude of the ^{13}C-^{19}F coupling constants were also used to prove the regiochemistry of **31** and **32**. In aliphatic molecules, two bond ^{13}C-^{19}F coupling constants are always larger than the three bond coupling constants.[5] One bond ^{13}C-^{19}F coupling constants are always substantially larger than both two and three bond coupling constants.[5] This generalisation is in agreement with the data presented in Table 2. The assignments listed in Table 2 were made after the regiochemistry of each of the cycloadducts was deduced.

Table 2: Summary of the chemical shifts (ppm) and ^{13}C-^{19}F coupling constants (Hz) exhibited by the methine carbons in the ^{13}C nmr spectra of **31** and **32**.

carbon assigned	cycloadduct **31**		cycloadduct **32**	
	δ (ppm)	J_{CF} (Hz)	δ	J_{CF} (Hz)
C_1	34.5	7.5, 10.6	57.8	23.3, 22.4
C_2	218.2	4.0, 0	212.2	3.0, 1.5
C_3	36.3	0, 0	36.7	4.0, 0
C_4	19.6	2.9, 5.8	27.0	2.8, 0
C_5	47.9	23.5, 25.1	25.6	6.1, 11.0
C_6	119.9	285, 282	40.3	22.4, 22.4
C_7	38.8	25.3, 25.3	115.8	282, 289

The following methodology was used in determining the regiochemistry of **31** and **32**. First, the ^{13}C nmr resonance due to the C_4 carbon was assigned for each adduct. This assignment was based on the relative magnitude of the ^{13}C-^{19}F coupling constant, the attached proton test (APT) spectrum, and the results of ^{13}C-^{1}H heteronuclear correlation (HETCOR) experiments. The ^{13}C-^{1}H HETCOR experiments were used in conjunction with ^{1}H-^{1}H high power decoupling in order to determine which methine ^{13}C nmr resonance originated from the carbon adjacent to C_4. In this way, methine carbon C_5 was assigned. The magnitude of the ^{13}C-^{19}F coupling constant observed for the C_5 resonance indicated whether the fluorine substituents were positioned α or β with respect to this methine carbon.

In the case of **31**, the ^{13}C resonance at 19.6 ppm (solvent: $CDCl_3$) was assigned to the C_4 position. This resonance was found to correlate with a ^{1}H resonance at 2.04 ppm in HETCOR experiments. The geminal coupling of 14.4 Hz exhibited by this ^{1}H nmr resonance was too small for this resonance to be assigned to the α-keto methylene protons.[6] The ^{1}H resonance at 2.04 ppm, which was observed as a doublet of quartets in the coupled spectrum, was decoupled to form a doublet of triplets by irradiation at the ^{1}H nmr resonance located at 3.36 ppm. The coupling constant between these two resonances was determined to be 9.6 Hz. The HETCOR results indicated that the proton resonance at 3.36 correlated with the lowest field methine ^{13}C nmr resonance located at 47.9 ppm which exhibited ^{13}C-^{19}F coupling constants of approximately 25 Hz. Therefore, this methine ^{13}C resonance was assigned to the carbon in the C_5 position. The other methine resonance in the ^{13}C nmr spectrum of **31** was located substantially further up-field at 34.5 ppm and exhibited ^{13}C-^{19}F coupling constants of 7.5 and 10.6 Hz. Based

on the relative magnitude of the ^{13}C-^{19}F coupling constants and the relative magnitude of the chemical shifts of the carbon signals, the fluorine substituents must be positioned β with respect to the C_5 methine carbon. Therefore, the regiochemistry of **31** must be head-to-tail.

In the case of compound **32**, the methylene ^{13}C nmr resonance at 27.0 ppm (solvent: $CDCl_3$) was assigned to the C_4 position of the ring system. One of the geminal proton resonances correlated with this ^{13}C resonance was located at 2.00 ppm in the ^1H nmr spectrum of **32**. Selective decoupling experiments indicated that the resonance at 2.00 ppm was coupled to an α-keto methylene proton at 2.61 ppm. The assignment of the 2.61 ppm resonance to the α-keto methylene protons was based on the fact that this resonance exhibited a large geminal coupling constant of 18.5 Hz.[6] Selective decoupling experiments were also used to show that the 2.00 ppm resonance was <u>not</u> coupled to an undetermined multiplet located at 3.23 ppm in the ^1H nmr spectrum of **32**. The multiplet at 3.23 ppm in the ^1H nmr spectrum was found to be correlated with a ^{13}C nmr resonance possessing a multiplicity representative of a methine carbon located at 57.8 ppm which exhibited ^{13}C-^{19}F coupling constants of approximately 23 Hz. Therefore, this methine carbon was assigned to the C_1 position of the ring system. The other methine ^{13}C resonance, located much further up-field at 25.6 ppm and exhibiting ^{13}C-^{19}F constants of 6 and 11 Hz, was assigned to the C_5 position. Based on the relative chemical shifts and ^{13}C-^{19}F coupling constants exhibited by these methine carbons, it was concluded that the methine carbon with the chemical shift of 57.8 ppm was positioned β with respect to the fluorine substituents. In this way, compound **32** was proven to have a head-to-head regiochemistry.

2.2.2 Attempted biradical trapping

Attempts were made to trap the biradicals generated in the photocycloaddition reaction between 1,1-difluoroethene and 2-cyclopentenone with hydrogen selenide. In these experiments, acetonitrile solutions containing 2-cyclopentenone (0.040 mole/L) and 1,1-difluoroethene (saturation concentration at -10°C in acetonitrile; 0.2 M) were irradiated in the presence of various concentrations of H_2Se. The reaction was investigated at three concentrations of H_2Se: the saturation concentration in acetonitrile at room temperature, 0.5 times the saturation concentration, and 0.15 times the saturation concentration. In all cases, the total time that the reaction mixture was irradiated was 45 minutes.

The only products observed when these solutions were irradiated with U.V. light were 2-cyclopentenone, cyclopentanone, **31**, **32**, and enone dimers. The relative yields of these products at the different concentrations of H_2Se used are summarized in Table 3. The data in this table demonstrate that as the concentration of H_2Se was increased, the relative yield of cyclopentanone also increased· however, the relative yield of **31**, **32** and the enone dimers decreased. (The origin of the cyclopentanone will be explained later.) In all of the experiments, no evidence of products resulting from H_2Se biradical trapping was detected by g.c.-m.s. Based on the analysis of the reaction mixture containing H_2Se that was not exposed to the light (see the first entry in Table 3), it was also conclude that no products resulting from dark reactions involving cyclopentenone and 1,1-difluoroethene in H_2Se-saturated acetonitrile were formed during the time period of the reaction.

carbonyl stretch at 1770 cm^{-1} as well as a characteristic O-H stretch at 3510 cm^{-1}. The presence of a lactone in the mixture of **37** and **38** was also confirmed by the presence of a carbonyl carbon resonance at 180.6 ppm. For purposes of comparison it may be noted that γ-butyrolactone has a carbonyl ^{13}C nmr resonance at 178.1 ppm and a carbonyl IR stretching frequency of 1770 cm^{-1}.[4] The ^{13}C nmr spectrum of the mixture of **37** and **38** exhibited methine resonances at 105.5, 86.0 and 85.5 ppm. The chemical shift of the former of these three resonances is representative of a hemiacetal while the latter two resonances are representative of ether α-carbon signals.[4] Therefore, after combining all of the spectroscopic evidence it seemed reasonable to assign the structures indicated in Scheme 4 to compounds **37** and **38**. The formation of compound **37** must be a result of over-reduction of lactone **38** by the $NaBH_4$. In hindsight, conversion of compound **37** to **38** by chromic acid oxidation would probably have been quite easy and might have provided more information; however, at the time the photocycloaddition of 2-cyclopentenone was being studied it was decided that, based on the spectral data observed for **33**, **37** and **38**, the identification of **33** was secure. Therefore, the oxidation of **37** was not performed.

Additional evidence for the regiochemical assignment of compound **33** was obtained by comparing the methine carbon ^{13}C nmr chemical shifts of this compound with those of the other cycloadducts (see Table 4). All of the methine resonances observed in the ^{13}C nmr spectra of **33** had chemical shifts which were very similar to the chemical shifts of the corresponding resonances observed in the ^{13}C nmr spectra of compound **34**; however, these chemical shifts were significantly different from the chemical shifts of the methine carbon resonance observed in the ^{13}C nmr spectra of **35** and **36**. The general

Scheme 14

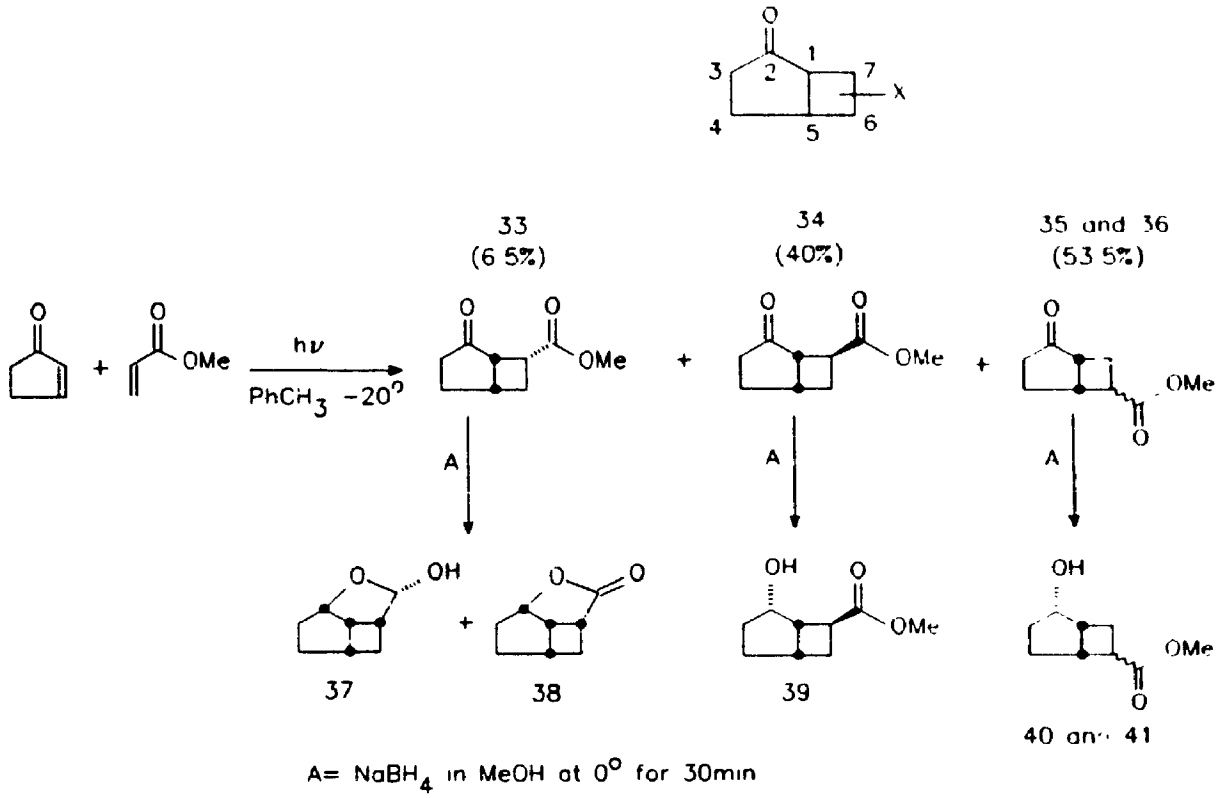

The ratio of cycloadducts **33:34:(35+36)** was not determined by g.c. since conditions could not be found under which compounds **34** and **35** did not co-elute. Therefore, it was necessary to determine the product ratios by performing quantitative ^{13}C nmr spectroscopy on reaction mixtures resulting from irradiation of a solution of 2-cyclopentenone and methyl acrylate in toluene. In these quantitative ^{13}C nmr experiments gated decoupling, in which the decoupler was turned on only during the acquisition and 90° pulse, was used. Small pulse widths (i.e. small flip angles) and long delay times between each pulse (35 seconds) were also used.[7] Reaction mixtures containing 2-cyclopentenone and methyl acrylate were irradiated at -20°C through a $SnCl_2$ in 10% HCl/H_2O light filter instead of just a Pyrex filter. This was done in order to prevent

secondary photolysis of the cycloadducts. The stability of the cycloadducts to light passing through this filter was determined by irradiating a solution of compounds **33**, **34**, **35** and **36** in $CDCl_3$. No change was detected in the cycloadduct ratios after 4 hours of irradiation; therefore, it was concluded that cycloadduct ratios measured by ^{13}C nmr spectroscopy were not altered by secondary photolysis. The ratio of cycloadducts **33**:**34**:(**35**+**36**) as determined by ^{13}C nmr spectroscopy was found to be 7:40:53. Proton nmr spectroscopy was not useful in quantifying the products since reaction mixtures containing all four cycloadducts were too complicated to allow the identification and accurate integration of ^1H nmr signals originating from each adduct.

In order to help elucidate the regio- and stereochemistry of the cycloadducts formed in the photocycloaddition of 2-cyclopentenone and methyl acrylate, sodium borohydride reductions were performed on each of the cycloadducts. The reason for performing these reduction studies was twofold. First, by reducing the ketone functionality it was hoped that some of the ^1H resonances which overlapped in the proton spectrum of each cycloadduct might become resolved in the proton spectrum of the alcohol reduction product. Secondly, it was hoped that the head-to-head cycloadduct possessing the *exo* stereochemistry would spontaneously lactonise upon reduction of the ketone to the alcohol. The formation of lactone **38** would unequivocally prove the stereochemistry of the *exo* head-to-head cycloadduct.

The reduction of adduct **34** with $NaBH_4$ in methanol resulted in the formation of one product which was characterised as alcohol **39**. No evidence of the epimeric alcohol (i.e. the alcohol possessing the exo stereochemistry) was detected in the $NaBH_4$ reductions of this cycloadduct. Similarly, only one epimer was observed in the

reductions of each of compounds **35** and **36**. In each case, it was hypothesised that the epimeric alcohol formed was that which was representative of exo attack of the metal hydride on the ketone carbon because this mode of reduction results in less steric hinderance relative to endo attack. The reduction of adduct **33** under the same conditions resulted in the formation of a lactone characterised as compound **38** as well as another product, compound **37**, which was characterised as a product resulting from over-reduction of the lactone. The only cycloadduct which possesses a stereochemistry from which lactonisation could occur, after reduction of the ketone group, is cycloadduct **33**.

Identification of 33.

Cycloadduct **33** was not obtained as a pure compound; rather, this cycloadduct was identified in a mixture containing **33** and **35** in a 25:75 ratio. Using this mixture in conjunction with a sample of pure **35**, it was possible to deduce that compound **33** reduces to compounds **37** and **38** upon treatment with sodium borohydride in methanol. A pure sample of compound **35** was reduced to a single alcohol labelled **40** (see below). The identity of compounds **37** and **38** was established by examination of the mass spectra of each compound as well as by examination of the ^{1}H and ^{13}C spectra obtained from a 4:6 mixture of **37** and **38**.

The mass spectrum of **38** contained a parent molecular ion at m/e=138. This mass is the equivalent of one methanol molecule less than the expected mass of a product resulting from the $NaBH_4$ reduction of the ketone functionality of cycloadduct **33**. On the other hand, the mass spectrum of **37** contained a parent molecular ion at m/e=140. The IR spectrum of the mixture containing **37** and **38** exhibited a characteristic lactone

carbonyl stretch at 1770 cm^{-1} as well as a characteristic O-H stretch at 3510 cm^{-1}. The presence of a lactone in the mixture of **37** and **38** was also confirmed by the presence of a carbonyl carbon resonance at 180.6 ppm. For purposes of comparison it may be noted that γ-butyrolactone has a carbonyl ^{13}C nmr resonance at 178.1 ppm and a carbonyl IR stretching frequency of 1770 cm^{-1}.[4] The ^{13}C nmr spectrum of the mixture of **37** and **38** exhibited methine resonances at 105.5, 86.0 and 85.5 ppm. The chemical shift of the former of these three resonances is representative of a hemiacetal while the latter two resonances are representative of ether α-carbon signals.[4] Therefore, after combining all of the spectroscopic evidence it seemed reasonable to assign the structures indicated in Scheme 4 to compounds **37** and **38**. The formation of compound **37** must be a result of over-reduction of lactone **38** by the $NaBH_4$. In hindsight, conversion of compound **37** to **38** by chromic acid oxidation would probably have been quite easy and might have provided more information; however, at the time the photocycloaddition of 2-cyclopentenone was being studied it was decided that, based on the spectral data observed for **33**, **37** and **38**, the identification of **33** was secure. Therefore, the oxidation of **37** was not performed.

Additional evidence for the regiochemical assignment of compound **33** was obtained by comparing the methine carbon ^{13}C nmr chemical shifts of this compound with those of the other cycloadducts (see Table 4). All of the methine resonances observed in the ^{13}C nmr spectra of **33** had chemical shifts which were very similar to the chemical shifts of the corresponding resonances observed in the ^{13}C nmr spectra of compound **34**; however, these chemical shifts were significantly different from the chemical shifts of the methine carbon resonance observed in the ^{13}C nmr spectra of **35** and **36**. The general

conclusion which seems to fit the data presented in Table 4 is that cycloadducts possessing a head-to-head regiochemistry exhibit a large downfield shift for the α-keto methine ^{13}C nmr resonance. This generalisation holds true for other examples of 2-cyclopentenone-alkene cycloadducts.[8,9]

Table 4: Chemical shifts of the methine ^{13}C nmr resonances in ppm for cycloadducts **33**, **34**, **35** and **36** (solvent: $CDCl_3$).

carbon assigned	cycloadduct **33**	cycloadduct **34**	cycloadduct **35**	cycloadduct **36**
C_1	47.1	47.2*	41.7	41.4*
α-ester C	36.5	38.1*	40.7	38.4*
C_5	32.3	33.0*	40.2	37.0*

*Positive assignment based on ^{13}C-^1H heteronuclear correlation experiment results.

Identification of 34.

The regiochemistry of cycloadduct **34** was proven by ^1H-^1H selective decoupling and ^{13}C-^1H heteronuclear correlation (HETCOR) experiments. The HETCOR experiments were used in conjunction with ^{13}C APT experiments in order to identify the geminal proton pairs. Table 5 summarises the chemical shifts and coupling patterns of the ^1H resonances. The assignments listed in this table are discussed in the following two paragraphs.

Based on the observed large geminal coupling constant of 18.5 Hz, the geminal protons at 1.89 and 2.15 ppm (solvent: C_6D_6) were assigned to the methylene group positioned α with respect to the ketone.[6] When each resonance in this geminal pair was

irradiated, decoupling of the resonances positioned at 1.21 and 1.44 ppm was observed. Therefore, the protons with the chemical shifts 1.21 and 1.44 ppm were assigned to methylene at the C_4 position.

Table 5: ^1H nmr assignments for compound **34** in C_6D_6 and $CDCl_3$.

Proton(s)	δ ppm (in C_6D_6)	δ ppm (in $CDCl_3$)	coupling pattern (J in Hz)
H_1	a	a	
H_3	1.89 2.15	2.29 2.58	dddd, 1.5, 4.1, 9.7, 18.4 dt, 18.6, 9.3
H_4	1.21 1.44	a	dddd, 2.3, 4.1, 9.4, 13.5 ddt, 7.7, 13.6, 9.8
H_5	2.57	3.01	broad quintet, 7 to 9 Hz
H_6	1.61 2.32	a	ddd, 5.5, 8.9, 12.4 dddd, 2.1, 5.5, 9.2, 12.5
H_7	a	a	
OCH_3	3.34	3.61	singlet

[a]Resonance not resolved due to overlap with other signals.

Irradiation of the resonance at 1.44 ppm resulted in decoupling the broad quintet (J=8 Hz) located at 2.57 ppm to form a broad quartet (J=8 Hz). The HETCOR results confirmed that the proton resonance at 2.57 ppm was correlated with the C_5 methine carbon. Irradiation of the resonance at 2.57 ppm resulted in decoupling the resonances at 1.61 and 2.32 ppm. The resonances at 1.61 and 2.32 ppm were identified, based on HETCOR experiments, as resonances resulting from a geminal pair of protons on a methylene centre. The selective decoupling of the resonance at 2.57 ppm resulted in the destruction of a splitting of 8.9 Hz for the resonance at 1.61 ppm and the destruction of

a splitting of 9.2 Hz for the resonance at 2.32 ppm. Since it was proven that the methine proton resonance (2.57 ppm) at the C_5 position of cycloadduct **34** was coupled to four methylene protons with large vicinal coupling constants, this adduct must have a head-to-head regiochemistry.

Identification of 35.

The regiochemistry of cycloadduct **35** was determined from the results of ^{1}H nmr selective decoupling experiments that were carried out in C_6D_6. Table 6 contains a summary of the ^{1}H nmr assignments for this compound. The ^{1}H nmr spectrum of **35** exhibited a complex pattern of resonances between 1.25 and 1.37 ppm which integrated for two protons. Decoupling this entire region resulted in the following: the doublet (J=18.8 Hz) of triplets (J=10.2 Hz) located at 2.03 ppm was collapsed to a doublet with J=18.8 Hz, and the broad quartet at 2.78 ppm was collapsed to sharp triplet with J=6.4 Hz. The ^{1}H nmr resonance at 2.03 ppm was assigned to one of the geminal protons positioned α to the ketone based on the observed large geminal coupling constant of approximately 19 Hz.[6] The other member of this geminal pair made up part of the complex pattern between 1.70 and 1.92 ppm; however, when the resonances between 1.25 and 1.37 ppm were decoupled this other geminal proton became visible as a doublet (J=18.8 Hz) of doublets (J=1.5 Hz) at 1.88 ppm. Since two splittings, each with J= 10.2 Hz, were collapsed at the 2.03 ppm resonance (C_3 geminal proton) when the complex pattern between 1.25 and 1.37 was decoupled, both geminal protons positioned at C_4 of compound **35** must be responsible for the complex pattern of resonances between 1.25 and 1.37 ppm. This means that the broad quartet at 2.78 ppm, which was coupled

with the two overlapping proton resonances located between 1.25 and 1.37 ppm, must be due to the methine proton at C_5. The decoupling experiments indicate that this methine proton is only coupled to two protons other than the methylene protons at C_4. This finding is consistent with the head-to-tail regiochemistry assigned to **35**.

Table 6: ^1H nmr assignments for compound **35** in C_6D_6 and $CDCl_3$.

Proton(s)	δ ppm (in C_6D_6)	δ ppm ($CDCl_3$)	coupling pattern (J in Hz)
H_1	a	a	
H_3	2.03 1.88	a 2.38	dt, 18.8, 10.2 dddd, 18.8, 9.0, 2.5, 1.5
H_4	1.25 to 1.37 complex	a	
H_5	2.78	3.23	broad quartet, 7 to 9 Hz
H_6	a	2.97	dt, 8.5, 7.0
H_7	a	a	
OCH_3	3.30	3.69	singlet

[a]Resonance not resolved due to overlap with other signals.

Identification of 36.

Table 7 contains a summary of ^1H nmr assignments for compound **36**. The resonance located at 1.88 ppm in the ^1H nmr spectrum (solvent: $CDCl_3$) of **36** was assigned to one of the geminal protons at the C_4 position. This assignment was based on the following two observations: first, this signal correlated with the highest field methylene ^{13}C nmr signal in HETCOR experiments, and secondly, the signal was coupled to only one methine proton which was located at 3.21 ppm. The methine resonance

located at 3.21 ppm was assigned to the C_5 proton. Decoupling experiments revealed that the C_5 methine proton was coupled in a vicinal fashion to two other methine protons, one being located at 2.76 ppm and the other at 3.46 ppm. This latter observation proves the head-to-tail regiochemistry of **36**. Unfortunately, the magnitudes of the coupling constants between each of the methine protons were not useful in determining the stereochemistry of **36**. Therefore, the stereochemistry of **36** was not assigned.

Table 7: ^{1}H nmr assignments for compound **36** in $CDCl_3$.

Proton(s)	δ ppm ($CDCl_3$)	coupling pattern (J in Hz)
H_1	2.76	dt, 9.3, 6.5; broad due to small long range coupling with H_3
H_3	a	
H_4	1.88 a	dddd, 14.2, 9.0, 5.1, 3.0
H_5	3.21	broad quartet, 7 to 9 Hz
H_6	3.46	dt, 8.3, 9.5
H_7	a	
OCH_3	3.69	singlet

[a]Resonance not resolved due to overlap with other signals.

2.3.2 Biradical trapping results

A solution of 2-cyclopentenone (0.200 mole/L) and methyl acrylate (1.00 mole/L) in toluene at -20°C was saturated with hydrogen selenide gas and then irradiated with Pyrex filtered light from a 450 watt Hanovia medium pressure mercury lamp. When the

reaction mixture was analyzed by coupled g.c./m.s. it was determined that the formation of cycloadducts was completely suppressed. Instead of the cycloadducts, five new products, **42**, **43**, **44**, **45**, and **46**, were separated from the reaction mixture and identified (see Scheme 15). These compounds were not formed in reaction mixtures containing 2-cyclopentenone, methyl acrylate, and hydrogen selenide that were not exposed to U.V. light. After determining the structures of these five compounds, we were able to conclude that the compounds were the reduction products resulting from an interaction between hydrogen selenide and each of the 1,4-biradicals generated in the cycloaddition reaction.

Scheme 15 shows the biradicals from which each of compounds **42**, **43**, **44**, **45**, and **46** were formed. In this scheme there are two pairs of biradicals which are diastereomers. Similarly, two pairs of trapped products were determined to be diastereomers. Each of the individual diastereomers in the pair was not separated and identified as an individual compound; rather, the diastereomers were isolated as a mixture and characterised accordingly. Thus, a mixture of **42** and **43** was characterised as a single fraction as was a mixture of **44** and **45**. Because the diastereomers were not individually characterised, the ratios of **42**:**43** and **44**:**45** were not determined. However, the combined yield of compounds **42** and **43** and the combined yield of compounds **44** and **45** were determined relative to the yield of trapped compound **46**. Therefore, the ratios of (**48**+**49**):(**50**+**51**):**52** for the relative rates of biradical formation were determined to be 5.0:45:50 respectively, based on the relative product yields of the trapped products measured at 6% conversion of 2-cyclopentenone. No product corresponding to **47**, resulting from the trapping of biradical **53**, was observed.

Scheme 15

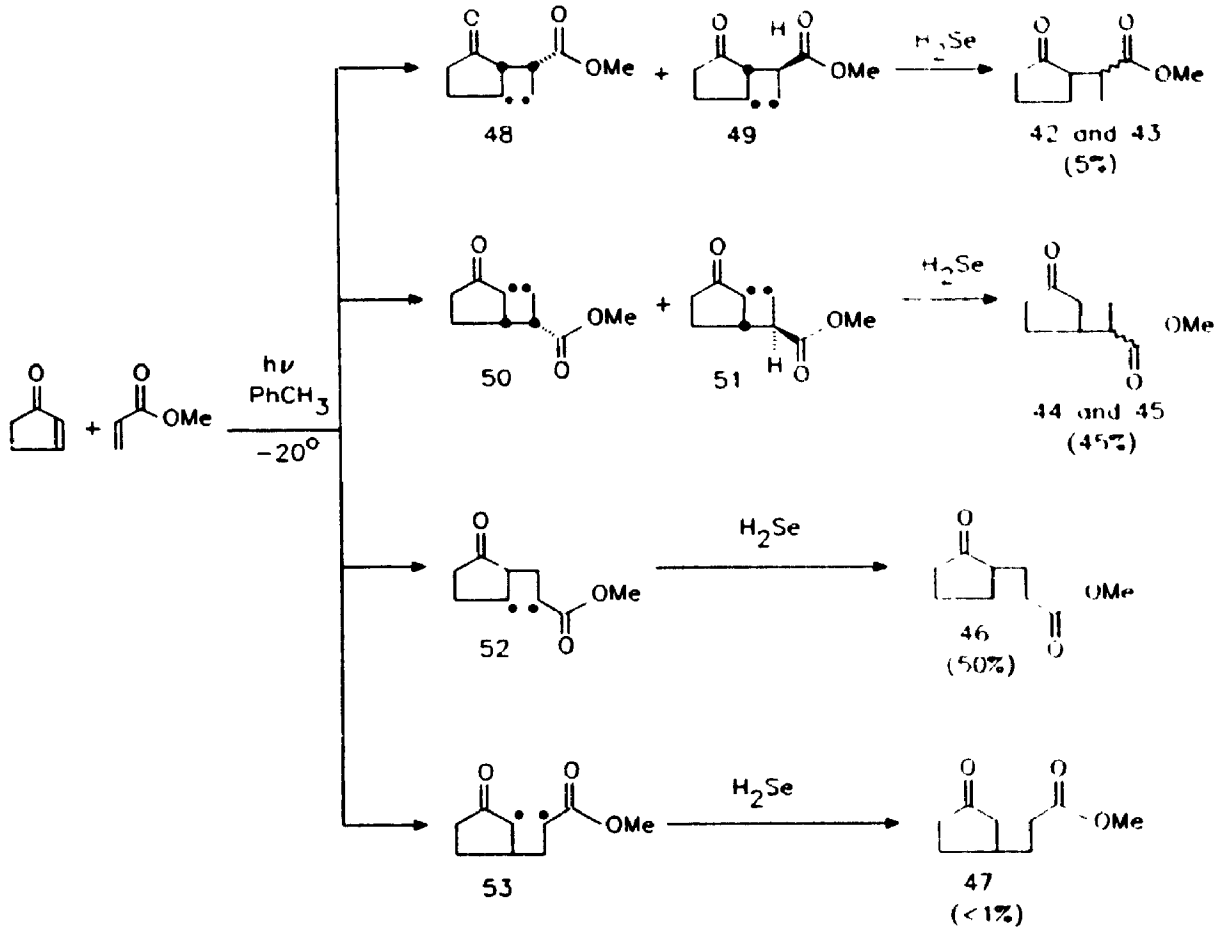

Small scale experiments in which varying amounts of hydrogen selenide were added to solutions of 2-cyclopentenone and methyl acrylate in toluene were also carried out. These solutions were irradiated with Pyrex filtered light from a 450 watt Hanovia medium pressure mercury lamp. The relative product yields of the trapped products and cycloadducts in each solution were determined by g.c. Figure 1 shows a plot of the ratio of the trapped product yield to the trapped product plus cycloadduct combined product yield (which also can be expressed as a ratio of quantum yields) versus the hydrogen selenide concentration. This plot does not extend in the vertical direction to 1.0 because

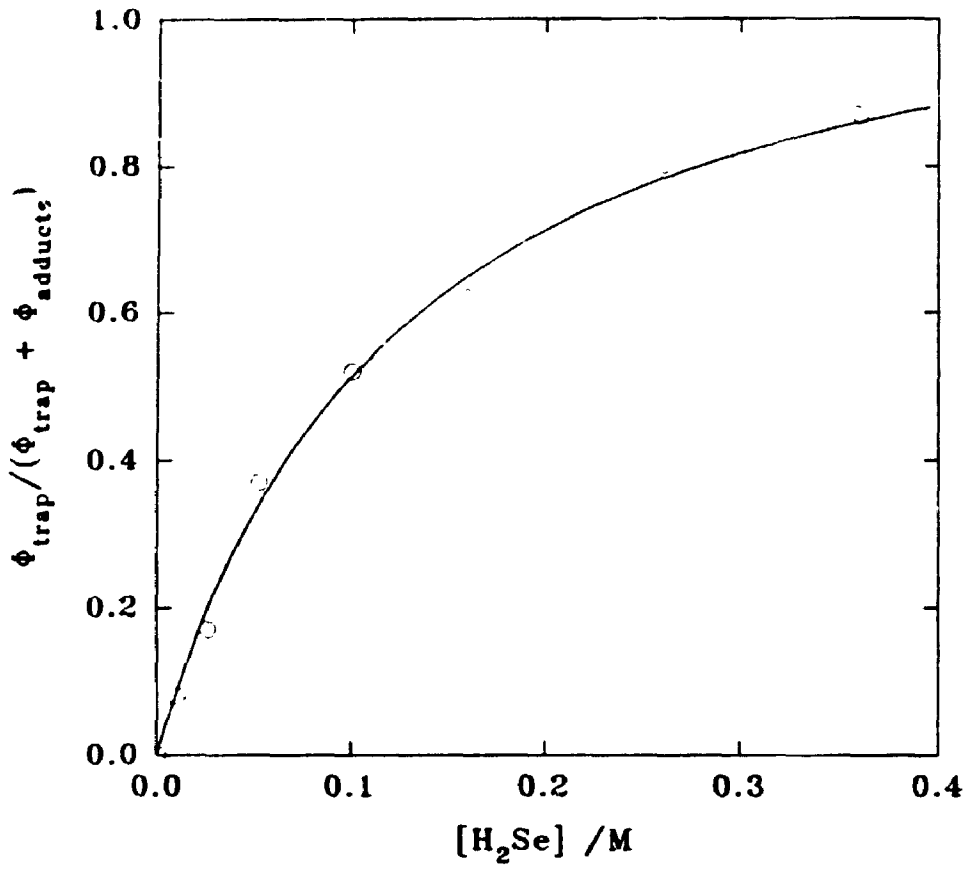

Figure 1: Dependence of the ratio of the yield of trapped products to the combined yield of trapped products plus cycloadducts on the hydrogen selenide concentration.

the saturation point concentration of H_2Se in toluene at 25°C is not high enough to effect complete trapping of the biradicals; however, according to the experiments described above, the concentration of H_2Se in toluene saturated with the gas at -20°C is high enough to completely suppress cycloadduct formation. Due to practical problems in handling saturated solutions of H_2Se in toluene at low temperatures, it was not possible to accurately determine the concentration of H_2Se in those mixtures in which complete biradical trapping was observed. The tendency of the plot shown in Figure 1 to approach a plateau at a trapped product yield to total product yield ratio of 1.0 does indicate that efficient trapping of the 1,4-biradicals begins to occurs at room temperature saturation

concentrations of the H_2Se in toluene.

Four additional products, other than those resulting from the reduction of 1,4-biradicals by hydrogen selenide, were isolated from the reaction mixture containing 2-cyclopentenone, methyl acrylate, and hydrogen selenide that was irradiated with U.V. light. These products were characterised as cyclopentanone, diastereomers **100** and **101**, and their isomer **102**. Cyclopentanone was not formed in reaction mixtures containing 2-cyclopentenone, methyl acrylate, and hydrogen selenide that were kept dark. Compounds **100**, **101**, and **102** were formed in the dark reaction mixtures; however, the rate of formation of these compounds in the dark reaction seemed to be considerably slower than the rate of formation in those reaction mixtures that were exposed to U.V. light.

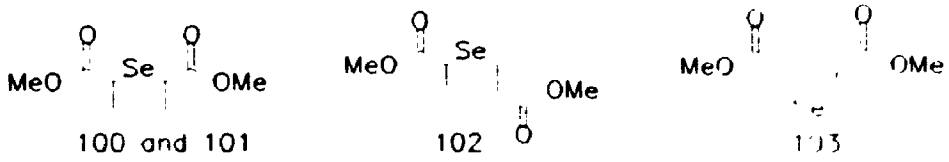

100 and 101 102 103

Compounds **100** and **101** are probably the result of addition of the hydrogen selenyl radical to the 2-position of methyl acrylate followed by radical addition of this intermediate to the 2-position of another methyl acrylate molecule. Compound **102** was probably formed by the addition of the methyl 2-hydroseleno-propanoate intermediate to the 3-position of methyl acrylate. In addition to compounds **100**, **101**, and **102**, the presence of a fourth compound exhibiting a parent molecular ion with an isotopic pattern consistent with the incorporation one selenium atom was also observed in coupled g.c./m.s. analyses of the trapping experiment reaction mixture. The m/e ratio of 254 observed for the parent molecular ion of this compound was the same as the m/e ratio

observed for the parent molecular ions observed in the mass spectra of **100**, **101**, and **102**. The compound apparently decomposed on silica gel since it was not isolated by column chromatography; however, we postulate that its structure is that of compound **103**.

We were concerned that the trapping of the biradicals generated in the cycloaddition reaction between 2-cyclopentenone and methyl acrylate might also yield products from processes other than simple reduction of each radical site by two successive hydrogen atom abstractions. It was hypothesised that the trapping of biradicals could also follow a course in which H_2Se intercepts a biradical and donates a hydrogen atom to one radical centre to form a radical pair which then undergoes a radical coupling reaction. The products resulting from this mechanism would have the same structure as the biradicals but with a hydrogen at one radical site and a selenol group at the other. Since alkyl selenols are quite reactive, trapped compounds such as these would easily be oxidized to diselenides following work-up and exposure to air, or react with excess methyl acrylate under the reaction conditions to yield in radical addition products. This is readily tested since all of the products resulting from secondary reactions involving trapped compounds that contain a selenol functionality would be reduced by Raney Nickel to give products identical to **42**, **43**, **44**, **45**, **46**, and **47**.[10]

When Raney Nickel reductions of the trapping reaction mixtures were carried out using a large excess of active Raney Nickel, no change in the ratio of the identified trapped products was observed; however, compounds **100**, **101**, **102**, and **103** were completely destroyed. Therefore, it was concluded that no selenol containing products representative of trapped biradicals were formed in the reactions involving 2-

cyclopentenone, methyl acrylate, and hydrogen selenide.

A mass balance based on 2-cyclopentenone was calculated for the trapping reaction. In a large scale reaction in which 2.132 g of 2-cyclopentenone was used as starting material, 2.123 g of 2-cyclopentenone was recovered in the form of trapped biradicals, cyclopentanone, and unreacted 2-cyclopentenone. This translates into a 99% recovery of the initial 2-cyclopentenone added to the reaction mixture. Based on this excellent recovery ratio, the conclusion can be made that all of the biradicals that were trapped by hydrogen selenide were recovered and isolated as the stable compounds described above. Therefore, a substantial degree of confidence can be placed in the method that was used for quantitatively trapping biradicals with hydrogen selenide.

Identification of 42 and 43.

The presence of two carbon-bonded CH_3 signals in the APT ^{13}C nmr spectrum of a mixture containing a 1:1 ratio of **42** and **43** indicates that these two compounds are products which result from a reaction between H_2Se and biradicals containing primary radical centres. Inspection of the other ^{13}C nmr signals reveals that there are seven pairs of resonances (excluding the carbonyl resonances) in which the two resonances of each pair have very similar chemical shifts and identical multiplicities (see Table 8). This observation supports the hypothesis that compounds **42** and **43** are diastereomers and not different structural isomers.

The resolved ^1H nmr resonances observed for the mixture of **42** and **43** are summarized in Table 9. Selective decoupling of the distinct resonances in the ^1H nmr spectrum of this mixture was useful in assigning these resonances. For example, it was

found that the doublet of quartets at 2.95 ppm was collapsed to a doublet by irradiating the methyl doublet at 1.07 ppm. Similarly, the doublet of quartets at 2.76 ppm was collapsed to a doublet by irradiating the other methyl doublet at 1.00 ppm. Therefore, the resonances at 2.95 and 2.76 ppm were assigned to be methine protons at the 2-position of the methyl propanoate appendage in **42** and **43**.

Table 8: ^{13}C nmr chemical shifts for the sp^3 carbon signals observed for the **42** plus **43** and **44** plus **45** mixtures (in $CDCl_3$).

multiplicity[a]	**42** and **43** mixture		**44** and **45** mixture	
	δ ppm	assignment[b]	δ ppm	assignment[b]
CH_3	51.7 (2 signals)	OCH_3	51.7 (2 signals)	OCH_3
CH	51.54, 51.47	α-keto	44.5, 44.4	β-keto
CH	39.1, 38.8	α-ester	40.3, 40.0	α-ester
CH_2	38.1 (2 signals)	α-keto	43.4, 42.7	γ-keto
CH_2	26.1, 25.9	β-keto	38.6, 38.5	α-keto
CH_2	20.6, 20.5	β-keto	27.7, 27.2	β-keto
CH_3	15.2, 13.7		15.9, 15.1	

[a]The multiplicity of each resonance was determined in APT ^{13}C nmr spectra.
[b]Position of the assigned carbon centre relative to either the ester or ketone functionality

Irradiation of the doublet of quartets located at 2.95 ppm resulted in collapsing a resonance located at 1.75 (multiplicity in coupled spectrum= ddd) to a doublet of doublets. This means that the resonance located at 1.75 ppm is coupled to no more than three protons in total. Therefore, the methine proton at 1.75 ppm must be in the 2-position of the cyclopentanone ring and not the 3- position. Similarly, irradiation of the resonance at 2.76 ppm resulted in collapsing the multiplet at 2.28 ppm to a doublet of

doublets of doublets. This means that the resonance located at 2.28 ppm is coupled to no more than four protons in total. One of these coupling constants is very small (1.2 Hz) and is probably due to long range coupling between the proton located at 2.28 ppm and one methylene protons on the opposite side of the carbonyl group. Therefore, the methine proton at 2.28 ppm must also be in the 2-position of the cyclopentanone ring and not the 3-position. These decoupling experiments confirm that compounds **42** and **43** have the 2-position of the methyl propanoate side-chain connected to the 2-position of the cyclopentanone ring.

Table 9: ^{1}H nmr assignments from the mixture containing **42** and **43** (in C_6D_6).

assignment[a]	δ (ppm)	coupling pattern (J in Hz)
methyl	1.085 1.237	d, 7.2 d, 7.3
α-ester methine	2.76 2.95	d. of quartets, 5.8, 7.1 d. of quartets, 4.4, 7.3
β-ester methine	1.75 2.28	ddd, 4.5, 8.2, 11.2 dddd, 1.2, 5.8, 8.1, 12.0

[a]Assignment relative to the ester functionality. It should be noted that for **42** and **43** the α-ester methine position is equivalent to the β-keto methine position. Similarly, the β-ester methine position is equivalent to the α-keto methine position.

Identification of 44 and 45.

The presence of two CH_3 signals at 15.9 and 15.7 ppm in the APT ^{13}C nmr spectrum of a mixture containing a 1:1 ratio of **44** and **45** indicates that these two compounds are products resulting from a reaction between H_2Se and biradicals containing primary radical centres. This conclusion was confirmed by the presence of two methyl

doublets at 1.20 and 1.17 ppm in the ^{1}H nmr spectrum of the mixture. Inspection of the other ^{13}C nmr signals reveals that there are seven pairs of resonances (excluding carbonyl resonances) in which the two resonances of each pair have very similar chemical shifts and identical multiplicities (see Table 8). The chemical shifts of the pairs of resonances in this mixture are not similar to the chemical shifts of resonances with similar multiplicities in the ^{13}C nmr spectrum of the mixture of **42** and **43**. The mass spectrum fragmentation patterns of **44** and **45** are identical; however, they are different from the common fragmentation pattern observed for **42** and **43**. These observations confirm that compounds **44** and **45** are a pair of diastereomers with different carbon-carbon connectivities than the diastereomers denoted as **42** and **43**.

Since the substitution of the cyclopentanone ring was determined to occur at the 2-position for both **42** and **43**, therefore the only remaining possibility for the structural assignment of **44** and **45** must include a cyclopentanone ring with the methyl 2-propanoate substituent at the 3-position. This substitution pattern is supported by the chemical shifts of the methine and methylene α-keto ^{13}C resonances listed in Table 8. For example, the lowest field pair of methine resonances (51.54 and 51.47 ppm) in the ^{13}C nmr spectrum obtained from the mixture of **42** and **43** are located 7 ppm further downfield relative to the lowest field pair of methine resonances (44.5 and 44.4) in the ^{13}C nmr spectrum obtained from the mixture of **44** and **45**. The other methine resonances identified in the ^{13}C nmr spectra of the two mixtures all have very similar chemical shifts. Therefore, the difference between the chemical shifts of the lowest field methine resonances in the mixture containing **42** and **43** relative to the mixture containing **44** and **45** is consistent with the regiochemistry assigned to these compounds.

Identification of 46.

The ^{13}C APT nmr spectrum of compound **46** was found to contain only one methine resonance and no methyl resonances. This indicates that compound **46** is the result of a hydrogen selenide reduction of a biradical which contained two secondary radical centres (i.e. either biradical **52** or **53**). Most of the resonances in the ^{1}H nmr spectrum of **46** overlapped each other; therefore, the regiochemistry of this compound could not be determined by relying on spectral data. The regiochemistry of the substitution pattern on the cyclopentanone ring was determined by preparing an authentic sample of **47** and comparing this compound with the product obtained from the trapping study. Compound **47** was prepared by acid catalysed methanolysis of bicyclo[3.3.0]octane-2,8-dione[11] (see Scheme 16). Since the spectral properties of **47** and the compound isolated from the trapping reaction mixture (**46**) were different, it was concluded that **46** must have a structure in which substitution occurs at the 2-position of the cyclopentanone ring.

Scheme 16

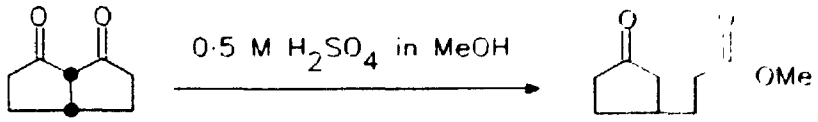

47

2.4 Discussion

The aim of the studies presented in this chapter was to investigate the mechanism of the photocycloaddition of 2-cyclopentenone to electron deficient alkenes and rationalise

the regiochemistry of the cycloadduct products that are formed in these reactions. As described in the introduction, the generalisation that had been accepted in the older literature states that alkenes bearing electron donating groups react with cyclic enones to give cycloadducts that are predominantly head-to-tail, while alkenes that bear electron withdrawing groups react to give cycloadducts that are predominantly head-to-head. The systems studied in the present investigation do not support this generalisation. The two examples of electron depleted alkenes that were studied, namely 1,1-difluoroethene and methyl acrylate, undergo photocycloaddition with 2-cyclopentenone to produce major cycloadducts that have a head-to-tail regiochemistry. In the case of the 1,1-difluoroethene addition to triplet 2-cyclopentenone the head-to-head:head-to-tail ratio was 1.0:2.8. In the case of the addition of methyl acrylate to the same enone the reaction proceeded almost non-regioselectively to give products with a head-to-head:head-to-tail ratio of 1.0:1.1. Therefore, the regiochemistry of the major products obtained from these reactions was found to be opposite to that predicted by the Corey-de Mayo exciplex theory.

Given the growing number of examples of electron deficient alkenes that do not obey the generalisation stated above, one begins to doubt the wide-spread applicability of this generalisation to all enone-alkene photocycloaddition. If one begins to doubt the applicability of the generalisation, then one must acquiesce to the fact that the mechanism proposed to try and explain the generalisation, that is the Corey-de Mayo mechanism, must also have questionable applicability and validity.

The intermediates that were proposed in the Corey-de Mayo mechanism in order to explain the regioselectivity of enone-alkene photocycloaddition reactions were the

orientated triplet excited state complexes or exciplexes. The main premise of the Corey-de Mayo mechanism was that relative orientation of the triplet enone and the polarised alkene in the exciplex dictates the regiochemical outcome of a photocycloaddition. If this were the case then the structures of the biradical intermediates, which are formed after the exciplexes on the reaction pathway, should reflect the regiochemistry of the major regioisomer to which they close. In summary, the Corey-de Mayo mechanism predicts that the biradicals which lead to production of the minor regioisomer have a slower rate of formation than the biradicals that lead to the production of the major regioisomer.

In the investigation described in this chapter, the Corey-de Mayo hypothesis was tested by determining the relative rates of formation and structures of all the biradicals that are formed during the photocycloaddition reaction of 2-cyclopentenone and methyl acrylate. This was accomplished by intercepting the biradicals generated in the photocycloaddition reaction using hydrogen selenide. This reagent successfully trapped all of the biradicals generated by the addition of methyl acrylate to triplet 2-cyclopentenone and gave stable products which revealed the structures of their biradical precursors. However, H_2Se did not trap the biradicals generated in the addition of 1,1-difluoroethene to triplet 2-cyclopentenone.

When 2-cyclopentenone was irradiated in the presence of methyl acrylate and hydrogen selenide, cycloadduct formation was quenched while products **42**, **43**, **44**, **45**, and **46** were formed in significant amounts. The ratio of **(42+43)**:**(44+45)**:**46** was 1.0:9.1:10.3. The complete suppression of all cycloadduct formation indicates that each triplet biradical responsible for cycloadduct formation was quantitatively trapped as a stable product before intersystem crossing to the singlet state surface followed by closure

Scheme 17

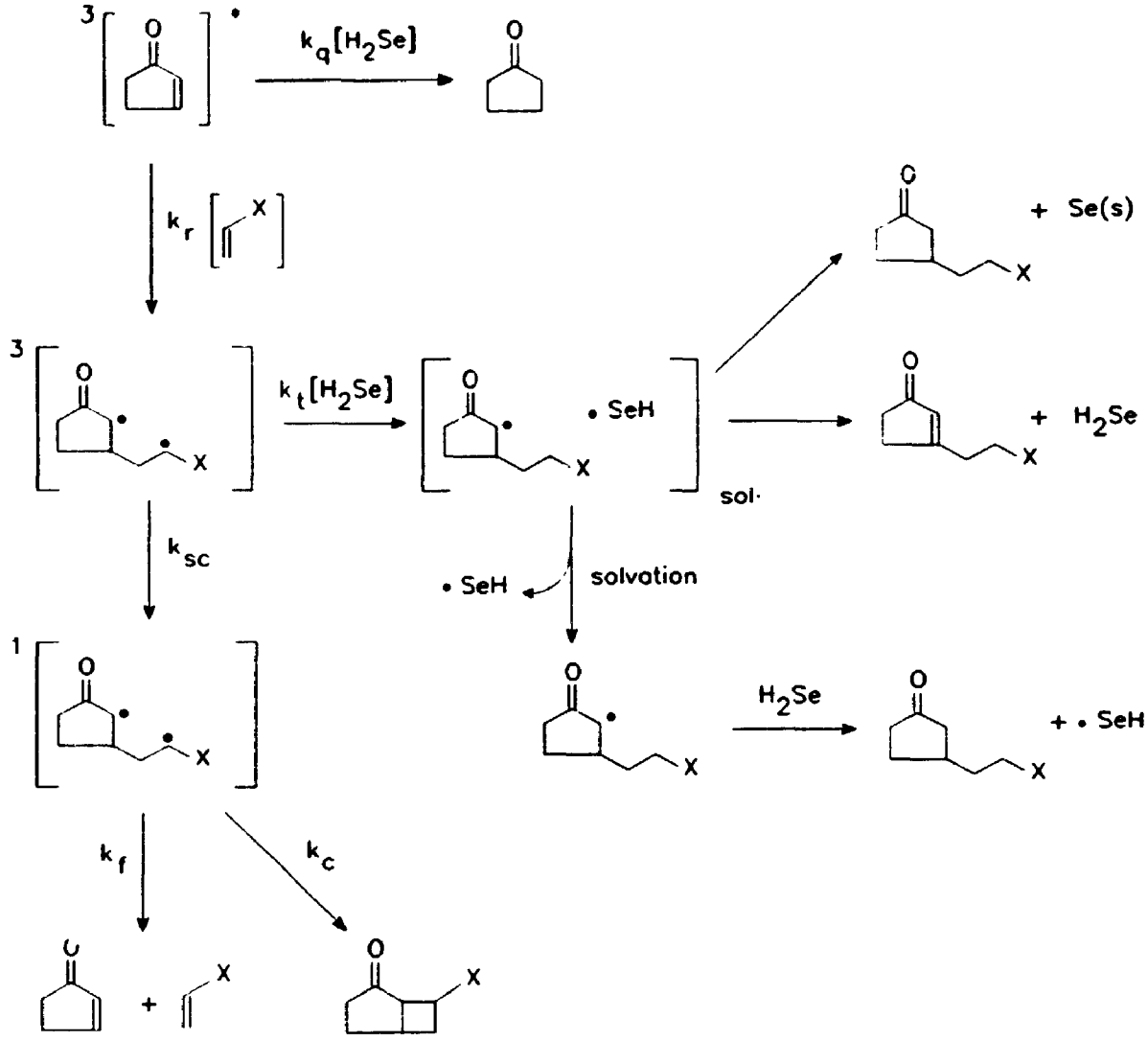

could occur. In terms of the rate constants defined in Scheme 17 this indicates that $k_T[H_2Se]$ is much larger than k_{sc}. Since closure and fragmentation are competing unimolecular processes for a common biradical intermediate, we can conclude that the absence of products resulting from one of the processes, namely the closure process, indicates that both processes are effectively quenched by the bimolecular reaction of H_2Se with the biradical intermediate.

The formation of compounds **42**, **43**, **44**, **45**, and **46** was a result of complete reduction of the corresponding biradicals. No products resulting from a disproportionation reaction between the hydrogen selenyl radical and partially reduced biradicals (see Scheme 17) were observed in the photoreaction mixtures containing 2-cyclopentenone, methyl acrylate and hydrogen selenide. This particular reaction pathway was, however, important in the experiments carried out by Hastings and Weedon[2] on the photocycloaddition of 2-cyclopentenone and ethyl vinyl ether.

The absence of **47** in the cycloaddition reactions that were carried out in the presence of H_2Se was confirmed by independently synthesising the compound and comparing its nmr spectra with all of the chromatographic fractions of the trapping reaction mixture that were collected. Based on the detection limit of the g.c./m.s. method, it was concluded that the relative yield of compound **47** was less than 1% of the combined yield of all other trapped products. So far, we have been unable to explain why the rate of formation of biradical **53** is so much slower than the rate of formation of biradical **52**.

The relative yields of the trapped products that were isolated when 2-cyclopentenone plus methyl acrylate photocycloaddition reaction was carried out in the presence of H_2Se indicate that 95% of all the biradicals formed could result in head-to-tail cycloadduct formation while only 5% of the biradicals could result in head-to-head cycloadduct formation. In the absence of H_2Se, a head-to-head:head-to-tail ratio of 1.0:1.1 was observed for the formation of cycloadducts. This product ratio clearly does not reflect the regioselective formation of the biradical precursors. In addition, the structures and rates of formation of the major biradicals are not in agreement with what

one might predict using the Corey-de Mayo exciplex theory. Therefore, it can be concluded that the regiochemical outcome of this reaction is controlled by the way each biradical partitions between closure and reversion to starting materials and not by the relative rates of formation of the biradicals.

It is interesting to compare the structures of the biradicals that Weedon and Hastings identified in the reaction between 2-cyclopentenone and ethyl vinyl ether (see Scheme 12) with the biradicals that are formed in the reaction between 2-cyclopentenone and methyl acrylate. Several differences between these two systems may be noted. For instance, biradicals containing primary radical centres are not formed in the 2-cyclopentenone plus ethyl vinyl ether photocycloaddition but they are formed in significant amounts in the photocycloaddition reaction between 2-cyclopentenone and methyl acrylate. The reason for this dissimilarity is not obvious. It is possible to make inconclusive generalisations about the relative stabilities of primary radicals versus secondary radicals adjacent to a carbonyl group, which may act as a destabilising or stabilising group depending on whether inductive or resonance effects dominate; however, such generalisations do not result in useful mechanistic insights. The most important conclusion that can be made about this particular difference between the two photocycloaddition reactions is that it is almost impossible to know which biradicals may be excluded from consideration, if any, when attempting to make mechanistic simplifications of the enone-alkene reaction.

Another difference between the trapped products resulting from the biradicals generated in the reaction of 2-cyclopentenone with ethyl vinyl ether and the trapped products resulting from the biradicals generated in the reaction of 2-cyclopentenone with

methyl acrylate was also noted. In the former reaction, a large proportion of the trapped products were the result of an in-cage disproportionation reaction, while in the latter reaction the no disproportionation products were observed. The reasons for this difference also remain unclear.

One of the by-products resulting from the trapping reactions that has not yet been discussed is cyclopentanone. This product was produced in large quantities in all of the photocycloaddition reactions that were carried out in the presence of H_2Se. Cyclopentanone is the result of direct quenching of the excited enone triplet by H_2Se (see Scheme 17). This quenching process results in the formation of a cyclopentanone radical with the radical centred on either the α or β carbon.[8] This cyclopentanone radical abstracts a second hydrogen atom from the hydroselenyl radical or another H_2Se molecule to form cyclopentanone. It is possible to envisage reaction pathways in which the cyclopentanone radical is not reduced by a second molecule of H_2Se and therefore proceeds to add to an alkene molecule. The radical resulting from this addition could then react with H_2Se to form products which would be identical to products representative of trapped biradicals. The presence of this pathway can be argued against with a high degree of certainty by comparing the rate of radical addition to double bonds with the rate of alkyl radical hydrogen abstraction from H_2Se. For example, the rate of alkyl radical addition to double bonds[12] (10^3 to 10^5 $Lmol^{-1}sec^{-1}$) is known to be at least three orders of magnitude less than the rate at which a carbon centred radical can abstract hydrogen from H_2Se ($> 10^8$ $Lmol^{-1}sec^{-1}$)[13]. Therefore, the trapped products observed

---

[8] It is important to note that the enolised form of this radical may also play a significant role.

in the photocycloaddition reactions that were carried out in the presence of H_2Se are not the result of addition of the cyclopentanone radical to the alkene followed by disproportionation of the intermediate or reduction of the intermediate by hydrogen abstraction. The trapped products must be the result of a reaction between the hydrogen donor and the biradicals.

The biradicals generated in the reaction between photochemically excited 2-cyclopentenone and 1,1-difluoroethene were not trapped by hydrogen selenide. When this photocycloaddition was carried out in the presence of hydrogen selenide no evidence of products resulting from the H_2Se induced reduction of the intermediate biradicals was detected. Addition of hydrogen selenide to this reaction resulted in a reduction in the rate of cycloadduct formation; however, this reduction was probably due to a quenching process of the enone triplet by hydrogen selenide and not interception of the biradicals by hydrogen selenide. The presence of cyclopentanone in the reactions carried out in the presence of H_2Se confirmed the fact that the enone triplet was being quenched and reduced. When the concentration of H_2Se was increased to the saturation point (in acetonitrile at 22°C), the cycloaddition reaction was completely suppressed. Thus, at high concentrations of H_2Se quenching of the enone triplet occurs much faster than the reaction of the enone triplet with 1,1-difluoroethene which was present at a concentration of 0.20 ± 0.05 mole/L. That is to say, the magnitude of the rate of triplet quenching by H_2Se, shown as $k_q[H_2Se]$ in Scheme 17, was larger than the magnitude of k_r[alkene] at high H_2Se concentrations. It was also concluded that the lifetimes of the biradicals present in the photocycloaddition reaction between 1,1-difluoroethene and 2-cyclopentenone are too short for H_2Se to be an effective trapping agent; the rate of

reaction between H_2Se and the biradicals must be slower than the rate at which the triplet biradicals intersystem cross to singlet biradicals. Therefore, the term $k_T[H_2Se]$ in Scheme 17 must be smaller than k_{ic} for the case were 1,1-difluoroethene is the alkene.

In general, the biradicals formed in photocycloaddition reactions involving cyclic enones and electron deficient alkenes appear to be more difficult to trap with H_2Se than the biradicals formed in photocycloadditions which involve electron rich alkenes. Weedon and Hastings[2] demonstrated that the biradicals generated in the photocycloaddition of 2-cyclopentenone and ethyl vinyl ether can be trapped completely at saturation concentration of H_2Se in benzene at room temperature (approx. 0.35 M); however, the biradicals generated in the photocycloaddition of 2-cyclopentenone and methyl acrylate were not completely trapped at this H_2Se concentration. For the photocycloaddition reaction involving methyl acrylate, the ratio of the relative yield of trapped products to the combined yield of trapped products plus cycloadducts was 0.9 at an H_2Se concentration of 0.35 M in benzene. The ratio indicates that less than 90% of the biradical were trapped in the 2-cyclopentenone plus methyl acrylate system at 0.35 M H_2Se. At the same concentration of H_2Se, 100% of the biradicals were trapped in the 2-cyclopentenone plus ethyl vinyl ether system. These comparative observations indicate that the lifetimes of the biradicals formed in photoaddition reactions involving 2-cyclopentenone and electron deficient alkenes are shorter than the lifetimes of the biradicals formed when an electron rich alkene is involved. Alternately, the observations could reflect significantly different rates of reaction between H_2Se and the biradicals formed in each of these two types of photocycloadditions.

2.5 Conclusions

The structures and relative rates of formation of all the biradicals generated in the photocycloaddition reaction between 2-cyclopentenone and methyl acrylate were determined by reacting each biradical quantitatively with H_2Se and trapping it as a stable product. The results of these experiments indicate that the regiochemistry of the intermediate biradicals generated in the photocycloaddition of 2-cyclopentenone to a representative electron deficient alkene does not reflect the regiochemistry of the cycloaddition products. In the case of 2-cyclopentenone reacting with methyl acrylate, a high degree of regioselectivity was observed in the formation of the biradicals; however, the regioselective formation of the biradicals did not translate into a regioselective formation of cycloadducts. The way in which each biradical partitions between closure and fragmentation has a much greater influence on the regiochemical outcome of the enone-alkene photocycloaddition reaction than the rate at which each biradical is formed. This conclusion disagrees with the Corey-de Mayo exciplex theory which predicts that the regiochemistry of the products resulting from an enone-alkene cycloaddition is determined by the nature and behaviour of intermediates existing prior to biradical formation.

The photoaddition of 1,1-difluoroethene to 2-cyclopentenone is another example of a enone cycloaddition reaction involving an electron deficient alkene that does not give the expected head-to-head cycloadduct as the major regioisomer. Attempts to trap the biradicals formed in this reaction with H_2Se were unsuccessful. The presence of H_2Se in photo-reaction mixtures of 2-cyclopentenone and 1,1-difluoroethene resulted in quenching the formation of cycloadducts by quenching the triplet enone. No products

were obtained from this trapping study that would indicate that biradicals were intercepted by H_2Se. The ineffectiveness of H_2Se at trapping the biradicals formed in the photocycloaddition of 2-cyclopentenone and 1,1-difluoroethene may be due to shorter lifetimes for the biradicals present in this system.

The results of the biradical trapping experiments involving the photoaddition of 2-cyclopentenone to methyl acrylate were quite different from the results of similar trapping experiments performed by Weedon and Hastings on the photocycloaddition reaction of 2-cyclopentenone and ethyl vinyl ether. In the photocycloaddition of 2-cyclopentenone to ethyl vinyl ether, the biradicals responsible for the formation of head-to-head cycloadducts were formed at the same rate as the biradicals responsible for the formation of head-to-tail cycloadducts; however, this photocycloaddition results in the regioselective formation of head-to-tail products as the major cycloadducts. In the photocycloaddition involving 2-cyclopentenone and methyl acrylate biradical formation occurred regioselectively, but product formation occurred non-regioselectively. The results described in this chapter together with the results published by Hastings and Weedon[2] demonstrate that fates of the biradicals control the product distribution observed in enone-alkene photocycloaddition reactions. Therefore, it can be concluded that any future studies which attempt to develop methods by which the regiochemistry of the enone-alkene photocycloaddition reactions can be controlled should focus on the structure and behaviour of the biradical intermediates and less on the relative dipole moments of the excited triplet enone and ground state alkene.

2.6 References

1. Corey, E. J.; Bass, J. D.; LeMahieu, R.; Mitra, R. B. *J. Am. Chem. Soc.* **1964**, *86*, 5570.

2. Hastings, D. J.; Weedon, A. C. *J. Am. Chem. Soc.* **1991**, *113*, 8525.

3. Wagner, P. J.; Bucheck, D. J. *J. Am. Chem. Soc.* **1969**, *91*, 5090.

4. Pretdch, E.; Seibl, J.; Simon, W.; Clerc, T. *Tables of Spectral Data for Structural Determination of Organic Compounds*, Springer-Verlag: Berlin Heidelberg, 1989.

5. (a) Emsley, J. W.; Phillips, L.; Wray, V. *Prog. Nucl. Magn. Reson. Spectrosc.* **1977**, *10*, 85. (b) Bovey, F. A. *Nuclear Magnetic Resonance Spectroscopy 2nd Ed.*, Academic Press Inc.: San Diego, 1988; pp 457-460. (c) Breitmaier, E.; Voelter, W. *^{13}C NMR Spectroscopy*, Verlag Chemie: Weinheim Bergstr., 1974; pp 133-137. (d) Grutzner, J. B.; Jautelat, M.; Dence, J. B.; Smith, R. A.; Roberts, J. D. *J. Am. Chem. Soc.* **1970**, *92*, 7107. (e) Maciel, G. E.; Dorn, H. C. *J. Am. Chem. Soc.* **1971**, *93*, 1268.

6. Geminal coupling constants of 17 to 19 Hz are typical for methylene protons located α with respect to a ketone in a five membered ring. See: Bovey, F. A. *Nuclear Magnetic Resonance Spectroscopy 2nd Ed.*, Academic Press Inc.: San Diego, 1988.

7. A methodology for performing quantitative ^{13}C nmr on complex mixtures has been developed by Shoolery. See: Shoolery, J.N. *Prog. Nucl. Magn. Reson. Spectrosc.* **1977**, *11*, 79.

8. (a) Berenjian, N.; de Mayo, P.; Sturgeon, M. E.; Sydnes, L. K.; Weedon, A. C.; *Can. J. Chem.* **1982**, *60*, 425. (b) Sydnes, L. K.; Meling, H. L. *Acta Chem. Scand.* **1987**, *b 41*, 660.

9. Tobe, Y.; Nakayama, A.; Kakiuchi, K.; Odaira, Y.; Kai, Y.; Kasai, N. *J. Org. Chem.* **1987**, *52*, 2639.

10. Raney Nickel cause the reductive deselenisation of selenols and selenoethers by addition of hydrogen. See: Nicolaou, K. C.; Lysenko, Z. *Tetrahedron Lett.* **1977**, 1257 and Sevrin, M.; Van Ende, D.; Krief, A. *Tetrahedron Lett.* **1976**, 2643.

11. Bicyclo[3.3.0]octa-2,8-dione was generously donated by Andreas Rudolph. The compound was prepared by Dr. Rudolph according to the method of Duthaler and

Maienfisch. See: Duthaler, R. O.; Maienfisch, P. *Helv. Chim. Acta* **1984**, *67*, 856.

12. (a) Denisov, E. T. *Liquid-Phase Reaction Rate Constants*, Plenum Press: New York, 1974; pp 351-362. (b) Kochi, J. K. *Free Radicals*, John Wiley & Sons: New York, 1973; pp 91-94.

13. The lifetime of the biradical generated in the Norrish Type II reaction of valerophenone has been determined by laser flash photolysis to be 100 ns (Hayashi, H.; Nagakura, S. *Bull. Chem. Soc. Jpn.* **1980**, *53*, 1519). Kambe, et al. (Kambe, N.; Masawaki, T.; Kondo, K.; Miyoshi, N.; Ogawa, A.; Sognoda, N. *Chem. Lett.* **1987**, 1907) were able to trap this 1,4-biradical with H_2Se and measure the trapped product to biradical closure product ratio. By using the biradical lifetime, Kambe et al. were able to assign a lower limit of 1.6×10^8 $Lmol^{-1}sec^{-1}$ to the rate of valerophenone biradical trapping by H_2Se.

CHAPTER 3

2+2 PHOTOCYCLOADDITION REACTIONS OF METHYL-SUBSTITUTED 2-CYCLOPENTENONES WITH 2-METHYLPROPENE

3.1 Introduction

Part of the work described in the previous chapter included an investigation of the photocycloaddition reaction of 2-cyclopentenone and methyl acrylate. In this investigation, hydrogen selenide was used to trap the 1,4-biradicals formed in the reaction as stable products. The structures of the trapped products were used to deduce the structures of the biradical intermediates. It was found that of all the biradicals identified, the fraction of biradicals in which one of the radical sites was located at the 2-position of the cyclopentanone ring was the same as the fraction in which one of the radical sites was located at the 3-position of the cyclopentanone ring. That is to say, no preference was observed for bonding to either the α- or the β-position of 2-cyclopentenone upon biradical formation. Hastings and Weedon also demonstrated that in the photocycloaddition reactions of 2-cyclopentenone with ethyl vinyl ether and cyclopentene α- and β-bonded biradicals were formed in equal amounts.[1] Therefore, these studies indicate that possible resonance effects of the carbonyl group do not enhance the rate of formation of biradicals resulting from initial bond formation at the β-position of the enone.

The original goal of the studies described in this chapter was to determine if alkyl-substitution at the 2- or 3-position of 2-cyclopentenone could be used to effect

changes in the relative rates of formation of regioisomeric biradicals resulting from enone-alkene photocycloaddition reactions. In particular, the photocycloaddition reactions between 2-methylpropene and each of 2-cyclopentenone, 2-methyl-2-cyclopentenone, and 3-methyl-2-cyclopentenone were studied. Hydrogen selenide was used to trap the biradicals formed in each of these photocycloaddition reactions as stable products. The relative yields and structures of each of the stable products observed in the trapping studies were used to deduce information about the biradical intermediates present in each photocycloaddition.

It was hypothesised that alkyl-substitution at the 2- or 3-position of 2-cyclopentenone might encourage formation of biradicals containing tertiary radical sites on the cyclopentanone ring as opposed to secondary radical containing biradicals. This argument was based on the generalisation that tertiary alkyl radicals are more stable than secondary alkyl radicals. Alternatively, it was reasoned that steric hindrance by an α- or β-methyl substituent might discourage biradical formation resulting from bonding to the substituted site. It was also hypothesised that alkyl substitution at the 2- or 3-positions of 2-cyclopentenone might have dramatic effects on the relative efficiencies of the closure and reversion pathways available to each biradical. Therefore, the quantum yield of cycloadduct formation was measured for each reaction at various concentrations of 2-methylpropene. These quantum yield measurements were used in conjunction with the relative rates of biradical formation determined in the trapping studies to calculate the relative fraction of each biradical population which closes to form cycloadducts.

3.2 Results of the photocycloadditions.

3.2.1 Photocycloaddition of 2-methylpropene and 2-cyclopentenone.

The photochemical cycloaddition of 2-methylpropene and cyclopentenone has been described in the literature.[2] The regiochemistry of each of the 2+2 cycloadducts obtained from this reaction were previously assigned based on the chemical shift differences of the two methyl groups in each adduct.[2a] In the work described in this thesis, the reaction was repeated in order to characterise the two major 2+2 cycloadducts more completely and to characterise any other minor products resulting from the reaction that were not previously isolated.

The irradiation of a benzene solution of cyclopentenone and 2-methylpropene with Pyrex filtered light from a medium pressure mercury lamp resulted in the formation of products **54**, **55**, **56**, and **57** in the ratios 2.8%:6[illegible]%:18.6%:9.1% (see Scheme 18). These ratios were determined at 5% conversion of cyclopentenone. Compounds **55** and **56** were isolated in 90% and 85% purity respectively after column and thin layer chromatography on silica gel. They were confirmed to be 2+2 cycloadducts based on the positions and multiplicities of the signals in the ^{13}C nmr spectra of these compounds. Compounds **54** and **57** were isolated in mixtures contaminated by **55** and **56**. The spectral properties of these compounds were deduced by comparing the spectra obtained from the mixtures with the spectra obtained for relatively pure **55** and **56**. Compounds **54** and **57** were identified as biradical disproportionation products since these two compounds exhibited ^{1}H and ^{13}C nmr spectra that contained resonances indicative of a double bond. Previous descriptions of this reaction in the literature made no mention of **54** and **57** as minor products.[2]

Scheme 18

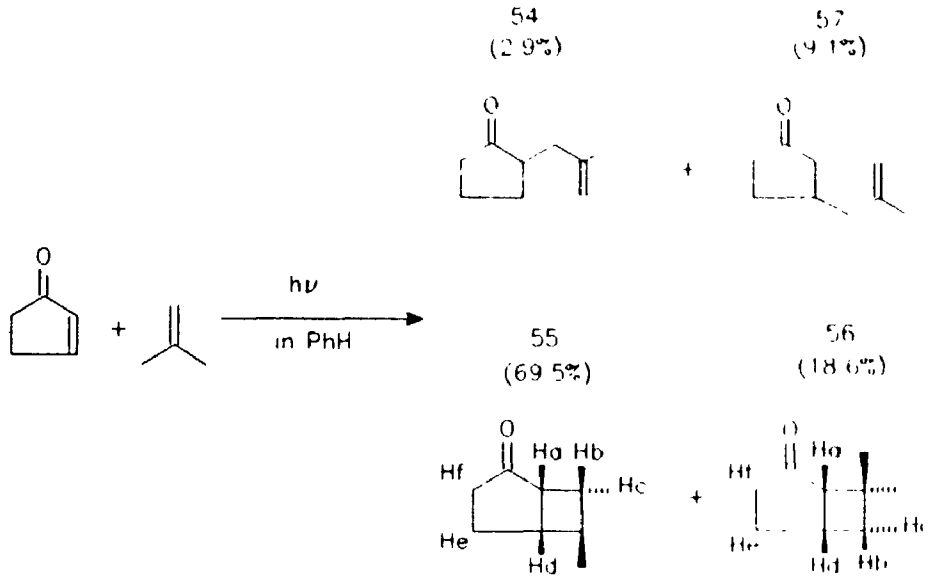

The regiochemistries of compounds **55** and **56** were determined by inspection of the ^{1}H nmr spectra of the two cycloadducts. In order to disperse some of the overlapping resonances observed in the ^{1}H nmr spectra of these two cycloadducts, shift reagent studies were carried out in which the lanthanide metal complex tris(1,1,1,2,2,3,3-heptafluoro-7,7-dimethyl-4,6-octanedionato) europium(III) (commonly referred to as Eu(fod)$_3$) was added to solutions of the adducts. The Eu(fod)$_3$ species complexes with molecules that possess basic functional groups such as the carbonyl groups in compounds **55** and **56**. When complexation occurs, the lanthanide ion induces resonance shifts that exhibit a geometric dependence on the mode of complexation. The use of shift reagents in identifying enone plus alkene photocycloadducts will be discussed in more detail in Chapter 4. The important generalisation to note before discussing the structural

elucidation of **55** and **56** is that, in many cases, the presence of a lanthanide shift reagent results in the dispersion of overlapping ^1H nmr signals.

The clearly resolved resonances observed in the ^1H nmr spectrum of **55**, which was acquired in the absence of $Eu(fod)_3$, are listed in Table 10. The doublet of doublets at 1.68 ppm listed in the table was coupled to the resonance at 2.09 ppm with a coupling constant of 12.5 Hz. This was proven in ^1H-^1H COSY experiments as well as in ^1H-^1H selective decoupling experiments. When $Eu(fod)_3$ was added to a $CDCl_3$ solution of **55**, the resulting ^1H nmr spectrum also exhibited a doublet of quartets (J=2 Hz and J=6 Hz respectively) that was not resolved in the unshifted spectrum due to other overlapping signals. Heteronuclear correlation (HETCOR) ^{13}C-^1H experiments as well as APT experiments were performed on solutions containing **55** and $Eu(fod)_3$ in order to determine which ^1H nmr signals were methine protons and which were methylene protons. Based on the results of these experiments, the doublet of quartets was assigned to a methine proton and the resonances observed at 1 68 and 2.09 ppm in the unshifted spectrum were assigned to a geminal pair of methylene protons. The methine proton which was observed a doublet of quartets in the ^1H nmr spectrum of **55** was assigned as Hd. This assignment is made using the results of the ^1H-^1H selective decoupling experiments described below.

In a cycloadduct derived from the photoaddition of 2-cyclopentenone and 2-methylpropene, only the Hb or Hc proton could appear as a simple doublet of doublets with a geminal coupling constant of 12.5 Hz. The rest of the methylene protons (i.e. He and Hf) would all exhibit multiplicities more complex than a doublet of doublets due to the fact that these protons have more than one vicinal proton with which to couple. In

addition, the α-keto methylene protons would also exhibit a much larger geminal coupling constant.[3] Therefore, the resonance at 1.68 and 2.09 ppm in the unshifted ^1H nmr spectrum were assigned to the Hc and Hb protons.

Table 10: ^1H nmr resonances observed for compound **55** in $CDCl_3$.

Protons[a]	δ (ppm)	coupling pattern (J in Hz)
methyl	0.99	singlet
methyl	1.15	singlet
Hc	1.68	dd, 12.5, 5.9
Hb	2.09	ddd, 12.5, 10.7, 1.8

[a]Only the clearly resolved and non-overlapping resonances are listed.

The selective ^1H-^1H decoupling experiments carried on **55** in the presence of the shift reagent revealed that the Hd proton was not coupled to the geminal proton assigned as Hc; however, Hd was coupled to Hb with a small coupling constant of approximately 2 Hz. Based on this evidence, it was concluded that the Hd proton identified in the ^1H nmr spectrum acquired in the presence of $Eu(fod)_3$ must be located diagonally across the cyclobutane ring with respect to the methylene protons Hc and Hb. The small coupling observed between Hd and Hb was assigned to a diagonal cross-ring coupling for the cyclobutane system. Therefore, the only regiochemical assignment for **55** which is consistent with the results of the selective decoupling experiments is the head-to-tail regiochemistry.

The ^{1}H nmr spectrum and ^{13}C APT results obtained for **56** indicated that this compound was also a cyclobutane ring-containing photoaddition product. Since a head-to-tail regiochemistry was assigned to **55**, the regiochemistry of **56** must be head-to-head. The ^{1}H nmr spectra of **56** which were obtained in the presence and absence of Eu(fod)$_3$ prove this assignment of regiochemistry to be correct.

The non-overlapped signals in the ^{1}H spectrum of **56** that were observed in the absence of Eu(fod)$_3$ are listed in Table 11. The results of a ^{13}C-^{1}H HETCOR experiment demonstrated a correlation between the 2.94 ppm ^{1}H resonance and a methine ^{13}C resonance at 29.9 ppm. The only other methine ^{13}C signal was positioned much further downfield at 55.4 ppm and was therefore assigned to an α-keto methine carbon. Based on the results of the ^{13}C-^{1}H heteronuclear correlation experiment, the 2.94 ppm quintet was assigned to Hd. The fact a quintet was observed for Hd indicates that this resonance must be coupled to four vicinal protons. Selective decoupling experiments indicated the doublet of doublets at 1.69 ppm was one of the vicinal protons coupled to Hd; however, this resonance was not coupled to the multiplet at 2.50 ppm. Based on the large geminal coupling constant of 19 Hz observed at the 2.50 ppm resonance, this signal was assigned to one of the α-keto methylene protons.[3] Therefore, the doublet of doublets at 1.69 ppm can be assigned to either the Hc or Hb proton but not the He protons. The only structural assignment for **56** which is consistent with Hd coupling to Hb or Hc as well as 3 other vicinal protons is one in which the relative regiochemical orientation of the geminal dimethyl groups and the carbonyl group is head-to-head.

Table 11: ^{1}H nmr resonances observed for compound **56** in $CDCl_3$.

Protons*	δ (ppm)	coupling pattern (J in Hz)
methyl	0.89	singlet
methyl	1.21	singlet
Hb or Hc	1.69	dd, 12.3, 7.3
one of Hf	2.50	ddd, 19, 9.2, 12.2
Hd	2.94	quintet, 7.5

*Only the clearly resolved and non-overlapping resonances are listed.

Compounds **54** and **57** were determined to be products resulting from the disproportionation of two different 1,4-biradicals. Their mass spectra showed them to be isomeric with **55** and **56** while their ^{1}H and ^{13}C nmr spectra possessed the appropriate spectral features for a double bond, unsubstituted at one end, disubstituted at the other end, and possessing allylic methyl protons. For example, the ^{1}H nmr spectrum of compound **54** exhibited a multiplet with very small coupling constants at 1.65 ppm which integrated for 3 protons. This signal was assigned to an allylic methyl group. The ^{1}H nmr spectrum of compound **57** also exhibited a signal indicative of an allylic methyl group which appeared at 1.64 ppm. The ^{13}C nmr spectrum of **54** contained vinylic signals at 143.4 and 111.6 ppm with multiplicities representative of carbons bonded to none and two protons, respectively. Similarly, the ^{13}C nmr spectrum of **57** contained vinylic signals at 143.5 and 111.6 ppm with the same multiplicities as the 143.4 and 111.6 ppm resonances in the spectrum of **54**. Therefore, these spectral data allowed the determination of the position of the alkene functionality in the disproportionation products.

The regiochemistry of **54** and **57** was determined by examining the chemical shift differences between the methine resonances in the ^{13}C nmr spectra of the two compounds. Table 12 contains a summary of the chemical shifts and multiplicities of the sp^3 ^{13}C nmr resonances for **54** and **57**. The data in the table demonstrate that the methine carbon in **54** is located approximately 12 ppm further downfield relative to the position of the methine carbon in **57**. This observation is consistent with a regiochemical assignment for **54** in which the cyclopentanone ring is substituted in the 2-position and not the 3-position. Similarly, the data is also consistent with a regiochemical assignmert for **57** which includes a 3-substituted cyclopentanone. Therefore, the structures of **54** and **57** were completely determined.

Table 12: Chemical shifts and multiplicities of the sp^3 ^{13}C nmr signals for compounds **54** and **57** in $CDCl_3$.

Multiplicity	Compound **54**		Compound **57**	
	δ (ppm)	assignment	δ (ppm)	assignment
CH	47.3	α-keto	34.7	β-keto
CH_2	38.0[a]	α-keto	44.8	α-keto
CH_2	38.0[a]	β-keto	43.7	α-keto
CH_2	29 3		38.0	
CH_2	20.5		29.0	
CH_3	21.9	allylic methyl	22.2	allylic methyl

[a]Isochronous signals.

3.2.2 Photocycloaddition of 2-methylpropene and 2-methyl-2-cyclopentenone.

The irradiation of a benzene solution of 2-methylcyclopentenone and 2-methylpropene with Pyrex filtered light from a medium pressure mercury lamp resulted in the formation of products **58** to **65** inclusively (see Scheme 19). Products **58** and **59** were only present at high conversion of the enone. At 3% conversion of the enone starting material the ratios of products **60**:**61**:**62**:**63**:**64**:**65** were determined by g.c. to be 7.3:46:5.2:28.9:3.4:9.3, with no trace of compounds **58** and **59** detected.

Compounds **58** and **59** were proven to be secondary photochemical products resulting from irradiation of the cycloadducts formed in the photocycloaddition of 2-methyl-2-cyclopentenone and 2-methylpropene. In the photocycloaddition, the increase in concentration of products **58** and **59** parallelled the decrease in concentration of products **60** and **61** relative to the other three products.

In a separate experiment a benzene solution containing **60**, **61**, and **62** in a 3:29:1 ratio was irradiated with Pyrex filtered light from a 400 W Hanovia medium pressure mercury lamp to result in the formation of a 1.4:15:1.4:16:1.0 mixture of **58**, **59**, **60**, **61**, and **62**, respectively. An inert internal standard was also present in the reaction mixture. The ratio of the total g.c. peak area of the products to g.c. peak area of the internal standard, before and after the reaction, was used to establish a mass balance. This mass balance indicated that compounds **58** and **59** were the only photolysis products. Therefore, it was concluded that photolysis of **61** results in the formation of **59**. The results also suggest that photolysis of **60** results in the formation of **58**; however, this cannot be confirmed absolutely since a more enriched sample of **60** was not isolated.

Compounds **58** and **59** were isolated as a 1:7 mixture from the 2-methyl-2-

each of **58** and **59** was confirmed by the chemical shifts and multiplicities of the vinylic signals in the compounds' ^{13}C nmr spectra. Therefore, it was concluded that **58** and **59** were formed as a result of the homolytic α-cleavage of ketones **60** and **61** followed by disproportionation of the intermediate biradical (see Scheme 19).

Compounds **60**, **61** and **62** were isolated as mixtures by chromatography. In all of the chromatographic fractions containing these products, compound **61** was the major compound. The spectral data for **61** were obtained from a highly enriched mixture consisting of **60**, **61** and **62** in a 3:29:1 ratio. The spectral data for compounds **61** and **62** were obtained by analyzing several different mixtures, each of which contained a different ratio of the three products. An accurate assignment of the ^{13}C nmr signals for the two minor products was accomplished by performing quantitative nmr spectroscopy on each of the mixtures.

Compounds **60** and **61** were determined to be 2+2 cycloadducts based on the chemical shifts and multiplicities of the signals observed in the ^{13}C nmr spectrum of each compound. The regiochemistry of **61** was determined by inspection of the compound's ^{1}H nmr spectrum. An obvious AB pattern was observed at 1.71 ppm with $J_{AB}=12.5$ Hz and $\Delta\delta_{AB}=0.071$ ppm. The relatively large coupling constant observed in this pattern was indicative of a geminal coupling. The integrity of the AB pattern was confirmed by the addition of the lanthanide shift reagent $Eu(fod)_3$ to a $CDCl_3$ solution of **61**. In the presence of the shift reagent, the AB pattern became an AX pattern as the Hc proton moved downfield relative to the Hb proton. Of both the regioisomers of the possible cycloadduct product, the only two geminal protons that have no vicinal neighbours are the Hb and Hc protons of the head-to-tail regioisomer. Therefore, the major compound

Scheme 19

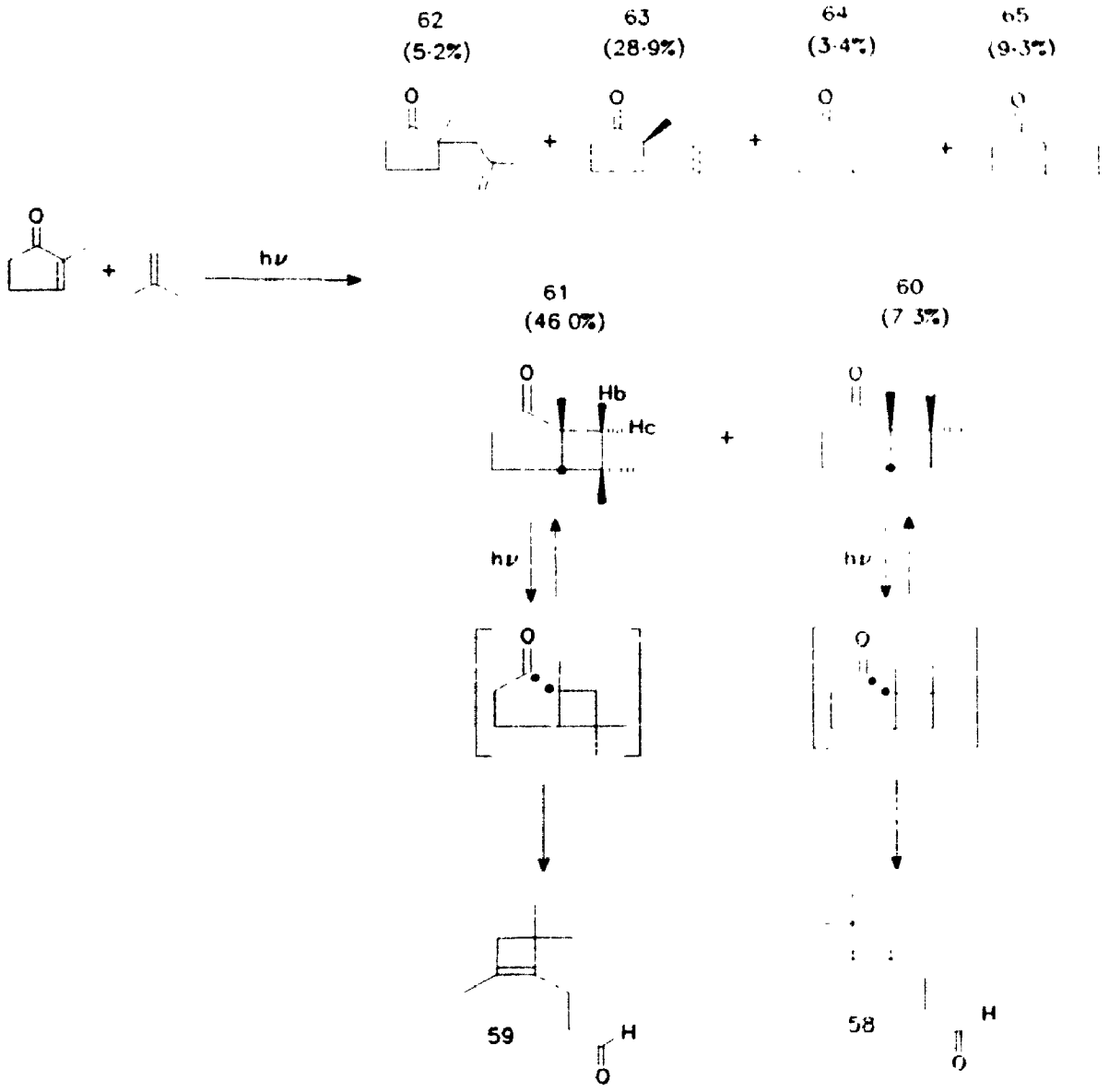

cyclopentenone plus 2-methylpropene reaction mixture by chromatography and their structures were determined by ^{1}H and ^{13}C nmr spectroscopy. The ^{1}H nmr spectra for **58** and **59** both contained triplets at very low field (9.74 and 9.75 ppm respectively) which were assigned to aldehydic protons. The presence of the cyclobutene functionality in

each of **58** and **59** was confirmed by the chemical shifts and multiplicities of the vinylic signals in the compounds' ^{13}C nmr spectra. Therefore, it was concluded that **58** and **59** were formed as a result of the homolytic α-cleavage of ketones **60** and **61** followed by disproportionation of the intermediate biradical (see Scheme 19).

Compounds **60**, **61** and **62** were isolated as mixtures by chromatography. In all of the chromatographic fractions containing these products, compound **61** was the major compound. The spectral data for **61** were obtained from a highly enriched mixture consisting of **60**, **61** and **62** in a 3:29:1 ratio. The spectral data for compounds **61** and **62** were obtained by analyzing several different mixtures, each of which contained a different ratio of the three products. An accurate assignment of the ^{13}C nmr signals for the two minor products was accomplished by performing quantitative nmr spectroscopy on each of the mixtures.

Compounds **60** and **61** were determined to be 2+2 cycloadducts based on the chemical shifts and multiplicities of the signals observed in the ^{13}C nmr spectrum of each compound. The regiochemistry of **61** was determined by inspection of the compound's ^{1}H nmr spectrum. An obvious AB pattern was observed at 1.71 ppm with $J_{AB}=12.5$ Hz and $\Delta\delta_{AB}=0.071$ ppm. The relatively large coupling constant observed in this pattern was indicative of a geminal coupling. The integrity of the AB pattern was confirmed by the addition of the lanthanide shift reagent $Eu(fod)_3$ to a $CDCl_3$ solution of **61**. In the presence of the shift reagent, the AB pattern became an AX pattern as the Hc proton moved downfield relative to the Hb proton. Of both the regioisomers of the possible cycloadduct product, the only two geminal protons that have no vicinal neighbours are the Hb and Hc protons of the head-to-tail regioisomer. Therefore, the major compound

61 was identified as the head-to-tail regioisomer. The regiochemistry of compound **60** was determined to be head-to-head by elimination.

Compound **63** was isolated relatively pure while compounds **64** and **65** were isolated as a mixture. The ^{1}H and ^{13}C nmr spectra of **63** and **65** were assigned by analyzing mixtures containing different ratios of **63** and **65**. Compounds **62**, **63**, **64**, and **65** were all determined to be alkene containing products resulting from the disproportionation of various 1,4-biradicals. The ^{13}C nmr spectrum of each of these compounds contained two vinylic signals; one exhibited a multiplicity representative of a CH_2 carbon and the other exhibited a multiplicity representative of a fully substituted carbon. The position of the double bond in **62** and **63** was confirmed by the presence of an allylic methyl proton resonance in the ^{1}H nmr spectrum of each compound at 1.64 and 1.61 ppm respectively. The regiochemistry of **62** and **63** was easily determined from the multiplicity of the high-field methyl resonance in the ^{1}H nmr spectrum of each compound as well as from the number of methine carbon resonances in the ^{13}C nmr spectrum of each compound.

The stereochemistry of **63** was assigned as *trans* about the cyclopentanone ring. This conclusion was based on two observations: first, it is geometrically impossible for the *cis* isomer (**66**) to form from an intramolecular disproportionation of the biradical precursor; and secondly, compound **63** was the preferred stereoisomer (relative to **66**) under epimerisation conditions in strong base. It is important to note that none of **66** was formed in the photo-reaction between excited 2-methylcyclopentenone and 2-methylpropene.

The presence of an α,β-unsaturated ketone functionality in **64** and **65** was

confirmed by the fact that the carbonyl carbon chemical shifts for these compounds were at approximately 12 ppm higher field than the chemical shifts for the carbonyl carbons in compounds **60** to **63** inclusively. The presence of the t-butyl group in compound **64** was confirmed by the presence of a sharp singlet at 0.91 ppm integrating for 9 protons in the ^{1}H nmr spectrum of this compound. In addition to this evidence, the chemical shifts and multiplicities of the signals observed in the ^{13}C nmr APT spectrum of **64** also confirmed the presence of the t-butyl group. Compound **65**, on the other hand, exhibited two diastereotopic methyl doublets in its ^{1}H nmr spectrum. The presence of these signals confirmed that compound **65** contained the 1-(2-methylpropyl) sub-unit. The multiplicity and chemical shifts of the ^{13}C nmr signals also confirmed the identity of this compound.

The structures of compounds **63** and **65** were confirmed by the results of hydrogenation and epimerisation studies carried out on the compounds and their derivatives. Scheme 20 illustrates the results of these studies.

The hydrogenation of **65** had to be carried out on mixtures containing **65** and **64** since it was not possible to isolate **65** in pure form. Hydrogenation of a 1:2.5 mixture of **64** and **65** resulted in the formation of a 2.8:1.0:1.4:3.0 mixture (g.c. ratio) of **67**, **69**, **70**, and **68** respectively. The ratio of **69**+**70** to **67**+**68** was determined to be 1:2.4 by g.c. Epimerisation of this mixture of four compounds resulted in a mixture containing **67**, **69**, and **68** in a 11:5.1:1 ratio. The ratio of **69** to **67**+**68** in the epimerised mixture was determined to be 1:2.4. In a separate experiment hydrogenation of a 2:1 mixture of **64** and **65** resulted in the formation of a 1:1.9:2.3:1.2 mixture of **67**, **69**, **70**, and **68** respectively. Epimerisation of this mixture resulted in a mixture containing **67**, **69**, and **68** in a 10:18:1 ratio. The identity of **67** and **68** was confirmed by comparing the g.c.

Scheme 20

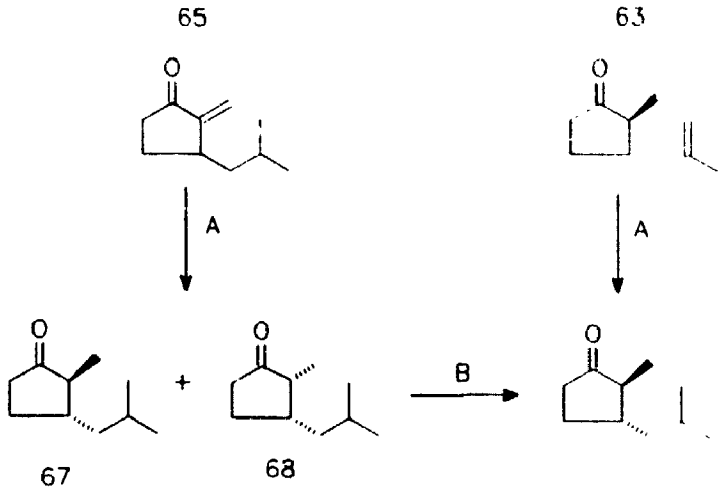

A= H_2, 10% Pd on carbon, in EtOH

B= NaOMe in MeOH

retention times and g.c.-m.s. results obtained for these compounds with those obtained from the hydrogenation and epimerisation products of compound **63**. Therefore, the results of these experiments indicate that hydrogenation of **65** results in the formation of a 1:1 mixture of **67** and **68** which can be epimerised under basic conditions to a 10:1 mixture.

The products resulting from the palladium metal catalysed hydrogenation of compound **64** can be deduced from the results described in the previous paragraph. Scheme 21 illustrates that compound **64** hydrogenates to a 1:1.3 mixture of **69** and **70**. Treatment of this mixture with a solution of sodium methoxide in methanol causes the ratio of the components of the mixture to change so that the resulting mixture is comprised almost entirely of compound **69**. Therefore, compound **69** was assigned a

Scheme 21

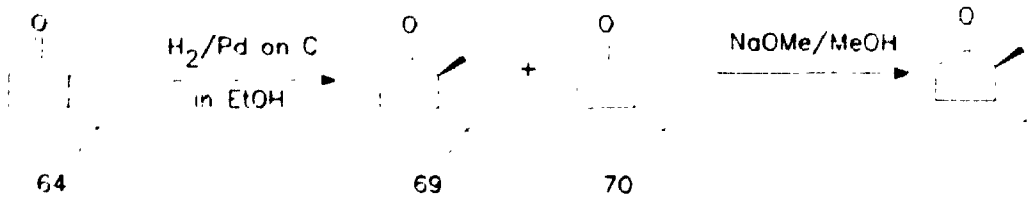

64 69 70

trans stereochemistry for the substituents on the cyclopentanone ring.

The hydrogenation of compound **62** was also performed over a palladium catalyst supported on carbon. Only one compound, **71**, was formed in this reaction (see Scheme 22). When compound **71** was treated with sodium methoxide in methanol no reaction was observed; therefore, it was concluded that **71** is not susceptible to epimerisation. These results are consistent with the structure which was assigned to **62** based on ^{1}H and ^{11}C nmr evidence.

Scheme 22

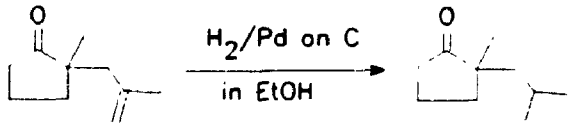

62 71

3.2.3 Photocycloaddition of 2-methylpropene and 3-methyl-2-cyclopentenone.

The irradiation of a benzene solution containing 3-methylcyclopentenone and 2-methylpropene with Pyrex filtered light from a medium pressure mercury lamp resulted in the formation of products **72**, **73**, **74**, and **75** in the ratio 20.8:4.5:47.4:27.3 (see Scheme 23). These product ratios were determined at 5% conversion of 3-methylcyclopentenone.

Scheme 23

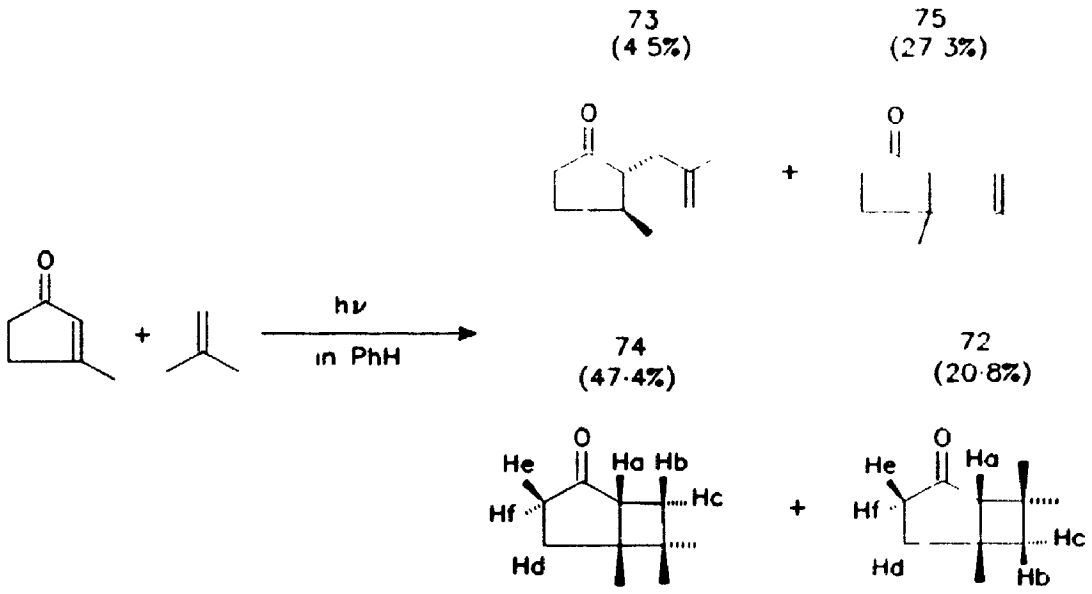

Compounds **72** to **74** were separated by chromatography and isolated in greater than 90% purity. Compound **75** was isolated as a mixture with **74**. Compounds **72** and **74** were confirmed to be 2+2 cycloadducts based on the positions and multiplicities of the signals in the ^{13}C nmr spectra of these compounds. Compounds **73** and **75** were confirmed to be "ene" type products since they are isomeric with **72** and **74**, and their

^1H and ^{13}C nmr spectra exhibited resonances indicative of a double bond.

The regiochemistry of the two cycloadducts **72** and **74** was determined by examining their ^1H nmr spectra. An ABX pattern with $J_{AB}=12.5$ Hz, $J_{AX}=0$ Hz, $J_{BX}=2.0$ Hz, and $\Delta\delta_{AB}=0.104$ ppm was observed at 1.84 ppm in the ^1H nmr spectrum of **72**. The AB part of this ABX pattern was assigned to protons Hb and Hc (see Scheme 23). Irradiation of a broad singlet at 2.02 ppm, which was subsequently assigned to Ha, resulted in collapsing the small J_{BX} coupling; therefore, the small coupling constant in the ABX pattern was assigned to a cross ring coupling between protons Ha and Hb or Hc. Based on the lack of a large vicinal coupling constant between Ha and Hb or Hc, compound **72** was assigned a head-to-head regiochemistry.

The ^1H nmr spectrum of **74** contained evidence in support of a head-to-tail regiochemical assignment for this compound. This evidence was based primarily on the coupling constants observed for the ^1H nmr signals originating from the geminal methylene protons Hc and Hb. These signals were located at 1.74 ppm and 2.00 ppm respectively. Both signals exhibited a multiplicity representative of a doublet of doublets with the large geminal coupling constant equal to 12 Hz. In addition to the geminal coupling, the signal assigned to Hb exhibited a large vicinal of 10 Hz while the signal assign to Hc exhibited a moderate vicinal coupling of 7 Hz. These vicinal coupling constants were assigned to coupling between Ha and each proton of the geminal pair. Therefore, based on the presence of large vicinal coupling constants at the ^1H nmr signals assigned to Hb and Hc in compound **74**, the regiochemistry of this compound was proven to be representative of a head-to-tail orientation between the enone and 2-methylpropene.

Compounds **73** and **75** were both determined to be alkene containing products

resulting from the disproportionation of different 1,4-biradicals. Both **73** and **75** had ^{13}C nmr spectra that exhibited a vinylic resonance with a multiplicity representative of a CH_2 carbon as well as a vinylic resonance with a multiplicity representative of a fully substituted carbon. The ^1H nmr spectra of these compounds further indicated that **73** and **75** both contain allylic methyl groups since broad singlets integrating for 3 protons each were observed at 1.66 and 1.75 ppm respectively. The regiochemistries of **73** and **75** were easily determined by counting the number of ^{13}C nmr resonances with multiplicities representative of methine and quaternary carbons.

The stereochemistry of **73** was determined to be *trans* about the cyclopentanone ring. This determination was based on the fact that formation of the *cis* stereochemistry by biradical disproportionation is impossible due to the constraints imposed by the five-membered ring. In addition, it was found that, upon addition of sodium methoxide in methanol, compound **73** epimerised to a mixture of two compounds, **73** and **76**, with **73** being strongly favoured (see Scheme 24). One might expect that under these epimerisation conditions the *trans* stereoisomer (**73**) would be preferred over the higher energy *cis* stereoisomer.

Hydrogenation of **73** over a palladium catalyst supported on carbon resulted in the formation of **77** (see Scheme 24). When **77** was subjected to epimerisation conditions involving sodium methoxide in methanol a minor product, compound **78**, was formed. The ratio of **77**:**78** after epimerisation was 6.3:1.0. A 6.8:1.0 mixture of **77** and **78** was also formed by hydrogenating the 6.9:1.0 mixture of **73** and **76** which resulted from the epimerisation of pure **73**. These results confirm the assignment of a *cis* stereochemistry to compounds **76** and **78**.

Scheme 24

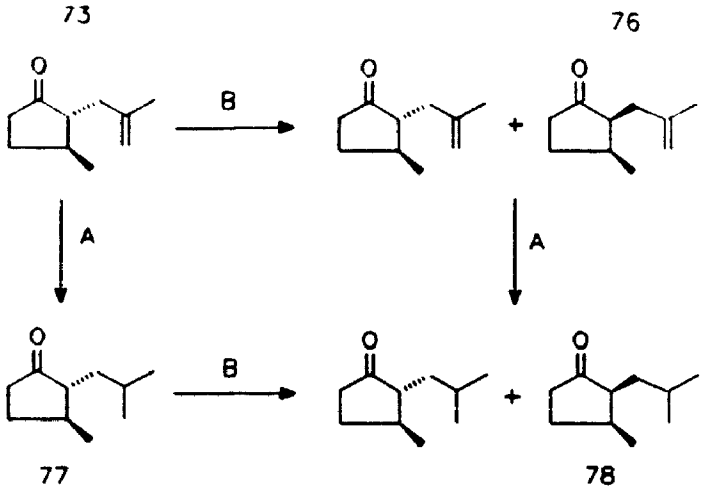

A= H_2, 10% Pd on carbon, in EtOH

B= NaOMe in MeOH

Scheme 25

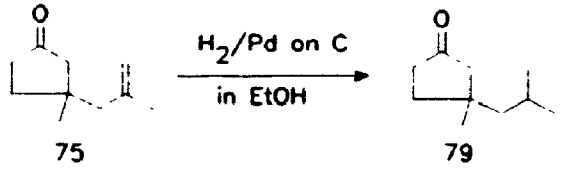

Compound **75** was also hydrogenated using the same conditions used to hydrogenate **73**. Scheme 25 illustrates that hydrogenation of **75** results in the formation of **79**. Treatment of **79** with a solution of sodium methoxide in methanol did not result in the formation of any new products.

3.2.4 Quantum yield determinations.

The quantum yield of formation of each product obtained in the three enone plus alkene reactions discussed above was measured at various alkene concentrations in benzene. The concentration of the enone was kept constant as the 2-methylpropene concentration was varied: the concentration of cyclopentenone was 0.0401 mol/L and the concentration of both 2- and 3-methylcyclopentenone was 0.0407 mol/L. All quantum yield measurements were made using a PTI QUANTACOUNT instrument. This instrument was calibrated using the rearrangement of azoxybenzene to 2-hydroxyazobenzene in KOH saturated ethanol as an actinometer.[4]

Figure 2 contains a plot of the total quantum yield of product formation versus the concentration of 2-methylpropene for the photocycloaddition of 2-cyclopentenone and 2-methylpropene. Similar plots were obtained for the quantum yield determinations performed on the corresponding photocycloaddition reactions involving the 2- and 3-methyl-2-cyclopentenones. (See the Experimental Section in Chapter 7 for the original data). The relative yield of each product obtained from the three photo-cycloadditions did not vary as the alkene concentration was increased from 0.08 to 2.5 mol/L.

An excellent linear correlation was obtained when the reciprocal of the quantum yield of formation of each product was plotted versus the reciprocal of the 2-methylpropene concentration. Figure 3 contains a linear plot of the reciprocal of the total quantum yield of the products formed in tne photocycloaddition reactions of the three cyclopentenones studied and 2-methylpropene. The slope and intercept parameters obtained from the weighted least squares regression analyses of the $1/\Phi$ versus 1/[alkene]

plots are listed in Table 13. The corresponding slope and intercept parameters for each individual product obtained in the photocycloaddition reactions were calculated by dividing the regression parameters that were obtained for the plots shown in Figure 3 by the relative yield of each product (normalised to 1). The errors quoted for each slope and intercept parameter represent one standard deviation unit for the parameter as determined in the weighted least squares analysis of the data. The significance of the intercept and slope parameters obtained from the double inverse plots will be examined in the kinetic analysis described in the Discussion Section below.

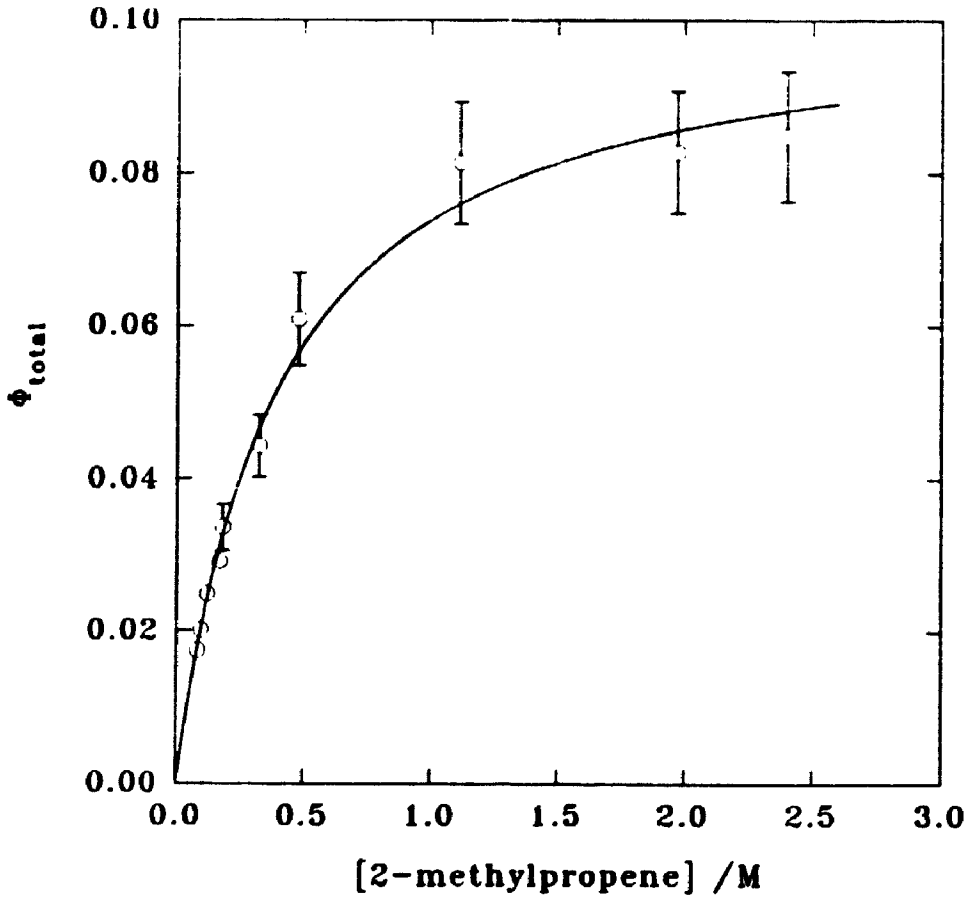

Figure 2: Dependence of the quantum yield of product formation on the concentration of alkene for the photocycloaddition of 2-cyclopentenone and 2-methylpropene in benzene.

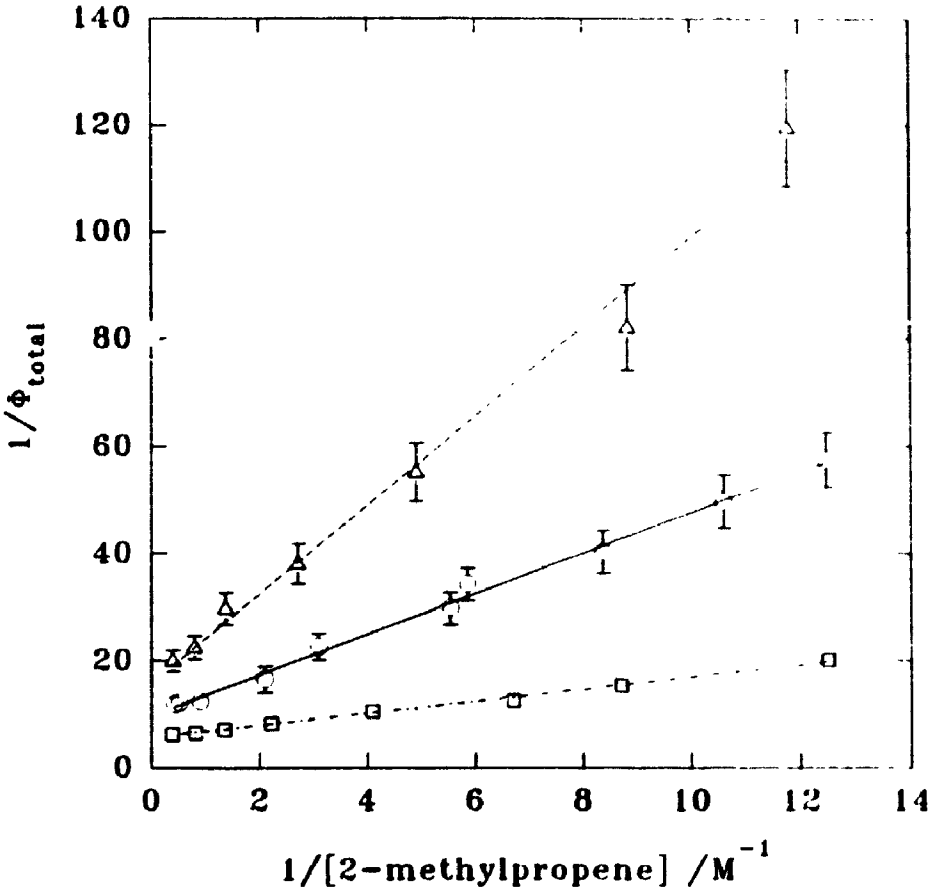

Figure 3: Dependence of the reciprocal of the total product quantum yield on the reciprocal of the alkene concentration for the photocycloaddition reactions of 2-cyclopentenone (○), 2-methyl-2-cyclopentenone (△), and 3-methyl-2-cyclopentenone (□) with 2-methylpropene.

Table 13: Weighted least squares regression analysis results for the quantum yield determinations made for the photocycloaddition of 2-methylpropene and substituted 2-cyclopentenones.

Product	Relative Product Yield[a]	1/Φ versus 1/[alkene] regression parameters			
		slope (M^{-1})	intercept	1/intercept	r
Photocycloaddition of 2-methylpropene and 2-cyclopentenone					
All		3.8±0.1	9.7±0.6	0.10±0.01	0.998
54	2.9	131±4	336±21	0.0030±0.0002	
55	69.5	5.4±0.1	14.0±0.9	0.071±0.004	
56	18.5	20.4±0.5	52±3	0.019±0.001	
57	9.1	41.6±1.0	107±7	0.0093±0.0006	
Photocycloaddition of 2-methylpropene and 2-methyl-2-cyclopentenone					
All		8.3±0.4	15.6±2.3	0.063±0.009	0.993
60	7.3	114±5	216±31	0.0046±0.0006	
61	46.0	18.1±0.8	34±5	0.029±0.004	
62	5.2	160±8	306±44	0.0033±0.0004	
63	28.9	29±2	55±8	0.018±0.002	
64	3.4	244±12	465±67	0.0022±0.0003	
65	9.3	89±4	170±25	0.0059±0.0007	
Photocycloaddition of 2-methylpropene and 3-methyl-2-cyclopentenone					
All		1.13±0.05	5.6±0.3	0.18±0.01	0.998
72	20.8	5.4±0.2	27±1	0.037±0.002	
73	4.5	25±1	125±5	0.0080±0.0005	
74	47.4	2.4±0.1	11.8±0.5	0.084±0.004	
75	27.3	4.1±0.2	20.6±0.8	0.049±0.003	

[a]Relative error of 2%.

3.3 Biradical trapping experiment results.

3.3.1 General description of the H_2Se trapping experiments.

Each of cyclopentenone, 2-methylcyclopentenone, and 3-methylcyclopentenone was irradiated with UV light ($\lambda > 300$nm) in benzene solutions containing H_2Se and 2-methylpropene. The appearance of products in these reaction mixtures was monitored by g.c. and coupled g.c./m.s. The appearance of products in identical reaction mixtures that were not exposed to light was also monitored. No cycloadducts were observed in the irradiated solutions containing enone, 2-methylpropene, and H_2Se; however, products resulting from the reduction of the 1,4-biradicals formed from the reaction of triplet enone with alkene were observed. Evidence of products resulting from trapped 1,4-biradicals was not observed in any of the "dark" reactions.

In addition to the products resulting from the reduction of 1,4-biradicals, cyclopentanone, 2-methylcyclopentanone, or 3-methylcyclopentanone were observed in the reaction mixtures exposed to UV light. The formation of each of these cyclic ketones was a result of the quenching reaction between the corresponding enone triplet and H_2Se. This quenching reaction is presumed to be initiated when excited triplet enone abstracts a hydrogen atom from a molecule of H_2Se. The resulting radical may abstract another hydrogen atom from the hydrogen selenyl radical before this species leaves the solvent cage, or the radical may leave the solvent cage and abstract a hydrogen atom from an another H_2Se molecule. As discussed in Chapter 2, the rate of hydrogen abstraction by the photoreduced enone radical is expected to be several orders of magnitude faster than its rate of addition to the alkene. Therefore, this radical is excluded as a source of products possessing the same structures as the reduced biradical intermediates.

Some products were observed in the reaction mixtures that were not exposed to UV light. These products were also observed in the solutions that were exposed to UV light. It was determined by g.c.-m.s. that all of the dark reaction products contained two selenium atoms each. The dark reaction products were not isolated or characterised. The formation of these products was of no significance with regard to the kinetic analyses described in the Discussion Section.

3.3.2 The 2-methylpropene plus 2-cyclopentenone system.

The irradiation of a benzene solution containing H_2Se, 2-methylpropene and cyclopentenone with Pyrex filtered light from a 450 W medium pressure Hanovia mercury lamp resulted in the formation of the products **80**, **81**, **54**, **82**, **83**, and **84** (see Scheme 26). The ratio of these products was determined at 5% conversion of cyclopentenone to be 2.3:15.3:10.0:7.5:0.4:64.5. The mass spectra of **81**, **83**, and **84** exhibited a molecular ion at a mass of 140. The other 3 products exhibited a molecular ion at a mass of 138 in their electron impact mass spectra. Therefore, it was concluded that compounds **81**, **83**, and **84** were the result of complete reduction of the corresponding biradicals while compound **80**, **54**, and **82** were formed by partial reduction followed by radical pair disproportionation.

Compounds **83** and **80** were recovered together in a 1:1.5 mixture. The low relative yields of these two compounds along with their chromatographic similarity resulted in unsuccessful separation of these compounds. The ^{13}C nmr spectrum of the mixture exhibited two methine signals with chemical shifts indicative of vinylic carbons. Assuming that the 5-membered cyclic ketone moiety is present in **80**, then the only

Scheme 26

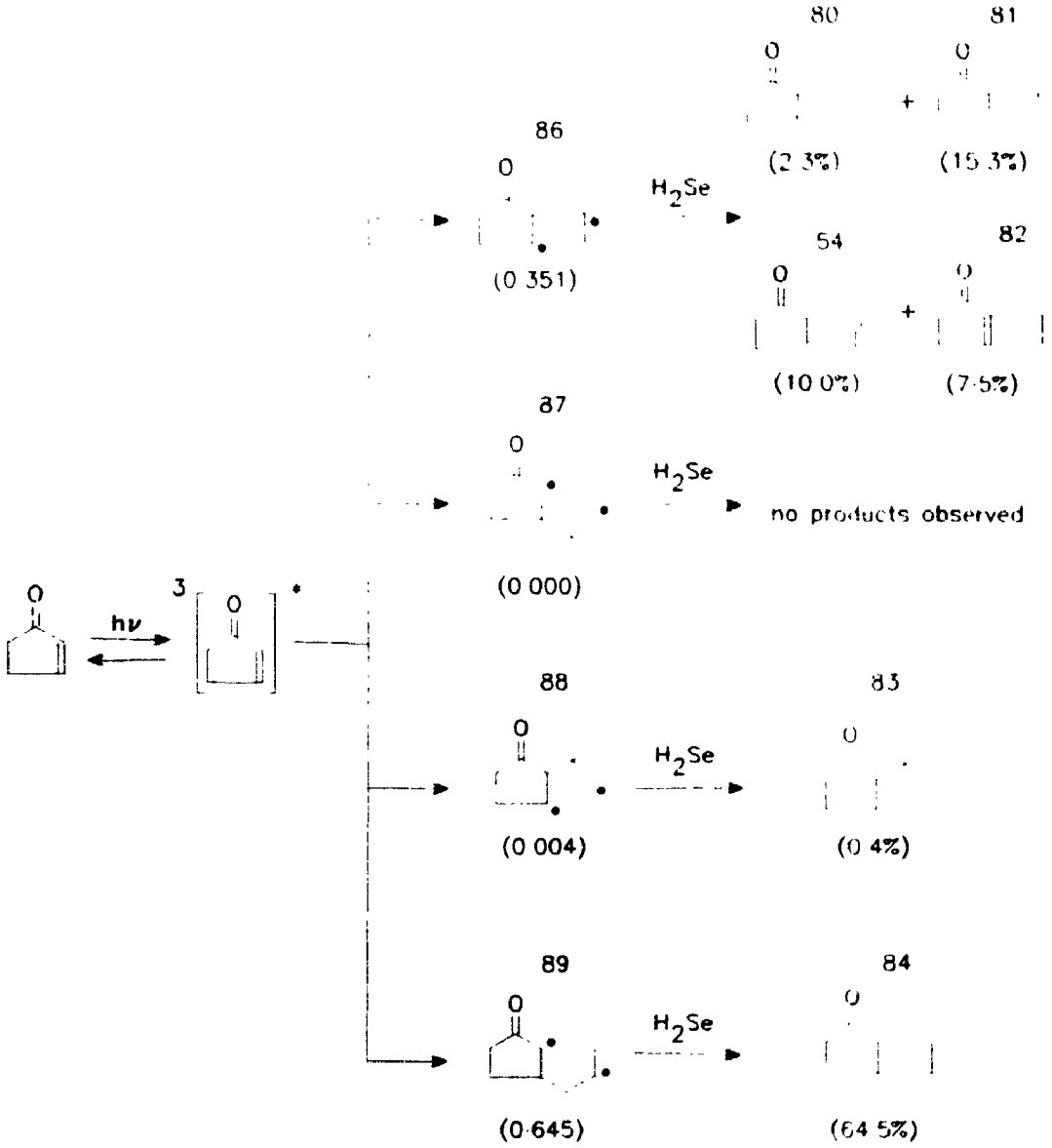

position that the double bond could occupy and still exhibit two methine vinylic ^{13}C signals is the 3-position of the 5-membered ring. The vinylic resonance at 6.07 ppm in the ^{1}H nmr spectrum of the mixture, which integrated for 2 protons, confirmed the position of this double bond in compound **80**. The two carbonyl resonances at 220.5 and

219.7 ppm in the ^{13}C nmr spectrum, and the major fragments at m/e of 84 and 82 in the mass spectra of **83** and **80** are a strong indication that both **83** and **80** contain the 5-membered cyclic ketone moiety.

The presence of a t-butyl group in either **83** or **80** was confirmed by the appearance of a 9 proton singlet in the ^{1}H nmr spectrum, a very intense methyl ^{13}C resonance at 27.7 ppm, and a quaternary ^{13}C resonance at 32.5 ppm. In principle, the t-butyl group could be attributed to either **83** or **80** based on the fact that **83** and **80** were isolated as a mixture; however, the t-butyl group can be assigned to the fully reduced biradical (**83**) based on the following deductive argument. The only other two compounds, **81** and **84**, positively identified as products resulting from complete reduction of 1,4-biradicals were found not to contain t-butyl groups. Since there are only four 1,4-biradical species which may be postulated, two of which upon complete reduction by H_2Se give compounds containing t-butyl groups and two which give compounds **81** and **84**, therefore by deduction compound **83** must contain a t-butyl group.

The position of substitution on the cyclopentanone ring of **83** was determined from the ^{13}C nmr spectrum of the mixture of **83** and **80**. The α-keto carbons in **83** and **80** were assigned to the sp^3 ^{13}C nmr resonances shifted furthest downfield. The multiplicity of the two sp^3 resonances located furthest downfield (57.9 and 50.5 ppm) was determined to be representative of a methine carbon. The only other methine resonance observed in the ^{13}C nmr spectrum of the mixture of **83** and **80** occurred at 26.1 ppm. This methine signal was assigned to the carbon bearing the geminal methyl groups which exhibited doublets at 0.88 and 0.90 ppm in the ^{1}H nmr of the mixture. Since no other high-field methine resonances were observed in the ^{13}C nmr spectrum of the mixture,

therefore both of these compounds were assigned a regiochemistry representative of substitution at the 2-position of the cyclopentanone ring.

Additional evidence for the structure of **80** was obtained by subjecting the mixture containing **83** and **80** to palladium metal catalysed hydrogenation. It was found that hydrogenation of the 1:1.5 mixture of **83** and **80** resulted in the formation of a 1:1.5 mixture of **83** and **81**. Therefore, it was concluded that **80** and **81** must have the same regiochemisry. This finding is consistent with the structures assigned to compounds **80** and **81** based on ^{1}H and ^{13}C nmr spectra of the two compounds.

Compounds **81** and **84** were determined to be products resulting from complete reduction of 1,4-biradicals based on mass spectral data. This assignment was confirmed by the ^{1}H and ^{13}C nmr spectral data obtained for each of the compounds. The regiochemistry of each compound was deduced by comparing the multiplicities of the ^{13}C nmr signals assigned to the α-keto carbons in each compound. Compound **81** was found to have a methine resonance at 47.5 ppm and a methylene resonance at 38.9 ppm as the furthest downfield signals in its ^{13}C nmr spectrum. On the other hand, compound **84** was found to have two methylene resonances (45.3 and 45.0 ppm) as the furthest downfield signals in its ^{13}C nmr spectrum. The lowest field methine signal in the ^{13}C nmr spectrum of **84** was located at 34.8 ppm. Therefore, it was determined that compound **81** is substituted at the α-position of the cyclopentanone ring and that compound **84** is substituted at the β-position of the cyclopentanone ring.

The structure of **82** was easily assigned based on its ^{1}H nmr spectrum. The most important feature of the ^{1}H nmr spectrum of **82** was the presence of a multiplet at 7.24 ppm which integrated for one proton. By comparing this spectrum with the spectrum of

2-methylcyclopentenone, the 7.24 ppm resonance was assigned to the proton attached to the β carbon of enone **82**. (In 2-methylcyclopentenone the β proton comes at 7.23 ppm while in 3-methylcyclopentenone the α proton comes at 5.86 ppm).[5] The ^{13}C nmr spectrum of the mixture also confirmed the structural assignment given to **82**. The ^{13}C APT spectrum contained vinyl resonances at 158.3 and 145.1 ppm which exhibited multiplicities representative of a methine and a fully substituted carbon. It was also found that the diastereotopicity of the two methyl groups observed in the ^{13}C nmr spectrum of **81** was not present in the ^{13}C spectrum of **82**. The achirality of **82** removes the possibility of diastereotopic methyl resonances.

The presence of compound **54** in the reaction mixture resulting from the irradiation of a benzene solution containing 2-methylpropene, 2-cyclopentenone, and hydrogen selenide was confirmed. This was accomplished by comparing the ^{1}H and ^{13}C nmr spectral properties of the chromatographic fractions isolated in the trapping experiment with the spectral properties of the corresponding compound isolated in the photocycloaddition reaction. It was determined that compound **54** originated from an interaction between H_2Se and biradical **86** and not from disproportionation of the biradical. This conclusion is based on the fact that no cycloadducts were identified in the trapping reaction mixture; therefore, H_2Se must intercept all of the triplet biradicals before closure or disproportionation can occur.

3.3.3 The 2-methylpropene plus 2-methyl-2-cyclopentenone system.

The irradiation of a benzene solution containing H_2Se, 2-methylpropene and 2-methylcyclopentenone with Pyrex filtered light from a 400 W medium pressure

Scheme 27

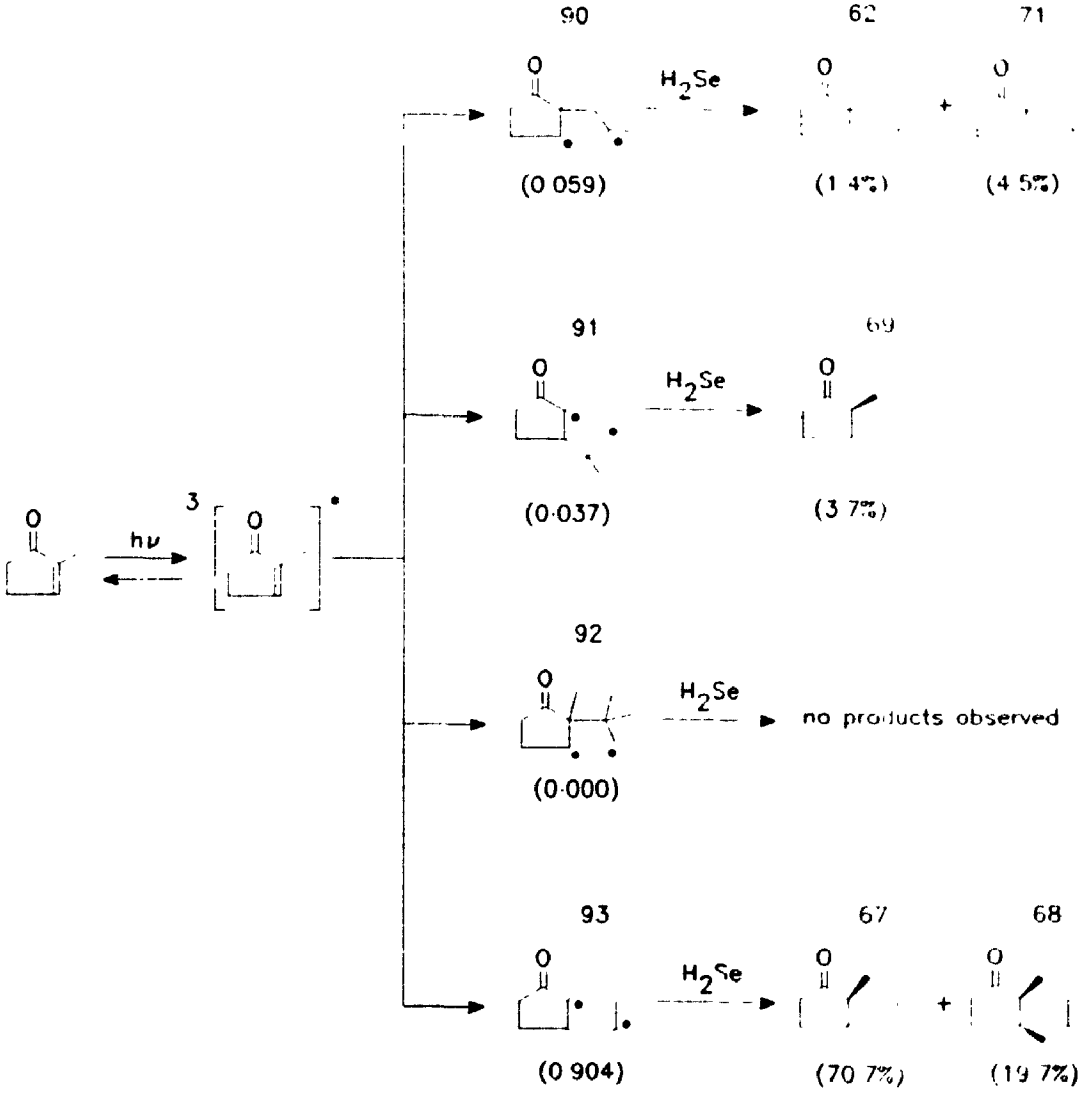

Hanovia mercury lamp resulted in the formation of the products **71**, **62**, **67**, **69**, and **68** in the ratio 4.5:1.4:70.7:3.7:19.7 (see Scheme 27). Due to the inefficiency of this reaction caused by the high rate of quenching of 2-methylcyclopentenone by H_2Se, it was impossible to synthesize enough of these products so that they could be isolated and characterised. Identification of the products was accomplished by g.c. co-injection of

authentic samples of each of the five products with the mixture obtained from the irradiations carried out in the presence of H_2Se. Their mass spectra were also compared to confirm the identifications. Authentic samples of **71**, **62**, **67**, **69**, and **68** were obtained directly from the photo-cycloaddition between 2-methylpropene and 2-methylcyclopentenone or from hydrogenation and epimerisations carried out on products obtained from the photo-cycloaddition.

3.3.4 The 2-methylpropene plus 3-methyl-2-cyclopentenone system.

The irradiation of a benzene solution containing H_2Se, 2-methylpropene and 3-methylcyclopentenone with Pyrex filtered light from a 400 W medium pressure Hanovia mercury lamp resulted in the formation of the products **73**, **76**, **77**, **78**, and **79** in the ratio 5.6:4.9:13.5:5.5:70.5 (see Scheme 28). It was impossible to synthesize enough of these products so that they could be isolated and characterised due to the same reason mentioned above. Identification of these products was accomplished by the same techniques employed in the identification of the products obtained from the irradiated solutions of 2-methylcyclopentenone, 2-methylpropene, and H_2Se.

Scheme 28

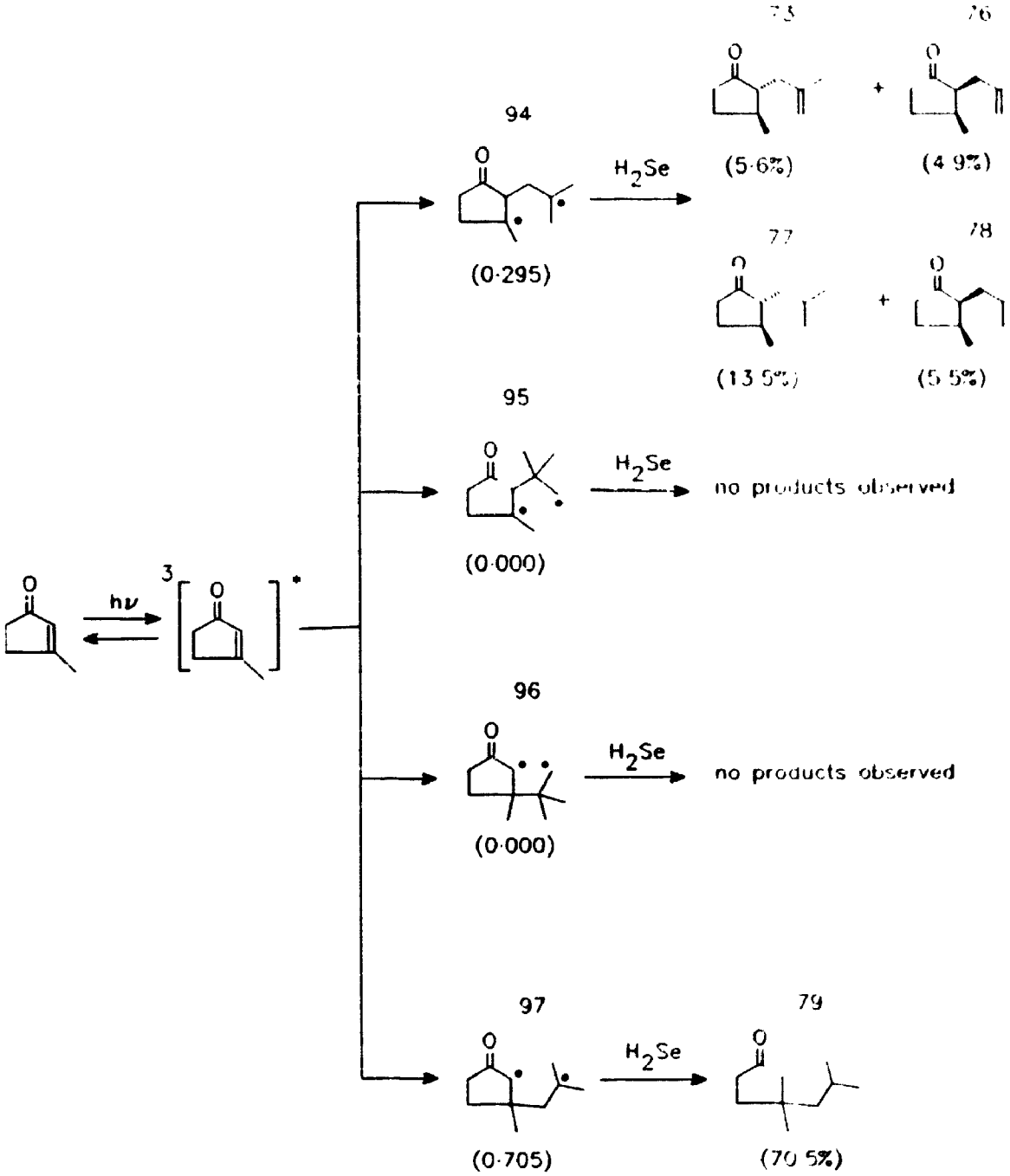
hν
3
94
(0·295)
H2Se
75
76
(5·6%)
(4·9%)
77
78
(13·5%)
(5·5%)
95
(0·000)
H2Se
no products observed
96
(0·000)
H2Se
no products observed
97
(0·705)
H2Se
79
(70·5%)

3.4 Discussion.

The results of the trapping studies presented above were used to determine the relative rates of formation for the biradicals generated in the photo-cycloaddition reactions between 2-methylpropene and each of the three enones cyclopentenone, 2-methylcyclopentenone, and 3-methylcyclopentenone. Once the structure of each trapped product was determined, it was possible to deduce from which biradical each product originated. Schemes 26, 27, and 28 summarize all of the compounds identified as trapped products which originated from an interaction between H_2Se and each of the biradicals formed in the photo-cycloaddition of 2-methylpropene with cyclopentenone, 2-methylcyclopentenone, and 3-methylcyclopentenone. By summing over the relative yields of all trapped products originating from a particular biradical, the relative rate of formation of that particular biradical was calculated. In these schemes the relative rate of formation of each biradical, normalized to unity, is listed in parentheses below each structure.

The most obvious feature indicated by the results summarised in Schemes 26, 27 and 28 concerns the rates of formation of the primary radical-containing biradicals relative to the rates of formation of the tertiary radical-containing biradicals. For example, the results shown in Scheme 26 demonstrate that biradicals **86** and **89** are formed at much faster rates relative to biradicals **87** and **88**. The results shown in Scheme 28 demonstrate a similar trend; that is, the biradicals containing primary radical sites are formed slower than the other biradicals. On the other hand, the results summarised in Scheme 27 do not support this trend. Based on the results shown in this

scheme it appears as though biradical **90**, which contains secondary and tertiary radical sites, is formed at a rate similar to that of biradical **91**, which contains primary and tertiary radical sites. Therefore, primary radical-containing biradicals may be ignored in the kinetic analysis of the photocycloaddition reaction of 2-methylpropene and each of 2-cyclopentenone and 3-methyl-2-cyclopentenone. However, these kinds of biradicals may not be ignored in the kinetic analysis of the photocycloaddition between 2-methylpropene and 2-methyl-2-cyclopentenone.

One of the main goals of this study was to determine if methyl substitution at either the 2- or 3-position of 2-cyclopentenone resulted in changing the regiochemistry of the major biradical intermediates which are formed when these substituted enones participate in photocycloaddition reactions with alkenes. It was thought possible that alkyl substitution at either of these positions on 2-cyclopentenone might favour radical formation at the substituted site upon generation of the biradical intermediates. The increased stability offered by a tertiary radical site relative to a secondary radical site might direct biradical formation so that the more stable intermediates would be formed at the faster rates. It was also recognised that the steric interactions between a methyl substituent and the attacking alkene might be important. The results shown in Schemes 26, 27, and 28 will now be discussed in terms of these hypotheses.

Scheme 27 demonstrates that methyl substitution at the 2-position of the 2-cyclopentenone ring results in directing the photocycloaddition reaction toward the formation of biradicals in which initial bonding occurs at the 3-position of the enone. Thus, biradical **93** is the major biradical formed in the photocycloaddition of 2-methylpropene and 2-methyl-2-cyclopentenone. A comparison of Schemes 26 and 27

demonstrates that the rate of formation of β-bonded biradicals relative to the rate of formation of α-bonded biradicals is enhanced by alkyl-substitution at the 2-position of 2-cyclopentenone. This observation is in agreement with the hypothesis mentioned above which suggests that the thermodynamically more stable biradicals are formed at faster rates.

The results presented in Scheme 28 demonstrate that methyl-substitution at the 3-position of 2-cyclopentenone does not result in directing the photocycloaddition reaction towards the formation of a major biradical which results from bonding at the α-position of the enone. For example, in the case of the photocycloaddition reaction between 2-methylpropene and 2-cyclopentenone the ratio of α-bonded biradical to β-bonded biradicals was determined to be 35:65, whereas in the case of the photocycloaddition involving 3-methyl-2-cyclopentenone the ratio was determine to be 30:70. The enhanced stability of the tertiary radical site in **94** relative to secondary site radical **86** does not result in an increase in the relative rate of formation of α-bonded biradicals in the photocycloaddition reaction of 3-methyl-2-cyclopentenone and 2-methylpropene. This observation is not consistent with the hypothesis that the thermodynamically more stable biradicals are formed at faster rates.

It is possible that the relative rates of biradical formation shown in Schemes 26, 27, and 28 are more dependent on steric factors than the relative thermodynamic stabilities of the biradicals. These steric factors can be explained by assuming that the enone is twisted in the triplet excited state with the α-position sp^2 (and conjugated) and the β-position sp^3.[6] Therefore, attack of the alkene at the α-position would be more susceptible to the steric effects associated with changing the substituent at this position

from hydrogen to a methyl group: the steric effects at the sp^3 β-position of the excited enone would be less. This model correlates with the observation that the photocycloadditions of 2-cyclopentenone and 3-methyl-2-cyclopentenone with 2-methylpropene give very similar biradical distributions while α-bonded biradical formation in the photocycloaddition of 2-methyl-2-cyclopentenone is relatively slow.

It is difficult to determine whether thermodynamic factors or kinetic factors are responsible for controlling which end of the alkene molecule participates in initial bonding during biradical formation. The results summarised in Schemes 26, 27, and 28 indicate that initial bonding to the less substituted end of the alkene is favoured. This might be due to the fact that a more stable radical site is formed in this mode of attack. Alternatively, the steric hindrance at the more substituted end of the alkene might discourage initial bonding during biradical formation at this terminus. Therefore, the very slow relative rate of formation for biradicals containing primary radical sites could be a consequence of the fact that both thermodynamic and steric factors disfavour such intermediates.

Another goal of the studies presented in this chapter was to determine how the triplet biradical intermediates shown in Schemes 26, 27, and 28 partition between closure and reversion after intersystem crossing to the singlet state surface. In order to make these determinations, it is first necessary to analyze the steady state kinetics of an enone-alkene photocycloaddition reaction mechanism which involves more than one biradical intermediate. This provides a relationship between the product quantum yield and two factors; the rates of formation of the isomeric biradical intermediates, and the partitioning factors for cyclisation versus reversion for each biradical. Since the relative rates of

Scheme 29

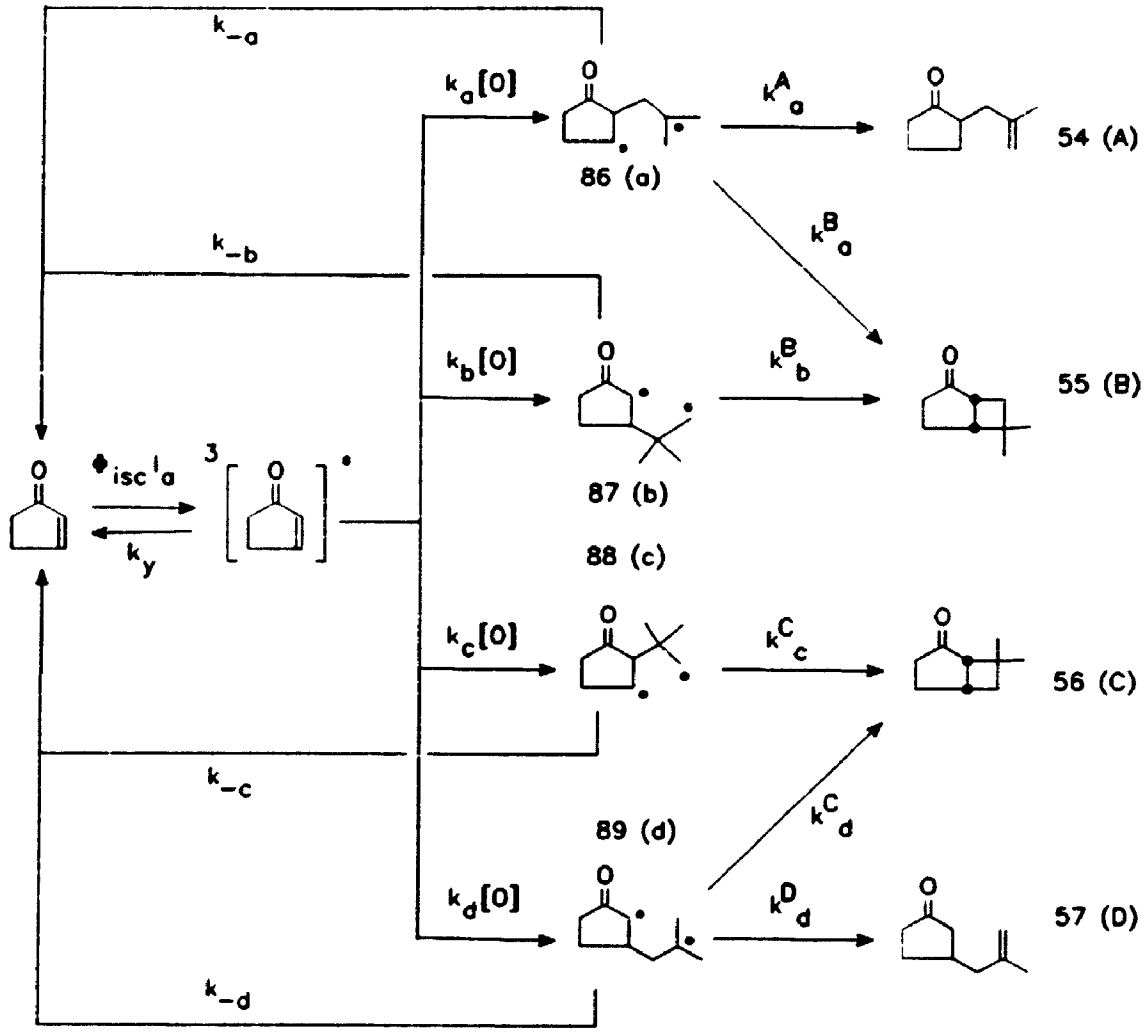

formation of each biradical intermediate are known from the H_2Se trapping experiments, it is then possible to determine the partitioning factors.

A reaction mechanism which describes the addition of 2-methylpropene to triplet cyclopentenone is proposed in Scheme 29. The products denoted as **54**, **55**, **56**, and **57** have been assigned the temporary designations **A**, **B**, **C**, and **D**, respectively, in Scheme

29. Similarly, biradicals **86**, **87**, **88**, and **89** have been assigned the temporary designations **a**, **b**, **c**, and **d** respectively. These temporary assignments were made in order to simplify the equations resulting from the following kinetic derivations.

The steady state approximation was applied to the appropriate intermediates in Scheme 29. This allowed expressions to be derived for the quantum yield of formation for each product obtained from the cycloaddition, namely compounds **A**, **B**, **C**, and **D**. For example, Equation 2 defines the quantum yield of formation of **B** in terms of the rate constants shown in Scheme 29:

$$\Phi_B = \Phi_{isc}\left[\left(\frac{k_a^B}{k_{-a}+k_a^A+k_a^B}\right)\left(\frac{k_a[O]}{(k_a+k_b+k_c+k_d)[O]+k_y}\right)+\left(\frac{k_b^B}{k_{-b}+k_b^B}\right)\left(\frac{k_b[O]}{(k_a+k_b+k_c+k_d)[O]+k_y}\right)\right] \qquad (2)$$

In this equation, Φ_{isc} represent the quantum yield of formation of the triplet enone and [O] represents the concentration of 2-methylpropene. The quantum yield of intersystem crossing for cyclopentenone has been determined by Wagner and Bucheck to be 1.0.[7] This value was substituted into the reciprocal of equation 2 in order to derive equation 3 below:

$$\frac{1}{\Phi_B} = \frac{1}{\rho_a^B\alpha_a+\rho_b^B\alpha_b}+\frac{k_y}{\rho_a^B k_a+\rho_b^B k_b}\cdot\frac{1}{[O]} \qquad (3)$$

Here, the quantities ρ_a^B, ρ_b^B, α_a, and α_b have the following definitions: $\rho_a^B = k_a^B/(k_a^B+k_a^A+k_{-a})$, $\rho_b^B = k_b^B/(k_b^B+k_{-b})$, $\alpha_a = k_a/(k_a+k_b+k_c+k_d)$, and $\alpha_b = k_b/(k_a+k_b+k_c+k_d)$. In general, the various ρ_i^I represent the fraction of biradical "i"

which results in the formation of product "I" while the quantities denoted as α_i represents the rate of formation of each biradical "i" relative to the other biradicals.

Quantum yield expressions for the disproportionation products **A** and **D** were also derived. The expressions which define the quantum yield of formation for these products are simpler than the expressions which define the quantum yields of products **B** and **C** since each of products **A** and **D** result from the disproportionation of a single biradical. For example, the quantum yield of formation of disproportionation product **A** is defined by equation 4:

$$\Phi_A = \Phi_{isc}\left(\frac{k_a^A}{k_{-a}+k_a^A+k_a^B}\right)\left(\frac{k_a}{(k_a+k_b+k_c+k_d)[O]+k_y}\right) \qquad (4)$$

By taking the reciprocal of equation 4 and substituting $\Phi_{isc}=1.0$, equation 5 can be derived:

$$\frac{1}{\Phi_{1A}} = \frac{1}{\rho_a^A\alpha_a} + \frac{k_y}{\rho_a^A k_a}\cdot\frac{1}{[O]} \qquad (5)$$

In equation 5, α_a has the same definition as in equation 3 and $\rho_a{}^A=k_a{}^A/(k_{-a}+k_a{}^A+k_a{}^B)$. Equations 3 and 5 predict the linear dependence of the reciprocal of the quantum yield of formation of products **B** and **A** on the reciprocal of the 2-methylpropene concentration.

Quantum yield expressions were also derived for products **C** and **D**. These expressions have forms similar to the equations derived for products **B** and **A**. Quantum yield expressions were also derived for each of the products obtained in the

2-methylcyclopentenone plus 2-methylpropene and 3-methylcyclopentenone plus 2-methylpropene photocycloaddtions. The quantum yield expressions for these latter two reactions were derived by applying the steady state approximation to the rate of formation of the intermediates preceding product formation in each system. These expressions have a form similar to the equations derived for the cyclopentenone plus 2-methylpropene system.

The quantum yield expressions for the products formed in the photocycloadditions of 2-methylpropene to each of 2-cyclopentenone, 2-methyl-2-cyclopentenone, and 3-methyl-2-cyclopentenone can yield information about the way each biradical partitions between closure and reversion. This information is contained in the various ρ_i^1 parameters defined above. In equations 3, and 5 each ρ_i^1 is multiplied by the relative rate of formation of biradical "i" (i.e. α_i). The various α_i were determined in the hydrogen selenide trapping studies and are listed under each biradical in Schemes 26, 27 and 28. These relative rates of formation for each biradical were substituted into the appropriate quantum yield expressions. It is important to note that it is impossible to solve equation 3 and 5 for the various ρ_i^1 parameters without first determining the relative rates of formation of each biradical.

The linear regression parameters shown in Table 13 were obtained from plotting the reciprocal of the quantum yield of formation of each product versus the reciprocal of the 2-methylpropene concentration. These parameters were fitted to the equations derived form steady state kinetics. The intercept components of equations 3 and 5, in conjunction with the α_i values obtained from the trapping study, were then used to calculate values for the various ρ_i^1. The fraction of biradicals which revert to ground

state enone and alkene (ρ_{-i}) was obtained from the normalisation condition $\rho_{-i}=1-\rho_i^I-\rho_i^Y$, where "I" an "Y" denote the two possible products that could be formed by biradical "i". The various ρ_i^I calculated for the three enone-alkene systems studied are listed in percent in Schemes 30, 31, and 32.

Scheme 30

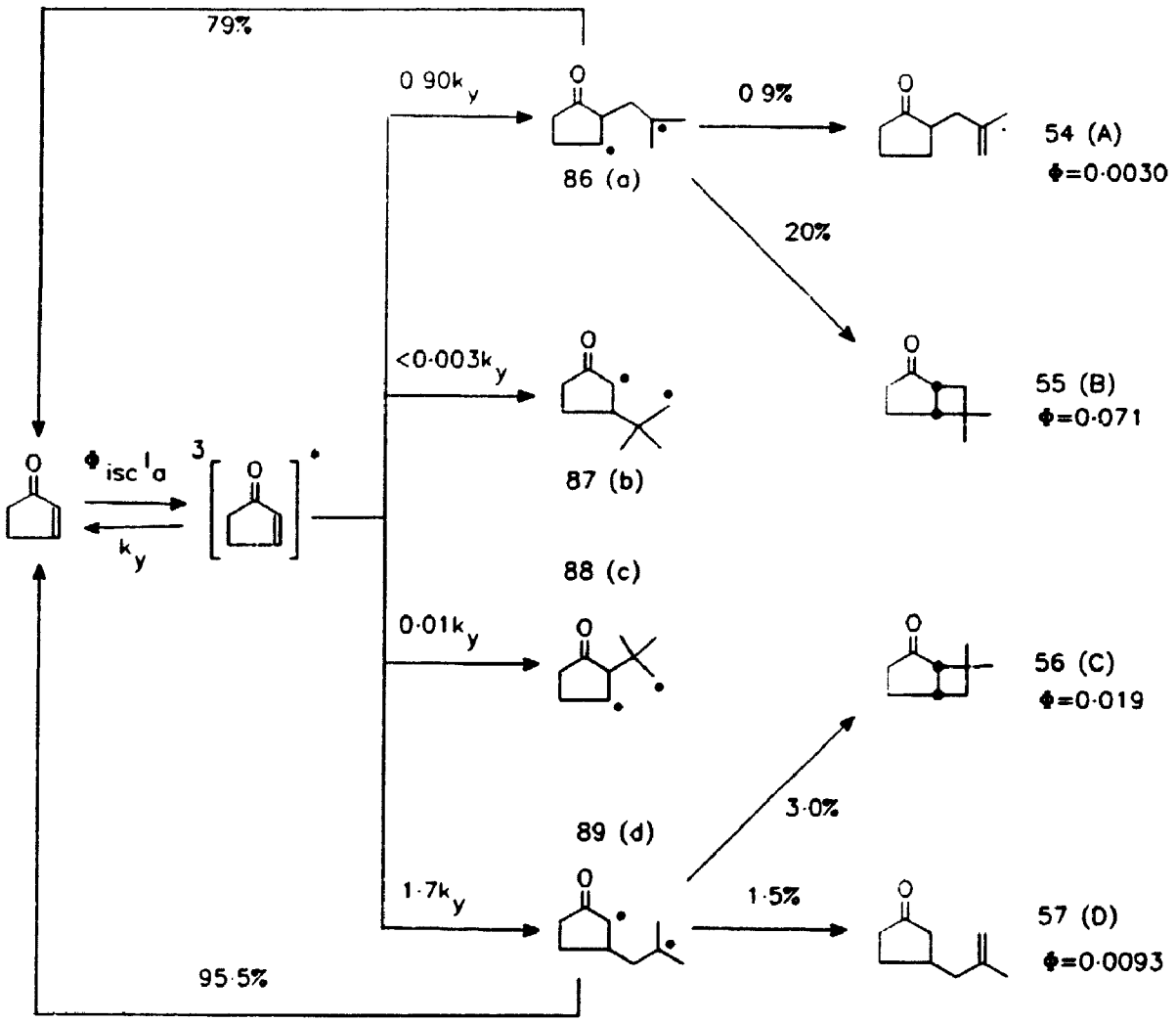

Scheme 31

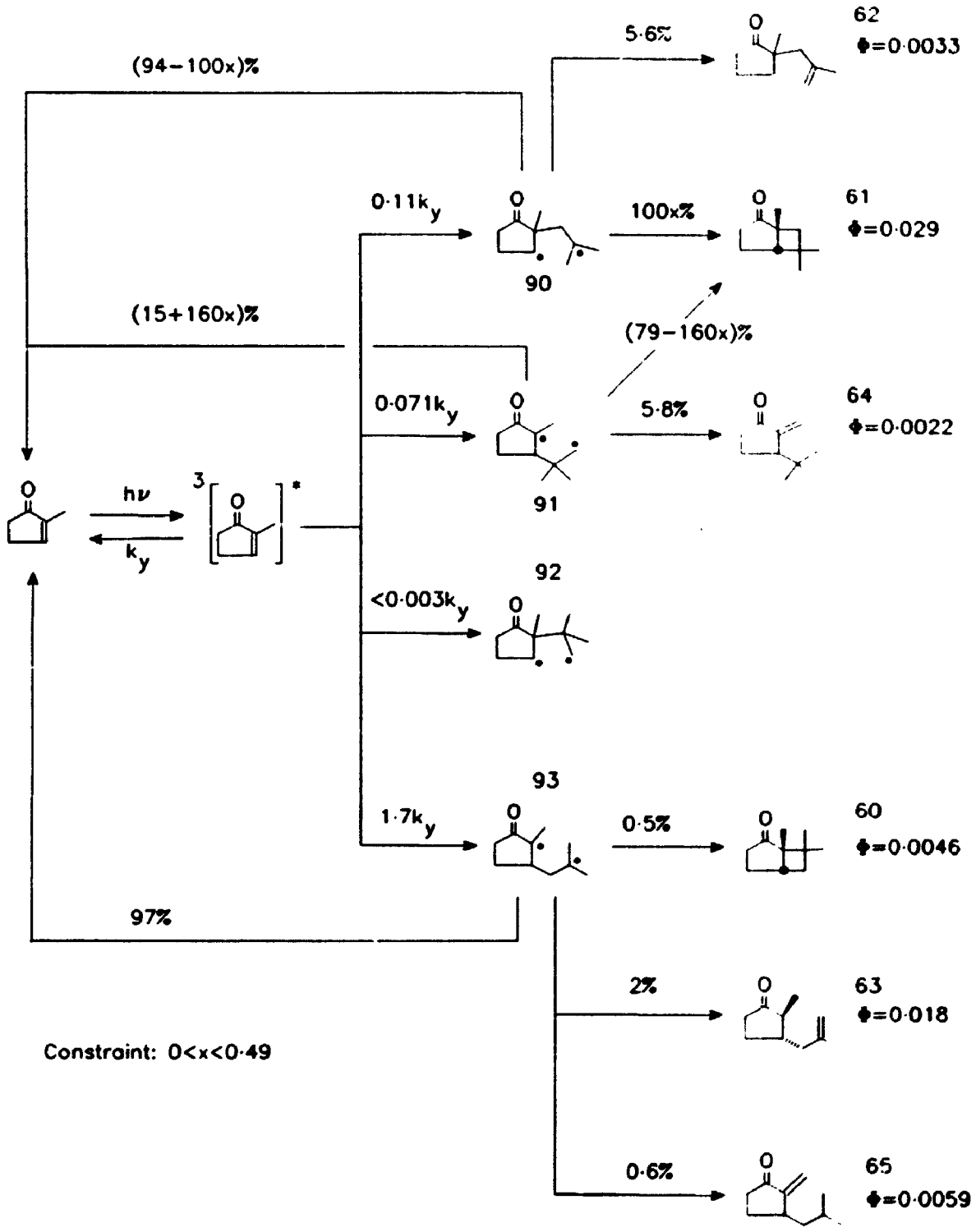
(94−100x)%
5·6%
62
Φ=0·0033
0·11k_y
100x%
61
Φ=0·029
90
(15+160x)%
(79−160x)%
0·071k_y
5·8%
64
Φ=0·0022
91
hν
k_y
3
*
92
<0·003k_y
93
1·7k_y
0·5%
60
Φ=0·0046
97%
2%
63
Φ=0·018
0·6%
65
Φ=0·0059
Constraint: 0<x<0·49

Scheme 32

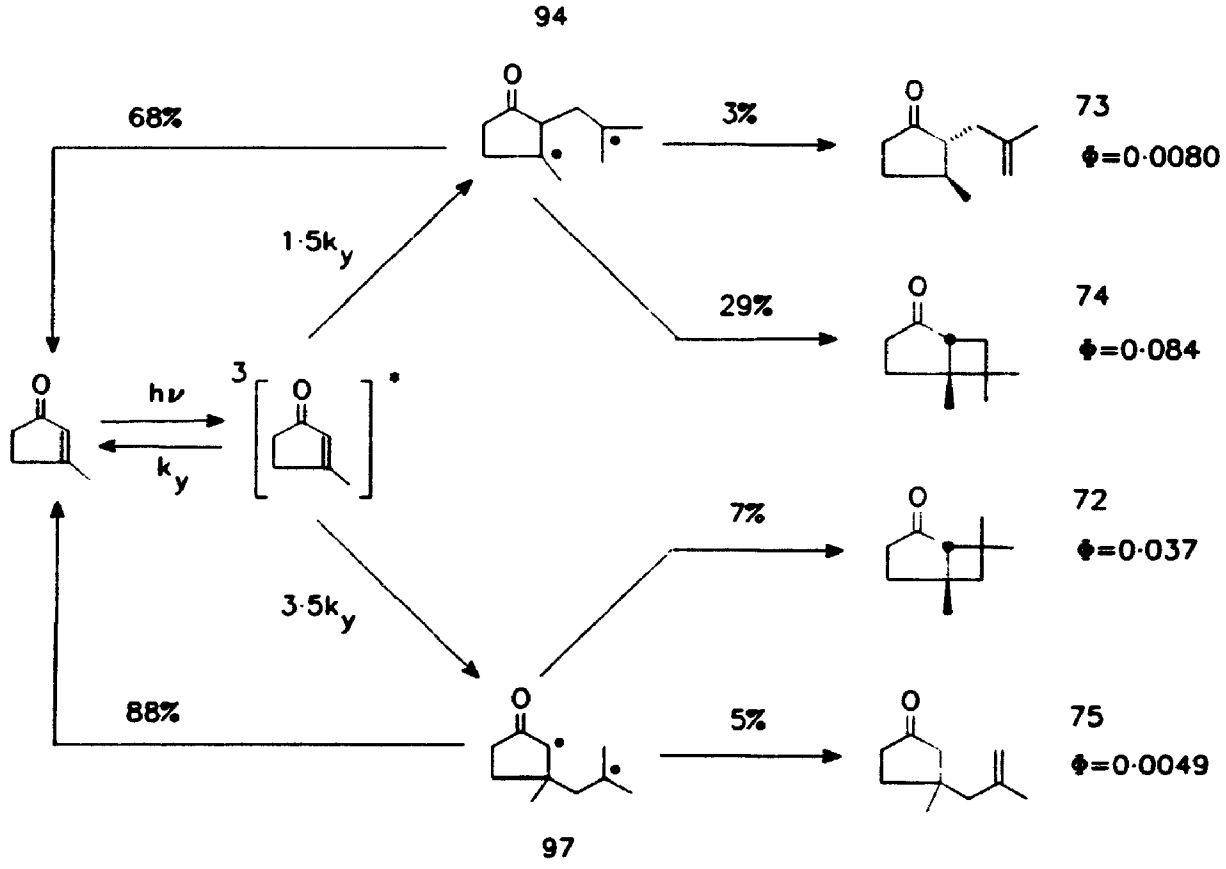

The contribution of the biradicals containing primary radical sites to product formation was ignored in the kinetic analysis of the photocycloaddition reactions of 2-methylpropene with 2-cyclopentenone and 3-methyl-2-cyclopentenone. This assumption is valid because the trapping experiments demonstrated that the rates of formation of biradicals **87**, **88**, **95**, and **96** was very slow compared to the rate of formation of the other biradicals. On the other hand, the significance of biradical **91** in the photocycloaddition of 2-methylpropene and 2-methylcyclopentenone could not be ignored.

The relative rate of formation of biradical **91** was, in fact, similar to the rate of formation of biradical **90**. Therefore, the kinetic analysis of this photocycloaddition reaction included the contribution from biradical **91** with regard to product formation.

The importance of biradical **91** in the photocycloaddition of 2-methylpropene and 2-methyl-2-cyclopentenone resulted in an unresolved kinetic ambiguity. This ambiguity developed when attempts were made to determine how much of cycloadduct **61** was the result of closure of biradical **91** and how much was the result of closure of biradical **90**. Scheme 31 demonstrates that some of the ρ_i^1 values which characterise each biradical are parametrically dependent on "x". This parameter is constrained only by the normalisation condition for the ρ_i^1 values associated with each biradical (i.e. $0 < x < 0.49$). The only way in which the kinetic ambiguity present in scheme 31 could be resolved would be to generate either biradical **90** or **91** independently and observe how much of the biradical resulted in product formation relative to how much resulted in formation of 2-methylcyclopentenone. This was not done.

The rate of formation of each biradical relative to the rate of decay of the enone triplet (k_y) was calculated from the slope/intercept ratio of the appropriate $1/\Phi$ versus 1/[O] linear regression analysis. For example, the slope/intercept ratio for the linear relationship defined by equation 5 is $(k_y\alpha_a)/k_a$. By substituting the value for α_a in to this ratio, it was possible to determine the ratio of k_y/k_a. Similarly, the ratio of the rate of triplet enone decay to the rate of biradical formation was determined for the other biradicals formed in all three of photocycloadditions studied. The rate of biradical formation relative to the rate of decay of each triplet enone are shown in Schemes 30, 31, and 32.

Using flash photolysis, Caldwell and co-workers measured the lifetime of the triplet state of 2-cyclopentenone at various enone concentrations in cyclohexane.[8] Equation 1 in Chapter 1 defines the concentration dependence of the rate of decay of triplet 2-cyclopentenone that was observed by Caldwell and co-workers. According to this equation, a 2-cyclopentenone concentration of 0.0401 M (the concentration used in the quantum yield determinations) results in an apparent first order rate constant of decay of 2.9×10^7 sec^{-1} for the triplet enone. By assuming that Equation 1 can also be applied to benzene solutions of 2-cyclopentenone, this rate constant was used to determine the absolute values of the rates of formation of biradicals **86** and **89** in benzene solution. It was found that the rates of formation of biradicals **86** and **89** are 2.6×10^7 and 4.9×10^7 $M^{-1}sec^{-1}$. The concentration dependencies of the triplet lifetimes of 2-methylcyclopentenone and 3-methylcyclopentenone have not been determined; therefore, absolute rate constants for the formation of the 1,4-biradicals generated in these systems could not be calculated.

The most obvious general conclusion that may be extracted from all the kinetic data presented in Schemes 30, 31, and 32 is that the major products formed in each of the photocycloaddition reactions do not originate from the biradicals formed at the fastest rates. In each of the three photocycloaddition reactions studied, the biradical formed by initial bonding at the 3-position of the enone had the fastest rate of formation; however, these β-bonded biradicals were responsible for the formation of the minor cycloaddition products. Schemes 30, 31, and 32 demonstrate that the β-bonded biradicals revert to starting materials more efficiently than the α-bonded biradicals. Therefore, the product distributions resulting from each photocycloaddition reaction are controlled by the way

each biradical partitions between reversion to starting materials and disproportionation or closure.

The fates of the biradicals generated in the cyclopentenone plus 2-methylpropene and 3-methylcyclopentenone plus 2-methylpropene systems are similar. The kinetic data presented in Schemes 30 and 32 indicate that the presence of the methyl group in biradicals **94** and **97** does not sterically hinder closure of these biradical relative to closure of biradicals **86** and **89**; in fact, a slightly greater fraction of biradicals **94** and **97** close to form cycloadducts compared to biradicals **86** and **89**. Thus, methyl substitution at the 3-position of 2-cyclopentenone does not seem to result in any significant effect on the photocycloaddition reaction with 2-methylpropene. The rates of formation of the biradical intermediates and the quantum yields of product formation are similar for the reaction of 2-methylpropene with triplet 2-cyclopentenone and triplet 3-methyl-2-cyclopentenone.

The pattern followed in the photocycloaddition reaction of 2-methylpropene with 2-methyl-2-cyclopentenone is significantly different from that observed in the other two photocycloaddition reactions studied. The β-bonded biradicals formed in the photocycloaddition reactions involving 2-cyclopentenone and 3-methyl-2-cyclopentenone each prefer closure over disproportionation. On the other hand, biradical **93**, which is formed in the photocycloaddition of in the 2-methylcyclopentenone and 2-methylpropene, favours disproportionation over closure by ratio of 5.4:1.0. In this system, closure of biradical **93** might by inhibited due to steric factors. If these steric factors are caused by the presence of the methyl group in biradical **93**, then why does the presence of a methyl group in biradcial **94** not seem to inhibit closure relative to biradical **86**?

In order to explain why steric factors might be responsible for inhibiting the closure of biradical **93**, it is useful to consider the hybridisation of the radical site on the enone component of the biradical. Biradical **93** has a radical site which is conjugated with the carbonyl group and therefore is probably sp^2 hybridised at the α-keto site. On the other hand, biradical **94** has a radical site located on the β-carbon of the enone. The hybridisation of this radical site might have more sp^3 character. It is possible that the steric hindrance caused by the methyl group in biradical **94** is much less significant than the steric hinderance caused by the methyl group in **93** because of the differences in hybridisation at the α- and β-positions of the enone. Therefore, the very low closure efficiency of biradical **93** may be a result of the increased steric hindrance associated with the methyl group at the sp^2 hybridised α-keto position of the biradical.

3.5 Conclusions

Hydrogen selenide was found to be an effective reagent for trapping the biradicals formed in the photocycloaddition reactions of 2-methylpropene with each of 2-cyclopentenone, 2-methyl-2-cyclopentenone, and 3-methyl-2-cyclopentenone. The products obtained from these trapping experiments were used to determine information about the structures and relative rates of formation of the biradicals formed in each reaction. It was found that the relative rates of formation of the biradical intermediates did not exert a pronounced influence on the product distribution obtained from each photocycloaddition. This conclusion is based on the observation that, in all cases, the

biradical formed at the fastest rate was responsible for the minor cycloaddition products; the major reaction products originated fror · the biradicals formed at slower rates. The way each biradical partitions between reversion to starting materials and closure or disproportionation was also determined. By comparing the relative fates of each biradical, it was possible to make draw conclusion the product distribution obtained from each photocycloaddition reaction is controlled primarily by the relative efficiencies of the reversion, disproportionation, and closure pathways available to each biradical. This conclusion disagrees with the Corey-de Mayo exciplex mechanism (see Chapter 1) which suggests that product distribution obtained from enone-alkene photocycloaddition reactions is determined prior to biradical formation.

The results obtained from the experiments described in this chapter did not permit any general conclusions to be made regarding the effect of alkyl-substitution at the 2- and 3-positions of 2-cyclopentenone on the reaction mechanism involving the photocycloaddition of 2-cyclopentenones and alkenes. The results obtained indicate that methyl substitution at the 3-position has little effect on the rates of formation of the biradical intermediates or their relative fates. However, the results also demonstrate that substitution at the 2-position of 2-cyclopentenone has a significant effect on the photocycloaddition reaction mechanism. In the case of the reaction between 2-methylpropene and 2-methyl-2-cyclopentenone, the relative rate of formation of the β-bonded biradical (93) is much greater than the relative rate of the β-bonded biradicals formed in the other two photocycloaddition reactions. In addition to having a greater relative rate of formation, biradical 93 closed less efficiently compared to the other β-bonded biradicals.

The effect of methyl substitution at the 2- and 3-positions of 2-cyclopentenone on the relative rates of biradical formation, as well as on the efficiencies of closure for each biradical, can be rationalised in terms of the increased steric hindrance caused by the presence of the substituent. It is possible than the steric hindrance caused by the methyl substituent in 2-methyl-2-cyclopentenone might be increased relative to that in 3-methyl-2-cyclopentenone due to difference in hybridisation at the 2- and 3-positions of the enone. If the 2-position of enone is more sp^2 in character, then the steric effects resulting from placing a methyl substituent at this site would be enhance. On the other hand, sp^3 hybridisation at the 3-position would decrease the steric hindrance at this centre. These steric arguments can be used to explain differences in the relative rates of biradical formation as well as differences in the relative efficiencies of biradical closure for the three systems studied.

3.6 References

1. Hastings, D. J.; Weedon, A. C. *J. Am. Chem. Soc.* **1991**, *113*, 8525.

2. (a) Crowley, K. J.; Erickson, K. L.; Eckell, A.; Meinwalld, J. *J. Chem. Soc. Perkin Trans. 1* **1973**, 2671. (b) Swenton, J. S.; Fritzen, E. L. *Tetrahedron Lett.* **1979**, 1951.

3. Geminal coupling constants of 17 to 19 Hz are typical for methylene protons located α with respect to a ketone in a five membered ring. See: Bovey, F. A. *Nuclear Magnetic Resonance Spectroscopy 2nd Ed.*, Academic Press Inc.: San Diego, 1988.

4. Bunce, N. J.; LaMarre, J.; Vaish, S. P. *Photochem. Photobiol.* **1984**, *39*, 531.

5. Al-Jallo, H. N. A.; Waight, E. S. *J. Chem. Soc., (B)* **1966**, 73.

6. Yamauchi, S.; Hirota, N. *J. Phys. Chem.* **1988**, *92*, 2129.

7. Wagner, P. J.; Bucheck, D. J. *J. Am. Chem. Soc.* **1969**, *91*, 5090.

8. Caldwell, R. A.; Tang, W.; Schuster, D. I.; Heibel, G. E. *Photochem. Photobiol.* **1991**, *53*, 159.

CHAPTER 4

2+2 PHOTOCYCLOADDITION OF 2-CYCLOPENTENONE AND *CIS*- AND *TRANS*-2-BUTENE: A MECHANISTIC INVESTIGATION OF STEREOCHEMISTRY

4.1 Introduction

The previous two chapters focused on the regiochemistry of the cycloadducts resulting from the photocycloaddition of cyclic enone and alkenes. In particular, these two chapters described investigations in which the factors controlling the regiochemistry of photocycloaddition reactions were studied. The main thrust of these regiochemical investigations centred on the fates and rates of formation of the biradical intermediates. In keeping with the general theme of investigating the nature of biradical intermediates, the purpose of the work described in this chapter was to study the effect of the biradical intermediates on the stereochemistry of the cycloadducts which result from enone-alkene photocycloaddition reactions.

It was demonstrated by de Mayo and co-workers that *cis* and *trans* symmetrically substituted alkenes add to 2-cyclopentenone to form structurally identical cycloadduct products.[1] The relative yield of formation of each stereoisomer resulting from these types of photocycloaddition reactions is, however, dependent on the stereochemistry of the alkene.[1] The fact that dissimilar product distributions are obtained for the photocycloaddition reaction of cyclic enones and *cis* and *trans* symmetrically substituted alkenes indicates that the relative rates of formation of the isomeric biradical

intermediates must be different. The idea that the fates of the biradical intermediates must be responsible for the dissimilar product distributions cannot be true since the structures of the biradicals formed from alkene geometrical isomers are identical.

Scheme 33

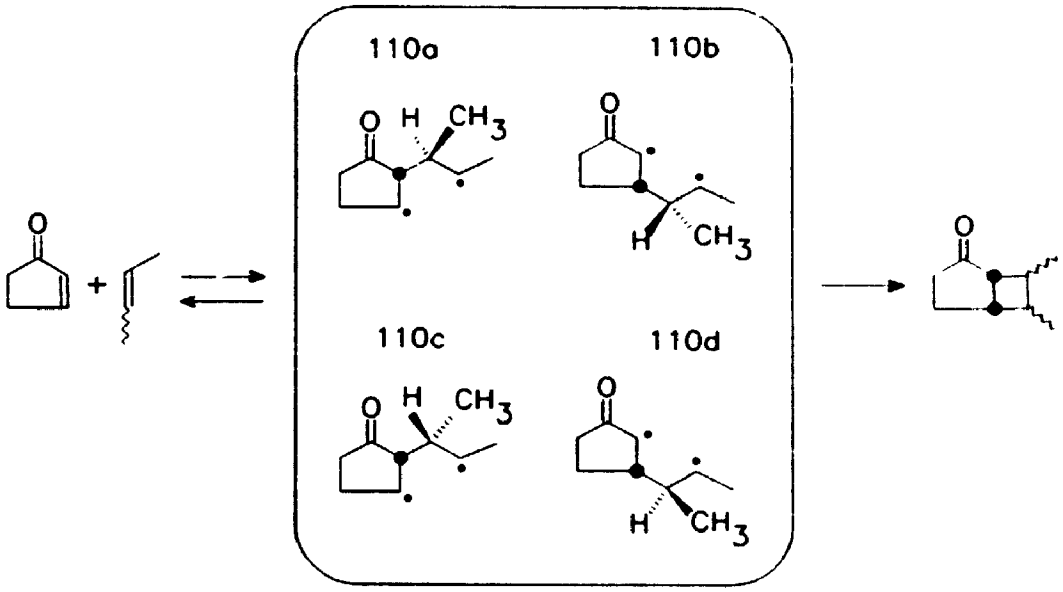

In the investigation described in this chapter, the rates of biradical formation in the photoreactions of *cis*- and *trans*-2-butene with triplet 2-cyclopentenone were studied. This was accomplished by using hydrogen selenide to trap the biradicals formed in each photocycloaddition reaction quantitatively. The four isomeric biradicals that could be formed in the photocycloaddition of *cis*- or *trans*-2-butene with 2-cyclopentenone are shown in Scheme 33. By determining the structure and relative yields of the products resulting from the trapping studies, we hoped to obtain information about the relative rates of formation of the biradicals from which the trapped products originated. In

addition to determining the rates of formation of these biradicals, we also hoped to determine the fates of the biradicals.

Some time ago, Bauslaugh suggested that the fates of biradicals could be influenced by the relative stabilities of the conformations available to each biradical.[2] In particular, Bauslaugh analyzed the conformations of the biradicals resulting from the photocycloaddition reaction of 2-cyclohexenone and 2-methylpropene in order to explain the formation of *trans*-fused cyclobutane adducts. Focusing on the head-to-tail cycloadducts, he suggested that conformation **111** would lead to a *trans*-fused adduct, **112** would lead to a *cis*-fused adduct, and **113** would give neither. He then used steric arguments to rationalise a greater stability for conformer **111** relative to conformer **112.**

111 112 113

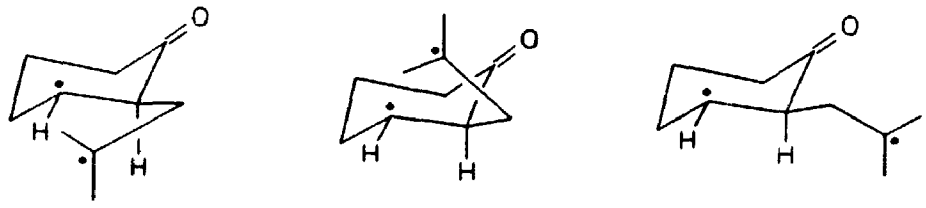

Therefore, the presence of the intrinsically less stable *trans*-fused cycloadduct was hypothesised to be due to the presence of a greater population of precursory biradicals possessing the conformation exemplified by structure **111.** In general, Bauslaugh concluded that the distribution of the products resulting from a photocycloaddition reaction is controlled by the relative populations of the conformations available to each biradical and by the ease with which each conformer closes to form each particular products. Bauslaugh did not, however, make any predictions regarding the control which the biradical conformation populations might exert over the relative rates of reversion and

closure for each biradical.

This chapter describes an attempt to investigate the structural factors which control the relative rates of reversion and closure for the biradicals shown in Scheme 33. By comparing the fates of the diastereomeric pairs of biradicals shown in this scheme, we hoped to determine if differences in the populations of the biradical conformers have an effect on the relative rates of reversion and closure. The diastereomeric pair of biradicals consisting of **110a** and **110c** as well as the pair consisting of **110b** and **110d** are excellent examples of biradicals which may be used to study conformational effects on the relative rates of reversion and closure. Both biradicals in each of these pairs differ only in the stereochemistry at two chiral sites, otherwise the intermediates are structurally very similar. Therefore, any difference in the fates of the biradicals comprising each diastereomeric pair may, in part, be attributed to differences in the relative energies of the conformations accessible to each biradical.

When analyzing the relative fates of biradical intermediates, it is important to remember that intersystem crossing from the triplet biradical surface to the singlet state surface must occur before the biradical is able to undergo fragmentation or closure. If the rate of intersystem crossing for a triplet biradical were independent of the biradical conformation then it would not be necessary to consider this process when investigating the effects of the relative stabilities of biradical conformations on the reversion and closure pathways available to each biradical. On the other hand, if the rate of intersystem crossing were dependent on the biradical conformation, the analysis would be much more difficult. In this latter case, the fate of each biradical would be dependent on the population of each biradical conformation as well as on the rate of intersystem

crossing from each triplet biradical conformation. The mechanistic implications of conformation dependent rates of triplet biradical intersystem crossing are discussed in detail in the Discussion Section of this chapter.

4.2 Results

4.2.1 Photocycloaddition of 2-cyclopentenone with *cis*- or *trans*-2-butene

The irradiation of a solution containing 2-cyclopentenone (0.10 mol/L) and *cis*-2-butene (1.5 mol/L) in benzene resulted in the formation of the four products **114a**, **114b**, **114c**, and **114d** in the ratio 43:44:2.2:12. Similarly, the irradiation of a benzene solution containing 2-cyclopentenone and *trans*-2-butene resulted in the formation of the same four products but in the ratio 50:29:2.1:19. These products are shown in Scheme 34. The product ratios were determined under conditions in which insufficient Schenck isomerisation of the 2-butene had occurred to perturb the relative yield of each cycloadduct.

Compounds **114b** and **114d** were isolated 90 and 92% pure respectively by chromatography on silica gel. The impurities consisted of minor amounts of the other cycloadducts. Compound **114a** was isolated in mixture consisting of **114a**, **114b** and **114d** in a 72:15:13 ratio. Characterisation of **114a** was accomplished by analysis of this mixture. The very low relative yield of **114c** made it impossible to isolate chromatographic fractions significantly enriched in this compound. Therefore, this particular compound was synthesised by an independent method and then the spectral properties of the pure compound were compared with the spectral features of mixtures containing **114c** isolated from the photocycloaddition reaction mixture (*vidi infra*).

Scheme 34

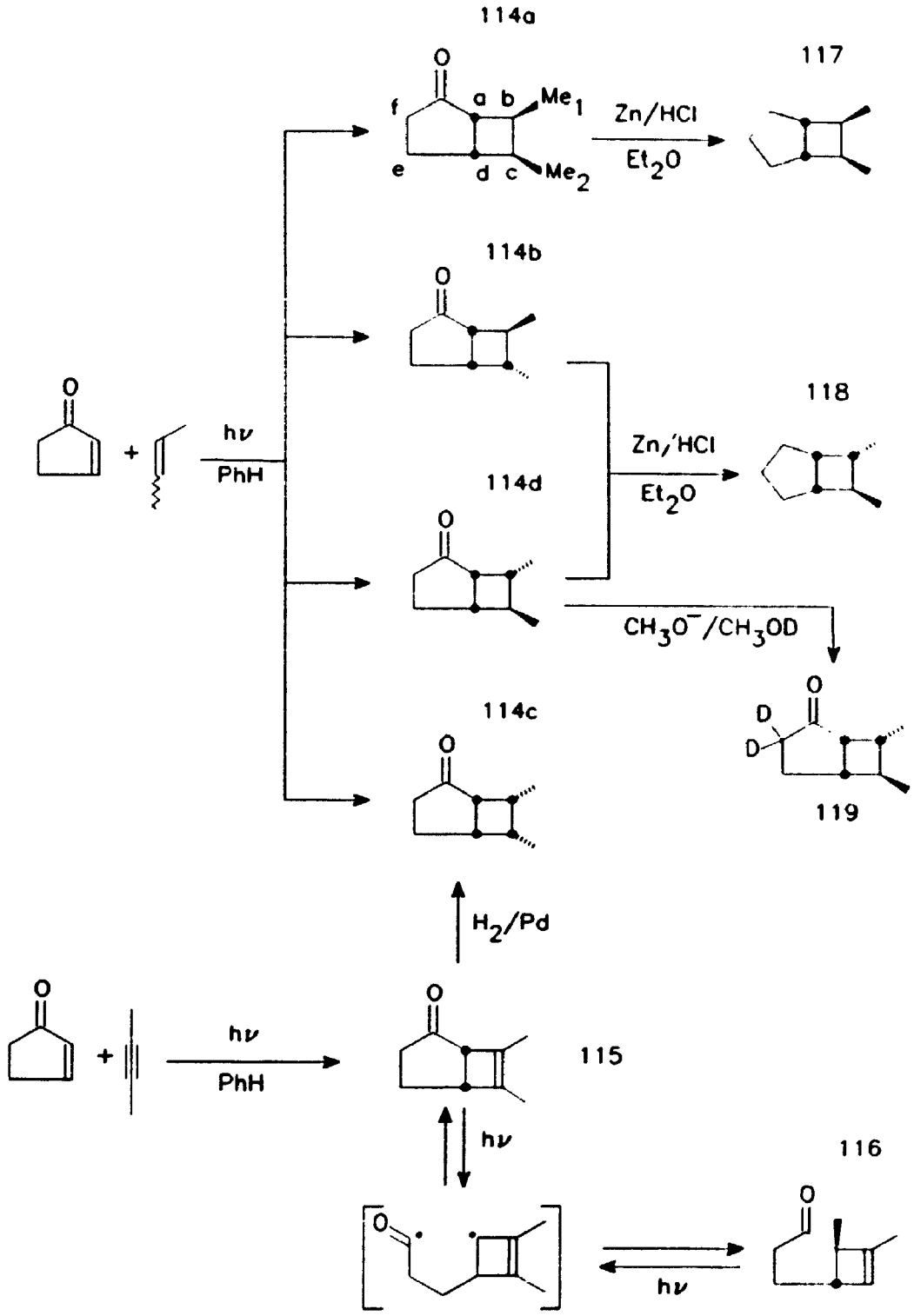
114a
117
Zn/HCl
Et2O
114b
118
Zn/HCl
Et2O
114d
CH3O⁻/CH3OD
114c
119
hν
PhH
H2/Pd
115
hν
116
hν
PhH

Each of the four products exhibited ^{13}C nmr spectra and mass spectrum fragmentation patterns that were indicative of 2+2 enone plus alkene cyclobutane adducts; however, these spectroscopic methods were of little use in analyzing the stereochemistry of **114a**, **114b**, **114c**, and **114d**. The methods used to determine the stereochemistry of the four photocycloadducts are described below.

The stereochemistry of the minor product resulting from both cycloadditions was determined by preparing an authentic sample of compound **114c** and then comparing the g.c. retention times and spectroscopic properties of the minor product observed in the cycloadditions with the corresponding properties of the authentic sample. The authentic sample of **114c** was prepared by irradiating 2-cyclopentenone with ultra-violet light in the presence of 2-butyne and then reducing the resulting cycloadduct in a metal surface catalysed hydrogenation reaction (see Scheme 34).

The products resulting from the photocycloaddition reaction between 2-cyclopentenone and 2-butyne have been characterised previously by Criegee and Furrer.[3] Criegee et al. also demonstrated that a considerable amount of secondary photolysis occurs during the photocycloaddition reaction due to the Type I cleavage of product **115**. This α-carbonyl bond cleavage results in the formation of **116**. We were able to improve the ratio of **115**:**116**, which was found by Criegee et al. to be 2:1, to 10:1 by using a $SnCl_2$ in 10% HCl/H_2O light filter during the photocycloaddition. This light filter minimises the light absorbed by the primary photo-product . The palladium metal catalysed hydrogenation of **115** resulted in the formation of two products, **114c** and **114a**, in a 93:7 ratio. Due to the fact that *exo* approach of **115** to the catalyst surface is much less sterically hindered relative to *endo* approach, the major product (**114c**) was

assigned the *endo,endo*-dimethyl stereochemistry.

The ketone functionality of each of **114a**, **114b**, and **114d** was reduced to a methylene group as part of the stereochemical elucidation of these compounds. A modified Clemensen reduction of each of compounds **114b** and **114d** resulted in the formation of one product, compound **118** (see Scheme 34). Identification of **118** was facilitated by comparison of the ^{1}H nmr spectrum of the product with the ^{1}H nmr spectrum of **118** reported in the literature.[4] The presence of two methyl doublets in the ^{1}H nmr spectrum of **118** indicates that the molecule does not belong to the C_s symmetry group. On the other hand, the reduction of the carbonyl group in **114a** under the same conditions used to reduce the ketone functionality of **114b** and **114d** resulted in the formation of **117**. The presence of a single methyl doublet in the ^{1}H nmr spectrum of this compound indicated that the molecule was in fact symmetrical. The ^{1}H nmr spectroscopic properties of **117** were identical to those reported in the literature.[4] Therefore, these reduction studies indicate that cycloadducts **114b** and **114d** have a stereochemistry in which the methyl groups are *trans* with respect to one another and that cycloadduct **114a** has a stereochemistry in which the methyl groups are mutually *cis*.

The relative stereochemistry of **114b** and **114d** was obtained by performing ^{1}H nmr NOE difference experiments on these compounds. Before these experiments could be conducted, it was necessary to assign the resolved proton resonances in the ^{1}H nmr spectra of the two compounds. For example, the proton resonance at 2.81 ppm in the ^{1}H nmr spectrum of **114b** was assigned to Hd. This assignment was based on the fact that this resonance (a quartet, J=7.2 Hz, of doublets, J=3.6 Hz) did not exhibit a large geminal coupling constant and was not decoupled by irradiation of either methyl doublet.

The fact that this proton was coupled to four other vicinal protons with relatively large coupling constants excluded the possibility that the resonance at 2.81 ppm might be due to Ha.

In order to simplify the ^{1}H nmr spectrum of cycloadduct **114d** the methylene protons α to the carbonyl group were exchanged for deuterons under conditions utilising base catalysis (see Scheme 34).[§] The ^{1}H nmr spectrum of the exchanged product, compound **119**, revealed three well separated methine proton resonances. Each of these methine protons was assigned based on the results of decoupling experiments. A doublet (9.9 Hz) of doublets (8.6 Hz) of quartets (7.0 Hz) at 2.12 ppm was assigned to proton Hb, the doublet (1.4 Hz) of quartets (6.5 Hz) at 2.45 ppm was assigned to Hd, and a doublet (9.9 Hz) of doublets (6.5 Hz) at 2.63 ppm was assigned to Ha. Having assigned proton Hb, it was possible to use the results of the ^{1}H-^{1}H nmr decoupling experiments to assign each methyl doublet to either Me1 or Me2 (see Scheme 34 for assignment). It was found that an assignment of Me1 to a doublet at 0.91 ppm and an assignment of Me2 to a doublet at 1.12 were consistent with the decoupling experiment results. Therefore, all of the resolved resonances in the ^{1}H nmr spectrum of **119** were assigned.

The relative magnitude of the NOE enhancement observed at each of the ^{1}H nmr resonances assigned to Ha, Hb, Hd in compound **119** was determined when the doublets assigned to Me1 and Me2 were irradiated. In addition, the relative magnitude of the NOE enhancement observed at the ^{1}H nmr resonance assigned to Hd in compound **114b**

[§] Integration of the ^{1}H nmr spectrum of product **119** revealed that the methine proton α to the carbonyl was not exchanged. This proton is less acidic than the methylene protons due to the fact that the methine carbon is locked in the sp^3 geometry and cannot adopt the planar geometry necessary for enolate stabilization.

was also determined when each methyl doublet was irradiated. The results obtained from the NOE ^{1}H nmr experiments are summarised in Table 14. The relative NOE results in Table 14 indicate that cycloadduct **114d** has a closer spacial relationship between Me2 and proton Hd compared to cycloadduct **114b**. This indicates that the methyl group denoted as Me2 is *syn* with respect to Hd in cycloadduct **114d** and *anti* in cycloadduct **114b**. In addition to this, the lack of an NOE observed at Ha of cycloadduct **114d** when the methyl protons designated Me1 were irradiated indicates that *anti* stereochemical relationship exists between these groups. Therefore, it was concluded that the stereochemistry of the methyl groups in compounds **114d** and **114b** is *exo,endo*-6,7-dimethyl and *endo,exo*-6,7-dimethyl, respectively.

Table 14: Results of ^{1}H nmr NOE difference spectroscopy (in $CDCl_3$) for cycloadducts **114b** and deuterated **114d** (i.e. **119**).

Signal irradiated	Relative Magnitude of NOE Observed[a]		
	Ha	Hb	Hd
Compound **114b**			
Me1	NR	NR	none
Me2	NR	NR	none
Compound **119** (**114d**-d_2)			
Me1	none	large	none
Me2	small	large	large

[a] NR indicates that the particular resonance was not resolved.

The lanthanide shift reagent tris(1,1,1,2,2,3,3-heptafluoro-7,7-dimethyl-4,6-octanedionato) europium (III), abbreviated as $Eu(fod)_3$, was useful in separating overlapping proton resonances in the ^1H nmr spectra of each cycloadduct. This facilitated the measurement of various ^1H-^1H nmr coupling constants. However, the importance of these coupling constants in assigning the stereochemistry of cycloadducts **114a**, **114b**, **114c** and **114d** was significantly diminished by the fact that the magnitudes of the coupling constants between vicinal methine protons around the cyclobutane ring are very sensitive to changes in the dihedral angles associated with the two puckered conformations of the 4-membered ring. That is to say, the *syn* and *anti* vicinal coupling constants depend on the dihedral angle between the coupled protons which in turn is dependent on the particular conformation of the cyclobutane ring adopted. Molecular mechanics computer modelling packages such as PCMODEL[5] show that the deviation from planarity (see the diagram below) of the cyclobutane ring in a 2-bicyclo[3.2.0]heptanone is as large as 16°. When the conformation of the cyclobutane

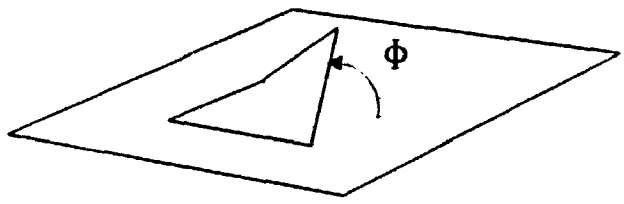

ring flips, the corresponding change in the dihedral angles that define the four membered ring is 32°. In the case of 2-bicyclo[3.2.0]heptanone, the angle between vicinal *anti* protons in one conformation is 110° while the angle between the same protons in the other conformation is 145°; hence, large changes in the ^1H-^1H vicinal anti coupling constants can accompany changes in the conformation of the cyclobutane ring. These

dihedral angle changes are consistent with other cyclobutane systems reported in the literature.[6]

The conformational dependence of the anti coupling constants makes stereochemical determination of the adducts difficult. Based on the simple Karplus equation, *anti* vicinal coupling constants should be significantly smaller than *syn* coupling constants in one ring conformation while in the other ring conformation vicinal *syn* and *anti* coupling constants should be similar. The coupling constants for some of the protons in adducts **114a**, **114b**, and **114d** which are listed in Table 15 demonstrate the lack of uniqueness possessed by *anti* and *syn* coupling constants.

Table 15: ^{1}H nmr vicinal coupling constants (in Hz) for the cyclobutane methine protons in the cycloadducts resulting from the photoaddition of 2-cyclopentenone and 2-butenes.

J	114a	114b	114c	114d
J_{ab}	4	7	9	10
J_{ad}	7		8	7
J_{bc}	7	7	9	9
J_{cd}	7		9	7

The coupling constant labelled J_{ab} in Table 15 did offer supportive evidence for the stereochemical assignment of cycloadduct **114a**. This coupling constant was assigned by analyzing the multiplicity of the signal attributed to Hb in the ^{1}H nmr spectrum of **114a**. Resonance Hb was identified as a quintet (J=7.2 Hz) of doublets (J=3.8 Hz). The assignment of Hb was confirmed by the fact that decoupling one of the methyl

doublets resulted in a collapse of the Hb resonance to a doublet (J=7.2 Hz) of doublets (J=3.8 Hz) as well as by the fact that decoupling the proton assigned Hd had no effect on Hb. In the presence of $Eu(fod)_3$, a sextet with J=7 Hz was observed in the ^1H nmr spectrum of **114a**. This resonance was assigned to Hc. The small coupling constant of 3.8 Hz was assigned to J_{ab} and not J_{bc} since irradiation of the resonance assigned to Hc did not affect the 3.8 Hz coupling observed for Hb. The only stereochemistry in which J_{ab} could be this small is one in which Hb and Ha exist in an *anti* relationship. Therefore, the magnitude of J_{ab}, in conjunction with the results obtained from the zinc metal reduction of **114a**, indicates that the stereochemistry of the methyl groups of **114a** is *exo,exo*-6,7-dimethyl.

The addition of shift reagent is useful not only in dispersing overlapped ^1H nmr resonances but also in determining the spacial relationship between the site of complexation and the various protons in a cyclobutane adduct. When the lanthanide ion complexes with a basic functional group in the adduct such as a ketone, the dipolar magnetic field of the lanthanide ion induces resonance shifts ($\Delta\delta_i$) that obey the geometrical dependence given by the McConnel-Robertson equation:[7]

$$\Delta\delta_i = K\frac{3\cos^2\phi_i - 1}{r_i^3} \qquad (6)$$

In this equation, K is a constant, r_i is the distance between nucleus *i* and the lanthanide ion, and Φ_i is the angle between the lanthanide ion-nucleus *i* vector and the bond defined by the coordination of the lanthanide with the function group. Equation 6 demonstrates that the lanthanide induced shifts (LIS) observed in an nmr spectrum are very dependent on the geometry with which the shift reagent coordinates to the molecule of interest. The

equation also predicts that structurally similar compounds will exhibit comparable LIS for ^{1}H nmr resonances that originate from protons possessing similar spacial relationships with respect to the site of lanthanide coordination.

Due to the structural similarity of cycloadducts **114a**, **114b**, **114c**, and **114d**, this series of compounds is a good example of a system in which valuable information could be gained by studying the relative change in chemical shift experienced by each ^{1}H nmr signal in the presence of Eu(fod)$_3$. The stereochemistry of each cycloadduct results in different spacial proximities for the methyl groups with respect to the site of lanthanide coordination. The position of one of the methyl groups in some pairs of cycloadducts is similar; for example, MeI in compounds **114c** and **114d** occupy the same region of space relative to the ketone oxygen. The LIS experienced by protons exhibiting similar spacial relationships will be similar according to the McConnel-Robertson equation. Therefore, in order to obtained additional evidence for the stereochemistry of each of the cycloadducts obtained in the photocycloaddition of 2-cyclopentenone and the 2-butenes, the LIS of the various ^{1}H nmr signals observed in the spectrum of each adduct were measured.

The experiments were carried out by adding successive amounts of Eu(fod)$_3$ to C_6D_6 or $CDCl_3$ solutions of a particular compound and observing the ^{1}H nmr spectrum of the compound after each addition. The change in the chemical shift of each proton ($\Delta\delta_i$), relative to its position in the ^{1}H nmr spectrum obtained in the absence of shift reagent, was then plotted against the change in the chemical shift of the *reference proton* ($\Delta\delta_r$). The reference proton was chosen as Hd since rigidity of the bicyclo[3,2,0]hepta-2-one ring system at this point ensured that this proton would have the same spacial

relationship with respect to the ketone functionality in each cycloadduct. In all cases, linear functions with linear correlation coefficients greater than 0.995 were obtained when $\Delta\delta_i$ was plotted against $\Delta\delta_r$. Figure 4 contains a plot of the change in chemical shift observed for each proton resonance in the ^1H nmr spectrum of **114c** relative to the proton Hd, that was caused by the addition of $Eu(fod)_3$ to a solution of the cycloadduct. The gradients of these plots are referred to as relative shift factors. The relative shift factors experienced by the protons in each of the cycloadducts are listed in Table 16.

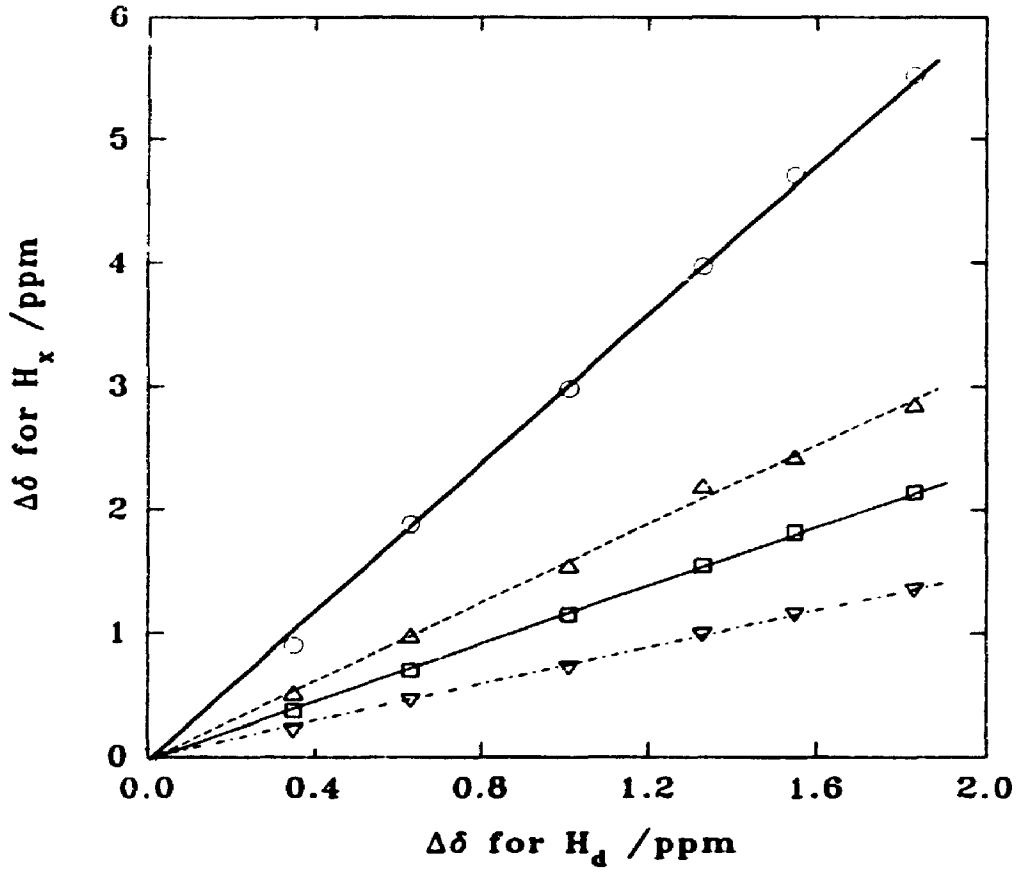

Figure 4: A plot of the change in chemical shift of proton Hx versus the change in chemical shift of proton Hd resulting from successive additions of $Eu(fod)_3$ to a $CDCl_3$ solution of compound **114c**. ○ represent Ha; △ represent Me1; □ represent Hb; and, ▽ represent Me2.

Table 16: Lanthanide induced chemical shift factors exhibited by the protons of cycloadducts **114a**, **114b**, **114c**, and **114d** relative to the chemical shift of the reference proton Hd.

Compound	Ha	Hb	Hc	Me1	Me2
114a	2.86	1.77	note a	0.68	0.46
114b	2.86	1.71	note a	0.71	0.54
114c	3.03	1.18	0.78	1.64	0.70
114d	2.94	1.12	note a	1.62	0.53

[a]The chemical shifts of these resonances were too obscured by other overlapping resonances to allow an accurate determination of the change in chemical shift of the resonance upon addition of shift reagent.

The relative shift factors summarised in Table 16 demonstrate that the proton Hb in cycloadducts **114a** and **114b** occupies the same region of space relative to the site of coordination of the lanthanide ion. Similarly, the relative shift factors for the Me1 resonance in cycloadducts **114a** and **114b** indicate that this methyl group must have the same stereochemical relationship in each of these cycloadducts. On the other hand, the relative shift factors exhibited by the Me1 resonance in the ^{1}H nmr spectra of cycloadducts **114c** and **114d** suggest that the stereochemical relationship of this methyl group is similar for **114c** and **114d** but different from the relationship exhibited by **114a** and **114b**. When the relative shift factors are put into the context of the other evidence use to assign the stereochemistry of the four cycloadducts, a consistent set of conclusions can be drawn. That is to say, the evidence obtained from the shift reagent studies discussed above is consistent with the evidence obtained from the ^{1}H NOE difference experiments and the coupling constant analysis. Therefore, the results obtained from the shift reagent study explicitly require that Ha and Hb have an *anti* stereochemical

relationship in **114a** and **114b** while the stereochemical relationship of these protons in **114c** and **114d** must be *syn*.

The shift reagent studies did not provide any evidence regarding the stereochemistry of the methyl group labelled Me2. The relative shift factors observed for the resonance originating from these protons did not result in any consistent trend among the four cycloadducts. Methyl group Me2 is considerably further away from the ketone functionality compared to the methyl group labelled Me1. The increased distance from the site of lanthanide ion complexation makes this group less sensitive to the presence of the shift reagent. Consequently, changes in the relative stereochemistry of this group did not result in large or consistent changes in the relative shift factor. Therefore, the relative shift factors of the Me2 group did not provide any support for the stereochemical assignment of each cycloadduct.

4.2.2 Quantum yield measurements

The dependence of the quantum yield of cycloadduct formation on the concentration of alkene in the cycloaddition reactions between cyclopentenone and each of *cis*-2-butene and *trans*-2-butene was determined. The conversion of 2-cyclopentenone was kept below 4% so that the formation of products resulting from the secondary photochemistry of the cycloadducts and Schenck isomerisation of the 2-butene did not interfere with the quantum yield determination. Figure 5 illustrates the total cycloaddition quantum yield as a function of the concentration of these alkenes. Figure 6 demonstrates that the reciprocal of the total quantum yield of product formation in the cycloaddition reaction is a linear function of the reciprocal of the concentration of the

2-butene. The product ratios observed in the addition of each 2-butene to 2-cyclopentenone were not dependent on the concentration of the alkene; therefore, the quantum yield of formation of each cycloadduct was calculated by multiplying the total quantum yield of product formation by the relative yield (normalised to 1.00) of each particular cycloadduct. The slope and intercept parameters corresponding to plots of the reciprocal of the quantum yield of formation of each cycloadduct versus the reciprocal of the 2-butene concentration were also calculated. These parameters were obtained by dividing the corresponding slope and intercept linear regression parameters determined for the plots illustrated in Figure 6 by the relative products yields of each particular adduct. Table 17 contains a summary of the regression parameters calculated from the double inverse plots illustrated in Figure 6.

Table 17: Linear regression parameters for plots of the inverse of the quantum yield of product formation versus the inverse of the alkene concentration (in M) for the photocycloaddition reaction of 2-cyclopentenone (0.0278 M) with 2-butene in benzene solution.

Cycloadduct (alkene)	Relative Yield (%)	slope (m) in $Lmol^{-1}$	intercept (b)	1/b	Correlation Coefficient
All products (E-2-butene)		1.71±0.05	2.5±0.2	0.40	0.9902
114a	50.2	3.4±0.1	4.9±0.4	0.20	
114b	28.5	6.0±0.2	8.7±0.7	0.11	
114c	2.1	81.0±2.4	117±9	0.0085	
114d	19.2	8.9±0.3	13±1	0.077	
All products (Z-2-butene)		0.71±0.02	2.7±0.2	0.37	0.9934
114a	42.6	1.66±0.04	6.3±0.5	0.16	
114b	43.5	1.63±0.04	6.2±0.5	0.16	
114c	2.2	32.2±0.8	123±9	0.0081	
114d	11.7	6.1±0.2	23±2	0.043	

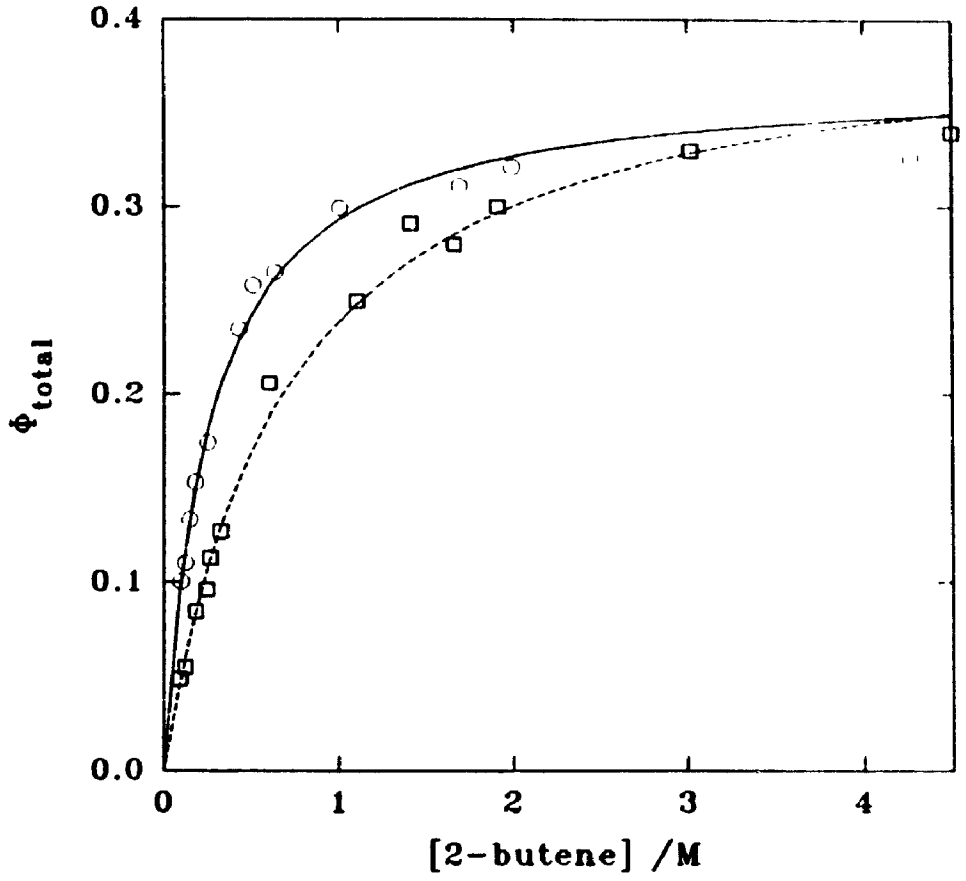

Figure 5: Dependence of the quantum yield of cycloadduct formation on the alkene concentration for the photoaddition 2-cyclopentenone and 2-butenes in benzene. o represent measurements for *trans*-2-butene; □ represent measurements for *cis*-2-butene.

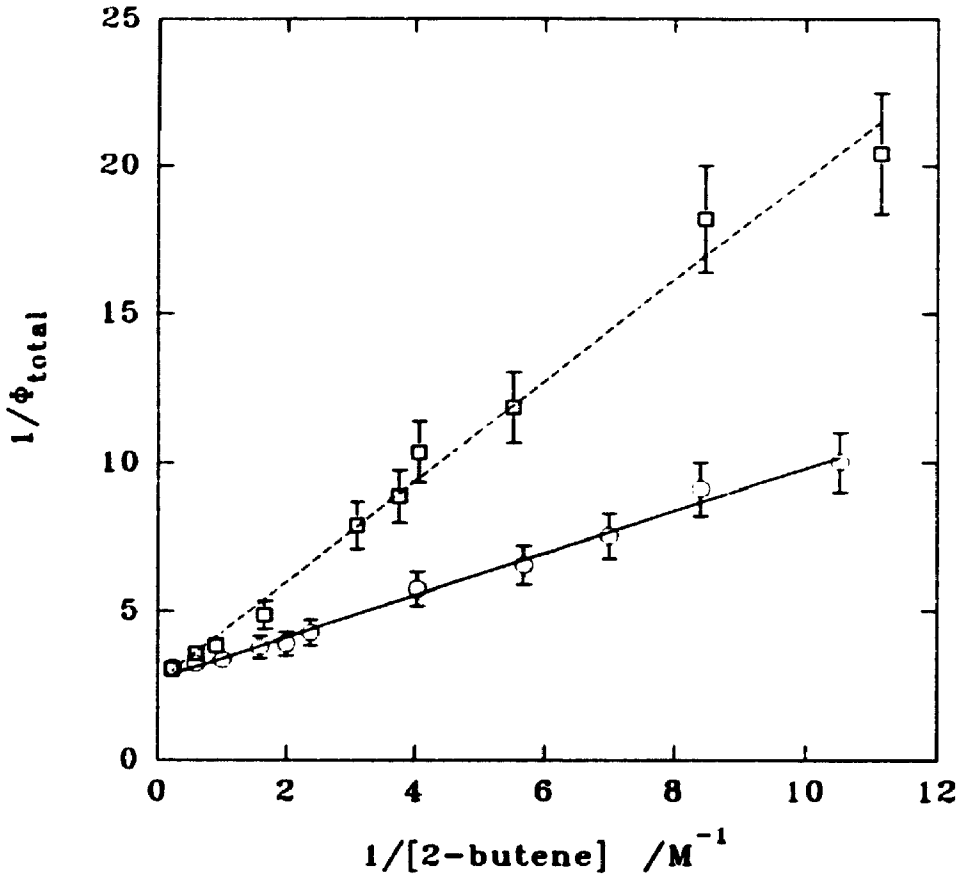

Figure 6: Plot of the reciprocal of the quantum yield of cycloadduct formation versus the reciprocal of the alkene concentration for the photocycloaddition of 2-cyclopentenone and 2-butenes in benzene. See Figure 5 caption for an explanation of the symbols.

4.2.3 Biradical Trapping with H_2Se

The UV light irradiation of a benzene solution of cyclopentenone (0.1 M) containing either *cis* or *trans*-2-butene (1.5 M) and H_2Se (0.3 M) with Pyrex filtered light from a 400 W Hanovia medium pressure mercury lamp resulted in the formation of the products **120** to **128** (see Scheme 35). No evidence of the formation of cycloadducts **114a** to **114d** was detected by coupled g.c./m.s. in these experiments. The relative yields of these products were determined by g.c. (FID detector) at 5% conversion of cyclopentenone. The relative product yields for **120**, **121**, **122**, **123**, **124**, **125**, **126**, and **127+128** combined when *cis*-2-butene was added to the triplet excited state of 2-cyclopentenone were found to be 2.3%, 2.0%, 13.2%, 10.3%, 2.1%, 2.0%, 12.6%, and 55.5%, respectively. The relative yields of the same compounds when *trans*-2-butene was used instead of *cis*-2-butene were 1.4%, 1.2%, 9.1%, 10.2%, 2.4%, 2.4%, 13.7%, and 59.6%, respectively.

Unfortunately, all attempts to isolate **120** and **124** as pure compounds were unsuccessful. The compounds could, however, be resolved on an analytical capillary G.C. column and so separate mass spectra were obtained. The mass spectra of **120** and **124** were found to be identical. The parent ion found at m/e=138 indicated that both **120** and **124** must have resulted from the disproportionation of a partially trapped biradical. The observation of fragments with m/e 82(100%) and 81(60%) suggested that the unsaturation was probably within the cyclopentanone ring. If the unsaturation were in the side chain then fragments with m/e 83 and 84 would be expected. The structural assignments of **120** and **124** were also confirmed by the ^1H nmr spectral data. The ^1H nmr spectrum of a 1:3 mixture of **120** and **124** contained a complicated multiplet centred

Scheme 35

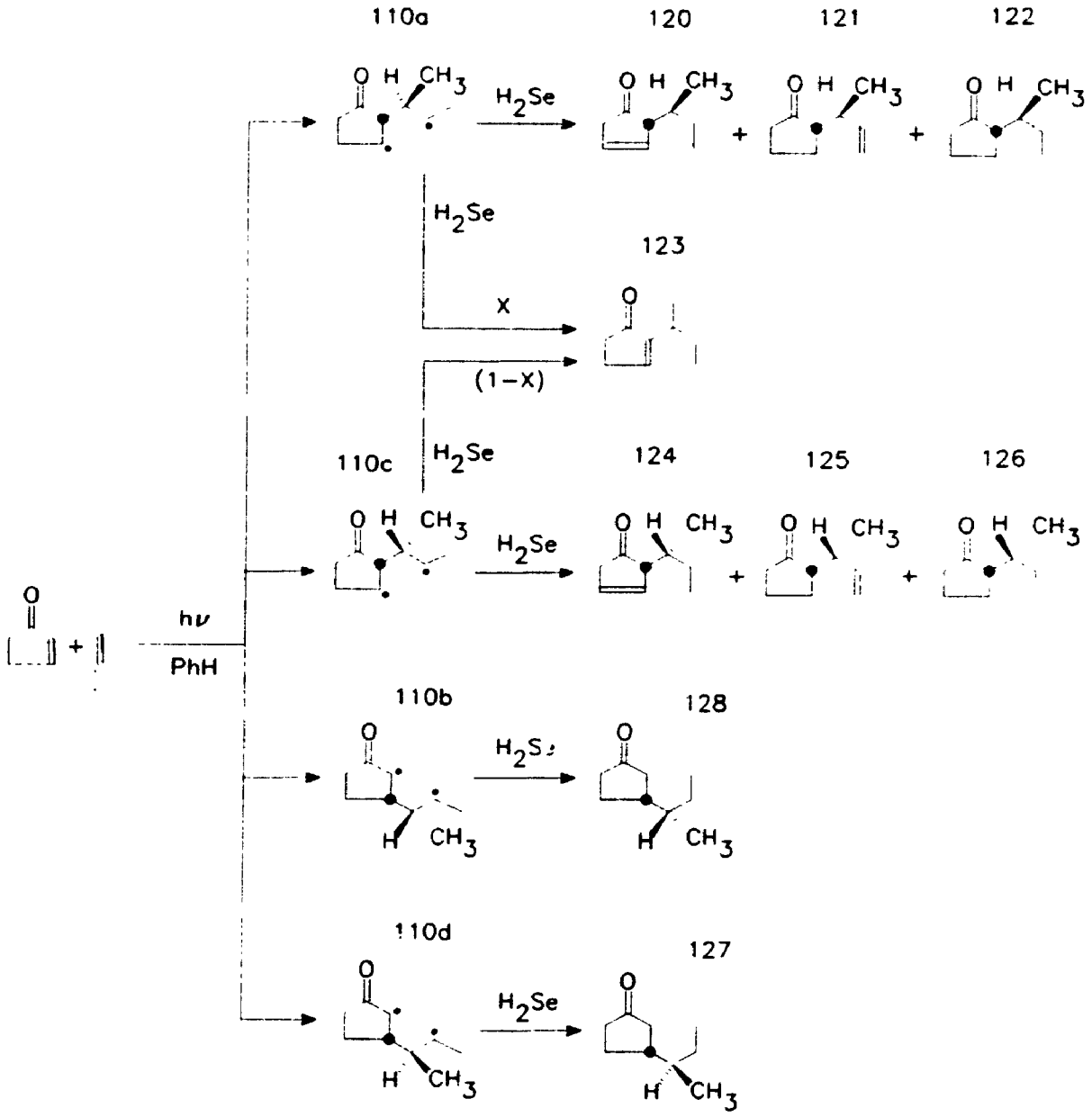
110a
120
121
122
H2Se
H2Se
123
X
(1−X)
110c
H2Se
124
125
126
hν
PhH
110b
128
H2Se
110d
127
H2Se

at 6.09 ppm which is characteristic of cyclopentene olefinic protons.[8] The ^{1}H nmr spectrum of the mixture also contained 2 triplets (0.93 and 0.85 ppm) and 2 doublets (0.74 and 0.97 ppm) each of which integrated for 3 protons. These resonances are obviously all due to methyl groups. The fact that 4 methyl groups with the chemical shifts and multiplicities noted above were observed in the ^{1}H nmr spectrum of the mixture of **120** and **124** is direct evidence against the possibility of side chain unsaturation in either compound.

Hydrogenation of the 1:3 mixture of **120** and **124** resulted in the formation of a 1:3 mixture of compounds **122** and **126** respectively. The stereochemistry of compounds **122** and **126** was positively determined by techniques discussed below. Based on the relative ratio of **120** to **124** in the starting mixture and the relative ratio of **122** to **126** in the product mixture, it was concluded that **120** hydrogenates to form **122** and **124** hydrogenates to **126**. Also, treatment of **120** and **124** with sodium methoxide (0.15 mole/L) in methanol resulted in 100% conversion to **123** in 20 minutes. The structure of **123** was characterized by nmr and mass spectral data (see later discussion). Therefore, based on the chemical and spectroscopic evidence presented above, the structures of **120** and **124** were confirmed.

Compounds **121** and **125** were also not isolated as pure compounds but rather as a 1:3.5 mixture. The mass spectra of these compounds were identical and included peaks with m/e 138(34%) and 84(100%). The parent ion mass indicated that both **121** and **125** were the result of disproportionation of partially trapped biradicals. The major fragment ion indicated that the double bond was probably in the side chain. The nmr spectra of the mixture of **121** and **125** confirmed the position of the double bond and the

regiochemistry of the side chain. The presence of two methyl doublets and the lack of two methyl triplets in the ^{1}H nmr spectrum indicated that the **121** and **125** must contain a monosubstituted double bond. The APT ^{13}C nmr spectrum of the mixture also confirmed the position of the double bond as two olefinic methylene resonances at 114.8 and 113.4 ppm and two methine resonances at 142.0 and 140.0 ppm were observed. The regiochemistry of substitution on the 5-membered ring was proven by the fact that in the ^{13}C nmr spectrum the two furthest down-field resonances (54.0 and 53.4 ppm), excluding vinyl and carbonyl resonances, had multiplicities representative of methine carbons. These resonances were assigned to the α-keto carbons that bear the substituent groups. Palladium surface catalysed hydrogenation of the 1:3.5 mixture of **121** and **125** resulted in the formation of a 1:3.5 mixture of **122** and **126**. Therefore, it was concluded that **121** has the same stereochemistry as **122** and that **125** has the same stereochemistry as **126**.

Compounds **122** and **126** were separated in a series of multiple chromatographic separations on silica gel. The mass spectra of the compounds indicated that they originated from two fully reduced biradicals. The APT ^{13}C nmr spectra of **122** and **126** confirmed that these compounds possess a regiochemistry representative of substitution at the carbonyl α-carbon in the cyclopentanone ring. This conclusion is based on the fact that the furthest down-field resonances in the ^{13}C nmr spectra of **122** and **126**, excluding carbonyl resonances, were found at 54.6 and 53.0, respectively, and both of these resonances were methines. Based on the chemical shifts of these methine resonances relative to the other resonances in the ^{13}C nmr spectra of **122** and **126**, these signals were assigned to the α-position of the cyclopentanone ring.

Scheme 36

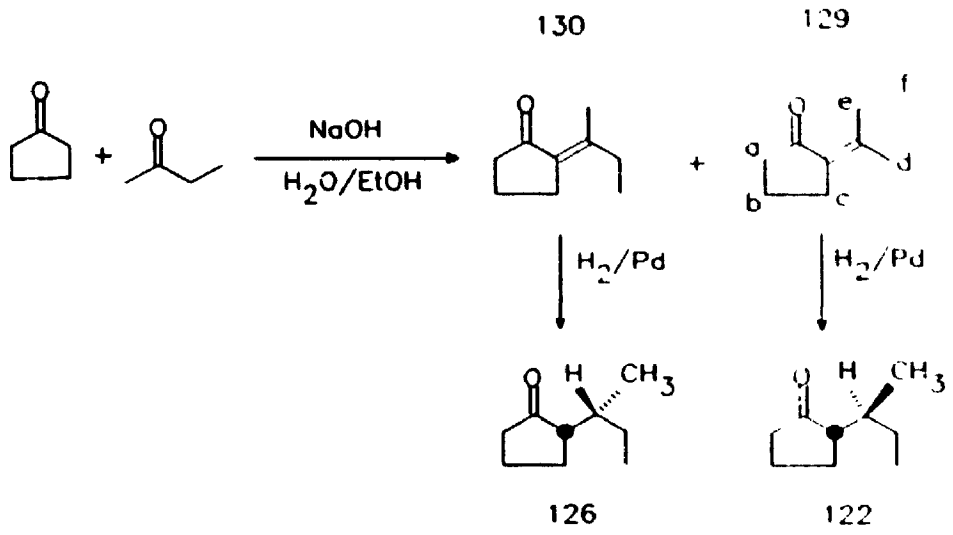

The similarities of the nmr spectra of compounds **122** and **126** made it impossible to distinguish between the two relative stereochemical configurations possible for the diastereomeric pair. In order to correctly identify these compounds, *E*- and *Z*-2-sec-butylidenecyclopentanone (**130** and **129** respectively) were prepared, isolated, and then reduced by catalytic hydrogenation to yield the two diastereomers requiring identification. Scheme 36 demonstrates that *E*-2-sec-butylidenecyclopentanone gives the corresponding R,S (and S,R) diastereomer and that *Z*-2-sec-butylidenenecyclopentanone gives the corresponding R,R (and S,S) diastereomer upon *syn* addition of H_2 to the appropriate alkylidene. Compounds **130** and **129** were easily synthesised via an Aldol condensation reaction between methyl ethyl ketone and cyclopentanone.[9] The isolated compounds were identified by comparing the spectral data of the pure compounds with those published in the literature.[9] The catalytic hydrogenation of each geometric isomer allowed generation of authentic samples of the diastereomers **122** and **126**. Gas

chromatographic co-injection of the authentic samples with both **122** and **126** allowed unequivocal confirmation of the stereochemistry of the compounds obtained from the hydrogen selenide trapping reaction.

The ^{13}C and ^{1}H nmr spectra of **123** proved that the double bond in **123** was endocyclic and conjugated with the carbonyl. The most obvious feature of the ^{1}H nmr spectrum of **123** was a doublet (J=0.8 Hz) of triplets (J=2.8 Hz) centred at 7.26 ppm integrating for 1 proton. This resonance was assigned to the β proton of a substituted 2-cyclopentenone by comparing the ^{1}H nmr spectrum of 2-methyl-2-cyclopentenone with the ^{1}H nmr spectrum of **123**.[10] The ^{13}C nmr resonances observed at 157.7 ppm (CH) and 131.0 ppm (C) were assigned to olefinic carbons positioned β and α with respect to the carbonyl. The other ^{13}C and ^{1}H nmr resonances were consistent with the structural assignment of 2-sec-butylcyclopent-2-enone to compound **123**. Also, hydrogenation of compound **123** over a palladium surface resulted in the formation of **122** and **126** in a 1:1 ratio. Based on the spectral evidence as well as the results obtained from the hydrogenation experiments, the structure of **123** was assigned with a high degree of certainty.

Compounds **127** and **128** were not isolated as pure compounds. In fact, these diastereomeric compounds were not resolved by gas chromatography using a DB-5 50m capillary column. The ^{1}H nmr spectrum of the mixture of compounds **127** and **128** was complicated by the fact that the resonances of each diastereomer severely overlapped each other. Addition of $Eu(fod)_3$ to the nmr sample of the mixture (1:1.5 mixture:$Eu(fod)_3$ mole ratio) resulted in separation of the two overlapping methyl triplets as well as separation of the two overlapping methyl doublets. The integrated area ratio

of the two methyl triplets resulting from *cis*-2-butene addition to cyclopentenone was found to be 1.0:1.0, while the ratio resulting from *trans*-2-butene addition to cyclopentenone was found to be 1.0:4.0. It was impossible to determine which of the two methyl triplets in the proton spectrum corresponded to **127** and which corresponded to **128**. For the purposes of the work described in this paper the inability to assign a stereochemistry to **128** and **127** does not represent a problem in the case of *cis*-2-butene addition to excited cyclopentenone since both diastereomers were formed in equal amounts. However, in the case of the *trans*-2-butene addition the lack of stereochemical assignment for **127** and **128** was a problem. The ambiguity resulting from the unassigned stereochemistry of **127** and **128** is discussed later in this section.

The regiochemistry of **127** and **128** was confirmed to be representative of β-substitution with respect to the carbonyl. This assignment was made by analyzing the ^{13}C APT spectrum of the mixture. The two most down-field resonances (44.4 and 43.8 ppm), excluding carbonyl resonances, had multiplicities representative of methylene carbons. If substitution on the cyclopentanone ring were α with respect to the carbonyl then one would expect to find methine resonances as the furthest down-field resonances and not methylene resonances. Therefore, it was determined that both **127** and **128** were 3-sec-butyl-cyclopentanones.

Additional evidence for the structures of **127** and **128** was obtained by preparing authentic samples of these two compounds via an independent method. Scheme 37 describes the conjugate addition of 2-butyl magnesium bromide to 2-cyclopentenone in the presence of (N, N, N', N'-tetramethylethylenediamine)zinc(II) chloride which results in the formation of a mixture of **127** and **128** in 52% yield.[11] This mixture of

diastereomers was characterised by ^{1}H and ^{13}C nmr spectroscopy. The chemical shifts and multiplicities of the ^{13}C nmr signals exhibited by the mixture of **128** and **127** formed in the conjugate addition were compared with the chemical shifts and multiplicities of the ^{13}C nmr signals exhibited by the products isolated from the reaction mixture formed in the H_2Se trapping study. In this way, the regiochemistry of the trapped products identified as **127** and **128** was confirmed.

Scheme 37

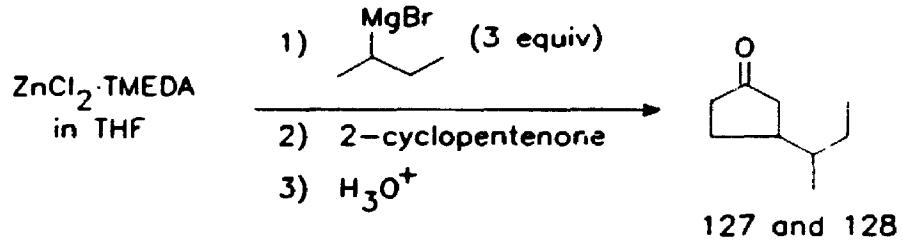

Having determined that **127** and **128** were in fact a pair of diastereomers, the problem of stereochemical identification for each compound still demanded a solution. As indicated above, the relative ratio of **127** to **128** resulting from the trapping experiments carried out on the addition of *cis*-2-butene to triplet 2-cyclopentenone was 1:1 so for this case the individual stereochemistries of **127** and **128** was irrelevant. In the case of the biradical trapping studies performed on the addition of *trans*-2-butene to triplet 2-cyclopentenone, compounds **127** and **128** were not formed in equal amounts and therefore steps were taken to determine the stereochemistry of each component of the mixture of diastereomers. The approach to the problem of stereochemical identification involved the attempted synthesis of each stereoisomer via an independent synthetic route. If a pure sample of each stereo-isomer were prepared, then the mixture of **127** and **128**

obtained from the trapping studies could be spiked with these samples which would allow the ^{13}C nmr and ^{1}H nmr signals exhibited by the mixture to be assigned to either diastereomer. Integration of these assigned signals would permit a determination of the relative product yield ratio of **127**:**128**.

Scheme 38

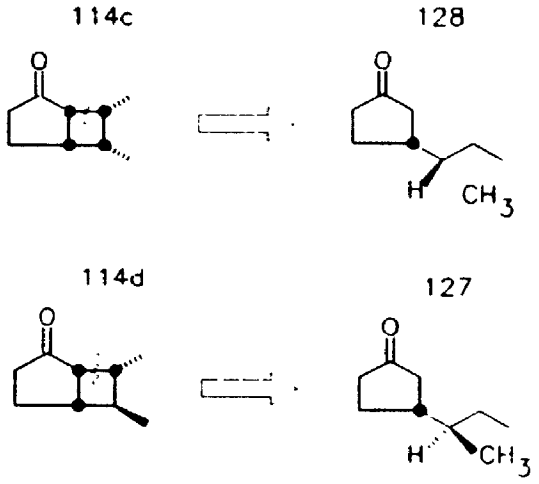

All of the attempts at selectively synthesising either **127** or **128** involved performing a cyclobutane ring opening reaction on one of the cycloadducts formed in the photocycloaddition of 2-cyclopentenone and the 2-butenes. Scheme 38 demonstrates the goal of this approach in the synthesis of **127** or **128**. The cycloadducts formed in the photocycloaddition reaction between 2-cyclopentenone and the 2-butenes were used as starting materials for the attempted synthesis of **127** and **128** since the stereochemistry of the methyl groups in each isolated cycloadduct was already assigned. Therefore, it was decided that a cyclobutane ring opening reaction was the easiest way in which the stereochemical assignment of the methyl groups of the cycloadducts could be translated into a stereochemical assignment of the chiral centres in **127** and **128**.

Crimmins and Mascarella have published a convenient method for cleaving the cyclobutane ring of the bicyclo[3,2,0]hepta-2-one moiety with trimethylsilyl iodide which can be generated *in situ* by reacting trimethylsilyl chloride and sodium iodide in acetonitrile.[12] This particular method was developed for use in the total synthesis of the sesquiterpene silphinene. The specific reaction to which the method was applied is shown in Scheme 39.[12] When cycloadduct **114c** was reacted with trimethylsilyl iodide in acetonitrile in the presence of an internal standard, less than 5% of the cycloadduct starting material was converted to products. Coupled g.c.-m.s. analysis of the reaction mixture indicated that none of the expected iodide containing ring-opened product was formed in the reaction. It is possible that the lack of reactivity demonstrated by **114c** towards cylobutane ring cleavage relative to compound **131** is a result of the fact that in the case of **114c** the ring cleavage must occur at a tertiary carbon centre whereas in the case of **131** the ring opening occurs at a secondary site. If the reaction mechanism involves an S_N2 type pathway in which iodide attacks the β-position with respect to the carbonyl, then the increased steric hinderance at this position in **114c** relative to **131** explains the lack of reactivity exhibited by **114c**. No attempts were made to carry out the trimethylsilyl iodide mediated cyclobutane ring opening reaction on any of the other 2+2 photocycloadducts. Given the lack of success of applying the method for cyclobutane ring cleavage that was developed by Crimmins and Mascarella to cycloadduct **114c**, we investigated another method for effecting the transformation shown in Scheme 38.

Examination of the structure of cycloadduct **114c** revealed that this compound has γ-hydrogens which are positioned in a fashion that would allow them to be involved in

Scheme 39

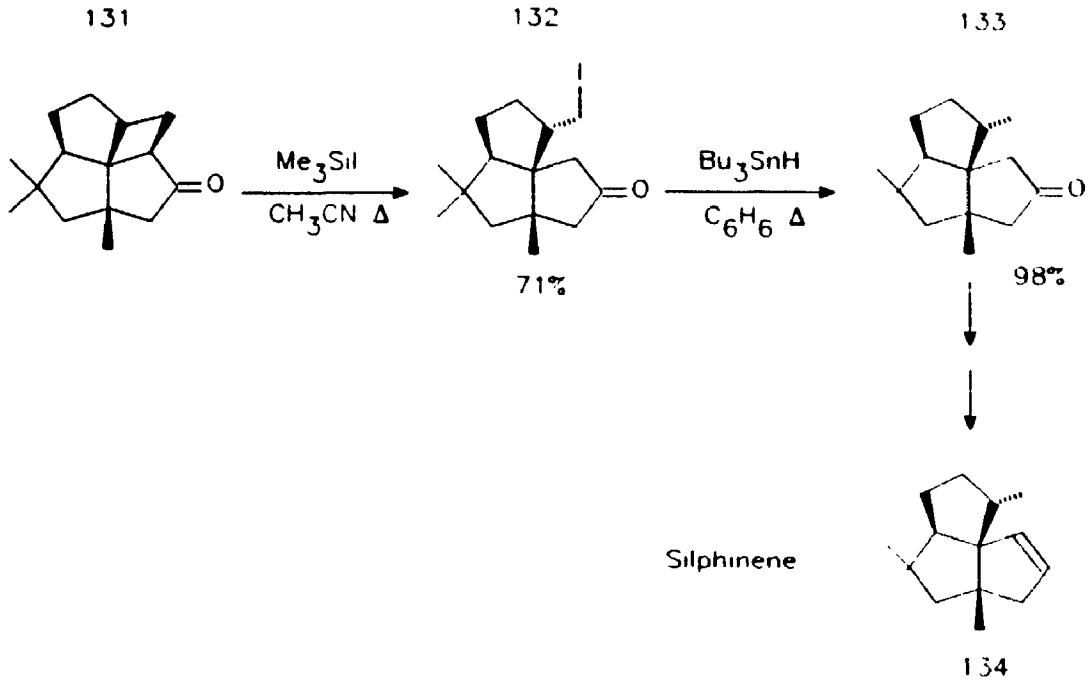

a Type II reaction upon excitation of the ketone functionality. Scheme 40 summarises the reaction mechanism tha. ould result from the Type II reaction of cycloadduct **114c**. This scheme demonstrates that the Type II reaction of **114c** could be used to open the cyclobutane ring without altering the stereochemistry present in compound **128**. Hydrogenation of the Type II fragmentation product labelled **135** would result in the formation of **128**. In order to investigate the Type II reactivity of **114c**, an acetonitrile solution of the cycloadduct was irradiated with Pyrex filtered light from a 400 W Hanovia medium pressure mercury lamp. One major product (**136**) was formed during this photolysis; however, the spectral properties of this compound revealed that it was not the result of a Type II process but rather the result of an α-cleavage or Type I reaction (see Scheme 40). The structure of **136** was confirmed by the ^{13}C nmr and ^{1}H spectra of this compound as both spectra contained evidence of an aldehyde group as well

as a cyclobutene ring system. The presence of two methyl doublets in the ^1H nmr spectrum of **136** confirmed the location of the alkene functionality in the four-membered ring. Performing the photolysis of **114c** in benzene under sensitised or direct irradiation conditions did not result in increasing the efficiency of the Type II process; under both conditions product **136** constituted more than 80% of the product mixture. Therefore, the high efficiency of the Type I reaction of **114c** relative to the Type II reaction made it impossible to use the Type II reaction of **114c** in the synthesis of **128**.

Scheme 40

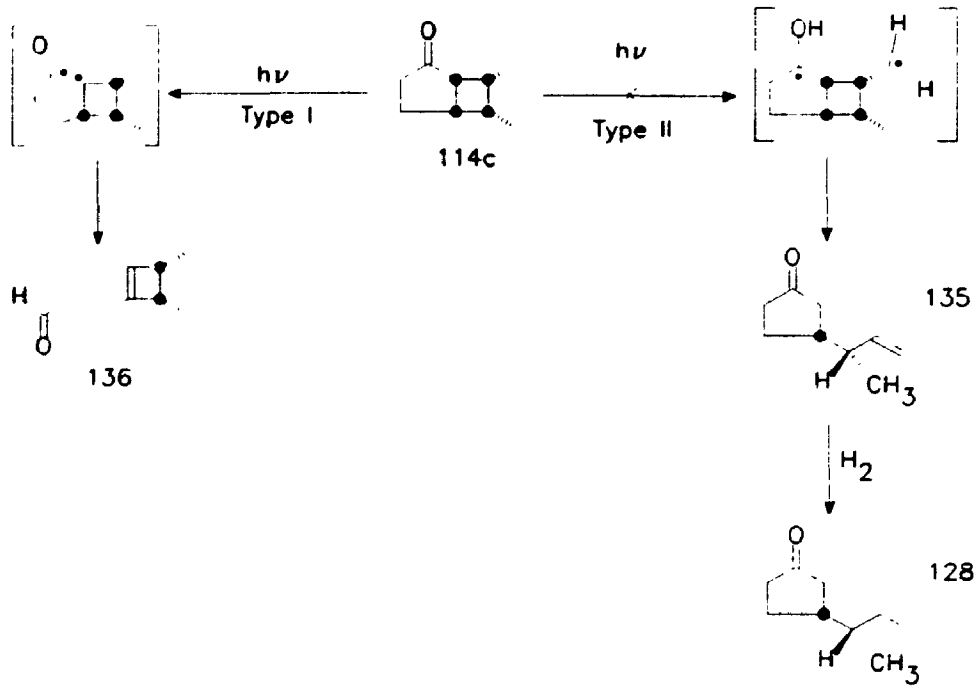

Due to the lack of success in synthesising either pure **127** or **128**, it was not possible to assign the stereochemistry of each of these compounds unequivocally. It was decided that the kinetic data made available by the trapping experiments should be evaluated given the explicit ambiguity resulting from the unknown relative

stereochemistries of **127** and **128**. The effect of the lack of stereochemical information for the pair of compounds comprised of **127** and **128** on the kinetic analysis of the results could then be determined. The arguments in the Discussion Section below demonstrate how we were able to minimise the effects of this ambiguity.

4.3 Discussion

4.3.1 Explanation of the kinetic treatment of the photocycloaddition reactions

A mechanism which describes the addition of *cis* or *trans*-2-butene to the triplet excited state of 2-cyclopentenone is shown in Scheme 41. The cycloadduct products **114a**, **114b**, **114c** and **114d** have been assigned the temporary designations **A**, **B**, **C** and **D**, respectively, in this scheme. Similarly, biradicals **110a**, **110b**, **110c** and **110d** have been assigned the temporary designations **a**, **b**, **c** and **d**, respectively. In summary, the cycloadducts have been assigned uppercase designations and the biradicals have been assigned lowercase designations. These temporary designations were made in order to simplify the rate constant definitions presented in Scheme 41.

In the mechanism shown in Scheme 41, the rate of formation of each biradical is represented as k_i multiplied by the alkene concentration, where "i" represents biradical **a**, **b**, **c**, or **d**. The rate of decay of triplet 2-cyclopentenone in the absence of 2-butene is denoted as k_y. The rate for the process in which each biradical reverts to ground state enone plus alkene is represented by the rate constant k_{-i}. The rate of closure of each biradical is represented by a rate constant with the form k_i^W, where "i" is the biradical from which closure occurs and "W" is the product for which closure results. Thus, "W" represents each of the four cycloadducts **A**, **B**, **C**, or **D**. It is important to note that each

Scheme 41

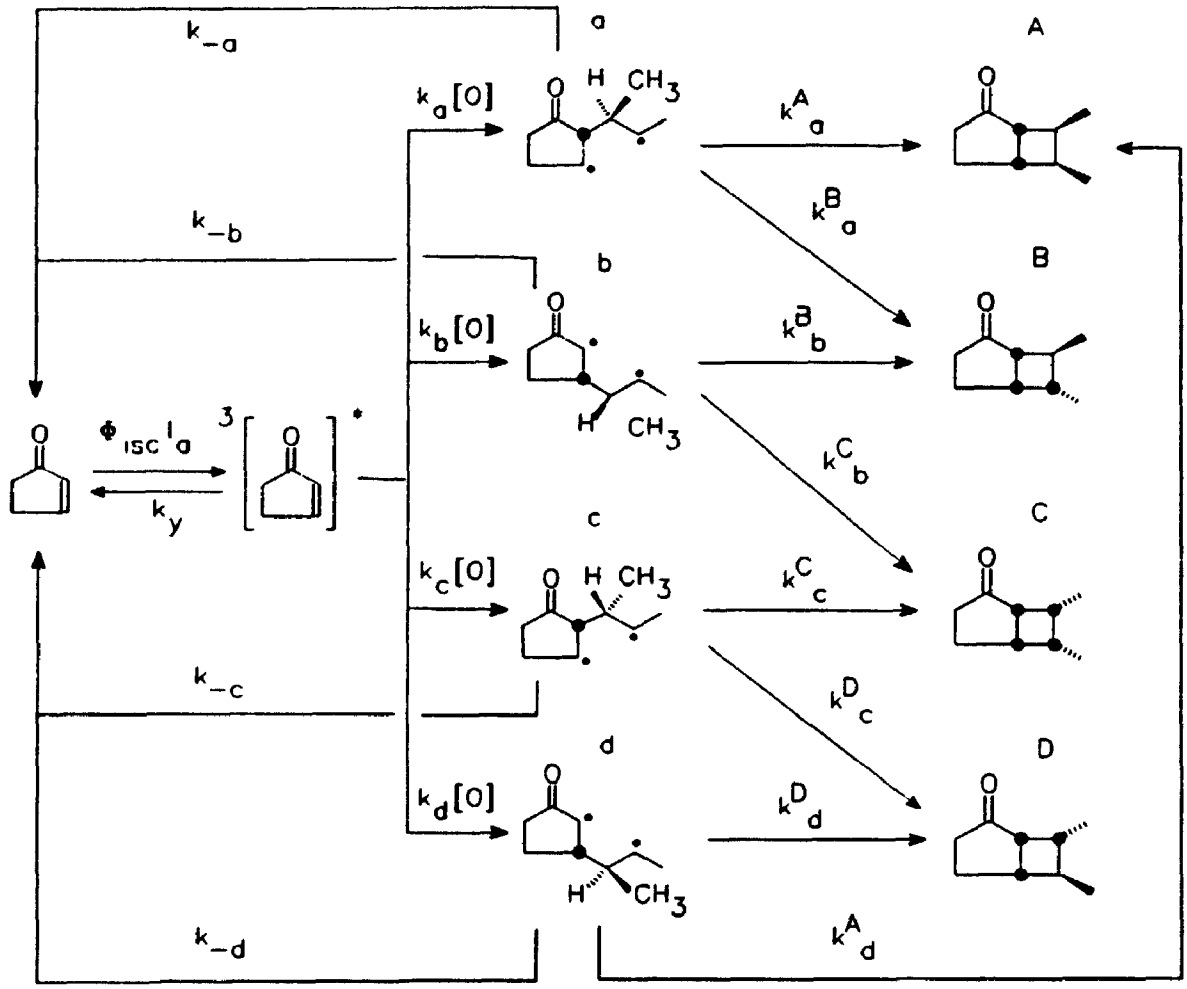

biradical is responsible for the formation of two cycloadducts. Similarly, each cycloadduct originates from the closure of two regio-isomeric biradicals. One of the primary goals of this study was to determine the relative proportions of reversion and closure for each biradical. Therefore, in terms of rate constants defined in Scheme 41, the goal of this investigation was to determine the ratio of k_{-i} to each of the two possible k_i^W for all four biradicals.

Equations which relate the quantum yield of the formation for each product

resulting from the cycloaddition between 2-cyclopentenone and each of the 2-butenes to the rate constants shown in Scheme 41 can be derived by applying the steady state approximation to the appropriate short lived intermediates. These short lived intermediates consist of the triplet and singlet excited states of the enone and each of the 1,4-biradicals. The quantum yield of formation of cycloadduct **114a** (i.e. **A**) is, for example, given by the following equation:

$$\Phi_A = \frac{\Phi_{isc}}{(k_a+k_b+k_c+k_d)[O]+k_y}\left[k_a[O]\left(\frac{k_a^A}{k_{-a}+k_a^A+k_a^B}\right)+k_d[O]\left(\frac{k_d^A}{k_{-d}+k_d^D+k_d^A}\right)\right] \quad (7)$$

In this equation, [O] is the concentration of 2-butene. It should be noted that the magnitude of the quantum yield Φ_A is dependent on the particular 2-butene geometric isomer being reacted with the enone triplet. This is because the magnitude of each rate constant denoted in the form k_i is also dependent on the alkene isomer. The parameter denoted as Φ_{isc} represents the quantum yield of intersystem crossing for 2-cyclopentenone. The magnitude of Φ_{isc} was found to be 1.0 by de Mayo[13,14] and by Wagner[15].

Taking the reciprocal of Equation 7 results in transforming the equation into an expression which describes a linear relationship between the reciprocal of the quantum yield of product formation and the reciprocal of the alkene concentration. If the following substitutions, along with $\phi_{isc}=1.0$, are applied to this reciprocal expression then Equation 8 is derived.

$$\text{Define:} \quad \alpha_a = \frac{k_a}{k_a+k_b+k_c+k_d} \quad \text{and} \quad \alpha_b = \frac{k_b}{k_a+k_b+k_c+k_d}$$

$$\text{Define:} \quad \rho_a^A = \frac{k_a^A}{k_a^A+k_a^B+k_{-a}} \quad \text{and} \quad \rho_d^A = \frac{k_d^A}{k_d^A+k_d^D+k_{-d}}$$

$$\frac{1}{\Phi_A} = \left(\frac{1}{\rho_a^A\alpha_a+\rho_d^A\alpha_d}\right) + \left(\frac{k_y}{\rho_d^A k_d+\rho_a^A k_a}\right)\cdot\frac{1}{[O]} \qquad (8)$$

Reciprocal quantum yield expressions that have the same general form as Equation 7 can also be written for the other cycloaddition products. Each of these expressions contains two ρ_i^W variables and two α_i variables that comply with the definitions stated above. The variables denoted as α_i represent the relative rate of formation of each biradical "i" and are dependent on the identity of the isomeric 2-butene reacting with the excited state triplet enone. The variables denoted as ρ_i^W represent the fraction of each biradical "i" population that closes to give cycloadduct "W" relative to all other decay processes available to the biradical.

If one assumes that each of the four triplet biradicals shown in Scheme 41 reaches conformational equilibrium before intersystem crossing followed by reversion or closure can occur, then the biradicals generated by the addition of *cis*-2-butene to triplet 2-cyclopentenone have exactly the same fates as the biradicals generated by the addition of *trans*-2-butene to triplet 2-cyclopentenone. If this assumption is correct then the value of each rate constant k_i^W or each parameter ρ_i^W does not depend on the identity of the 2-butene isomer. In order to test the validity of this assumption one must be able to

compare the rate of internal bond rotation in each triplet biradical with the lifetime of each triplet biradical. Approximate lifetimes for structurally similar biradicals are reported in the literature[16,17]; however, the activation energies for rotation about the various carbon-carbon σ-bonds of 1,4-biradicals generated in the cycloaddition react between cyclic enones and alkenes have not been determined. Consequently, the rate of conformational change in the triplet biradicals is not known. It is not realistic to suggest that the barriers to rotation about the carbon-carbon bonds of the biradicals shown in Scheme 41 are the same as the energy barriers in simple alkanes since extensive hyperconjugative interactions involving the partially filled radical orbitals may significantly affect these barriers.

The validity of assuming that the triplet biradicals involved in the cycloaddition between 2-cyclopentenone and 2-butene are conformationally relaxed can, however, be evaluated by studying the stereochemistry of the products obtained from the addition of each geometric 2-butene isomer to the triplet enone. The major cycloadduct resulting from the addition of *trans*-2-butene to 2-cyclopentenone, product **114a** (i.e. **A** in Scheme 41), was found to exhibit a *cis* relationship between the two methyl groups. On the other hand, one of the two major products resulting from *cis*-2-butene to 2-cyclopentenone, product **114b** (i.e. **B** in Scheme 41), was found to exhibit a *trans* relationship between the two methyl groups. The absence of any memory of 2-butene stereochemistry in the product distributions resulting from each isomeric 2-butene suggests that the rate of conformational motion in each biradical competes efficiently with the rate of intersystem crossing of the triplet biradical. This observation is consistent with lack of stereoselectivity in the products resulting from other systems in which *cis* and *trans*

symmetrical alkenes were added to excited cyclic enones.[18,19] Therefore, the assumption that the triplet 1,4-biradicals shown in Scheme 41 are conformationally relaxed is reasonable and has some experimental basis.

The relative rate of formation of each biradical was determined for each 2-butene isomer by carrying out the cycloaddition reactions in the presence of hydrogen selenide. In these experiments hydrogen selenide was used as a biradical trap in an effort to intercept all of the 1,4-biradicals generated in each of the cycloaddition reactions before intersystem crossing from the triplet to the singlet biradical, followed by either reversion or closure, could occur. In the presence of H_2Se, the biradicals formed by the reaction of either of the 2-butene geometrical isomers with the cyclopentenone triplet excited state were efficiently reduced to stable compounds before spin inversion could occur. In total nine products (**120** to **128**)--each the result of trapped or partially trapped 1,4-biradicals--were recovered from irradiated solutions of benzene containing cyclopentenone (0.05M), *cis* or *trans*-2-butene (1.5M), and H_2Se (0.3M). The conspicuous absence of any trace of cycloadducts **114a**, **114b**, **114c**, or **114d** indicated that the rate of reaction between each triplet biradical and hydrogen selenide was much faster than the rate of decay of the triplet biradicals. Therefore, it can be concluded that all of the triplet biradicals were intercepted before intersystem crossing could occur; both biradical closure and biradical reversion were prevented in the trapping experiments.

Before considering the conclusions to be drawn from the relative yields of the products resulting from the trapping experiments, the origin of each of the products will be considered. Compounds **122**, **126**, **127** and **128** (see Scheme 35) are the result of two successive hydrogen abstractions by each of the radical centres in the corresponding

biradicals. The first abstraction occurs when the 1,4-biradical abstracts a hydrogen atom from an H_2Se molecule to yield a radical pair consisting of the hydrogen selenyl radical and one of two possible alkyl radicals derived from the initial biradical. The second abstraction may occur when the alkyl radical abstracts a hydrogen atom from the hydrogen selenyl radical before the radicals can escape the solvent cage; however, if cage separation does occur then the second abstraction is from another H_2Se molecule. Compounds **120**, **121**, **123**, **124**, and **125** (see Scheme 35) are apparently the result of a hydrogen abstraction by the corresponding 1,4-biradical followed by disproportionation of the resulting radical pair. The formation of disproportionation products does not present a problem in the determination of the relative quantum yields of formation of each biradical if it is possible to determine from which biradical each partially trapped product is formed. Compounds **120** and **121** originate from biradical **110a** and compounds **124** and **125** originate from biradical **110c**. Compound **123**, however, presents a problem since either biradical **a** or **c** may be implicated in its formation. In order to determine the relative quantum yields of formation of each biradical, the parameter "x" must be introduced (see Scheme 35). If the fraction of **123** originating from biradical **110a** is "x", then the fraction originating from biradical **110c** is 1 - x. Under the assumption that the triplet biradicals have achieved conformational equilibrium, the parameter "x" is independent of the alkene (*cis* or *trans*-2-butene) involved in the initial reaction with triplet enone.

With a knowledge of the origins of each product recovered from the trapping reactions involving hydrogen selenide, one can assign specific values to the relative quantum yields of formation for each biradical resulting from the reaction between *cis*

or *trans*-2-butene and cyclopentenone triplet. The relative quantum yields correspond to the values of α_i in Equation 7. The various α_i values determined for the addition of each alkene to the enone triplet were calculated from the relative product yields of compounds **120** to **128** and are listed in Table 18.

There is an obvious problem with the values for α_b^{trans} and α_d^{trans} listed in Table 18. These parameters represent the relative quantum yields of formation of biradicals **110a** and **110d** when *trans*-2-butene was added to the triplet state of excited 2-cyclopentenone. As previously explained in the results section, the stereochemistry of some of the trapped product originating from these biradicals, specifically compounds **127** and **128**, could not be determined. In the case of *trans*-2-butene addition to triplet 2-cyclopentenone, these two compounds were formed in different amounts; therefore, two possible values have been listed for each of α_b^{trans} and α_d^{trans} in the table. In the case of *cis*-2-butene addition, **127** and **128** were formed in equal amounts and so there was no need to distinguish between **127** and **128** in order to quote single values for α_b^{cis} and α_d^{cis}. In the following two paragraphs, the method used to overcome this ambiguity will be described.

Table 18: Relative quantum yields of formation (α_i) for biradicals **110a**, **110b**, **110c**, and **110d** normalised to unity.

α_i	*cis*-2-butene addition	*trans*-2-butene addition
α_a	0.174 + 0.103x	0.116 + 0.102x
α_b	0.277	0.120 or 0.476
α_c	0.168 + 0.103(1-x)	0.185 + 0.102(1-x)
α_d	0.277	0.476 or 0.120

The α_i values determined in the H_2Se trapping experiments were substituted into the equations that define the inverse quantum yield of cycloadduct formation as a linear function of the inverse of the alkene concentration (Equation 8 is an example of these expressions). This results in the formation of eight linear equations--four equations for each of the two 2-butene isomers studied. In total, these eight equations contain eight unknown ρ_i^W variables. Each equation has a slope parameter, m, and an intercept parameter, b. The reciprocal of the intercept portions of these linear equations have the form $(1/b)_Y = \alpha_r\rho_r^Y + \alpha_s\rho_s^Y$, where "Y" is a cycloadduct and "r" and "s" are biradicals. The specific equations that were derived are listed as Equations 9 to 16.

$$I_A^{trans} = \rho_a^A(0.116 + 0.102x) + \rho_d^A(0.476 \text{ or } 0.120) \quad (9)$$

$$I_B^{trans} = \rho_a^B(0.116 + 0.102x) + \rho_b^B(0.120 \text{ or } 0.476) \quad (10)$$

$$I_C^{trans} = \rho_b^C(0.120 \text{ or } 0.476) + \rho_c^C(0.185 + 0.102(1-x)) \quad (11)$$

$$I_D^{trans} = \rho_c^D(0.185 + 0.102(1-x)) + \rho_d^D(0.476 \text{ or } 0.120) \quad (12)$$

$$I_A^{cis} = \rho_a^A(0.174 + 0.103x) + \rho_d^A(0.277) \quad (13)$$

$$I_B^{cis} = \rho_a^B(0.174 + 0.103x) + \rho_b^B(0.277) \quad (14)$$

$$I_C^{cis} = \rho_b^C(0.277) + \rho_c^C(0.168 + 0.103(1-x)) \quad (15)$$

$$I_D^{cis} = \rho_c^D(0.168 + 0.103(1-x)) + \rho_d^D(0.277) \quad (16)$$

In each of these equations I_i^{trans} and I_i^{cis} represent the reciprocal of the intercept parameters determined from plots of the inverse quantum yield of formation of each cycloadduct versus the inverse of the 2-butene concentration. These reciprocal intercept parameters are listed in Table 17 of the Results Section.

The solutions to the eight equations above are parametrically dependent on the particular set of values chosen for α_b^{trans} and α_d^{trans} (see Table 18) as well as on the choice of x. The following method was used to obtain homogeneous forms of Equations 9 to 16 and then exact solutions for each ρ_i^W. First, one of the sets of values for α_b^{trans} and α_d^{trans} in Table 4 was explicitly chosen and substituted into the equations. Secondly, the equations were solved, using matrix techniques, to obtain exact solutions for each ρ_i^W at a number of different values for the parameter x that satisfied the normalisation condition $0 \leq x \leq 1$. In this way, several solutions were obtained for the ρ_i^W, each of which corresponds to a particular value of x. The third step in obtaining values for each ρ_i^W from Equations 9 to 16 involved repeating steps one and two described above using the second set of possibilities for α_b^{trans} and α_d^{trans}. The value of each ρ_i^W when $\alpha_b^{trans} = 0.476$ and $\alpha_d^{trans} = 0.120$ is plotted as a function of x in Figure 7. Since all ρ_i^W are normalised to 1, acceptable values for the ρ_i^W must satisfy the condition $0 \leq \rho_i^W \leq 1$. Analysis of the solutions presented in Figure 7 indicates that three ρ_i^W have values which significantly violate this constraint throughout the entire allowable range of x values. When α_b^{trans} and α_d^{trans} are set equal to 0.120 and 0.476 respectively, the ρ_i^W taken on the values indicated in Figure 8. This figure indicates that if $0.3 \leq x \leq 1$ all ρ_i^W values fall within the constraint $0 \leq \rho_i^W \leq 1$. Therefore, the correct assignments of α_b^{trans} and α_d^{trans} must be 0.120 and 0.476 according to the mechanism shown in Scheme 41.

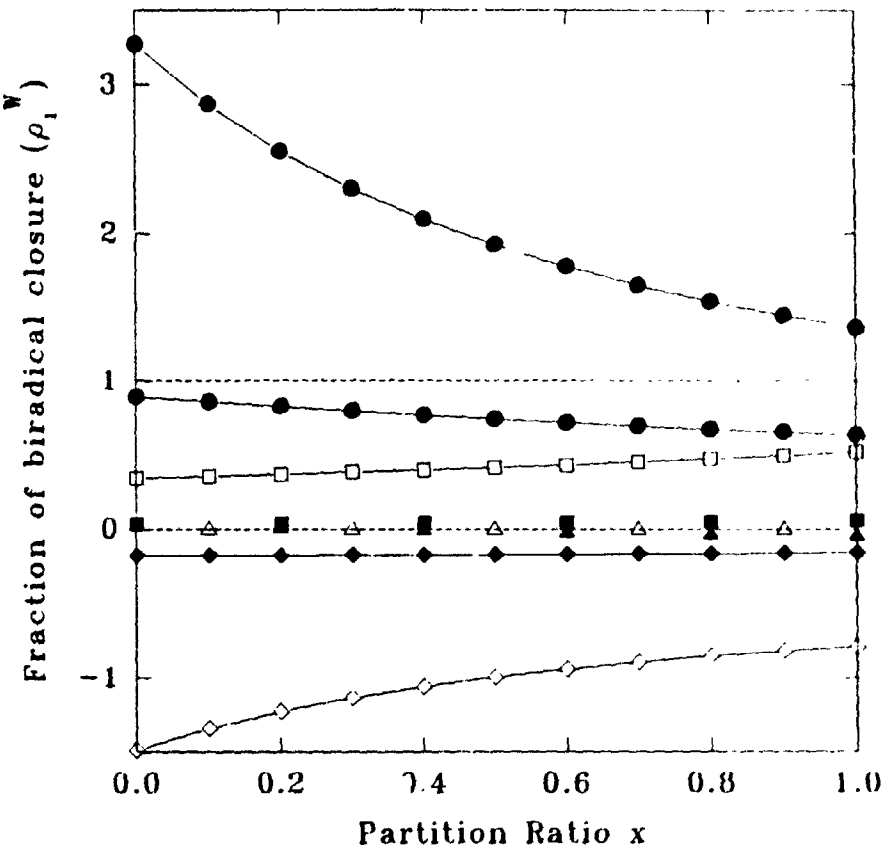

Figure 7: The dependence of each variable ρ_i^Y on the parameter x for the case $\alpha_b^{trans} = 0.476$ and $\alpha_d^{trans} = 0.120$. ● represent ρ_a^A; ○ represent ρ_a^B; ▲ represent ρ_b^B; △ represent ρ_b^C; ■ represent ρ_c^C; □ represent ρ_c^D; ◆ represent ρ_d^D; and, ◇ represent ρ_d^A.

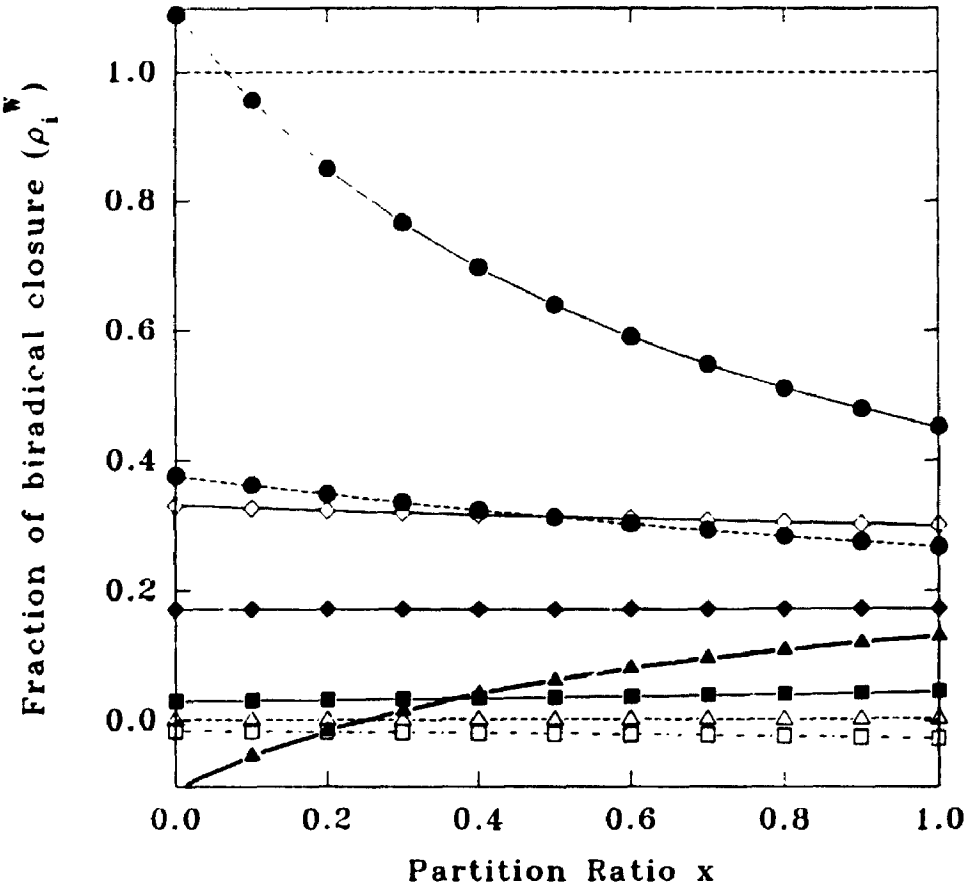

Figure 8: The dependence of each variable ρ_i^Y on the parameter x for the case $\alpha_b^{trans} = 0.120$ and $\alpha_d^{trans} = 0.476$. The symbols have the same definitions as in Figure 7.

The fraction of each biradical reverting to ground state cyclopentenone and alkene (ρ_{-i}) can be calculated from the ρ_i^I values described above. Since each ρ_i^I is normalized to 1, the fraction of each biradical i reverting to starting materials is given by the equation:

$$\rho_{-i} = 1 - \rho_i^I - \rho_i^Y \qquad (17)$$

Here, "I" and "Y" denote the two possible cycloadducts that biradical "i" may form. Figure 9 describes how each ρ_{-i} (calculated according to equation 11) behaves as a function of x when α_b^{trans} and α_d^{trans} are set equal to 0.476 and 0.120 respectively. Figure 10, on the other hand, shows the dependence of each ρ_{-i} on the parameter x when α_b^{trans} and α_d^{trans} are set equal to 0.120 and 0.476 respectively. Due the normalisation condition, acceptable values for each ρ_{-i} must lie between 0 and 1. When α_b^{trans} and α_d^{trans} are set equal to 0.476 and 0.120 respectively, this constraint is violated by ρ_{-a} and ρ_{-d} over all values of x indicating that these are not the correct assignments for α_b^{trans} and α_d^{trans}. However, when α_b^{trans} and α_d^{trans} are set equal to 0.120 and 0.476 the constraint is obey by all ρ_{-i} over the range $0.4 \leq x \leq 1$. It should be noted that the experimental error for each ρ_{-i} value is approximately 15% due to the error associated with the intercept values used to solve Equations 9 through 16.

The reversion ratios for each biradical obtained when $0.4 \leq x \leq 1.0$ are summarised in Scheme 42. Similarly, the relative fraction of each biradical closing to each cycloadduct, calculated when $0.4 \leq x \leq 1.0$, are also summarised in this scheme. The ranges in the quantities summarised in Scheme 42 correspond to the range of values possible for x.

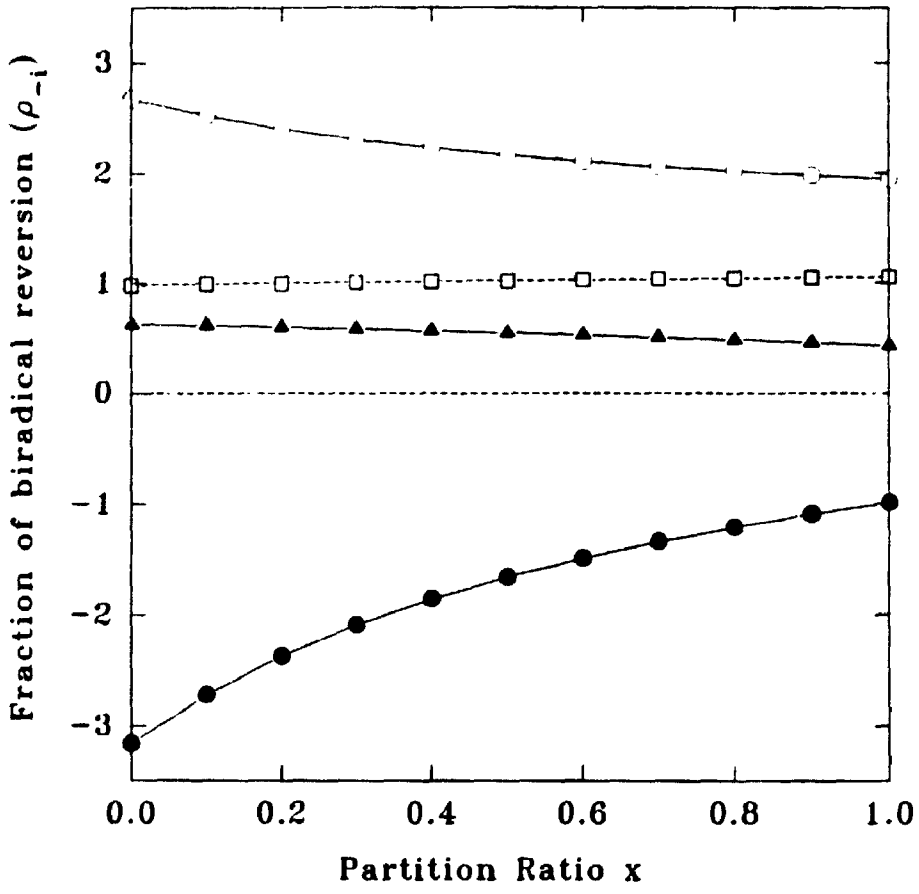

Figure 9: The dependence of each biradical reversion ratio ρ_{-i} on the parameter x for the case $\alpha_b^{trans} = 0.476$ and $\alpha_d^{trans} = 0.120$. ● represent ρ_{-a}; □ represent ρ_{-b}; ▲ represent ρ_{-c}; and, ○ represent ρ_{-d}.

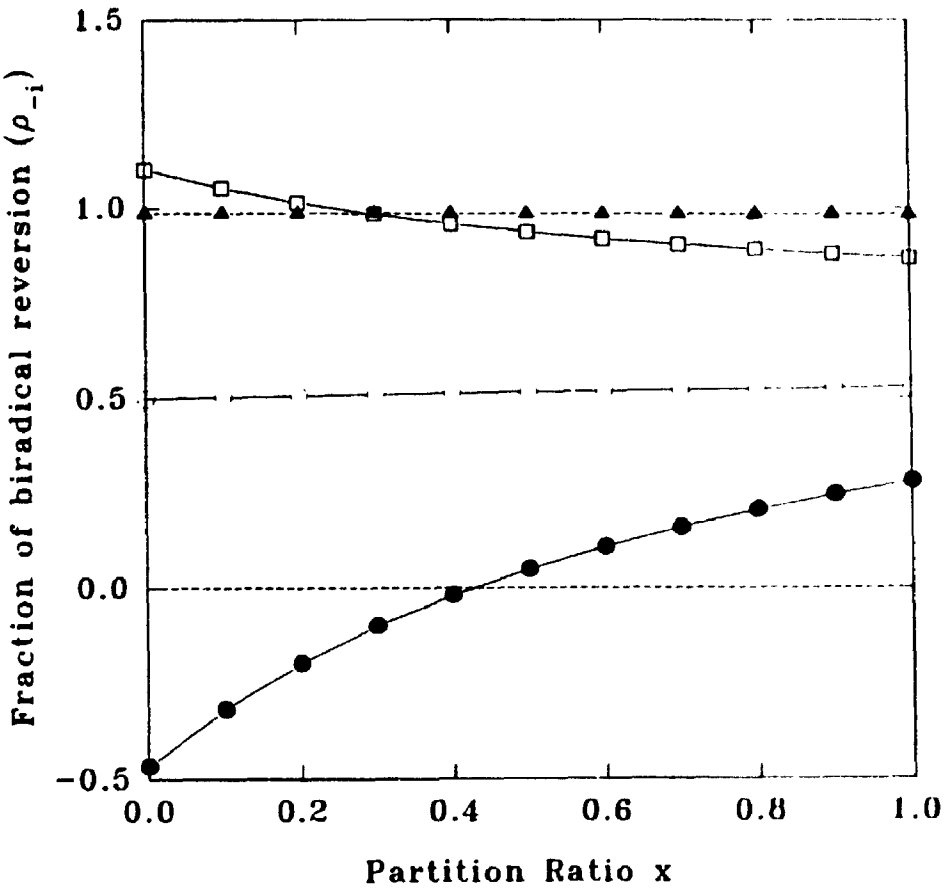

Figure 10: The dependence of each biradical reversion ratio ρ_{-i} on the parameter x for the case $\alpha_b^{trans} = 0.120$ and $\alpha_d^{trans} = 0.476$. The symbols have the same definitions as in Figure 9.

Scheme 42

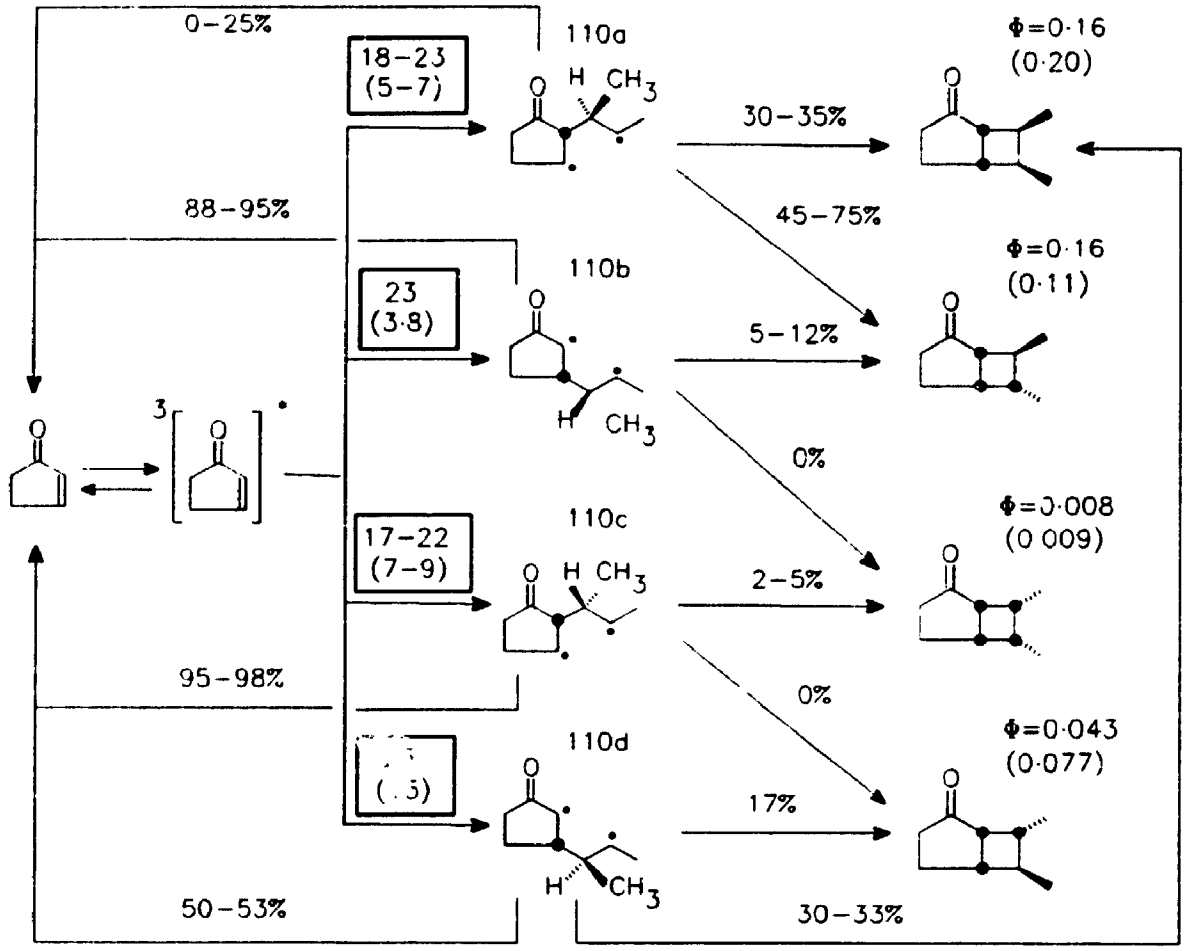

Boxed data are rate constants with units of 10^7 $M^{-1}sec^{-1}$
Product quantum yields are extrapolated to infinite alkene concentration
Trans–2–butene data in parentheses

So far, only the intercept components of the equations that define the inverse quantum yield of cycloadduct formation as a linear function of the inverse of the alkene concentration (see Equation 8) have been used to gain information about the kinetic parameters in Scheme 41. The slope components of these linear equations can also be used to access kinetic information. For example, if one divides the slope expression of linear Equation 3 by the equation's intercept expression then Equation 18 is derived.

$$\frac{\text{slope}}{\text{intercept}} = \frac{k_y\,(\rho_a^{\Lambda}\alpha_a + \rho_d^{\Lambda}\alpha_d)}{\rho_a^{\Lambda}k_a + \rho_a^{D}k_d}$$

$$= \frac{k_y}{k_a + k_b + k_c + k_d} \qquad (18)$$

Equation 18 can also be derived by taking the slope over intercept ratio for the quantum yield data pertaining to any of the other cycloaddition products. Only two distinct slope over intercept ratios exist: one corresponds to the quantum yield data obtained from the addition of *cis*-2-butene to 2-cyclopentenone, the other corresponds to the data obtained from the addition of *trans*-2-butene. Equation 18 indicates that the total rate of formation of all biradicals (i.e. $k_a+k_b+k_c+k_d$) can be calculated if one knows the rate of decay of the enone triplet in the absence of alkene.

Caldwell et. al.[20] have measured the lifetime of triplet cyclopentenone in cyclohexane by flash photolysis techniques. Caldwell also demonstrated that the rate of decay of triplet cyclopentenone is highly dependent on the concentration of enone. This dependence is described in more detail in Chapter 1 and summarised in Equation 1 of that chapter. For convenience, this equation, with the appropriate numerical values substituted for the rate of self quenching and the rate of decay of triplet 2-cyclopentenone at infinite dilution, is repeated below. Therefore, in cyclohexane, the rate of decay of the cyclopentenone triplet (k_y) is given by the following equation:

$$k_y = (5.41\times10^{6}\ s^{-1}) + (5.9\times10^{8}\ M^{-1}s^{-1})\,[enone] \qquad (19)$$

In all of the quantum yield determinations performed on the reactions described in this chapter the concentration of 2-cyclopentenone was fixed at 0.0278 M. Substitution of this concentration into Equation 19 results in a rate of decay for triplet 2-cyclopentenone (k_y) of 2.19×10^7 sec^{-1}. The total rate of triplet enone quenching by *cis*- and *trans*-2-butene ($k_a+k_b+k_c+k_d$) was calculated to be 8.3×10^7 $M^{-1}sec^{-1}$ and 3.2×10^7 $M^{-1}sec^{-1}$ respectively when this value of k_y was substituted into Equation 18. However, it is important to note that the quantum yield determinations were carried out in benzene and the rate constants substituted into Equation 19 were determined in cyclohexane. Therefore, the absolute rate constants determined above may have some inherent associated errors. The rates of formation of the individual biradicals were calculated by multiplying the total rate of biradical formation by the appropriate α_i value listed in Table 18. The results of these calculations, determined under the constraint $0.4 \leq x \leq 1.0$, are summarised in Scheme 42.

4.3.2 Significance of the kinetic parameters shown in Scheme 42

The data presented in Scheme 42 indicate that very different reversion to cyclisation ratios are exhibited by the biradical diastereomers denoted as **110a** and **110c**. Similarly, the diastereomeric pair of biradicals **110d** and **110d** also exhibit different reversion to cyclisation ratios. These dramatic differences are surprising since biradicals **110a** and **110c** are structurally identical, as are **110b** and **110d**, except for the stereochemistry about the 2,3-bond of the 1,4-biradical.

The differences in the reversion to cyclisation ratios exhibited by the diastereomeric pairs of biradicals can be rationalised in terms of the specific

conformations that must be accessed in order for biradical closure or reversion to occur. It can be easily demonstrated that certain conformations permit biradical fragmentation while others permit both fragmentation and cyclisation. Therefore, the population of biradicals occupying each conformation should have an impact on the reversion to cyclisation ratios as well as on the relative product ratios of the cycloadducts. According to this logic, the major products resulting from the decay of a specific biradical should come from the more stable biradical conformations. This argument is similar to the one presented by Bauslaugh[2] which is described in the introduction to this chapter. However, it is important to remember that the biradical reversion and biradical cyclisation pathways proceed from the singlet state and not the triplet state which is the state in which the biradical is formed initially. Therefore, it is important to consider how the intersystem crossing process could effect the products resulting from each biradical.

The lifetimes of the singlet biradicals involved in cyclic enone plus alkene photocycloadditions are probably extremely short. In fact, the lifetime of Norrish Type II singlet biradicals has been estimated by Scaiano to be between in the 10 to 500 ps range.[21] There is no reason to suggest that biradicals generated in cyclic enone plus alkene photocycloadditions have singlet lifetimes that are considerably longer than this. Therefore, it could be postulated that, due to very short singlet biradical lifetimes, the conformation in which a biradical finds itself after spin inversion has occurred is the conformation that dictates which products are formed.

In the case of Norrish Type II biradicals evidence exists to support this postulate. For example, Ito *et al.*[22] examined the direct and sensitised decomposition of valerophenone diperoxide, **137**, and found that the ratios of products **139** and **140** are

Scheme 43

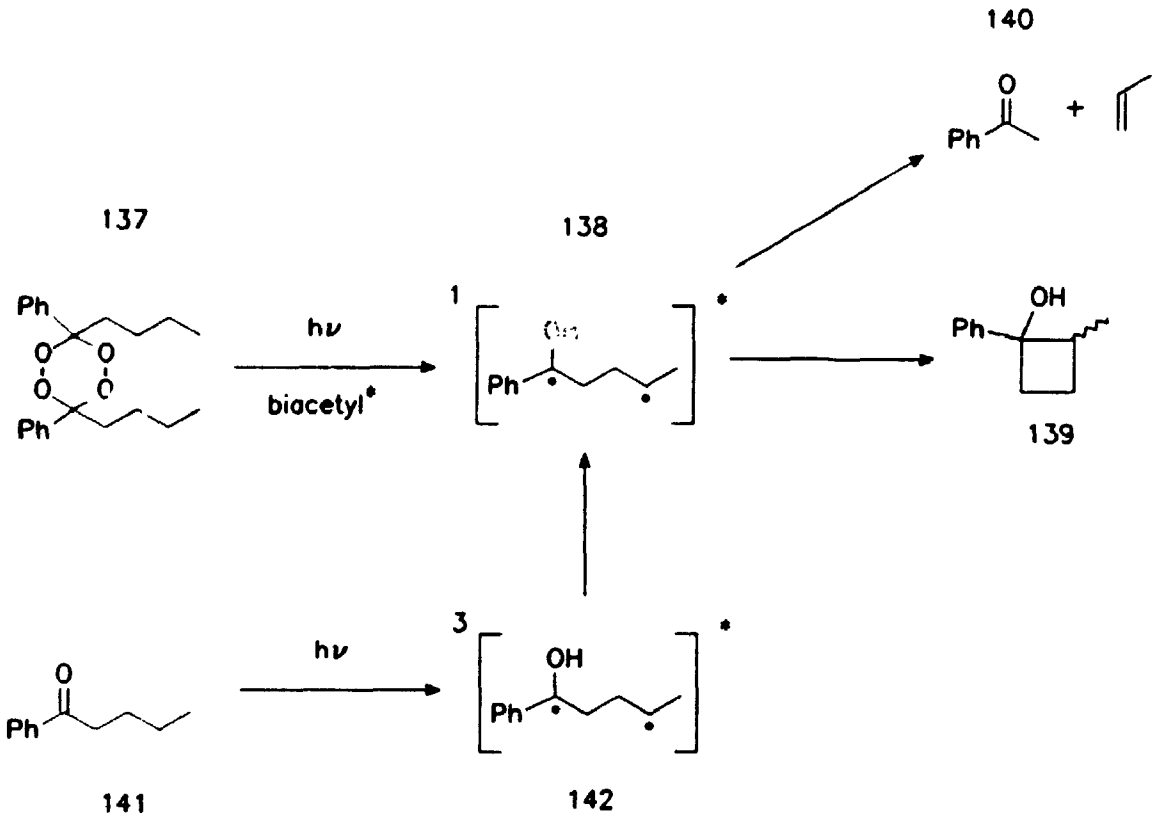

different from those obtained from the same singlet biradical, **138**, in the direct photolysis of valerophenone (see Scheme 43). One explanation for these differences is that the different sources of singlet biradical **137** result in the formation of different initial conformations and the collapse of this singlet biradical favours the reaction pathways with a transition state geometry resembling that of the initial biradical conformation. Therefore, it is reasonable to suggest that singlet biradicals retain a memory of the triplet biradical conformation from which they originated.

It is important to remember that the rate of intersystem crossing from the triplet state surface to the singlet state surface could be significantly different for each biradical conformation. In the case of biradicals generated in cyclic enone plus alkene

Scheme 44

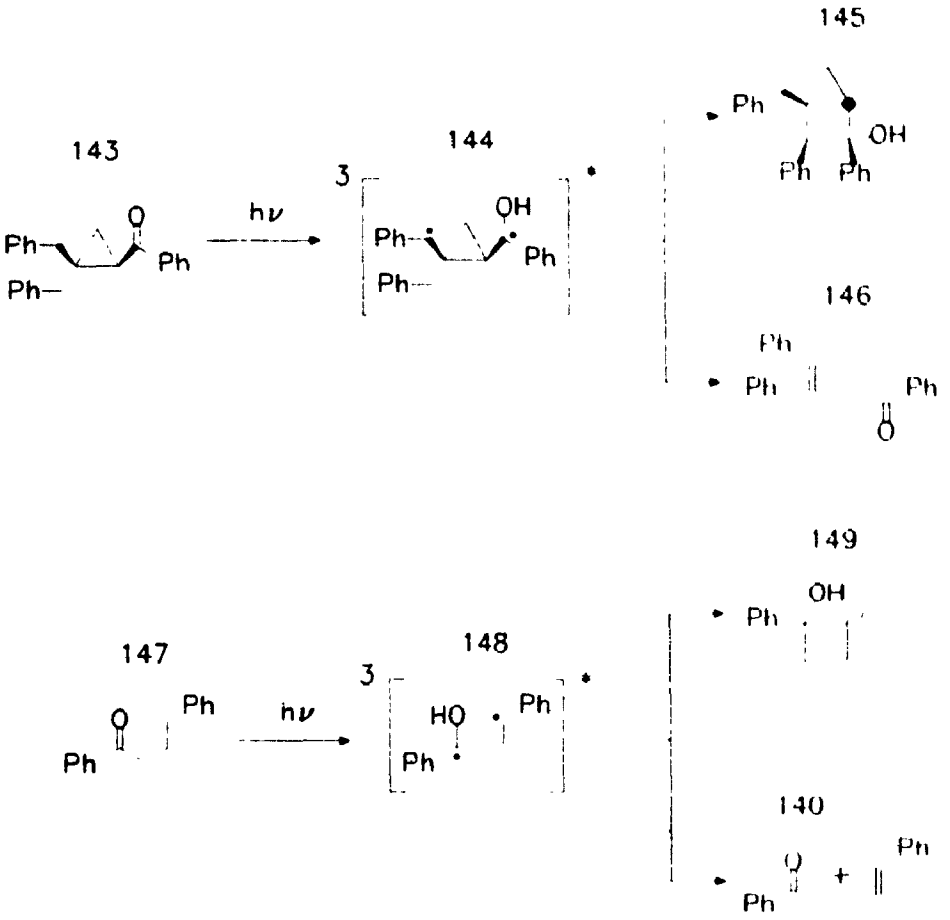

photocycloaddition reactions, each biradical conformation has a slightly different separation between the radical sites and so each conformation could exhibit a different spin-orbit coupling. It has been shown that with long flexible 1,n-biradicals the rate of intersystem crossing is dependent on the distance between the radical sites.[23] These systems demonstrate that a smaller separation between the radical sites translates into a larger spin-orbit coupling and therefore an increased rate of intersystem crossing. However, Caldwell has shown that the triplet lifetimes of Norrish Type II 1,4-biradicals exhibit a lack of conformational dependence.[24] In the latter study it was demonstrated that conformationally constrained biradical **144**, which is formed by photolysis of **143**, has a lifetime of 117 ns in methanol which is similar to the lifetime of 130 ns for the

more flexible biradical **148**[25] (see Scheme 44). Therefore, the smaller average separation of the radical sites in **144** relative to **148** does not seem to have an effect on the rate of intersystem crossing. A similar conclusion was reached when similar triplet lifetimes were observed for biradicals **150** (τ=242 ns in methanol) and **151** (τ=166 ns in methanol).[26] Given the lack of evidence to suggest that triplet 1,4-biradicals have conformation dependent lifetimes, we decided to evaluate the cyclisation to reversion ratios presented in Scheme 42 without invoking this additional complication. Therefore, we began by examining the relative energy differences between the various conformations available to each biradical in order to determine if the relative stabilities of the conformations can be correlated with the efficiencies of biradical reversion and biradical closure.

150

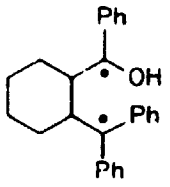

151

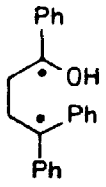

An inspection of the conformations available to biradicals **110a**, **110b**, **110c**, and **110d** reveals that for rotation about the 2,3-bond of each 1,4-biradical only one conformation exists in which gauche interactions between carbon-carbon bonds are minimised. Of the three possible conformations that may be accessed by rotation about this bond, two conformations result in three gauche interactions and one conformation results in two gauche interactions. The biradical conformations which result in two

gauche interactions are shown in Scheme 45. These conformations are characterised by a 180° dihedral angle between the hydrogens labelled H_2 and H_3 in this scheme. Molecular modelling calculations[5] were carried out on each biradical in which the energy differences due to rotation about the 2,3-bond were determined. Figure 11 demonstrates the energy surface that was mapped by plotting the heat of formation calculated by PCMODEL against the dihedral angle between H_2 and H_3 for biradicals **110b** and **110d**. The data in this figure confirm that the conformations of **110b** and **110d** shown Scheme 45 are the lowest energy conformations. Similar results were obtained for the biradicals **110a** and **110c**.

Scheme 45

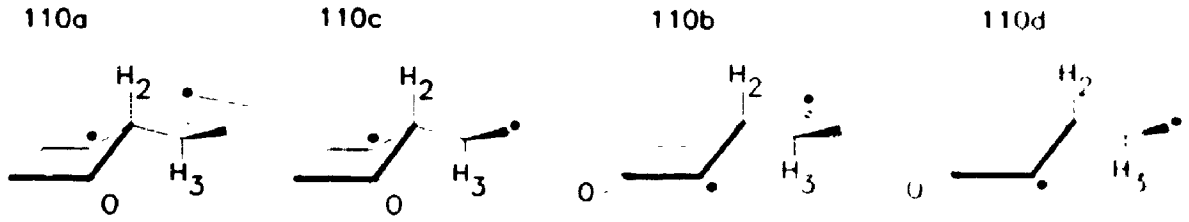

The lowest energy conformations of **110b** and **110c** exhibit an *anti* relationship between the two radical bearing carbon centres; hence, biradical fragmentation and not cyclisation is preferred from these conformations. On the other hand, the lowest energy conformations of **110a** and **110d** exhibit a *syn* relationship between the two radical bearing carbon centres; hence, both biradical fragmentation and cyclisation could result from these conformations. Indeed, the experimental data indicate that almost all of biradicals **110b** and **110c** revert to starting materials as opposed to closing to give

5.2 Results and discussion

5.2.1 Attempted biradical trapping with SO_2

A solution containing 0.15 M 2-cyclopentenone and 1.0 M 1-hexene in liquid SO_2 was prepared and then irradiated with acetone filtered light from a 400 W Hanovia medium pressure mercury lamp for 2 hours while the temperature was maintained at -50°C. After removal of the SO_2, a white polymeric residue was obtained. The residue was analyzed by g.c., coupled g.c.-m.s., ^1H nmr spectroscopy, ^{13}C nmr spectroscopy and IR spectroscopy. These analyses revealed that the reaction mixture contained a small amount of 2-cyclopentenone and 1-hexene starting material in addition to a large amount of a copolymer consisting of 1-hexene and sulfur dioxide which was identified as structure **195**. The identity of the polymer was confirmed by the presence of two characteristic sulfone peaks in the polymer's IR spectrum at 1308 and 1133 cm^{-1} as well as by presence of a common fragment ion at m/e=147 in the polymer's negative ion mass spectrum. The chemical shifts of the broad resonances in the ^{13}C and ^1H nmr spectra of the polysulfone also support the structural assignment.

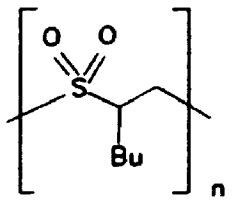

195

Reaction mixtures containing 2-cyclopentenone (0.1 M), 1-hexene (1 M) and concentrations of SO_2 between 1 and 5 M in benzene were prepared and irradiated with

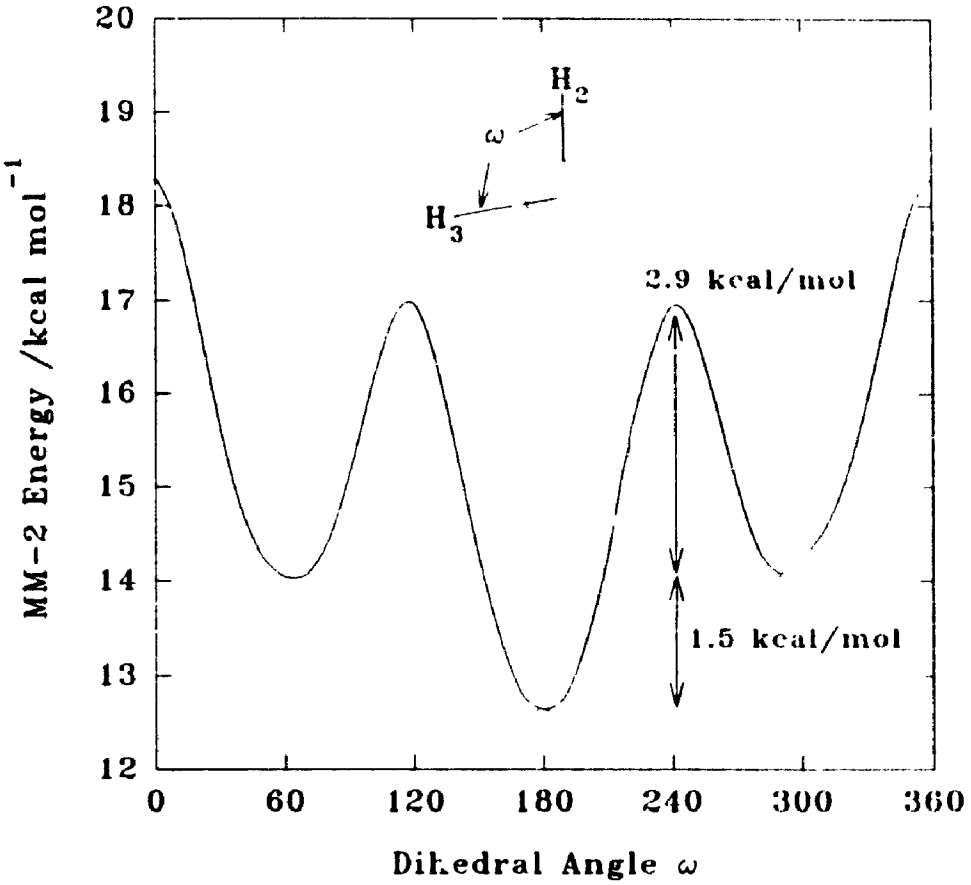

Figure 11: Potential energy surface for biradicals **110b** and **110d**.

cycloadducts. In the case of the biradicals that cyclise efficiently (i.e. **110a** and **110d**), we were unable to formulate any consistent theory that explains why certain product stereochemistries are favoured over others upon biradical closure.

The rate constants for biradical formation summarised in Scheme 42 exhibit some interesting features. For example, the rate constants k_b and k_d for *cis*-2-butene addition to 2-cyclopentenone indicate that the diastereomeric pair of biradicals labelled **110b** and **110d** are formed at the same rate. This observation indicates that the transition states leading to the formation of the respective biradicals are of similar energy. If overlap of the entire π-system of the alkene with the entire π-system of the enone were required,

Scheme 46

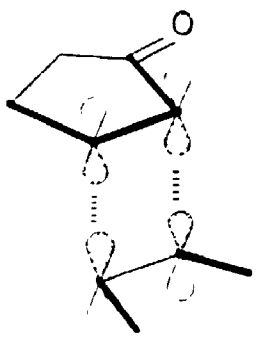

Exo approach

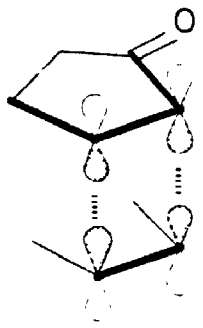

Endo approach

then the transition states leading to the formation of **110b** and **110d** would contain very different steric repulsions. In this case, the transition state leading to formation of **110b** would have the methyl groups of the alkene in an *endo* orientation with respect to the cyclopentenone ring and the transition state leading to formation of **110d** would have the methyl groups of the alkene in an *exo* orientation (see Scheme 46). These transition states would be different in energy and thus **110b** and **110d** would not be formed at the same rates.

If overlap of only one set of p-orbitals were required in the transition state, then enone-alkene orientations can be envisaged which would allow **110b** and **110d** to be formed at the same rate. Scheme 47 demonstrates two modes of approach of *cis*-2-butene to 2-cyclopentenone that could give rise to two diastereomeric biradicals. Each of these modes of approach might be expected to have similar steric interactions but do not require complete overlap of the π systems of the alkene and the enone. Therefore, the similarity of rate constants k_b and k_d for *cis*-2-butene addition suggest that biradical formation might not require full π-orbital overlap between the excited enone and the alkene.

Scheme 47

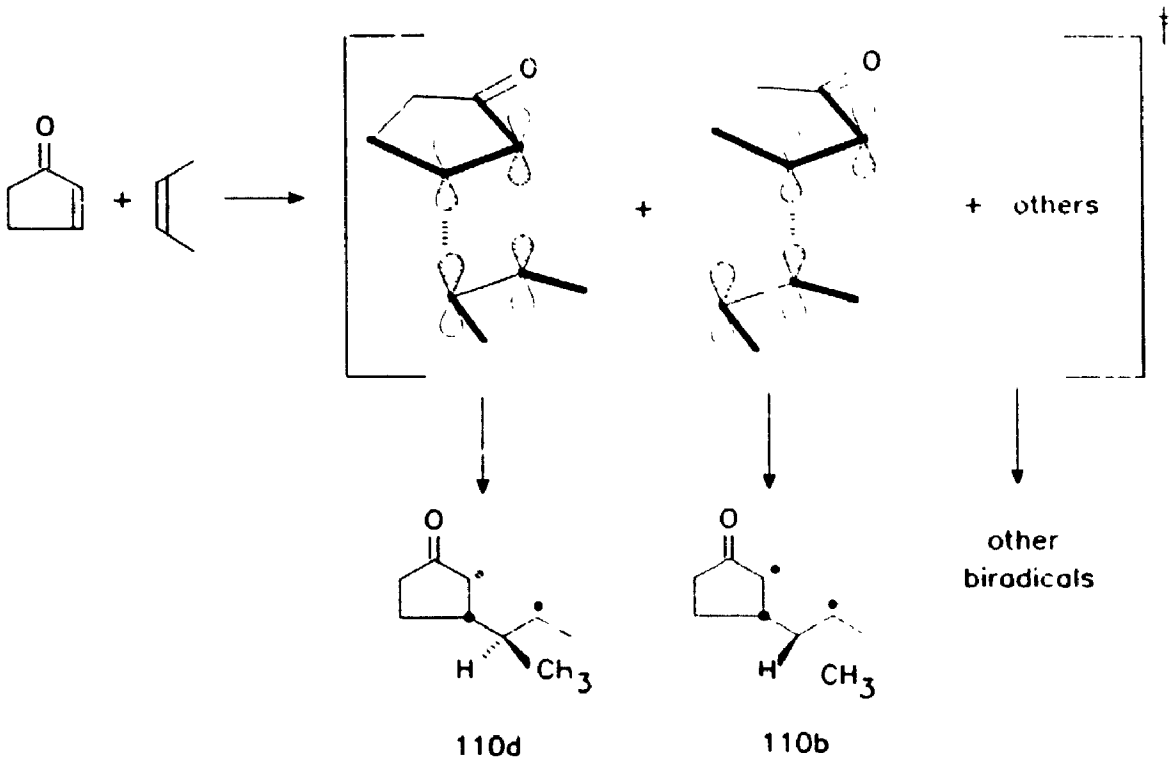

4.4 Conclusions

The use of hydrogen selenide as an effective reagent in trapping the 1,4-biradicals generated in t photocycloaddition reaction between *cis*- or *trans*-2-butene and 2-cyclopentenone made it possible to determine the relative rates of formation of each of the isomeric biradicals formed in these reactions. It was found that the structures of the biradicals formed in each photocycloaddition reaction were identical; however, the relative rates of formation of each biradical were dependent on the particular geometrical isomer of 2-butene added to the triplet enone. Therefore, the fact that different relative yields of cycloadducts result from the photocycloaddition of each 2-butene geometric isomer to 2-cyclopentenone can be rationalised in terms of the rates of formation of the

biradical intermediates.

The fraction of each biradical population which undergoes reversion to starting materials relative to the fraction which closes to form cycloadducts was determined for the 2-butene plus 2-cyclopentenone photocycloadditions. In determining these relative fractions, it was assumed that the triplet biradicals formed in the photocycloaddition reactions reach conformational equilibrium before intersystem crossing to the singlet state surface. The results indicate that relative fates of each member of the diastereomeric pair of biradicals **110a** and **110c** are very different. Similarly, the results also indicate that the relative fates of **110b** and **110d** are also very different. It was found that the fraction of the biradical **110a** population which undergoes reversion to starting materials relative to the fraction which closes to form cycloadducts was less than that determined for biradical **110c**. An analogous observation was made for the biradicals denoted **110d** and **110b**. In order to determine if the fates of the biradicals could be related to the molecular geometry of the lowest energy conformation, a semi-quantitative conformational analysis of all the biradicals was performed. In this analysis it was determined that biradicals **110b** and **110c** have a predicted lowest energy conformation from which only biradical reversion can occur. On the other hand, biradicals **110a** and **110d** have a predicted lowest energy conformation which facilitates biradical cyclisation. Therefore, the results of the conformational analysis indicate that the fates of the triplet biradicals formed in the photocycloaddition of the 2-butene isomers to 2-cyclopentenone are related to the structures of the lowest energy biradical conformations.

4.5 References

1. de Mayo, P.; Pete, J-P.; Tchir, M. *Can. J. Chem.* **1968**, *46*, 2535.
2. Bauslaugh, P. G. *Synthesis* **1970**, 287.
3. Criegee, R.; Furrer, H. *Chem. Ber.* **1964**, *97*, 2949.
4. Roth, W.R.; Enderer, K. *Liebigs Ann. Chem.* **1970**, *733*, 44.
5. PCMODEL (V.20), Serena Software Ltd., Bloomington IN. MM-2 parameters used.
6. Fleming, I.; Williams, D.H. *Tetrahedron* **1967**, *23*, 2747.
7. McConnell, H. M.; Robertson, R. E. *J. Chem. Phys.* **1958**, *29*, 1361.
8. Pretsch, E.; Seibl, J.; Simon, W. Clerc, T. *Tables of Spectral Data for Structure Determination of Organic Compounds*; Springer-Verlag: Berlin, 1989; p. H230.
9. Turro, N.J.; Morton, D.R. *J. Phys. Chem.* **1973**, *95*, 3947.
10. Al-Jallo, H.N.A.; Waight, E.S. *J. Chem. Soc. (B)* **1966**, 73.
11. Kjonaas, R. A.; Vawter, E. J. *J. Org. Chem.* **1986**, *51*, 3993.
12. Crimmins, M. T.; Mascarella, S. W. *J. Am. Chem. Soc.* **1986**, *108*, 3435.
13. de Mayo, P.; Pete, J.P.; Tchir, M.F. *Can. J. Chem.* **1968**, *46*, 2535.
14. de Mayo, P.; Nicholson, A.A.; Tchir, M.F. *Can. J. Chem.* **1970**, *48*, 225.
15. Wagner, P.J.; Bucheck, D.J. *J. Am. Chem. Soc.* **1969**, *91*, 5090.
16. Rudolph, A.; Weedon, A.C. *Can. J. Chem.* **1990**, *68*, 1590.
17. Becker, D.; Haddad, N.; Sahali, Y. *Tetrahedron Lett.* **1989**, *30*, 2661.
18. Peet, N.P; Cargill, R.L.; Bushey, D.F. *J. Org. Chem.* **1973**, *38*, 1218.
19. Dilling, W.L.; Tabor, T.E.; Boer, F.P.; North, P.P. *J. Am. Chem. Soc.* **1970**, *92*, 1399.
20. Caldweli, R.A.; Tang, W.; Schuster, D.I.; Heibel, G.E. *Photochem. Photobiol.* **1991**, *53*,159.

21. Scaiano, J. C. *Tetrahedron* **1982**, *38*, 819.

22. Ito, Y.; Matsuura, T.; Yokoya, J. *J. Am. Chem. Soc.* **1979**, *101*, 4010.

23. (a) Doubleday, C.; Turro, N.J.; Wang, J.F. *Acc. Chem. Res.* **1989**, *22*, 189. (b) Zimmt, M. B.; Doubleday, C.; Gould, I.; Turro, N. J. *J. Am. Chem. Soc.* **1985**, *107*, 6724. (c) Zimmt, M. B.; Doubleday, C.; Turro, N. J. *Ibid.* **1986**, *108*, 3618.

24. Caldwell, R.A.; Gupta, S.C. *J. Am. Chem. Soc.* **1989**, *111*, 740.

25. Caldwell, R. A. *Pure Appl. Chem.* **1984**, *56*, 1187.

26. Caldwell, R. A.; Dhawan, S. N.; Majima, T. *J. Am. Chem. Soc.* **1984**, *106*, 6459.

CHAPTER 5

INVESTIGATION OF POTENTIAL REAGENTS FOR TRAPPING 1,4-BIRADICALS

5.1 Introduction

The experiments described in Chapters 2, 3 and 4 involved the use of H_2Se as a reagent for trapping the 1,4-biradicals formed in enone-alkene photocycloaddition reactions. This reagent was successful in intercepting triplet biradicals and trapping them as stable products. Therefore, it was concluded that the rate of reaction between hydrogen selenide and the triplet biradicals was much faster than the rate at which each biradical intersystem crossed to the singlet state surface before closing to form cyclobutane adducts or fragmenting to form ground state starting materials. If the rate of reaction between H_2Se and the triplet biradicals was similar to the inverse lifetime of the biradicals, then complete trapping of the biradical would not have been observed. In this situation, some of the biradicals would react with H_2Se to form trapped products and some biradicals would undergo spin inversion followed by closure or fragmentation. The ratio of trapped biradicals to cyclobutane adducts would reflect the relative rate constants of biradical decay and H_2Se trapping.

In Chapter 2 it was demonstrated that the effective rate of biradical trapping can be adjusted by varying the concentration of H_2Se. In experiments described in that chapter, the ratio of the trapped products to cycloadducts was measured at each H_2Se concentration. However, these types of experiments were very difficult to perform since

H_2Se is a highly reactive and toxic gas which undergoes rapid oxidation upon exposure to air. Therefore, a considerable experimental error was associated with the determination of the concentration of H_2Se in solution. In order to obtain more information about the relative lifetimes of the triplet biradicals formed in a particular photocycloaddition, it would be of great benefit to have a reagent capable of trapping biradicals that is easier to handle than H_2Se and is a stable solid or a stable liquid at room temperature.

The initial goal of the studies described in this chapter was to find a suitable reagent capable of trapping triplet biradicals and then to use this reagent to study the effect of varying the concentration of the reagent on the ratio of the trapped product to cycloadducts. In these studies we hoped to obtain information about the relative lifetime of each of the biradicals formed in a particular cycloaddition reaction as well as information about the relative lifetimes of biradicals formed in different cycloaddition reactions. In addition to conducting these kinetic studies, the discovery of a new and useful reagent capable of intercepting biradical intermediates could be used to substantiate the results obtained from the biradical trapping experiments in which H_2Se was employed. That is to say, if the same relative rates of biradical formation were determined in trapping experiments involving a new reagent as were determined in the studies involving H_2Se, then additional credibility could be given to the H_2Se trapping experiments. Therefore, the investigation began by searching for a compound which showed promise as a biradical trapping reagent.

The main criterion that a potential biradical trapping reagent must satisfy is that the rate at which the reagent reacts with alkyl radical sites must be much greater than the

rate at which triplet biradicals formed in enone-alkene photocycloadditions decay. The products resulting from an interaction between the biradicals and the trapping reagent must also be relatively stable and isolable. In order to evaluate the former condition, one must have a general knowledge of the typical lifetimes of triplet 1,4-biradicals.

Scheme 48

155 156

There is a limited number of studies in the literature that report lifetimes for the biradical intermediates which are generated in enone-alkene photocycloadditions. For example, the lifetimes of the 1,4-biradicals generated in the cycloaddition of vinyl cyclopropane to cyclopentenone were determined to be approximately 50 ns.[1] In this study, Rudolph and Weedon used the rearrangement of the cyclopropylcarbinyl radical shown in Scheme 48 to "clock" the lifetime of the triplet biradicals formed in the cycloaddition. This rearrangement proceeds with an estimated rate constant of 1.2×10^8 sec^{-1}.[2] Scheme 49 demonstrates that two different types of products are formed in the photocycloaddition of vinyl cyclopropane with 2-cyclopentenone. One type of adduct contains a cyclobutane ring (i.e. products **160** and **164**) and is formed before the cyclopropylcarbinyl radical rearrangement has time to occur. The other type of product shown in Scheme 49 results from the disproportionation of a biradical which has undergone the cyclopropylcarbinyl radical rearrangement. Compounds **158** and **166** are examples of products resulting from this latter reaction. Therefore, the approximate average lifetime of 50 ns for the biradicals initially formed in the photocycloaddition of

vinyl cyclopropane and 2-cyclopentenone was determined by considering the relative ratio of products **160** and **164** to products **158** and **166**.[1]

Scheme 49

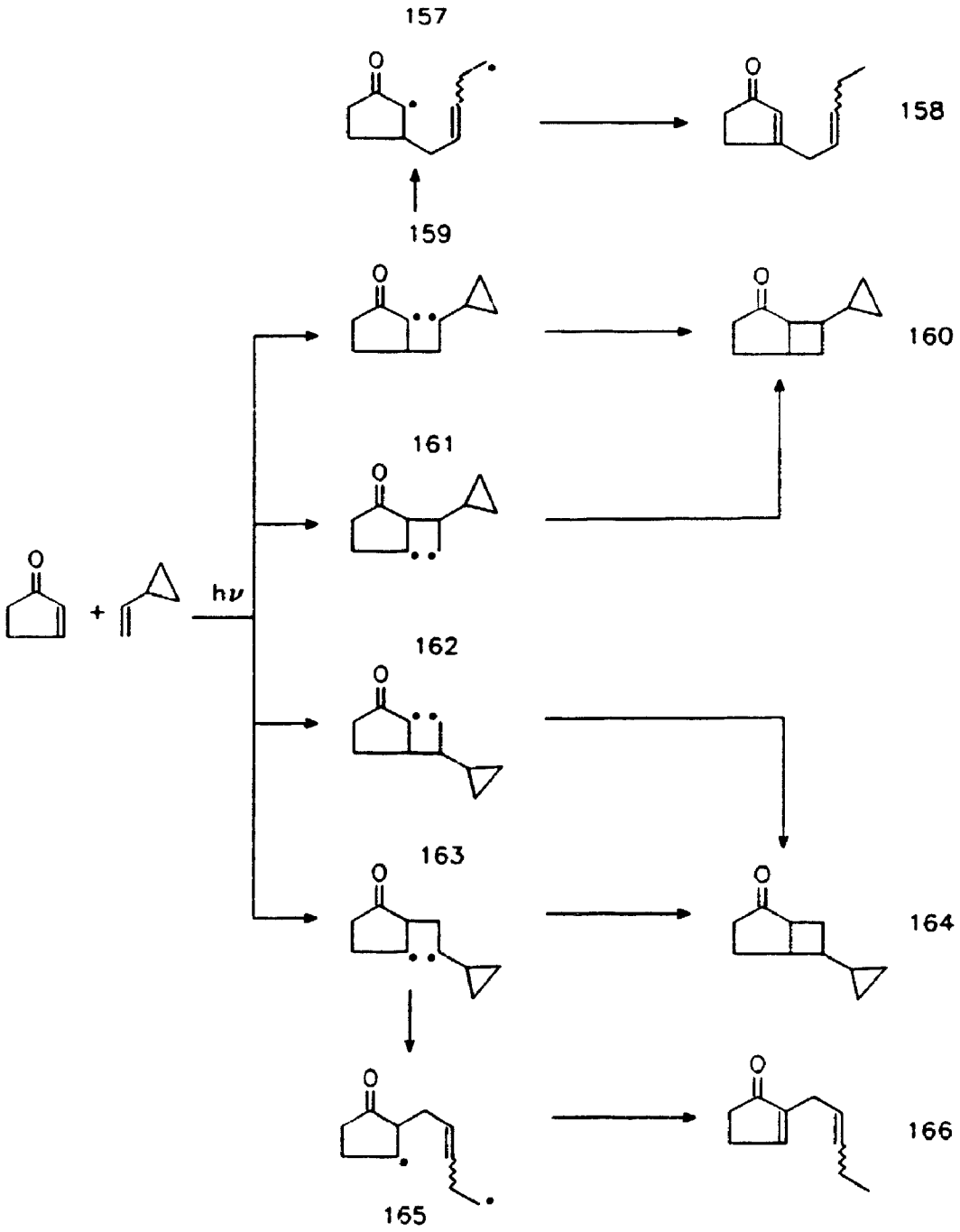

Scheme 51

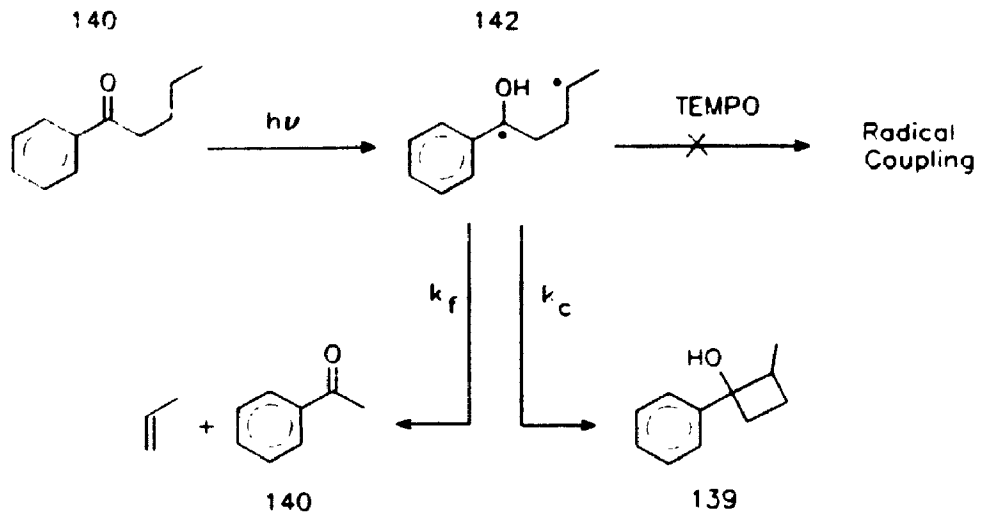

butyl radical with the 2,2,6,6-tetramethylpiperidinyloxyl radical (TEMPO) results in the formation of **167**. If each of the two radical sites in the triplet 1,4-biradicals generated in 2+2 enone-alkene photocycloaddition reactions behaved as separate radical species, then nitroxyl radicals such as TEMPO could couple to each radical site before the triplet biradical decayed. However, it has been shown that nitroxyl radicals do not react with the biradicals formed in the Type II intermolecular γ-hydrogen abstraction of phenyl ketones to form alkoxylamine type products.[5,6] In the case of Type II biradicals, the presence of TEMPO results in shortening the lifetime of the biradical and, in some instances, the relative ratio of the biradical closure and fragmentation products is also perturbed (see Scheme 51). Scaiano and co-workers have suggested that the presence of TEMPO causes an increase in the rate of intersystem crossing from the triplet biradical surface to the singlet surface which therefore decreases the lifetime of the triplet biradical.[5,7] The evidence that nitroxyl radicals do not couple with the radical sites of Type II biradicals indicates that these radicals are not suitable reagents for attempting to

trap the 1,4-biradicals formed in enone-alkene photocycloaddition reactions as stable products. The addition of TEMPO to enone-alkene photocycloaddition reaction would more than likely increase the rate of spin inversion for the triplet biradicals.

Scheme 52

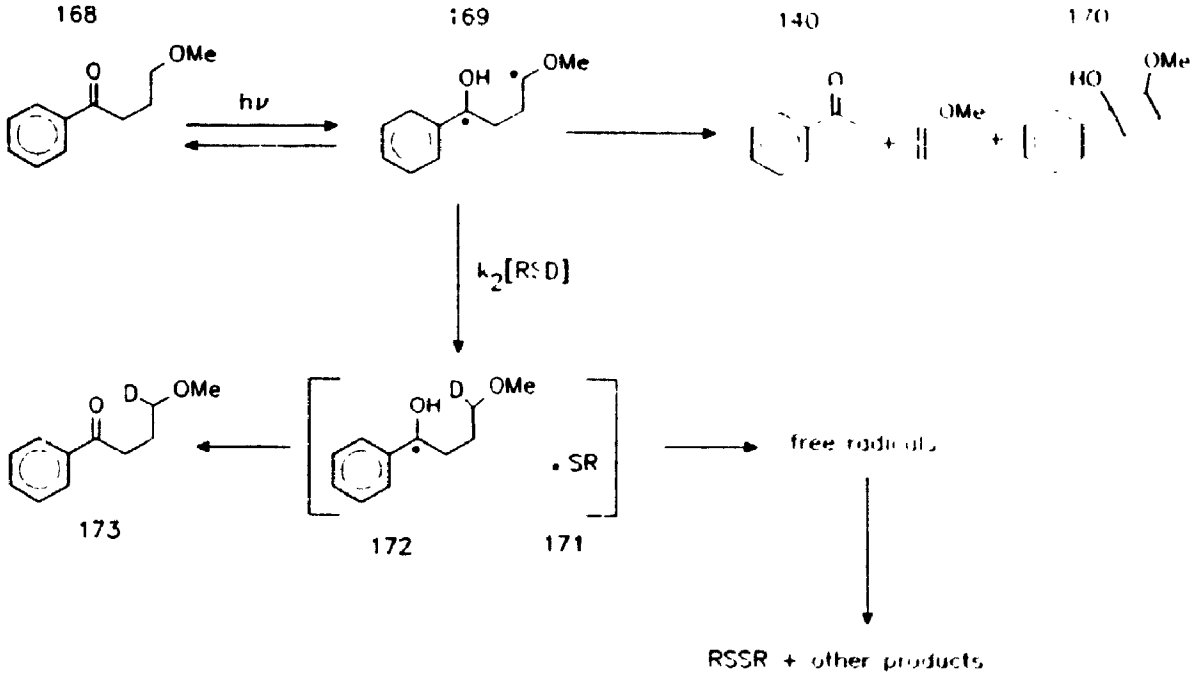

Wagner and co-workers have demonstrated that thiols can be used to trap the triplet biradicals formed in the Type II reaction of phenyl ketones.[8] In particular, Wagner and co-workers demonstrated that octanethiol and butanethiol are capable of intercepting the Type II biradicals generated in the photolysis of valerophenone and γ-methoxyvalerophenone (**168**). The products resulting from the reaction of octanethiol and valerophenone are shown in Scheme 52. The proportion of ketyl (**172**) and thiyl (**171**) radicals that disproportionate in the solvent cage relative to the proportion that react as free radicals was estimated to be 1:3 based on the relative quantum yields of γ-

deuterated γ-methoxyvalerophenone (**173**) and dioctyl disulfide.[8a] The rate constant k_2, which is defined in Scheme 52, was determined by measuring the rate of disappearance of biradical **169** and the rate of appearance of **172** in laser flash photolysis experiments at different concentrations of octanethiol.[8c] The lifetime of biradical **169** in a solution of 1.2 M pyridine in benzene which contained no octanethiol was determined to be 76 ns.[8c] The rate constant for reaction between **169** and octanethiol (k_2) was determined to be $1.1 \times 10^7\ M^{-1}s^{-1}$.[8c] The results of the experiments conducted by Wagner and co-workers indicate that the way thiols react with the radical sites in biradicals is similar to the way in which individual alkyl radicals react with thiols to form stable reduction products. Therefore, in the work described in this chapter alkylthiols were investigated as potential candidates for biradical trapping reagents in the photocycloaddition reaction of cyclic enones and simple alkenes.

Scheme 53

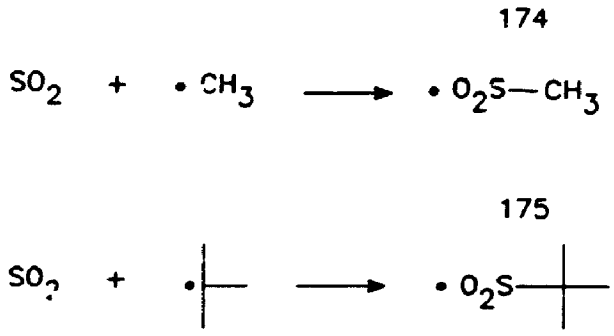

The reaction between alkyl radicals and sulfur dioxide is known to proceed at a relatively fast rate compared to the expected rate of decay of biradicals formed in photocycloadditions involving enones and alkenes. For example, the rate constant of the gas phase reaction between methyl radicals and sulfur dioxide has been reported by

James and co-workers to be 1.8×10^8 $M^{-1}s^{-1}$ at 22°C.[9] This radical trapping reaction, which is shown in Scheme 53, results in the formation of sulfonyl radical **174**. Similarly, the rate constant for the addition of the t-butyl radical to sulfur dioxide was estimated by ESR methods to be between 10^7 and 10^8 $M^{-1}s^{-1}$.[10]

Scaiano and Small examined the effect of sulfur dioxide on the lifetime of triplet biradical formed in the photodegradation of poly(phenyl vinyl ketone).[11] These investigations revealed that sulfur dioxide is capable of quenching the biradical intermediates formed in the photolysis with a rate constant of approximately 9×10^8 $M^{-1}s^{-1}$. Since no product studies were carried out by Scaiano and Small, the mechanism by which sulfur dioxide quenches the triplet biradicals is unknown. It is possible that addition of one of the radical sites of the biradical intermediates to sulfur dioxide might occur; however, it is also possible that the presence of sulfur dioxide might increase the rate of intersystem crossing from the triplet biradical to the singlet state surface via the spin-orbit coupling mechanism.

If a radical-type addition between sulfur dioxide and the triplet biradicals generated in an enone-alkene photocycloaddition were to occur, then it is possible that stable products could be formed and that these products would possess structures representative of the biradicals from which they came. Scheme 54 indicates the types of intermediates that could be formed by the reaction of sulfur dioxide with biradicals **176** and **179**; these are generated in the photoreaction of 2-cyclopentenone with a mono-substituted alkene. The scheme illustrates only two intermediates (i.e. **177** and **180**) although a number of other sulfonyl radical containing biradicals could also be formed. After intersystem crossing from the triplet state surface to the singlet state surface,

biradicals **177** and **180** could close to form cyclic sulfones **178** and **181**, respectively. In the studies described in this chapter, the irradiation of 2-cyclopentenone in solutions containing simple alkenes and sulfur dioxide was performed in order to test the validity of the mechanism shown in Scheme 54.

Scheme 54

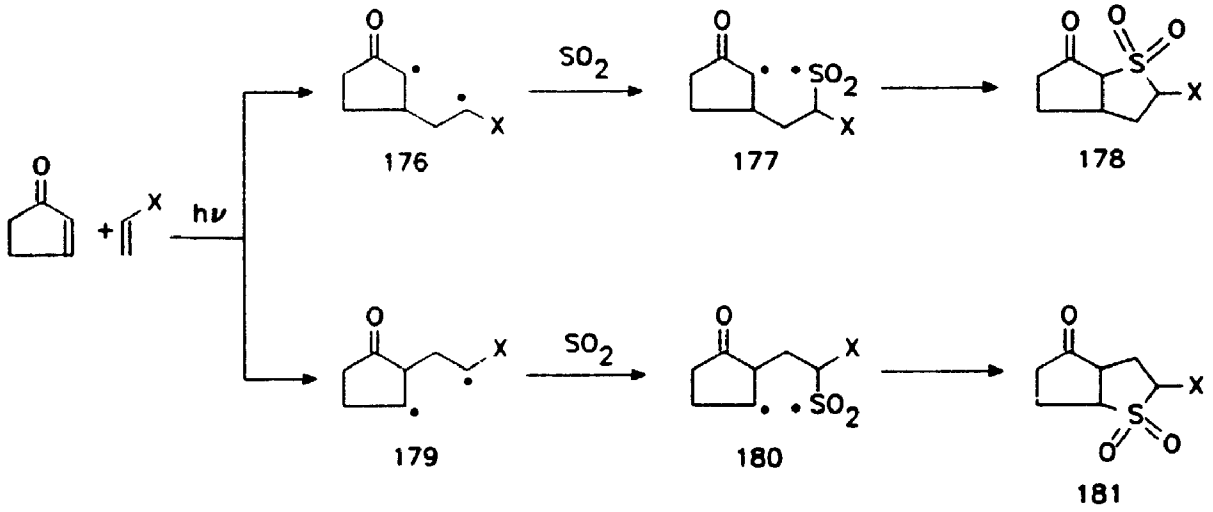

The potential effectiveness of compounds belonging to the nitrone class of compounds as biradical trapping reagents was also investigated in the studies described in this chapter. Nitrones contain the general structure indicated in compound **182.**

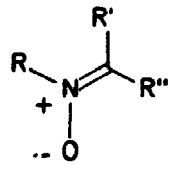

182

These types of compounds were investigated because they are known to undergo addition reactions with t-butoxyl radicals at very fast rates. For example, the addition of

t-butoxyl radical to nitrone **183** shown in Scheme 55 proceeds with a rate constant of $7x10^8$ $M^{-1}s^{-1}$.[12] Acyclic nitrones also react with the t-butoxyl radical at rates similar to this.[12b] Therefore, the rate constants for radical additions to nitrones are of the same order of magnitude required for an effective biradical trapping reagent.

Scheme 55

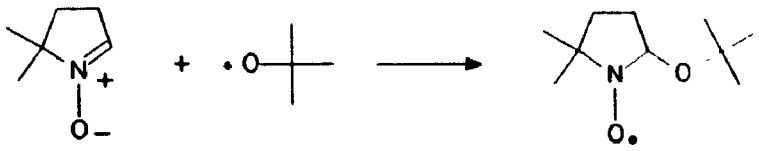

183 184

Scheme 56 illustrates the possible products that could be formed if nitrone **185** were to react with the triplet biradicals generated in an enone plus alkene photocycloaddition reaction. For example, the triplet biradicals could react with nitrones in radical-type addition reactions to form the nitroxyl radical intermediates **187** and **188** shown in this scheme. After spin inversion, these nitroxyl radical intermediates could close to form the stable heterocycles labelled **186** and **189**. The regiochemistry and relative yields of the heterocyclic compounds resulting from the reaction mechanism shown in Scheme 56 could be used to assign the structures and relative rates of formation of the biradicals from which the heterocyclic compounds originated. In this chapter, the attempt was made to trap the biradicals formed in the photocycloaddition reaction between 2-cyclopentenone and various alkenes with nitrone **185**.

The use of alkyl- and arylselenols as biradical trapping reagents will also be described in this chapter. These compounds are the logical analogues of hydrogen selenide which, according to the results described in the previous three chapters, is an

Scheme 56

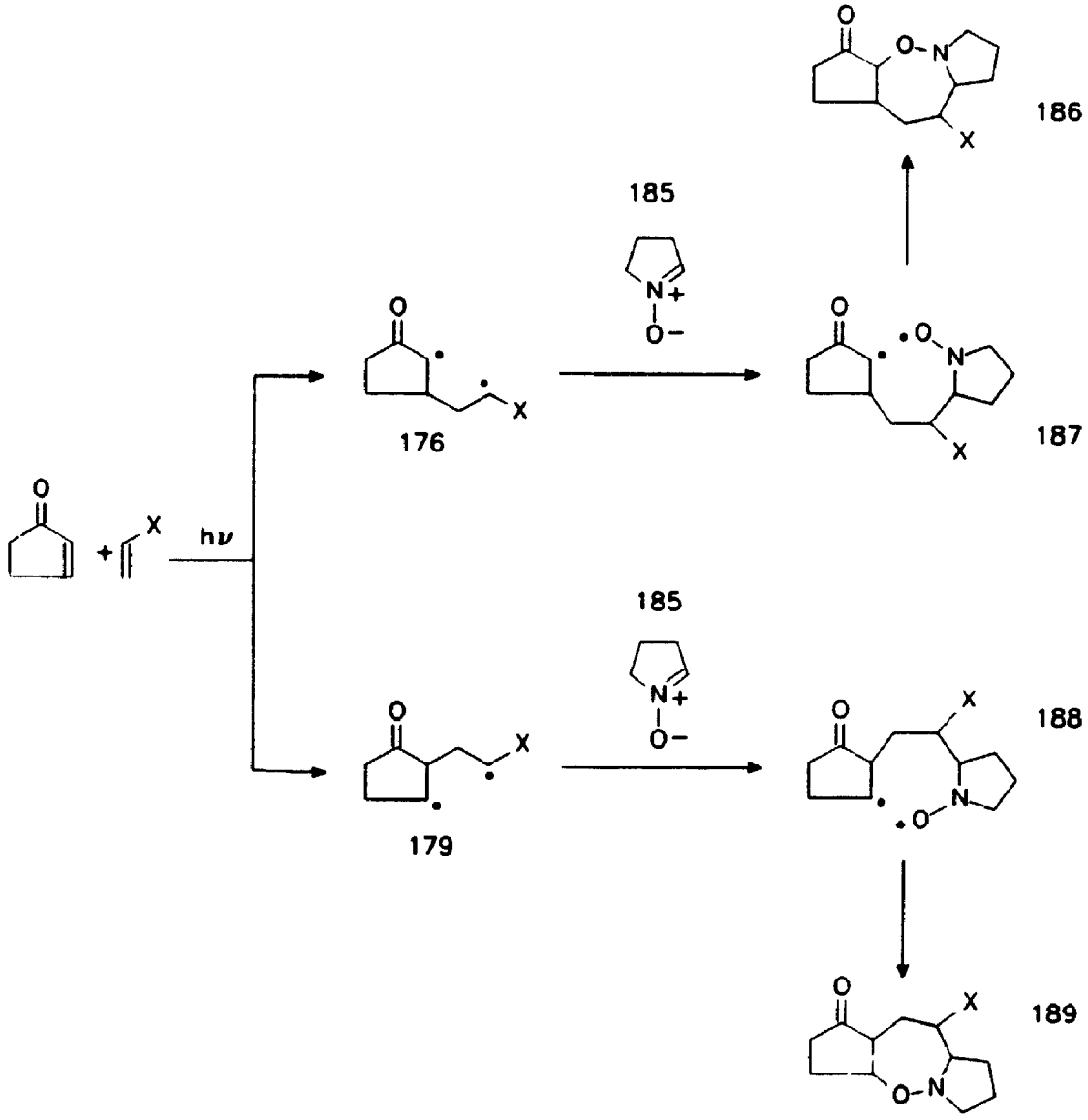

effective reagent for trapping the triplet biradicals formed in enone-alkene photocycloaddition reactions.

Rate constants for the abstraction of hydrogen from benzeneselenol by alkyl radicals have been determined by Newcomb and co-workers.[13] In these studies, the cyclopropylcarbinyl radical ring opening (see Scheme 48) was used to "clock" the rate of hydrogen abstraction from benzeneselenol. The relative yields of **193** and **194** shown in Scheme 57 were used to calculate a value of 2.1×10^9 $M^{-1}s^{-1}$ for k_t at 25°C. This rate

Scheme 57

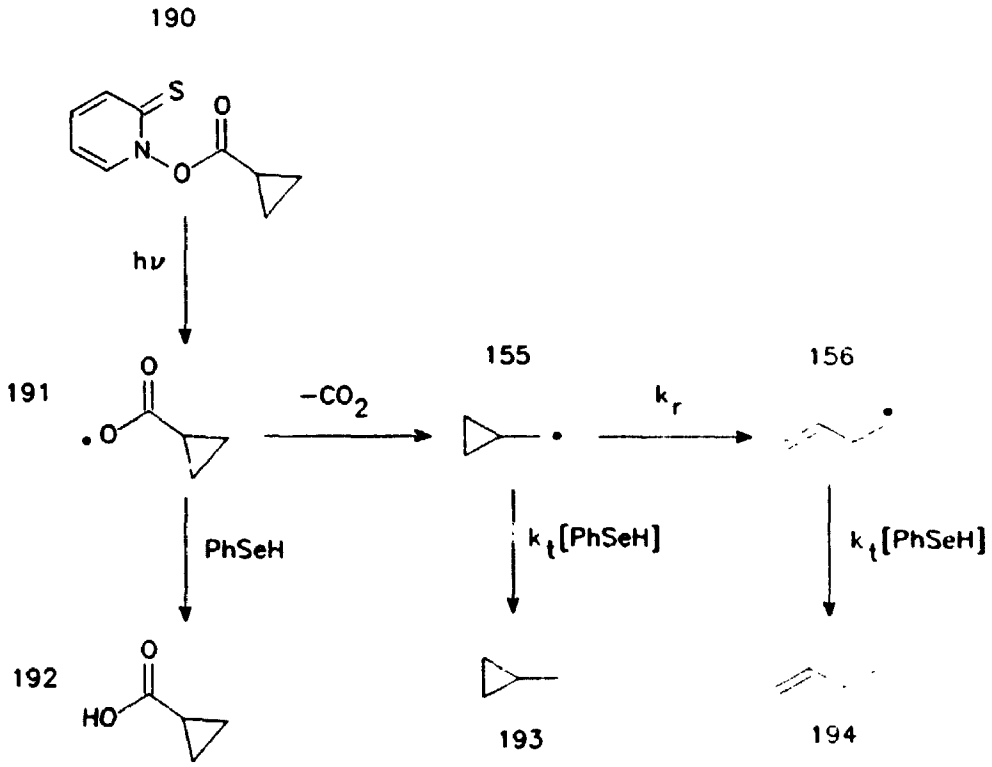

constant is 2 orders of magnitude greater than the approximate rate constant for decay of the triplet biradicals which are formed in photocycloadditions of cyclic enones and alkenes. No rate constants have been reported for the hydrogen abstraction reactions involving alkyl radicals and alkylselenols; however, the rate constants for these reactions are probably no more than an order of magnitude lower than the rate constant reported for benzeneselenol. Therefore, benzeneselenol and t-butylselenol were investigated as potential reagents for trapping the biradicals formed in the photoaddition of 2-cyclopentenone to 2-butene.

5.2 Results and discussion

5.2.1 Attempted biradical trapping with SO_2

A solution containing 0.15 M 2-cyclopentenone and 1.0 M 1-hexene in liquid SO_2 was prepared and then irradiated with acetone filtered light from a 400 W Hanovia medium pressure mercury lamp for 2 hours while the temperature was maintained at -50°C. After removal of the SO_2, a white polymeric residue was obtained. The residue was analyzed by g.c., coupled g.c.-m.s., ^1H nmr spectroscopy, ^{13}C nmr spectroscopy and IR spectroscopy. These analyses revealed that the reaction mixture contained a small amount of 2-cyclopentenone and 1-hexene starting material in addition to a large amount of a copolymer consisting of 1-hexene and sulfur dioxide which was identified as structure **195**. The identity of the polymer was confirmed by the presence of two characteristic sulfone peaks in the polymer's IR spectrum at 1308 and 1133 cm^{-1} as well as by presence of a common fragment ion at m/e=147 in the polymer's negative ion mass spectrum. The chemical shifts of the broad resonances in the ^{13}C and ^1H nmr spectra of the polysulfone also support the structural assignment.

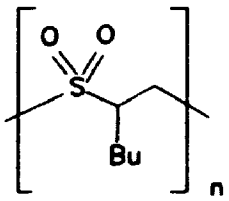

195

Reaction mixtures containing 2-cyclopentenone (0.1 M), 1-hexene (1 M) and concentrations of SO_2 between 1 and 5 M in benzene were prepared and irradiated with

acetone filtered light from a 400 W Hanovia medium pressure mercury lamp. The product mixtures obtained from these irradiations were very similar: all contained a large amount of unreacted starting material as well as a large amount of polysulfone **195**. No cycloadducts or products representative of sulfones **178** and **181** were formed in any of the reactions carried out in the presence of SO_2.

One problem with attempting to use SO_2 as a biradical trap in enone-alkene photocycloadditions is that benzene solutions of SO_2 absorb a small yet significant amount of light above 330 nm. The extinction coefficient of SO_2 at 350 nm was determined in a 2 M benzene solution to be 0.45 $M^{-1}cm^{-1}$. The extinction coefficient of 2-cyclopentenone at 350 nm in benzene solution is only about 10 $M^{-1}cm^{-1}$. Since the concentration of SO_2 must be kept above approximately 1 M in order to ensure a suitable potential biradical trapping rate, the problem of light being absorbed by SO_2 is impossible to avoid. The formation of polysulfone **195** is probably a direct consequence of the fact that SO_2 was absorbing light, forming either $^1(SO_2)^*$ or $^3(SO_2)^*$, which then reacted with the 1-hexene to initiate a radical polymerisation reaction. In fact, the copolymerization of alkenes and sulfur dioxide via a radical chain mechanism has been known for some time.[14] Based on the unsuccessful attempts to trap the biradicals generated in the photocycloaddition of 2-cyclopentenone and 1-hexene with SO_2, it must therefore be concluded that the hypothesised pathway shown in Scheme 54 does not operate.

5.2.2 Attempted biradical trapping with butanethiol

A solution containing 2-cyclopentenone (0.11 M), isobutene (1.7 M) and butanethiol (0.46 M) in benzene was prepared and irradiated with Pyrex filtered light

from a 400 W Hanovia medium pressure mercury lamp for 1 hour. The reaction mixture contained compounds **54**, **57**, **55**, and **56** in a 3:9:70:18 ratio (see Scheme 18 in Chapter 3); however, no evidence of products resulting from the trapping of biradicals was found. The distribution of these compounds was confirmed by comparing the g.c. retention times of the products resulting from this reaction with the products obtained in the absence of butanethiol. The characterisation of the cycloadducts and disproportionation products resulting from the cycloaddition of 2-cyclopentenone and isobutene has been described in Chapter 3. It is important to note that the presence of butanethiol did not affect the relative yields of the four products resulting from the cycloaddition reaction.

The results obtained for the experiments in which attempts were made to trap the biradicals formed in the photocycloaddition of 2-cyclopentenone and isobutene with butanethiol indicate that butanethiol is not a suitable reagent for intercepting these particular biradicals. The lack of formation of products representative of trapped biradicals indicates that the rate of reaction between butanethiol and the triplet biradicals formed in this cycloaddition must be considerably slower than the rate at which the triplet biradicals undergo spin inversion to the singlet state followed by fragmentation or closure. The similarity of the product ratios obtained in the presence and absence of butanethiol also indicates that incomplete trapping of triplet biradicals did not occur. If the butanethiol was intercepting some of the biradicals and was therefore partially responsible for the formation compounds **54** and **57** (see Chapter 3), the relative yields of the two disproportionation products and the cycloadducts would deviate from those observed in the reaction conducted in the absence of butanethiol. This was not the case. Therefore, it may be concluded that butanethiol is not an effective biradical trapping

reagent for use in photocycloaddition reactions involving cyclic enones and alkenes.

5.2.3 Attempted biradical trapping with nitrones

The particular nitrone that was investigated as a potential biradical trapping reagent was 1-pyrroline N-oxide (**185**). This cyclic nitrone is not commercially available and therefore had to be synthesised. Murahashi and co-workers reported the preparation of compound **185** by the tungstate-catalyzed hydrogen peroxide oxidation of pyrrolidine in aqueous solution (see Scheme 58).[15] The preparation of **185** can also be performed using selenium dioxide as the catalyst instead of sodium tungstate[16]; however, we were unable to obtained yields greater than 5%, which is substantially less than the 73% yield that Murahashi and co-workers reported, when selenium dioxide was used as the catalyst. The largest yield of **185** that was achieved in this investigation was 21% which was obtained using sodium tungstate as the oxidation catalyst. This yield is also substantially less than the reported yield of 44% for the reaction involving this particular catalyst.[15] The reasons for the poor yields of **185** that we obtained from both methods of preparation were not pursued.

Scheme 58

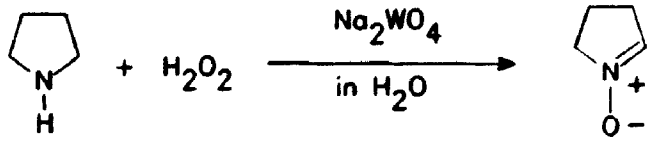

185

Before discussing the experiments in which the effectiveness of **185** as a biradical trap was studied, some attention must be given to the thermal reactions that **185** can undergo in the presence of alkenes. Nitrones such as compound **185** can add to alkenes in thermally initiated 1,3-dipolar additions.[17] Scheme 59 illustrates the types of products (i.e. compounds **196** and **197**) formed in the 1,3-dipolar addition reactions. Because these types of addition reactions are thermally initiated, it is possible to significantly slow the rate of reaction between a nitrone such as **185** and an alkene by lowering the reaction temperature.[18] In addition to lowering the reaction temperature, 1,3-dipolar additions of nitrones and alkenes can also be slowed by putting electron donating substituents on the alkene.[18] Therefore, the complication of 1,3-dipolar addition reaction products in trapping experiments involving nitrones, enones and alkenes must be minimized by lowering the reaction temperature and avoiding alkenes substituted with electron withdrawing groups.

Scheme 59

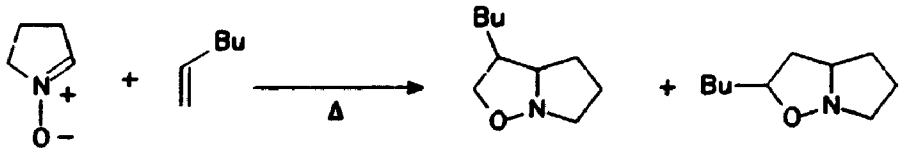

185 196 197

Attempts were made to trap the biradicals formed in the reaction between 2-cyclopentenone and cyclopentene with nitrone **185**. In these experiments, a methanol solution containing 0.22 M 2-cyclopentenone, 1.62 M cyclopentene, and 1.79 M nitrone **185** was irradiated with acetone filtered light from a 400 W Hanovia medium pressure mercury lamp while the reaction temperature was maintained at -78°C. The solution was

analyzed frequently by g.c. and it was determined that the only light initiated products formed were 2+2 photocycloadducts. The dark reaction products were identified by comparison of the g.c. analyses resulting from this irradiation with the g.c. analyses resulting from a reaction mixture containing 2-cyclopentenone, cyclopentene, and **185** that was not exposed to ultra-violet light. These dark reaction products exhibited molecular ions in their electron impact mass spectra indicating that they were 1,3-dipolar addition products resulting from reactions between cyclopentenone and **185** as well as from reactions between cyclopentene and **185**. The rate of formation of the cycloadducts was identical to the rate of formation of the cycloadducts resulting from a reaction in which a methanol solution containing the same concentrations of 2-cyclopentenone and cyclopentene as described above, but no nitrone **185**, was irradiated under the same conditions. Therefore, it was concluded that nitrone **185** is ineffective at intercepting the biradicals generated in this particular cycloaddition reaction.

In order to confirm the ineffectiveness of nitrone **185** as a biradical trapping reagent for enone-alkene photocycloaddition reactions, attempts were also made to trap the biradicals formed in the reaction between 2-cyclopentenone and ethyl vinyl ether. These experiments were conducted in a way similar to that described for the attempted trapping experiments involving 2-cyclopentenone and cyclopentene. The g.c. analyses of the reaction mixtures resulting from the photo-reactions containing 2-cyclopentenone, ethyl vinyl ether, and **185** indicated that nitrone **185** has no effect on the rates of formation of the cycloadducts. In addition, it was also observed that the presence of nitrone **185** did not affect the relative yields of the cycloadducts. Therefore, the results obtained from this attempted trapping confirm that nitrone **185** is incapable of

intercepting the biradicals formed in enone-alkene photocycloadditions in the way suggested in Scheme 56. It is possible that the ineffectiveness of **185** at trapping triplet biradicals is the result of a slow rate of reaction between the triplet biradicals and the nitrone relative to the rate of spin inversion of the biradicals.

5.2.4 Attempted biradical trapping with benzeneselenol and t-butylselenol

Benzeneselenol and t-butylselenol were also studied as potential reagents for trapping the biradicals formed in enone-alkene photocycloaddition reactions. These compounds were prepared by reacting phenyl magnesium bromide and t-butyl magnesium chloride with selenium metal in diethyl ether and quenching the reaction with an acidic work-up. Scheme 60 summarises the preparation of benzeneselenol.[19] Both of these selenols undergo rapid oxidation in the presence of air; therefore, each compound was prepared shortly before use in the trapping experiments and stored under nitrogen. The reactivity and toxicity of these compounds makes them just as difficult to use as hydrogen selenide. In fact, the relatively easy preparation of hydrogen selenide makes this proven biradical trap a more convenient reagent to add to enone-alkene photocycloaddition reactions. Nevertheless, attempts were made to trap the biradicals formed in the photocycloaddition of 2-cyclopentenone and *trans*-2-butene with benzeneselenol and t-butylselenol.

In order to evaluate the potential effectiveness of benzeneselenol as a biradical trap, a benzene solution of 2-cyclopentenone (0.083 M), *trans*-2-butene (1.5 M), and benzeneselenol (0.5 M) was irradiated with Pyrex filtered light from a 400 W Hanovia medium pressure mercury lamp. Analysis of this reaction mixture by g.c. revealed that

Scheme 60

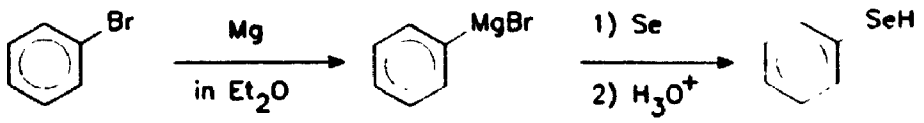

an horrendously complex mixture of products was formed in the reaction; however, no evidence of cycloadducts or products representative of trapped biradicals was found in the analyses. Most of the products formed in the photo-reaction were also observed in reaction mixtures containing benzeneselenol, 2-cyclopentenone, and *trans*-2-butene that were not exposed to ultra-violet light. Lowering the concentration of the benzeneselenol to 0.1 M did not have a significant effect on the complexity of the product mixture observed in the g.c. analyses. Due to the complexity of the product mixture, no attempt was made to separate the mixture's components.

The lack of success obtained in the experiments in which attempts were made to trap triplet biradicals with benzeneselenol could have been caused by the fact that benzeneselenol was absorbing a significant amount of light. The U.V. absorption spectrum of benzeneselenol exhibits a substantial tail out to 340 nm.[20] In retrospect, it would have been a good idea to filter the light coming from the mercury lamp with an acetone filter instead of a Pyrex filter in these trapping experiments. It is highly possible that some of the products observed in the reaction resulting from the trapping experiments in which benzeneselenol was used were a result of reactions stemming from excited benzeneselenol.

The trapping experiments that were conducted in the presence of t-butylselenol

2-cyclohexenone with fumaronitrile and maleonitrile in order to test the possibility of a reaction mechanism which involves triplet energy transfer and photocycloadduct formation as two competing pathways.[3] In this investigation, the quantum yield of product formation (Φ_p) and the quantum yield of isomerisation of each alkene (Φ_{iso}) were used in conjunction with quantum yields of triplet enone capture by each alkene (Φ_{tc}) in calculating the fraction of all intermediates, either triplet alkenes or biradicals, that reverted to fumaronitrile. The quantum yield of triplet capture was calculated according to the equation $\Phi_{tc} = k_q/(k_q + k_d)$, where k_q represents the rate of quenching of the enone triplet by the alkene and k_d represents the inverse lifetime of 3-methyl-2-cyclohexenone. Therefore, the fraction of all intermediates that revert to fumaronitrile (F) was determined from the equation $F = \Phi_{iso}/(\Phi_{tc} - \Phi_p)$, where each of the three quantum yields were measured for the addition of maleonitrile to 3-methyl-2-cyclohexenone. The value of F that was obtained was 0.72.[3] The authors of the work compared this fraction to the ratio of the photostationary state concentrations of maleonitrile and fumaronitrile (1:1) that result from the benzophenone or acetophenone sensitised photoisomerisation of the two alkenes. The difference between F and the photostationary state ratio of concentrations was explained in terms of a mechanism in which Schenck isomerisation of the intermediate biradicals accounted completely for the formation of fumaronitrile in the reaction of 3-methyl-2-cyclohexenone and maleonitrile.[3] One can also account for the difference between F and the photostationary state ratio by considering a mechanism in which both Schenck isomerisation and isomerisation induced by triplet energy transfer result in the formation of fumaronitrile. The latter possibility was not considered explicitly by Schuster and co-workers.

The build-up of these dark reaction products complicated the reaction mixture and therefore made it difficult to identify some of the cycloadducts and the trapped biradical products.

It is instructive to compare the product ratios obtained in the trapping experiments involving 2-cyclopentenone, *trans*-2-butene, and t-butylselenol with the product yields observed when H_2Se was used as the biradical trap (see Chapter 4). The presence of cycloadducts in the trapping experiments in which t-butylselenol (0.37 M) was used as the biradical trap indicate that, at the concentration used, this particular compound is incapable of quantitatively trapping all of the triplet biradicals. On the other hand, it was demonstrated in Chapter 4 that the presence of hydrogen selenide at a concentration of 0.3 M results in complete trapping of the triplet biradicals formed in the photocycloaddition of 2-cyclopentenone and *trans*-2-butene. Therefore, it appears that H_2Se reacts with triplet biradicals faster than t-butylselenol.

The ratios of cycloadducts **114a**, **114b**, and **114d** observed in the photocycloaddition of 2-cyclopentenone and *trans*-2-butene that was carried out in the presence of t-butylselenol (50:30:20) are very similar to the ratios that were observed in the absence of the biradical trap (51:29:20). The relative ratios of the cycloadducts **114a**, **114b**, and **114d** formed in the presence and absence of t-butylselenol can be used to assess the relative lifetimes of the biradical intermediates involved in the reaction. If the lifetimes of the triplet biradicals were substantially different from one another, then the addition of a biradical trapping reagent such as t-butylselenol would result in a perturbation of the ratios of the cycloadducts resulting from these biradicals. This perturbation would be caused by the fact that, in the case of a common rate constant for

biradical trapping, more of the longer lived biradicals would be intercepted by the trapping reagent relative the shorter lived biradicals. In this case, the contribution of cycloadduct formation from the shorter lived biradicals would be effectively enhanced relative to the longer lived biradicals. Since the ratios of the cycloadducts formed in the photo-addition reaction of 2-cyclopentenone and *trans*-2-butene are the same in the presence and absence of a biradical trapping reagent, then the biradicals responsible for the formation of these products must have similar lifetimes, if the assumption is correct that rate of trapping is the same for all biradicals.

Within experimental error, the ratio of trapped products **121**:**122**:**123**:**125**:**16**:(**127**+**128**) observed in the experiments in which H_2Se was used to trap the triplet biradicals (1.2:9.5:10.6:2.5:14.5:62.0) is similar to the ratio observed in the trapping experiments in which t-butylselenol was used (2:8:15:4:15:56). The similarity of the ratios of the trapped products observed in the product mixtures obtained from the reactions in which t-butylselenol and H_2Se were utilised suggests that the relative rates of formation of each of the biradicals generated in each reaction are the same. That is to say, the relative rates of formation of the biradicals formed in the photocycloaddition of 2-cyclopentenone and *trans*-2-butene are independent of the type of biradical trap used to determine the relative rates. This is an important conclusion because it demonstrates that the reaction between triplet 2-cyclopentenone and *trans*-2-butene which results in the formation of biradicals **110a**, **110b**, **110c**, and **110d** is not perturbed by the presence of the trapping reagent. Therefore, the relative ratios of the trapped products formed in the presence of the biradical trapping reagent accurately reflect the relative rates of formation of the biradicals formed in the absence of the trap.

5.3 Conclusions

The experiments described in this chapter indicate that butanethiol, sulfur dioxide, cyclic nitrones, and benzeneselenol are not suitable reagents for trapping the biradicals formed in enone-alkene photocycloaddition reactions. In the presence of butanethiol and nitrone **185**, the photocycloaddition reactions between 2-cyclopentenone and alkenes result in the formation of the same cycloadduct products observed in the absence of these compounds. This observation indicates that the rate of reaction between butanethiol or **185** and triplet biradicals is much slower than the rate at which the triplet biradicals formed in enone-alkene photocycloaddition reactions decay. The lack of success in using sulfur dioxide and benzeneselenol as reagents for biradical trapping was probably a manifestation of the fact that these compounds absorb a significant amount of light in the spectral region where most enones absorb.

The trapping experiments involving t-butylselenol indicated that this compound is effective at trapping triplet biradicals formed in enone-alkene photocycloaddition reactions. In the case of the 2-cyclopentenone plus *trans*-2-butene photocycloaddition reaction, the presence of either t-butylselenol or H_2Se resulted in the formation of a common mixture of products representative of trapped biradicals. The ratio of the trapped products observed in each trapping reaction were also similar thereby suggesting that the origin of the trapped products was not dependent on the nature of the trapping reagent.

The difficulties associated with preparing and storing t-butylselenol make this compound less convenient to use as a biradical trapping reagent relative to hydrogen selenide. In addition, more complex mixtures of dark reaction products resulted from

the solutions containing t-butylselenol, 2-cyclopentenone and *trans*-2-butene relative to the solutions which included H_2Se instead of t-butylselenol. The initial goal of the studies described in this chapter was to find a biradical trapping reagent that could be used for enone-alkene photocycloaddition reactions that was easier to handle than H_2Se. Due to the problem associated with t-butylselenol, this compound does not satisfy the initial goal. However, the similarity between the results obtained from both the H_2Se and t-butylselenol trapping experiments validate, to some extent, the results obtained in the trapping experiments described in Chapters 2, 3 and 4 in which H_2Se was used as the trapping reagent.

5.4 References

1. Rudolph, A.; Weedon, A.C. *Can. J. Chem.* **1990**, *68*, 1590.

2. (a) Newcomb, M.; Glenn, A. G.; Williams, W. G. *J. Org. Chem.* **1986**, *54*, 2675. (b) Bowry, V. W.; Lusztyk, J.; Ingold, K. U. *J. Am. Chem. Soc.* **1991**, *113*, 5687.

3. Kaprinidis, N. A.; Lem, G.; Courtney, S. H.; Schuster, D. I. *J. Am. Chem. Chem.* **1993**, *115*, 3324.

4. (a) Brownlie, I. T.; Ingold, K. U. *Can. J. Chem.* **1973**, *45*, 2427. (b) Kloplyankina, M. S.; Buchachenko, A. L.; Neiman, M. B.; Vasil'eva, A. G. *Kinet. Katal.* **1965**, *6*, 394. (c) Wilson, R. L. *Trans. Faraday Soc.* **1971**, *67*, 3008. (d) Schmid, P.; Ingold, K. U. *J. Am. Chem. Soc.* **1978**, *100*, 2493. (e) Chateauneuf, J.; Lusztyk, J.; Ingold, K. U. *J. Org. Chem.* **1988**, *53*, 1629. (f) Beckwith, A. L. J.; Bowry, V. W.; Moad, G. *J. Org. Chem.* **1988**, *53*, 1632. (g) Mathew, L.; Warkentin, J. *J. Am. Chem. Soc.* **1986**, *108*, 7981. (h) Busfield, W. K.; Jenkins I. D.; Thang, S. H.; Rizzardo, E.; Solomon, D. H. *Tetrahedron Lett.* **1985**, *26*, 5081.

5. Scaiano, J. C. *Tetrahedron* **1982**, *38*, 819.

6. Encinas, M. V.; Scaiano, J. C. *J. Photochem.* **1979**, *11*, 241.

7. Scaiano, J. C.; Lee, C. W. B.; Chow, Y. L.; Marciniak, B. *J. Phys. Chem.* **1982**, *86*, 2452.

8. (a) Wagner, P. J.; Zepp, R. G. *J. Am. Chem. Soc.* **1972**, *94*, 287. (b) Wagner, P. J.; Keslo, P. A.; Zepp, R. G. *Ibid.* **1972**, *94*, 7480. (c) Encinas, M. V.; Wagner, P. J.; Scaiano, J. C. *Ibid.* **1980**, *102*, 1357.

9. James, F. C.; Kerr, J. A.; Simons, J. *J. Chem. Soc. Faraday Trans.* **1973**, 2124.

10. Davies, A. G.; Robert, B. P.; Sanderson, B. R. *J. Chem. Soc. Perkin Trans. 2*, **1973**, 626.

11. Small, R. D.; Scaiano, J. C. *Macromolecules* **1978**, *11*, 840.

12. (a) Haire, D. L.; Janzen, E. G. *Can. J. Chem.* **1982**, *60*, 1514. (b) Evans, C. A.; Janzen, E. G. *J. Am. Chem. Soc.* **1973**, *95*, 8205.

13. Newcomb, M.; Varick, T. R.; Chau, H.; Manek, M. B.; Yue, X. *J. Am. Chem. Soc.* **1992**, *114*, 8158.

14. (a) Marvel, C. S.; Weil, E. D. *J. Am. Chem. Soc.* **1954**, *76*, 61.

15. Murahashi, S. I.; Mitsui, H.; Shiota, T.; Tsuda, T.; Watanabe, S. *J. Org. Chem.* **1990**, *55*, 1736.

16. Murahashi, S.; Shiota, T. *Tetrahedron Lett.* **1987**, *28*, 2383.

17. Tufariello, J. J. *Acc. Chem. Res.* **1979**, *12*, 396.

18. Ali, S. A.; Wazeer, M. I. M. *J. Chem. Soc. Perkin Trans. 2.* **1986**, 1789.

19. An adaptation of the method described by Arnold and Cantry was used for the preparation of t-butylselenol. See: Arnold, A. P.; Canty, A. J. *Inorg. Chim. Acta* **1981**, *55*, 171.

20. Mangini, A.; Trombetti, A.; Zauli, C. *J. Chem. Soc. (B)*, **1967**, 153.

CHAPTER 6

2+2 PHOTOCYCLOADDITION REACTIONS OF CYCLIC ENONES AND CYANO-SUBSTITUTED ALKENES

6.1 Introduction

This chapter will deal solely with the photocycloaddition reaction of cyclic enones with alkenes substituted by nitrile groups. After reading the title of this chapter, one might be compelled to ask the following question: Why are enone photocycloaddition reactions which involve cyano-substituted alkenes any different from photocycloaddition reactions which involve other kinds of alkenes? In fact, there is one very good reason why the photocycloaddition of cyclic enones with cyano-substituted alkenes should be treated as a special type of enone photccycloaddition reaction. The reason involves the relative ordering of the triplet energies of the triplet excited state of the cyclic enone and the triplet excited state of the alkene.

In most cases, the relaxed triplet energy of the cyano-substituted alkene is considerably lower than the triplet energy of the cyclic enone. For example, the triplet energy of fumaronitrile, according to photoacoustic calorimetry (PAC) measurements, is 48 ± 3 kcal/mol;[1] however, the triplet energy of 3-methyl-2-cyclohexenone, also according to PAC measurements, is 68.7 kcal/mol.[2] Based on the values of these two

triplet energies, energy transfer should be exothermic by more than 20 kcal/mol.[1] Consequently, rather than undergoing photocycloaddition the cyclohexenone would be expected to transfer energy to the singlet ground state of fumaronitrile, thereby generating the triplet excited state of fumaronitrile and singlet ground state enone. The excited triplet of fumaronitrile could then undergo twisting about the C=C bond, cross to the singlet potential energy surface, and decay to the ground state.

It has been demonstrated by Schuster and co-workers that fumaronitrile and 3-methyl-2-cyclohexenone do in fact form 2+2 photocycloadducts with a moderately high quantum yield (0.28 at an alkene concentration of 0.5 M) upon irradiation of the enone.[1] Therefore, either energy transfer is very inefficient in these systems, or photocycloaddition is unusually fast and, by some mechanism, competes with triplet-triplet energy transfer.

Before discussing possible mechanistic pathways for photocycloadditions of cyclic enones and cyano-substituted alkenes, it is important to indicate that there are other examples of cyclic enone and alkene systems in which the triplet energy of the alkene lies significantly below that of the enone. For example, there is a number of examples of photocycloaddition reactions involving cyclic enones and dienes which result in the formation of cyclobutane adducts.

---

[1] It should be noted that energy transfer from the excited enone to the alkene depends on the vertical triplet energy of the alkene and not the relaxed triplet energy. The vertical triplet energy of fumaronitrile has not been determined. However, in the case of acrylonitrile the vertical triplet energy is only 4 kcal/mol higher in energy than the relaxed triplet energy (see references 1 and 10 as well as the Discussion section of this Thesis)

Scheme 61

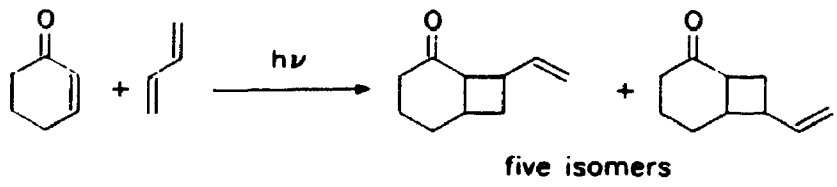

Scheme 62

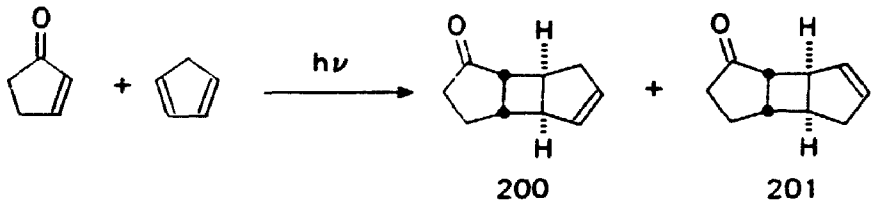

Some time ago Cantrell demonstrated that irradiation of a benzene solution containing 2-cyclohexenone and 1,3-butadiene results in the formation of 5 isomeric photocycloadducts all of which contain a cyclobutane ring (see Scheme 61).[4] Cantrell also demonstrated that 2-cyclopentenone reacts with cyclopentadiene to form cycloadducts **200** and **201** (see Scheme 62) in a 37:63 ratio.[4] Given that the triplet energies of 1,3-butadiene and cyclopentadiene are 59.7 and 58.3 kcal/mol respectively,[5] it is surprising that the photocycloaddition of these dienes to the triplets of 2-cyclohexenone and 2-cyclopentenone, which have triplet energies of 63 kcal/mol[2] and 72 kcal/mol,[23] respectively, occurs at all. Recently, Kumar and Rao demonstrated that 4,4-dimethyl-2-cyclohexenone (E_T=63 kcal/mol)[2] also reacts with cyclopentadiene to form 2+2 and 2+4 photoaddition products.[6] Based on the favourable energetics of triplet energy transfer, it is difficult to rationalise why photocycloadducts form at all in these systems. At the

present time there is little information in the literature regarding the mechanism by which cyclic enones react with dienes to form cycloadducts.

Scheme 63

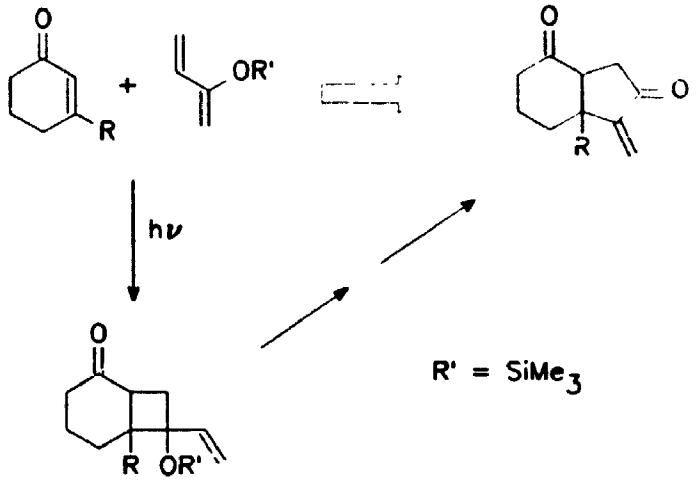

Despite the fact that little information exists regarding the mechanism of cyclic enone plus diene photocycloaddition reactions, this general type of reaction can be used in organic synthesis as an entry to penta-annulation.[7] Scheme 63 demonstrates a penta-annulation transform using 2-cycloalkenones and 2-trimethylsiloxybutadiene. This two step process consists of adding the diene to the enone in a 2+2 photocycloaddition, and then subjecting the adducts to a one-carbon ring expansion. Demuth has demonstrated that the photocycloaddition of 2-trimethylsiloxybutadiene to 3-methyl-2-cyclopentenone and 3-methyl-2-cyclohexenone is highly regioselective and stereoselective.[7] For example, these reactions result in the formation of head-to-tail regioisomers only (see Scheme 64). The preferred stereochemistry is that in which the trimethylsiloxy group is positioned *anti* with respect to the methyl group of the enone. Therefore, the photocycloaddition reaction of cyclic enones and dienes is a very useful synthetic reaction.

Scheme 64

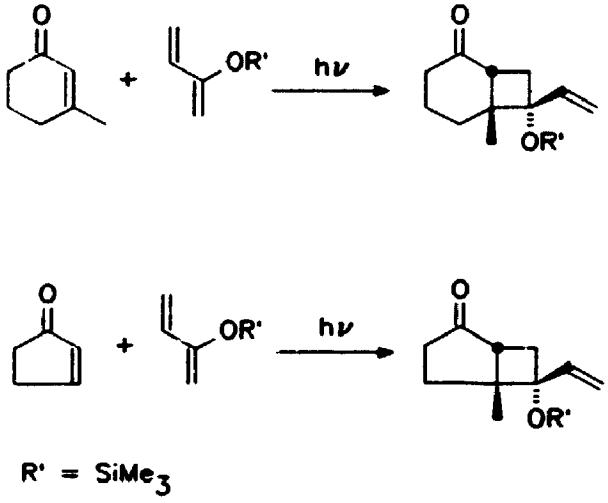

Schuster and co-workers recently published rate constants for the quenching interaction of various alkenes and cyclic enone triplets.[8] This was accomplished by using flash photolysis to measure the decrease in the lifetime of the triplet enone as the alkene concentration was increased. Some of the rate constants are summarised in Table 1 of Chapter 1. The quenching rate constants that Schuster and co-workers measured for those systems involving cyclic enones triplets and cyano-substituted alkenes are much larger than the rate constants for other alkenes. For example, fumaronitrile quenches the 2-cyclopentenone triplet with a rate constant of 4.6×10^9 $M^{-1}s^{-1}$ in cyclohexane while cyclopentene quenches the same enone triplet with a rate constant of 4.0×10^8 $M^{-1}s^{-1}$ in the same solvent.[8] The rate constant observed for the quenching of 2-cyclopentenone triplets by fumaronitrile is so large that it is even comparable to the rate at which oxygen quenches the 2-cyclopentenone triplet (5×10^9 $M^{-1}s^{-1}$).[9] The magnitudes of the rate constants for enone triplet quenching by cyano-substituted alkenes indicate that triplet

energy transfer might be a process which competes with photocycloadduct formation, and that the first step in photoadduct formation with fumaronitrile must be much faster than for other alkenes.

One reaction mechanism that has not yet been explicitly introduced includes the possibility of an interaction between the triplet alkene and the ground state cyclic enone. The first step in such a mechanism consists of an energy transfer interaction between the excited triplet enone and the alkene which results in the formation of the excited triplet alkene. In the second step of this reaction mechanism, the excited alkene triplet reacts with a ground state cyclic enone and forms an intermediary precursor to cycloadduct formation (i.e. an exciplex or a biradical).

The existence of this type of reaction has been investigated for the photocycloaddition reaction involving 2-cyclopentenone and acrylonitrile.[8] In this investigation, Schuster and co-workers attempted to sensitise the reaction between 2-cyclopentenone (E_T = 72 kcal/mol)[23] and acrylonitrile (E_T = 58-62 kcal/mol)[1,10] with the triplet sensitiser benzophenone (E_T = 69 kcal/mol)[5] which has a triplet energy between that of the enone and that of the alkene. The sensitisation experiments failed to result in the formation of any enone plus alkene cycloadduct; however, dimers of the alkene were formed. Therefore, it was concluded that a mechanism involving a reaction between the triplet alkene and the ground state enone does not result in adduct formation, at least for this particular case. This experiment does not, however, rule out the possibility that once energy transfer has occurred, a rapid in-cage reaction, or even exciplex formation may occur

Schuster and co-workers investigated the photocycloaddition reaction of 3-methyl-

2-cyclohexenone with fumaronitrile and maleonitrile in order to test the possibility of a reaction mechanism which involves triplet energy transfer and photocycloadduct formation as two competing pathways.[3] In this investigation, the quantum yield of product formation (Φ_p) and the quantum yield of isomerisation of each alkene (Φ_{iso}) were used in conjunction with quantum yields of triplet enone capture by each alkene (Φ_{tc}) in calculating the fraction of all intermediates, either triplet alkenes or biradicals, that reverted to fumaronitrile. The quantum yield of triplet capture was calculated according to the equation $\Phi_{tc} = k_q/(k_q + k_d)$, where k_q represents the rate of quenching of the enone triplet by the alkene and k_d represents the inverse lifetime of 3-methyl-2-cyclohexenone. Therefore, the fraction of all intermediates that revert to fumaronitrile (F) was determined from the equation $F = \Phi_{iso}/(\Phi_{tc} - \Phi_p)$, where each of the three quantum yields were measured for the addition of maleonitrile to 3-methyl-2-cyclohexenone. The value of F that was obtained was 0.72.[3] The authors of the work compared this fraction to the ratio of the photostationary state concentrations of maleonitrile and fumaronitrile (1:1) that result from the benzophenone or acetophenone sensitised photoisomerisation of the two alkenes. The difference between F and the photostationary state ratio of concentrations was explained in terms of a mechanism in which Schenck isomerisation of the intermediate biradicals accounted completely for the formation of fumaronitrile in the reaction of 3-methyl-2-cyclohexenone and maleonitrile.[3] One can also account for the difference between F and the photostationary state ratio by considering a mechanism in which both Schenck isomerisation and isomerisation induced by triplet energy transfer result in the formation of fumaronitrile. The latter possibility was not considered explicitly by Schuster and co-workers.

So far, it has been assumed that the enone excited state involved in the photocycloaddition of cyclic enones and alkenes possessing low triplet energies is a triplet. This assumption is based on the fact that early sensitisation and quenching studies indicated that in the case of simple alkyl substituted alkenes, the triplet state of the enone is the state responsible for the bimolecular reaction.[11] There are two problems with this assumption: first, none of the early sensitisation and quenching studies investigated the photocycloaddition reaction between cyclic enones and low triplet energy alkenes; and second, some of the early quenching studies involved the use of traditional diene quenchers, some of which were later shown to form photoadducts with cyclic enones. The possibility of singlet state reactivity in the bimolecular reaction between cyclic enones and low triplet energy alkenes has never been disproved. There have been no systematic quenching or sensitisation experiments carried out on cyclic enone plus low triplet energy alkene systems in order to rigorously exclude the possibility of singlet state reactivity. In the investigations described later in this chapter, these types of experiments were performed.

The goal of the experiments that are described in the remaining portion of this chapter was to obtain more kinetic data for the photocycloaddition reactions of 2-cyclopentenone with cyano-substituted alkenes. Initially, it was our intention to use hydrogen selenide to trap the biradicals which may form in photocycloaddition reactions involving cyclic enones and cyano-substituted alkenes. These trapping studies were unsuccessful. Consequently, most of the kinetic data described in this chapter were obtained by measuring the quantum yield of cycloadduct formation in the photoaddition of 2-cyclopentenone to each of acrylonitrile, maleonitrile and fumaronitrile at different

alkene concentrations. In no way are the results obtained from the experiments described in this chapter supposed to suggest a definitive mechanism for the reaction of cyclic enones with cyano-substituted alkenes. The results presented in this chapter can, however, be discussed in concert with the results published by other researchers in order to develop a probable mechanism for these types of reactions.

6.2 Results for the 2-cyclopentenone plus acrylonitrile photocycloaddition

The products resulting from the photocycloaddition of 2-cyclopentenone and acrylonitrile have been characterised by Weedon and co-workers.[12] In these investigations, it was found that the reaction results in the formation of four 2+2 cycloadducts in the ratio 15:25:45:15. The structures of the cycloadducts are shown in Scheme 65. Weedon and co-workers did not identify the individual stereoisomers; however, they were able to identify the pairs of regioisomers. The regiochemical ratio of head-to-head products to head-to-tail products (**203**:**204**) was determined to be 40:60. It is important to note that this ratio of regioisomers is opposite to that predicted by the Corey-de Mayo mechanism.[13]

Scheme 65

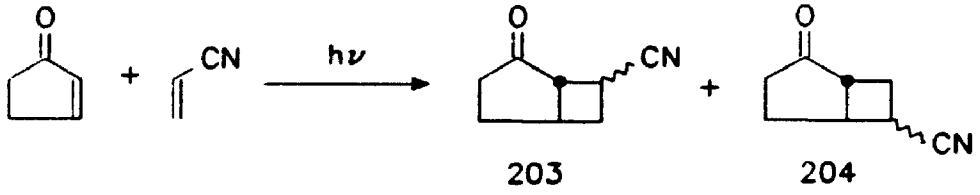

6.2.1 Triplet sensitisation and quenching studies

In order to prove rigorously whether the singlet excited state or the triplet state is directly involved in the mechanistic step in which excited 2-cyclopentenone and acrylonitrile react, careful sensitisation and quenching studies were performed. The first requirement in these studies was to find a triplet quencher that could be trusted to quench the triplet state of excited 2-cyclopentenone and not the singlet excited state. Obviously dienes are a poor choice since the mechanism by which dienes react with cyclic enones to form photoadducts is unclear. The triplet quencher that was chosen was 3,3,4,4-tetramethyl-1,2-diazetine 1,2-dioxide (**205**). This peculiar quencher was chosen because it has a very low triplet energy (36 to 42 kcal/mole) and because it is unable to quench singlets having energies below that of its own.[14] The quencher has one disadvantage--it is not commercially available and therefore must be synthesised.

Scheme 66

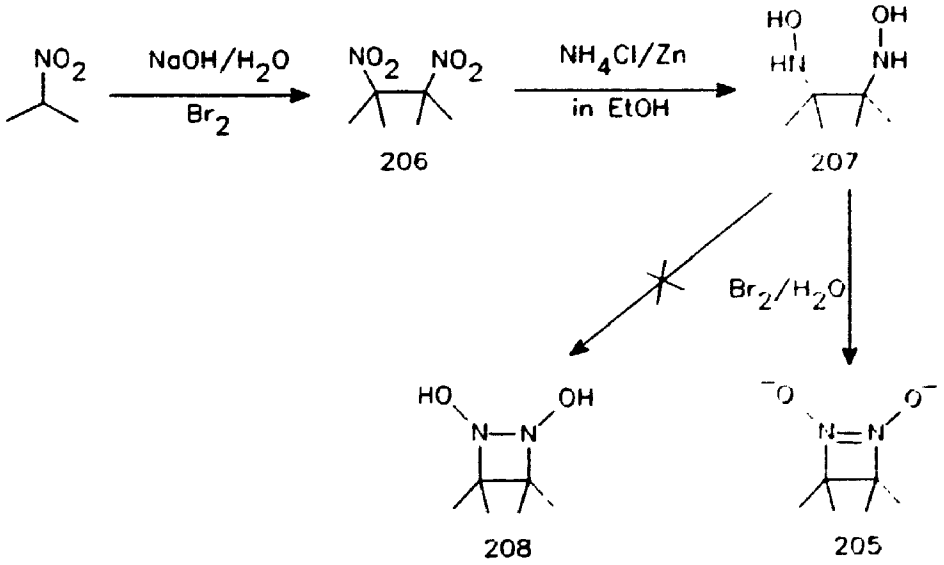

The multi-step synthesis of **205** is summarised in Scheme 66. Each of the steps shown in this scheme is a literature procedure and so the structure of each product was proven by comparison of the observed spectral data with the data published in the literature. The synthesis begins with the formation of 2,3-dimethyl-2,3-dinitrobutane (**206**) which was prepared by the oxidative coupling of two 2-nitropropane molecules in the presence of aqueous hydroxide and bromine.[15] Compound **206** was then reduced to the bis(hydroxylamine) **207** with zinc in the presence of weak acid.[16] Bromine was used to effect oxidation of **207** to the desired product.[14] In this last step no evidence of diol **208**, which is a possible oxidation product of **207**, was detected in the reaction mixture after work-up. Ullman and co-worker have demonstrated that magnesium dioxide facilitated oxidation of **207** results in the formation of **208** and not **205**.[17] Compound **205** was completely characterised by IR, ^{1}H nmr, ^{13}C nmr and mass spectrometry.

The quenching experiments involving 2-cyclopentenone, acrylonitrile and **205** were carried out in acetonitrile in the presence of cyclopentene. The purpose of these experiments was to observe the ratio of the relative yield of the cycloadducts resulting from the 2-cyclopentenone plus acrylonitrile reaction to the relative yield of the cycloadducts resulting from the 2-cyclopentenone plus cyclopentene reaction (see Scheme 67) at different concentrations of the quencher (**205**). Since all of the relevant evidence in the literature indicates that cyclopentene reacts with the triplet excited state of 2-cyclopentenone, any change in the ratio of the acrylonitrile derived products to the cyclopentene derived products (Φ_{AN}/Φ_{CP}) at different concentrations of **205** would indicate that the two alkenes react with different excited states of the enone.

Scheme 67

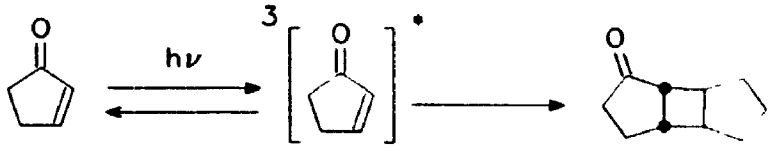

Acetonitrile solutions containing 2-cyclopentenone, acrylonitrile, cyclopentene and **205** were irradiated with acetone filtered light from a 400 W Hanovia medium pressure mercury lamp for 30 minutes. In these experiments, the concentrations of 2-cyclopentenone, cyclopentene (CP), and acrylonitrile (AN) were held constant and the concentration of **205** was varied. The results of these experiments, which are summarised in Table 19, indicate that **205** quenches the reaction of 2-cyclopentenone and cyclopentene as well as the reaction of 2-cyclopentenone and acrylonitrile since the amount of enone converted to product decreased relative to an internal standard as the concentration of **205** was increased. The results also indicate that the ratio Φ_{AN}/Φ_{CP} is insensitive to changes in the concentration of **205**. In addition, it is important to note that the product ratios of the four cycloadducts resulting from the photoaddition of 2-cyclopentenone and acrylonitrile were constant in each of the irradiations. Based on these quenching experiments, it is possible to conclude that cyclopentene and acrylonitrile both react exclusively with triplet excited state of 2-cyclopentenone in the formation of 2+2 photocycloaddition products.

Table 19: Results of experiments in which solutions containing 2-cyclopentenone, acrylonitrile (AN), cyclopentene (CP) and **205** were irradiated with UV light ($\lambda > 330$nm) in acetonitrile.

No.	Concentrations (M)				$\frac{\Phi_{AN}}{\Phi_{CP}}$	% conversion of enone
	enone	AN	CP	205		
1	0.0783	.162	.824	0	1.56	25
2	0.0783	.163	.823	0.034	1.64	21
3	0.0785	.162	.825	0.061	1.59	14
4	0.0784	.161	.824	0.170	1.64	6

Attempts were made to sensitise the 2-cyclopentenone plus acrylonitrile reaction using xanthone as a triplet sensitiser. The triplet energy of xanthone (E_T=74 kcal/mol)[5] is above the triplet energies of both 2-cyclopentenone (E_T=72 kcal/mol)[23] and acrylonitrile (E_T=58-62 kcal/mol).[1,10] A benzene solution containing cyclopentenone (0.107 M), acrylonitrile (1.01 M), and xanthone (0.106 M) was irradiated with Pyrex filtered light from a 400 W Hanovia medium pressure mercury lamp. Based on the extinction coefficients for xanthone (ϵ_{313}=3200, ϵ_{366}=100) and for 2-cyclopentenone (ϵ_{313}=28, ϵ_{366}=2) in benzene, it was determined that at these concentrations the xanthone was absorbing more than 98% of the light. A similar benzene solution containing the same concentrations of 2-cyclopentenone and acrylonitrile but no xanthone was also prepared and irradiated under the same conditions as the solution described above.

The reaction mixtures obtained from the sensitised and direct irradiations were analyzed by g.c. and coupled g.c./m.s. For the sensitised irradiation, these analyses

revealed that four cycloadducts resulting from photoaddition of 2-cyclopentenone and acrylonitrile were formed in a ratio of 16:25:46:13. This ratio is identical to the ratio of cycloadducts observed in the direct irradiation of 2-cyclopentenone and acrylonitrile. In addition to the cycloadducts, two acrylonitrile dimers and two enone dimers were formed in the sensitised irradiation. These dimers were identified by coupled g.c./m.s. Therefore, the combined ratio of acrylonitrile dimers to enone dimers to cycloadducts was calculated to be 29:4:67 in the sensitised irradiation. In the direct irradiation, no acrylonitrile dimers were observed (detection limit of analysis: about 2% of all product formed); however, the ratio of enone dimers to cycloadducts (6:94) was identical to that observed in the sensitised irradiation. These results support the conclusion deduced from the quenching studies; that is, acrylonitrile reacts with triplet 2-cyclopentenone directly to form 2+2 photocycloaddition products.

6.2.2 Attempted biradical trapping

When a benzene solution containing 2-cyclopentenone (0.102 M) and acrylonitrile (1.00 M) was saturated with H_2Se (0.35 M) and irradiated with Pyrex filtered light from a 400 W Hanovia medium pressure mercury lamp, cycloadduct formation was completely suppressed. Analyses of this reaction mixture by coupled g.c./m.s. also indicated that no products corresponding to trapped 1,4-biradicals were formed. The g.c. analyses did, however, indicate that a considerable amount of cyclopentanone was produced in the reaction. As described in Chapter 2, this product is assumed to be the result of reductive quenching of the 2-cyclopentenone triplet by H_2Se.

The absence of both cycloadducts and trapped biradicals in the irradiations of 2-cyclopentenone and acrylonitrile that were performed in the presence of H_2Se suggests that quenching of cyclopentenone triplets by H_2Se is faster than the reaction of the triplets with acrylonitrile. However, this is inconsistent with the known rate constants for quenching of the 2-cyclopentenone triplet by cyclopentene and by acrylonitrile combined with the observation that biradicals in the cyclopentene reaction can be reduced by H_2Se.

Scheme 68

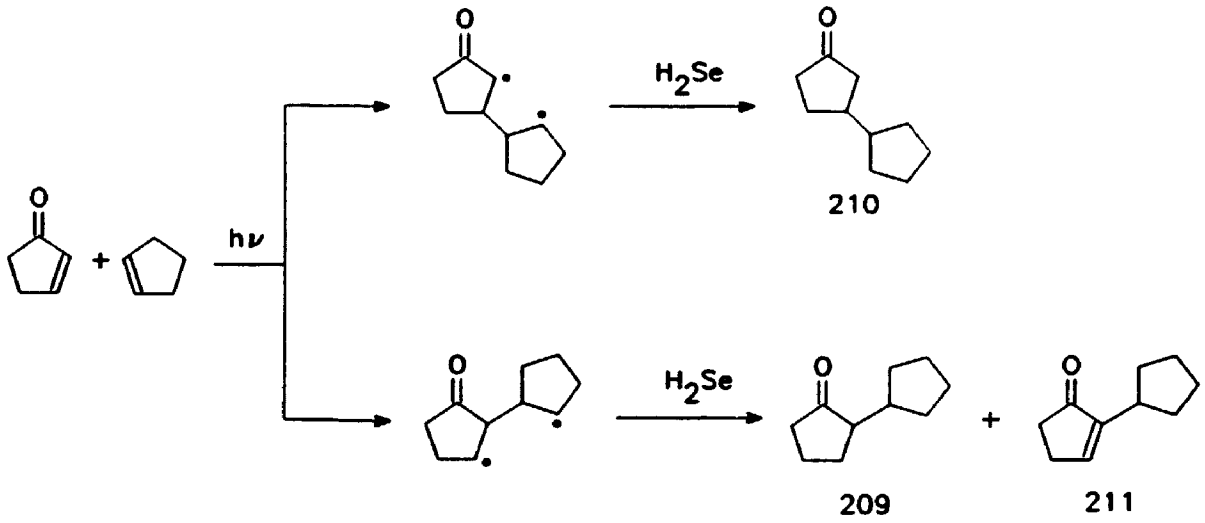

Schuster and co-workers determined that in cyclohexane acrylonitrile quenches the enone triplet at a rate 4.5 times faster than the rate at which cyclopentene quenches this triplet.[8] However, Hastings and Weedon demonstrated that at a concentration of 0.35 M H_2Se traps the biradicals generated in the photocycloaddition of 2-cyclopentenone and cyclopentene completely (see Scheme 68).[18] Based on Weedon and Hastings observation as well as Schuster's rate constants, one can not explain the lack of cycloadducts and trapped biradicals in the irradiated solutions containing 2-cyclopentenone, acrylonitrile and H_2Se by suggesting that the apparent lack of reactivity

is due to quenching of the triplet enone by H_2Se. This is because the reaction between 2-cyclopentenone and cyclopentene, which proceeds at the slower rate, should be more sensitive to a quenching process involving the enone triplet and H_2Se than the reaction between 2-cyclopentenone and acrylonitrile.

In order to investigate the apparent lack of cycloadduct or trapped biradical formation in the reaction involving 2-cyclopentenone, acrylonitrile and H_2Se, competition experiments were carried out in the presence of cyclopentene. In these competition experiments, a benzene solution containing 2-cyclopentenone (0.103 M), acrylonitrile (1.00 M), and cyclopentene (0.205 M) was prepared. Part of this solution was transferred to an irradiation vessel, saturated with H_2Se, and then irradiated with Pyrex filtered light from a 400 W Hanovia medium pressure mercury lamp. Another portion of the solution was irradiated in the absence of H_2Se. The ratio of the combined relative yield of the acrylonitrile adducts to the combined relative yield of the cyclopentene adducts in the reaction mixture not exposed to H_2Se was found to be 1.7:1.0 after irradiation. In the reaction mixture containing H_2Se, considerable amounts of the same trapped biradical products identified by Hastings and Weedon in the biradical trapping reaction involving 2-cyclopentenone and cyclopentene (that is, compounds **209** and **210**) were observed; however, no cycloadducts or trapped biradicals resulting from the reaction between 2-cyclopentenone and acrylonitrile were observed. The relative product ratio of **209**:**210** observed in the competition experiment[8] (1.0:1.8) was identical to the

---

[8] In the experiments in which H_2Se was used to trap the biradicals formed in the photocycloaddition of 2-cyclopentenone and cyclopentene, only trace amounts of disproportionation product **211** were observed. In trapping experiments reported by Hastings and Weedon this was a major product.[18] We have not been able to resolve this inconsistency.

ratio that was observed in reactions involving 2-cyclopentenone, cyclopentene and H_2Se. The results of these competition reactions are summarised in Scheme 69.

Scheme 69

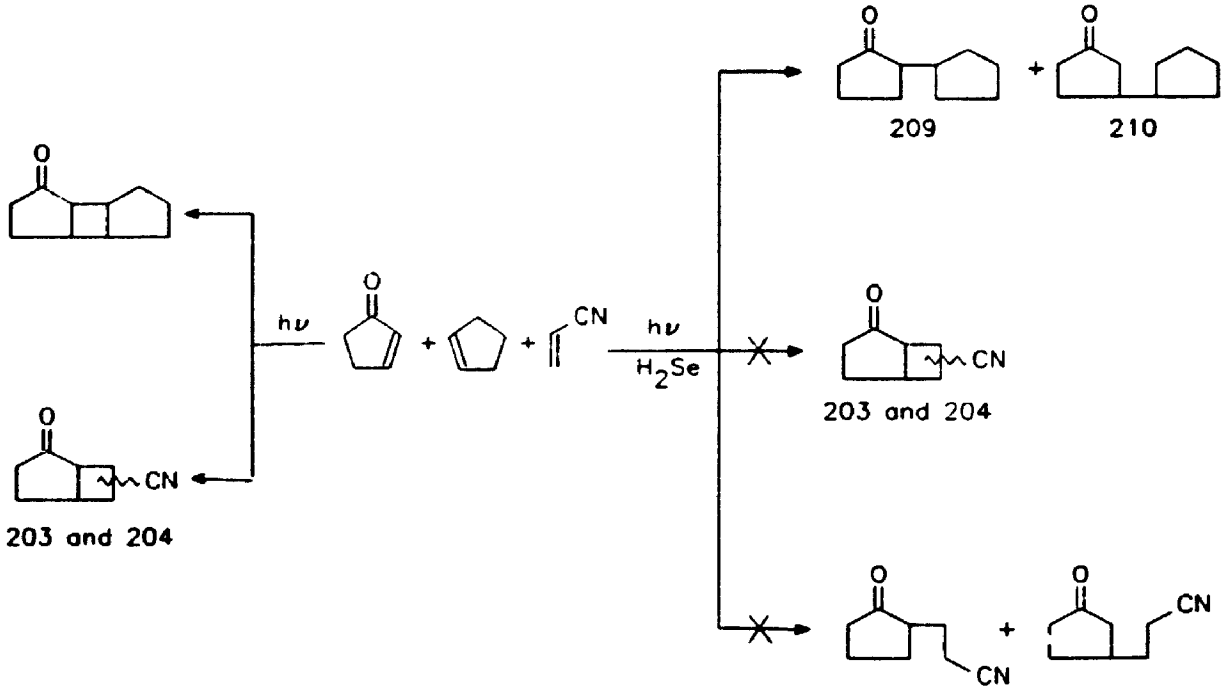

6.3 Results for the photocycloaddition of 2-cyclopentenone with fumaronitrile and maleonitrile.

When an acetonitrile solution containing 2-cyclopentenone (0.110 M) and fumaronitrile (0.620 M) was irradiated with Pyrex filtered light from a 400 W Hanovia medium pressure mercury lamp for 45 hours four 2+2 photocycloadducts (**212a**, **212b**, **212c**, and **212d**), two enone dimers, and maleonitrile were formed (see Scheme 70). The ratio of **212a**:**212b**:**212c**:**212d**, determined by g.c. at 3% conversion of the fumaronitrile, was found to be 21:16:30:33. The ratio of the combined relative yield of the two enone

dimers to the combined relative yield of the cycloadducts was determined to be 23:77 at this level of conversion. The isolated chemical yields of **212a**, **212b**, **212c**, and **212d** were found to be 13%, 8.5%, 16%, and 18% respectively based on the amount of 2-cyclopentenone starting material. Therefore, the combined chemical yield of all the isolated cycloadducts was 56% based on the amount of 2-cyclopentenone starting material.

The yield (in %) of each cycloadduct relative to the combined yield of all four cycloadducts did not change by more than 2% according to g.c. analyses as the amount of starting materials converted to products increased. However, the ratio of the combined relative yield of the two enone dimers to the combined relative yield of the cycloadducts decreased as the irradiation progressed. This decrease was probably due to secondary photolysis of the enone dimers.

Scheme 70

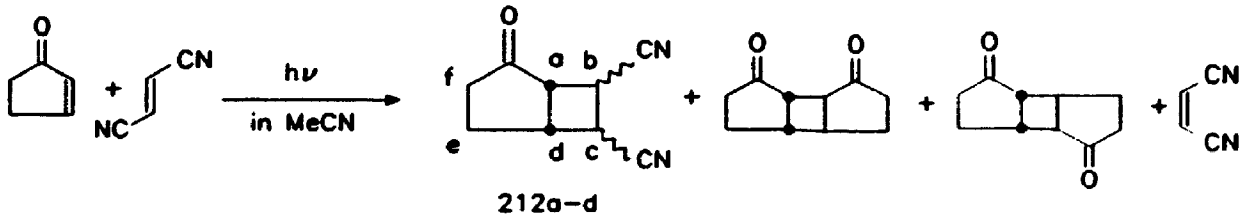

212a–d

The relative concentrations of maleonitrile and fumaronitrile were also determined by g.c. at regular time intervals throughout the photocycloaddition reaction of 2-cyclopentenone and fumaronitrile described above. The g.c. ratio of the concentration of maleonitrile to the concentration of fumaronitrile is plotted against irradiation time in Figure 12. The amount of maleonitrile formed in the reaction increased as the irradiation progressed until a photostationary state was achieved for the ratio of fumaronitrile to

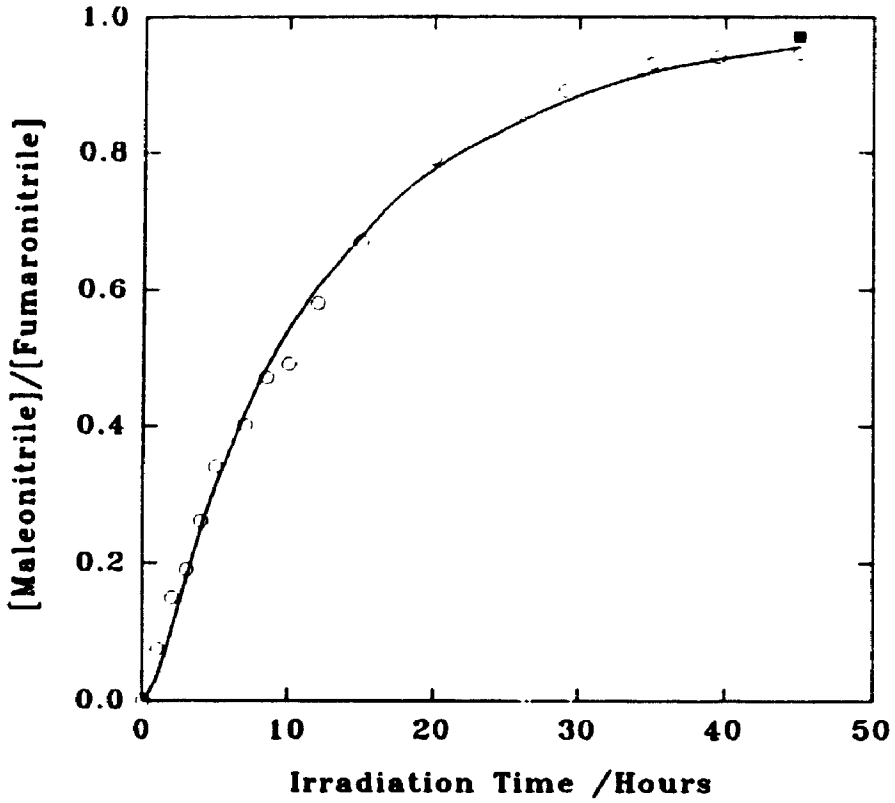

Figure 12: G.c. ratio of the concentration of maleonitrile to fumaronitrile at various irradiation times in the reaction of 2-cyclopentenone and fumaronitrile in acetonitrile. Recovered yield ratio indicated by a square.

maleonitrile. Figure 12 demonstrates that the photostationary state ratio of maleonitrile to fumaronitrile approached 0.94:1 after 45 hours of irradiation. The recovered chemical yields of maleonitrile and fumaronitrile were 44% and 46% respectively, based on the amount of fumaronitrile present as starting material. These yields indicate that only 10% of the fumaronitrile starting material was converted to cycloadduct products over the course of the reaction. (The recovered yield of cycloadducts corresponds to 9.9%, based on the amount of fumaronitrile initially present.) The ratio of the recovered yields of maleonitrile and fumaronitrile (0.96:1) is in excellent agreement with the g.c. ratio

measured at the end of the irradiation.

In order to study the products resulting from the reaction between maleonitrile an 2-cyclopentenone, a pure sample of maleonitrile had to be synthesised first. This synthesis involved photochemical isomerisation of a sample of commercially available fumaronitrile under conditions in which acetophenone (E_T=74 kcal/mol)[5] was used as a triplet sensitiser. Therefore, an acetonitrile solution containing fumaronitrile (0.330 M) and acetophenone (0.0502 M) was irradiated with Pyrex filtered light from a 400 W Hanovia medium pressure mercury lamp until a photo-stationary state of 0.92:1 for the ratio of maleonitrile to fumaronitrile was achieved. The maleonitrile was easily separated from this reaction mixture by chromatography on silica gel; however, the fumaronitrile and acetophenone were difficult to separate under the same conditions. If the yield of maleonitrile had been crucial, then the mixture of fumaronitrile and acetophenone could have been recycled in subsequent irradiations. The spectral properties and melting point of the isomerisation product resulting from this reaction confirmed that the product was in fact maleonitrile. It is important to note that no oxetane products or any other types of cycloadducts resulting from a reaction between acetophenone and either of the alkenes were formed in the sensitised irradiations.

The ratios of the products resulting from the reaction of 2-cyclopentenone and maleonitrile in acetonitrile were determined by irradiating an acetonitrile solution containing maleonitrile (1.51 M) and 2-cyclopentenone (0.110 M) with Pyrex filtered light from a 400 W Hanovia medium pressure mercury lamp. A ratio of 22:16:27:35 was determined for **212a:212b:212c:212d** by g.c. at 3% conversion of maleonitrile starting material. As the irradiation progressed, the yield of each cycloadduct product

(in %) relative to the combined yield of all of the cycloadducts did not change by an amount greater than the error of 1% to 2% associated with each relative yield. A photostationary state of 0.93:1 for the ratio maleonitrile to fumaronitrile was achieved at long irradiation times.

6.3.1 Product characterisation

The dimers of 2-cyclopentenone that were isolated in the reaction between 2-cyclopentenone and fumaronitrile were identified by g.c. co-injection with an authentic sample of the dimers. This authentic sample was prepared by irradiating an acetonitrile solution of 2-cyclopentenone with acetone filtered light ($\lambda > 330$ nm) from a 400 W Hanovia medium pressure mercury lamp. The maleonitrile was identified in the irradiation of 2-cyclopentenone and fumaronitrile by comparing the ^{1}H and ^{13}C nmr spectra of the isolated product with the spectra obtained from the product resulting from the acetophenone sensitised isomerisation of fumaronitrile.

The identification of the 2+2 cycloadducts formed in the photocycloaddition of 2-cyclopentenone and fumaronitrile or maleonitrile was based on the ^{1}H nmr, ^{13}C nmr, and mass spectra of the isolated adducts. The general structure of **212a**, **212b**, **212c**, and **212d** was confirmed by a combination of mass spectrometry and ^{13}C nmr spectroscopy. For example, the mass spectra of all of the cycloadducts exhibited an M+1 parent ion peak at m/e=161 under chemical ionisation conditions using isobutane. The APT ^{13}C nmr spectrum of each 2+2 cycloadduct in DMSO-d_6 exhibited one carbonyl ^{13}C resonance between 215 and 216 ppm, two nitrile ^{13}C resonances between 116 and 119 ppm, four methine ^{13}C resonances, and two methylene ^{13}C resonances. The number and

multiplicity of ^{13}C nmr resonances observed for each adduct indicated that all of the 2+2 cycloadduct contained a bicyclo[3.2.0]heptan-2-one ring system and that none were oxetane type products.

Each of the resolved ^1H nmr signals in the cycloadducts' spectra were assigned by conducting ^1H-^1H selective decoupling experiments. In these decoupling experiments, the characteristic large geminal coupling constant of α-keto methylene protons (J ~ 20 Hz) was used to identify the Hf protons (see Scheme 70 for the proton labelling key). With the Hf protons identified, it was relatively easy to deduce the assignments of all the other protons in the spectra of **212b** and **212c** from the results of the decoupling experiments. Table 20 contains a summary of the proton signals observed in the ^1H nmr spectra of **212b** and **212c**.

In the case of compound **212a**, too many resonances were overlapping in the ^1H spectrum to allow complete assignment of protons Ha to Hf. Compound **212d** also exhibited a considerable number of overlapping resonances in the ^1H nmr spectrum obtained in DMSO-d_6; however, changing the nmr solvent to C_6D_6 resulted in alleviating this problem considerably. In addition to changing the solvent, a lanthanide induced chemical shift study in which Eu(fod)$_3$ was also used to help disperse some of the overlapping resonances observed in the ^1H nmr spectrum obtained in C_6D_6. The proton signals in the shifted and unshifted spectra of **212d** were assigned by following the same logic used to assigned the signals observed in the spectra of **212b** and **212c**. The problem of overlapping ^1H nmr resonances in the spectra obtained for compound **212a** was not solved by changing the solvent. Table 20 contains a summary of the assignments for the proton resonances observed in the ^1H nmr spectra of **212a** and **212d**.

Table 20: ^{1}H nmr chemical shifts (ppm) and coupling constants (Hz) for adducts **212a**, **212b**, **212c**, and **212d**.

Proton	**212a** in DMSO-d_6	**212b** in DMSO-d_6	**212c** in DMSO-d_6	**212d** in C_6D_6
Ha	3.05 to 3.25 (overlaps Hd)	2.94 (brd. t., 9)	3.08 (dd, 8, 4.0)	a (brd. t., 9)
Hb	4.28 (overlaps Hc)	4.26 (t, 9.5)	3.81 (dd, 9.3, 4.0)	2.25 (t, 9.3)
Hc	4.28 (overlaps Hb)	4.04 (dd, 9.5, 7.2)	3.91 (dd, 9.3, 6.1)	2.19 (dt, 1.2, 9.3)
Hd	3.05 to 3.25 (overlaps Ha)	3.32 (brd. quart. 8±1)	3.43 (qd, 7±1, 2.4)	a (brd. quart. 8.5±1)
He	complex	1.9 to 2.2 complex	1.9 to 2.2 complex	1.04 (dddd, 14.8, 10.7, 9.9, 8.7)
				complex
Hf	complex	2.37 (dddd, 19, 8.1, 3.0, 1.7)	2.32 (dddd, 19, 8.8, 4.6, 1.5)	2.49 (dt, 19, 10)
		2.72 (dt, 19, 10)	2.63 (19, 9.3)	a (dddd, 19, 10.5, 3.6, 1.7)

[a]Resonance resolved in lanthanide induced chemical shift study.

Assignment of the stereochemistry of each 2+2 photocycloadduct by inspection of the coupling constants exhibited by each methine proton resonance was attempted. It was hoped that coupling between methine protons positioned *anti* with respect to one another would exhibit a significantly smaller coupling constant than protons positioned *syn* with respect to one another. Dilling and co-workers demonstrated that this general trend holds true for cycloadducts derived from 2-cyclopentenone and the two geometrical

isomers of 1,2-dichloroethene.[19] In addition, Griesbeck and co-workers demonstrated that the ^{1}H nmr spectra obtained from the cycloadducts resulting from the photocycloaddition of 2-cyclopentenone to ethyl vinyl ether also follow this trend.[20] If the trend were to hold true for the 2-cyclopentenone plus fumaronitrile of maleonitrile products, then the stereochemistry of the methine protons around the cyclobutane ring could be identified.

Table 21 contains a summary of the vicinal 3-bond coupling constants observed for the cyclobutane methine protons in cycloadducts **212b**, **212c**, and **212d**. Compound **212a** is not included in this table due the problem of overlapping ^{1}H nmr resonances discussed above. The magnitudes of the J_{ab} coupling constants presented in this table indicate that compound **212c** probably has a stereochemistry in which protons Ha and Hb are positioned *anti* with respect to one another. The relative magnitudes of the J_{cd} coupling constants may suggest that compounds **212b** and **212c** possess a stereochemistry in which Hc and Hd are *anti* and compound **212d** possesses a stereochemistry in which Hc and Hd are *syn*. On the other hand, the relative magnitude of the J_{ad} and J_{bc} coupling constants do not seem to vary among the three cycloadducts. This latter observation is not consistent with the hypothesis that *anti* coupling constants around the cyclobutane ring are smaller than *syn* coupling constants. Therefore, the stereochemistry of four 2+2 cycloadducts resulting from the photocycloaddition of 2-cyclopentenone to fumaronitrile or maleonitrile cannot be assigned with any real degree of confidence. This lack of stereochemical assignment is not really of any major significance for the work in this thesis since the relative ratios of the four adducts resulting from the addition of maleonitrile and fumaronitrile to 2-cyclopentenone are almost identical; a knowledge of

the stereochemistry of the adducts would not provide any significant mechanistic information.

Table 21: Summary of methine proton coupling constants (Hz) for **212b**, **212c**, and **212d**.

Coupling	212b	212c	212d
J_{ab}	9	4.0	9.3
J_{bc}	9.5	9.3	9.3
J_{cd}	7.2	6.1	9.3
J_{ad}	9	8	9

6.4 Quantum yield studies

The initial goal of the quantum yield studies was to measure the quantum yield of adduct formation in the photocycloaddition reactions of 2-cyclopentenone with each of maleonitrile, fumaronitrile, and acrylonitrile in cyclohexane and acetonitrile, and then to compare these data with the flash photolysis data obtained by Schuster and co-workers.[8]

All of these quantum yield determinations were carried out on a PTI QUANTACOUNT instrument at 340 nm. The instrument was calibrated by using the rearrangement of azoxybenzene to 2-hydroxyazobenzene in KOH saturated 95% ethanol as an actinometer.[21] The 2-cyclopentenone and acrylonitrile were both purified by fractional distillation immediately prior to use. This purification procedure was particularly important for acrylonitrile since the commercially available form of this reagent is stabilised with 0.005% 4-methoxyphenol. Fumaronitrile and maleonitrile were

purified by multiple recrystallizations prior to use. In all of the reactions involving fumaronitrile and maleonitrile, the quantum yields of cycloadduct formation were determined at less than 6% conversion of the alkene starting material. In the case of the reactions which involved the photocycloaddition of 2-cyclopentenone and acrylonitrile, the quantum yields of cycloadduct formation were determined at less than 5% conversion of the enone.

Significant practical problems were encountered in some of the quantum yield determinations. For example, a considerable amount of insoluble material resulting from polymerisation of the alkene was formed after very short irradiation times in the quantum yield determinations involving 2-cyclopentenone and acrylonitrile in cyclohexane. The light scattering caused by the build up of this insoluble polymeric material made it impossible to accurately measure quantum yields for cycloadduct formation in this solvent. The quantum yields of cycloadduct formation resulting from the photoaddition of 2-cyclopentenone and fumaronitrile or maleonitrile were also not measured in cyclohexane since both of these alkenes are insoluble in cyclohexane.

The quantum yields of cycloadduct formation resulting from the photocycloaddition reaction between 2-cyclopentenone and each of acrylonitrile, fumaronitrile and maleonitrile in acetonitrile solution are summarised in Table 22. The quantum yields listed in this table represent the combined quantum yield of formation of all four of the cycloadduct products (i.e. compounds **212a**, **212b**, **212c**, and **212d**). It is important to note that the relative ratios of these products did not vary from as the alkene concentration was changed.

The data in Table 22 indicate that the quantum yields of cycloadduct formation

resulting from these reactions appear to be insensitive to the concentration of alkene over the concentration range studied. Of the three reactions studied, only the reaction between 2-cyclopentenone and acrylonitrile exhibited a quantum yield of cycloadduct formation that began to decrease at the low alkene concentrations. The reason for the apparent insensitivity of the quantum yields of cycloadduct formation to the alkene concentration is examined in more detail in the Discussion section.

Table 22: Quantum yields of cycloadduct formation from the photocycloaddition reaction of 2-cyclopentenone with acrylonitrile, fumaronitrile, and maleonitrile in acetonitrile.

acrylonitrile		fumaronitrile		maleonitrile	
[alkene] M	$\Phi_{adducts}$	[alkene] M	$\Phi_{adducts}$	[alkene] M	$\Phi_{adducts}$
0.0269	0.11±0.02	0.0289	0.019±0.002	0.0394	0.020±0.002
0.0497	0.15±0.02	0.0501	0.023±0.003	0.102	0.026±0.003
0.0665	0.17±0.02	0.0991	0.027±0.003	0.206	0.024±0.003
0.110	0.22±0.03	0.203	0.027±0.003	0.415	0.026±0.003
0.199	0.20±0.03	0.501	0.026±0.003	0.823	0.025±0.003
0.502	0.21±0.03	1.00	0.024±0.003	1.51	0.023±0.003
1.00	0.20±0.03				

The total quantum yield of formation of the two enone dimers resulting from the photocycloaddition reactions involving 2-cyclopentenone and each of acrylonitrile, fumaronitrile, and maleonitrile were also determined at different concentrations of alkene. These experiments were conducted in order to determine the relative rates at which each of the alkenes quenched the enone triplet. It was found that the quantum yield of enone dimerisation decreased significantly as the concentration of each alkene was increased.

In this equation, Φ_o represents the quantum yield of dimer formation at the concentration of 2-cyclopentenone denoted as E in the absence of the alkene. The rate constant k_q represents the total rate of triplet enone quenching by the alkene A, $k_{sq}[E]$ represents the total rate of enone self quenching, and k_d represents the unimolecular rate of decay of the enone triplet. The slope over intercept ratio for a plot of $1/\Phi_{dimer}$ versus the concentration of alkene is equal to $k_q/(k_d + k_{sq}[E])$ Since k_d and k_{sq} are known for 2-cyclopentenone in acetonitrile from flash photolysis data,[24] therefore the absolute magnitude of k_q can be calculated from the slope over intercept ratio obtained from the quantum yield measurements. The concentration of 2-cyclopentenone used in all of the quantum yield determinations involving acrylonitrile, maleonitrile and fumaronitrile was 0.0940 M. Using this concentration and the values of 2.6×10^6 and 2.7×10^8 for the rate constants k_d and k_{sq} respectively,[24] the sum of $k_d + k_{sq}[E]$ was calculated to be 5.1×10^7 sec^{-1}. Therefore, the rates for the quenching of triplet 2-cyclopentenone by acrylonitrile, fumaronitrile, and maleonitrile were calculated to be $1.0\pm0.3\times10^9$, $2.4\pm0.5\times10^9$, and $3.8\pm0.7\times10^9$ M^{-1} sec^{-1} respectively. These rate constants are in agreement with the corresponding rate constants measured by laser flash photolysis[8] (see Table 1 in Chapter 1) when experimental error is taken in to account.

The rate constants for quenching triplet 2-cyclopentenone with acrylonitrile, fumaronitrile and maleonitrile are in agreement with the mechanism proposed in Scheme 71. The data indicate that reaction between acrylonitrile and 2-cyclopentenone is slower than the reaction between the 1,2-dicyanoethenes and 2-cyclopentenone. Since the triplet energies of the 1,2-dicyanoethenes are lower than the triplet energy of acrylonitrile (see above), the trend exhibited by the rate constants is consistent with an triplet energy

Table 23: Weighted least squares regression parameters for the plots of $1/\Phi_{dimer}$ versus alkene concentration shown in Figure 13.

alkene	Slope (M^{-1})	Intercept	standard deviation of parameters	
			slope (M^{-1})	intercept
acrylonitrile	72	3.5	9	0.6
fumaronitrile	186	3.9	11	0.4
maleonitrile	306	4.1	25	0.6

The quantum yields of cycloadduct formation for the photocycloaddition reaction of 2-cyclopentenone and acrylonitrile in benzene solution were also measured at different concentrations of acrylonitrile. It was found that the quantum yield of cycloadduct formation in this solvent increased significantly as the concentration of the alkene was increased (see Figure 14). When the reciprocal of the quantum yield of cycloadduct formation was plotted against the reciprocal of the concentration of acrylonitrile, a linear relationship was observed (see Figure 15). The data shown in Figure 15 were subjected to a weighted least squares analysis. The slope and intercept parameters obtained from this analysis were summarised in Table 24.

Table 24: Weighted least squares regression parameters for the plot of $1/\Phi_{adduct}$ versus the reciprocal of the alkene concentration shown in Figure 15.

system	Slope (M^{-1})	Intercept	standard deviation of parameters	
			slope (M^{-1})	intercept
acrylonitrile + 2-cyclopentenone in benzene	1.01	3.4	0.06	0.2

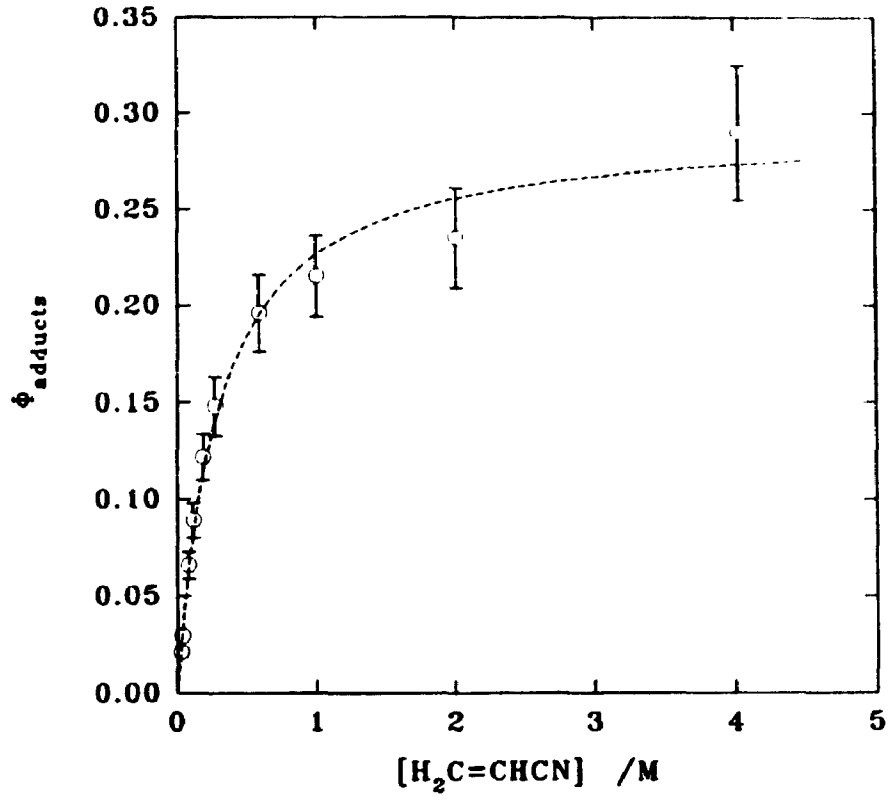

Figure 14: Plot of the quantum yield of cycloadduct formation versus the alkene concentration for the photocycloaddition of 2-cyclopentenone to acrylonitrile in benzene.

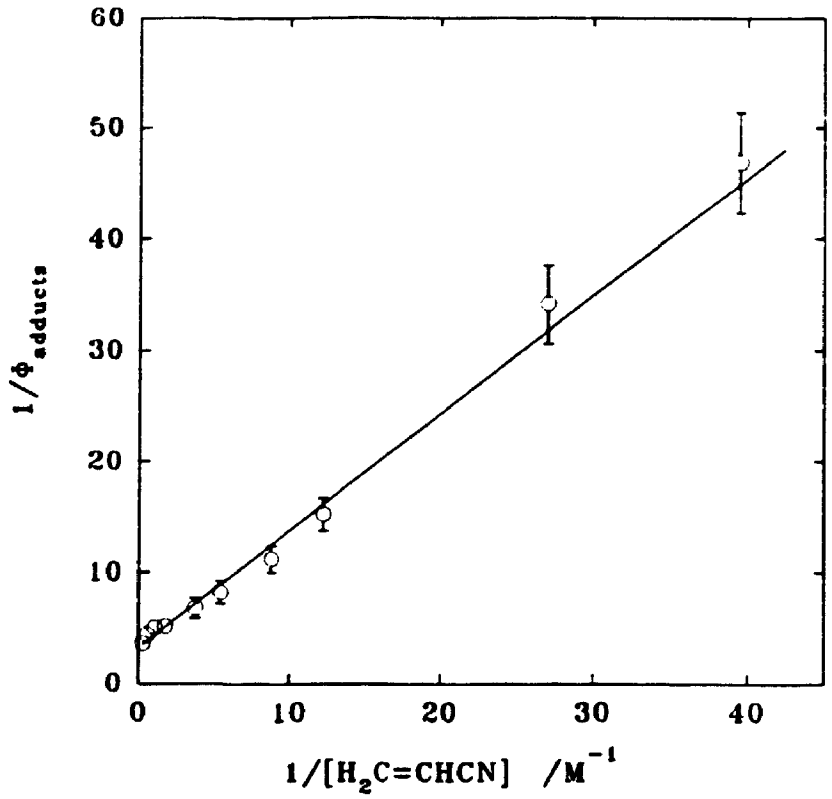

Figure 15: Plot of $1/\Phi_{adducts}$ versus the reciprocal of the concentration of acrylonitrile for the photocycloaddition of 2-cyclopentenone and acrylonitrile in benzene.

6.5 Discussion

As described in the results section, solutions containing a fixed concentration of 2-cyclopentenone, acrylonitrile, and cyclopentene and various concentrations of compound **205** were irradiated with acetone filtered light from a medium pressure mercury lamp. It was found that the ratio of the yield of the cyclopentene derived adducts to yield of the acrylonitrile derived adducts did not vary as the concentration of the triplet quencher **205** was increased. The combined yield of all cycloadduct products

did, however, decrease as the concentration of the triplet quencher increased. These experiments indicate that the same triplet excited state is involved in the formation of the cycloadducts resulting from the reaction between excited 2-cyclopentenone and cyclopentene and the reaction between 2-cyclopentenone and acrylonitrile. If different excited states were involved in these two reactions, then one might expect that triplet quencher **205** would quench the formation of cycloadducts resulting from each reaction at different rates.

In addition to the quenching studies, the experiments in which xanthone was used to sensitise the photocycloaddition of 2-cyclopentenone and acrylonitrile also rule out the possibility of direct involvement of the singlet state in the bimolecular photoaddition reaction. Even though a triplet energy transfer process in which acrylonitrile quenches triplet 2-cyclopentenone is energetically very favourable, it appears that the triplet state of 2-cyclopentenone is also directly responsible for the formation of cycloadducts.

The photocycloaddition reaction of 2-cyclopentenone and fumaronitrile or maleonitrile results in the formation of four stereoisomers identified as **212a**, **212b**, **212c**, and **212d**. The stereochemistry of each of the individual stereoisomers was not assigned. The relative product ratio of the four cycloadducts obtained from the reaction of fumaronitrile with 2-cyclopentenone (21:16:31:33) was the same as the product ratio obtained from the reaction of maleonitrile with 2-cyclopentenone (22:16:27:36), within experimental error. These cycloadduct ratios were determined at 3% conversion of the alkene and did not vary as the reactions progressed. The similarity of the product ratios obtained from these reactions indicates that both reactions have a common set of intermediates. In the context of a reaction mechanism which involves four

conformationally equilibrated isomeric biradicals, the identical product distributions for the reaction of 2-cyclopentenone and fumaronitrile and the reaction of 2-cyclopentenone and maleonitrile require that the relative rates of formation of the individual biradicals are identical in the two reactions.

The fact that identical product distributions are observed for the photocycloaddition of the two geometrical isomers of 1,2-dicyanoethene to 2-cyclopentenone is a little surprising. Other examples of reactions in which two geometrical alkene isomers are added to triplet cyclopentenone usually result in the formation of significantly different product distributions. The work described in Chapter 4 demonstrated that the different product distributions obtained from the addition of the two geometrical isomers of 2-butene to 2-cyclopentenone are a result of different relative rates of biradical formation for the two reactions. That is to say, the rate of formation of each biradical relative to rate of formation of all the biradicals was different in the reaction between *cis*-2-butene and triplet 2-cyclopentenone compared to the reaction involving *trans*-2-butene.

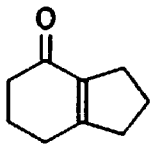

213

Cargill and co-workers also found that the ratios of the cyclobutane containing adducts formed in the photocycloaddition reaction of bicyclo[4.3.0]non-1(6)-en-2-one (213) and each of the geometrical isomers of 2-butene were different.[22] In addition, de Mayo and co-workers demonstrated that the photocycloaddition of 2-cyclopentenone to the geometrical isomers of hexene and 1,2-dichloroethene results in the formation of

significantly different product distributions.[23] In fact, the only other example of a photocycloaddition reaction which results in identical product distributions for addition of both geometrical isomers of a 1,2-disubstituted alkene to a cyclic enone involves the photoaddition of fumaronitrile and maleonitrile to 3-methyl-2-cyclohexenone.[3]

The reason why the different geometrical isomers of 1,2-cyanoethene add to excited cyclic enones to give identical product distributions while the geometrical isomers of other 1,2-disubstituted alkenes add to excited cyclic enones to give different relative product yields is unclear, but it may be relevant. It could suggest that the orthogonal alkene triplet reacts with the enone along the reaction pathway. If this were the case, the stereochemical identity of the ground state alkene would have no impact on the photocycloaddition reaction products.

In addition to formation of the four cycloadducts, isomerisation of the alkene starting material also occurred in the 2-cyclopentenone plus fumaronitrile and maleonitrile photocycloaddition reactions. The photo-stationary state ratio of the concentration of maleonitrile to the concentration of fumaronitrile was determined to be 0.94:1.0 for both reactions. This photo-stationary state ratio was achieved after less than 10% of the alkene was converted to cycloadducts.

The steady state ratio for the concentrations of maleonitrile and fumaronitrile observed in the photocycloadditions with 2-cyclopentenone is identical to the photo-stationary state ratio of 0.92:1.0 observed in the acetophenone sensitised isomerisation of fumaronitrile. Since no photoaddition products were observed in the acetophenone sensitised reaction, it was concluded that isomerisation of the alkene in this case proceeded from triplet fumaronitrile which was formed via energy transfer from triplet

acetophenone to ground state fumaronitrile. In the case of the reaction between fumaronitrile or maleonitrile and cyclopentenone, isomerisation of the alkene could have occurred via a Schenck mechanism involving a triplet 1,4-biradical, an energy transfer pathway, or a combination of both processes. If the Schenck pathway were the dominant mode of isomerisation, then it is very surprising that the photo-stationary state ratio of the concentration of maleonitrile to the concentration of fumaronitrile observed for the photocycloaddition involving 2-cyclopentenone was the same as that observed for the acetophenone sensitised reaction. One might expect that the triplet 1,4-biradicals would partition between reversion to fumaronitrile and reversion to fumaronitrile differently from the perpendicular 1,2-dicyanoethene triplet. Therefore, it is reasonable to suggest that the alkene isomerisation might result from an energy transfer process involving the formation of triplet fumaronitrile or triplet maleonitrile.

At this point, the proposal of a new reaction mechanism for the photocycloaddition of high triplet energy cyclic enones with low triplet energy alkenes is in order. The mechanism shown in Scheme 71 includes a pathway for energy transfer from the triplet cyclic enone to the alkene in addition to a pathway which results in biradical formation. The energy transfer process results in lowering the maximum quantum yield of cycloadduct formation by acting effectively as another energy loss pathway. The mechanism shown in Scheme 71 predicts that as the energy transfer process becomes more favourable relative to the biradical formation pathway, the quantum yield of the formation of cycloadducts should drop. One could test this prediction by measuring the limiting quantum yield of cycloadduct formation for various systems in which the exergonicity of the energy transfer process is different.

Scheme 71

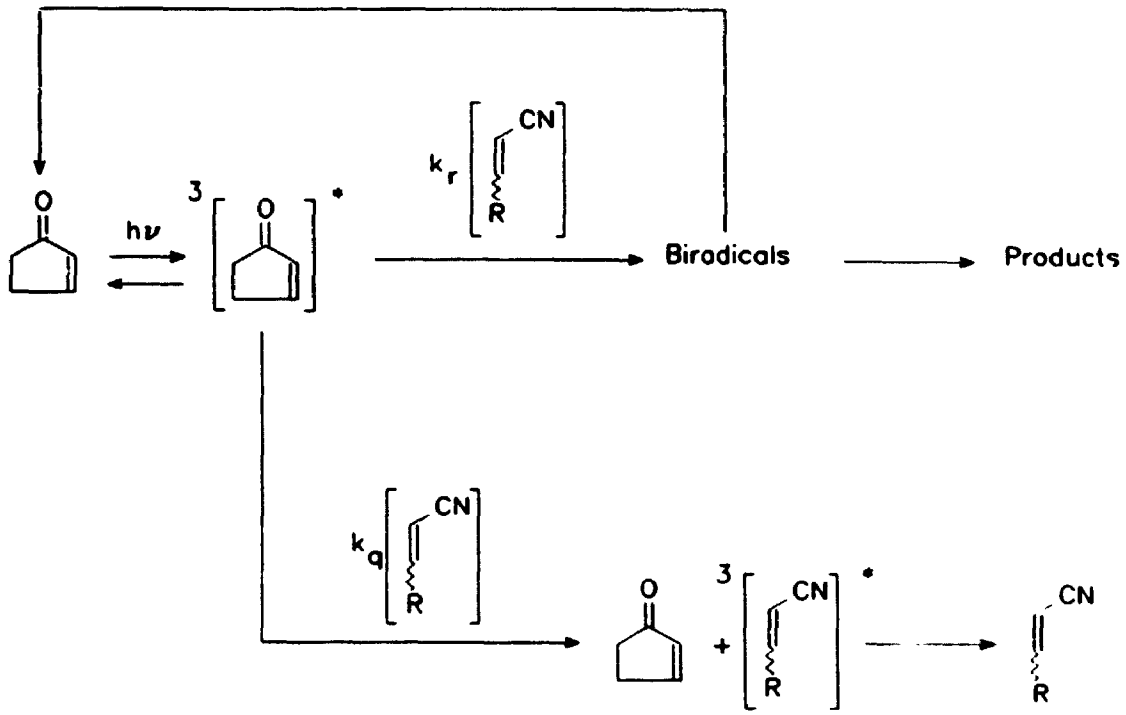

The total quantum yield of cycloadduct formation in the photocycloaddition reactions of 2-cyclopentenone with acrylonitrile, fumaronitrile, and maleonitrile were measured at various alkene concentrations in acetonitrile. It was found that the quantum yields of cycloadduct formation in these systems were relatively insensitive to alkene concentration over the concentration range studied. This observation indicates that the rate at which the alkene reacts with the triplet enone to form cycloadducts is much faster than the rate at which the triplet enone decays by processes which do not involve the alkene.

The maximum quantum yields of cycloadduct formation resulting from the reactions between 2-cyclopentenone and each of acrylonitrile, fumaronitrile and

maleonitrile in acetonitrile were 0.21 ± 0.03, 0.026 ± 0.003, and 0.025 ± 0.003 respectively. Since the relaxed triplet energies of acrylonitrile and fumaronitrile have been determined by photoacoustic calorimetry to be 58 ± 4 and 48 ± 3 respectively,[1] it is possible to conclude that the cyano-substituted alkene with the lower triplet energy exhibits the lower quantum yield of cycloadduct formation in the photocycloaddition reaction with triplet 2-cyclopentenone. This trend is consistent with the prediction suggested earlier; that is, as the triplet energy transfer process becomes more favourable[¶¶], the quantum yield of cycloadduct formation should decrease. However, the difference between the quantum yields of cycloadduct formation determined for the reactions between cyclopentenone and each of the cyano-substituted alkenes could also be attributed to differences in the way in which any biradicals intermediates partition between closure and reversion. More examples of photocycloaddition reactions involving 2-cyclopentenone and low triplet energy alkenes are required in order to develop a more convincing trend.

Additional indirect evidence in favour of the presence of an energy transfer pathway which competes with cycloadduct formation (see Scheme 71) in enone photocycloadditions that involve low triplet energy alkenes comes from the rates at which acrylonitrile quenches the triplet state of different enones. If triplet energy transfer is an important reaction pathway for enone photocycloadditions involving low triplet energy

---

[¶¶] It must be noted that the unrelaxed vertical triplet energies of the alkenes are the quantities that should be compared when predicting the relative efficiencies the triplet energy transfer process. The vertical triplet energy of acrylonitrile has been determined to be approximately 62 kcal/mol by sensitising the photodimerisation of this alkene with sensitisers of various triplet energies.[10] However, the vertical triplet energies of fumaronitrile and maleonitrile have not been determined.

alkenes, then those cyclic enones which exhibit the higher triplet energies should be quenched by acrylonitrile at faster rates. The quenching rate constants measured by Schuster and co-workers demonstrate this trend. For example, the rate constant of triplet enone quenching by acrylonitrile for bicyclo[4.3.0]non-1(6)-en-2-one (**213**), 2-cyclopentenone, testosterone acetate (**214**), and 3-methyl-2-cyclohexenone were found to be $130x10^7$, $63x10^7$, $24x10^7$, and $15x10^7$ M^{-1} sec^{-1} respectively.[8] Based on photoacoustic calorimetry measurements, the triplet energies of **213**, **214**, and 3-methyl-2-cyclohexenone are 73.8, 70.3, and 68.7 kcal/mol.[2] The triplet energy of 2-cyclopentenone has been estimated to be 72 kcal/mol in accordance with the results obtained from experiments in which various sensitisers of various triplet energies were used to sensitise cycloaddition reactions.[23] Therefore, these literature data demonstrate that as the predicted efficiency of triplet energy transfer increases for reactions involving cyclic enones and acrylonitrile so does the observed rate of alkene facilitated triplet enone quenching. This trend is in agreement with the mechanism proposed in Scheme 71.

The relative rates at which acrylonitrile, fumaronitrile, and maleonitrile quench the triplet state of 2-cyclopentenone were determined by measuring the quantum yield of formation of the 2-cyclopentenone dimer at different concentrations of each alkene in acetonitrile. Equation 20 relates the reciprocal of the quantum yield of dimer formation ($1/\Phi_{dimer}$) to the concentration of the alkene ([A]) for a mechanism possessing any number of biradical intermediates, all of which may undergo reversion to ground state stating materials:

$$\frac{1}{\Phi_{dimer}} = \frac{1}{\Phi_o} + \frac{k_q[A]}{\Phi_o(k_d + k_{sq}[E])} \qquad (20)$$

In this equation, Φ_o represents the quantum yield of dimer formation at the concentration of 2-cyclopentenone denoted as E in the absence of the alkene. The rate constant k_q represents the total rate of triplet enone quenching by the alkene A, $k_{sq}[E]$ represents the total rate of enone self quenching, and k_d represents the unimolecular rate of decay of the enone triplet. The slope over intercept ratio for a plot of $1/\Phi_{dimer}$ versus the concentration of alkene is equal to $k_q/(k_d + k_{sq}[E])$ Since k_d and k_{sq} are known for 2-cyclopentenone in acetonitrile from flash photolysis data,[24] therefore the absolute magnitude of k_q can be calculated from the slope over intercept ratio obtained from the quantum yield measurements. The concentration of 2-cyclopentenone used in all of the quantum yield determinations involving acrylonitrile, maleonitrile and fumaronitrile was 0.0940 M. Using this concentration and the values of 2.6×10^6 and 2.7×10^8 for the rate constants k_d and k_{sq} respectively,[24] the sum of $k_d + k_{sq}[E]$ was calculated to be 5.1×10^7 sec^{-1}. Therefore, the rates for the quenching of triplet 2-cyclopentenone by acrylonitrile, fumaronitrile, and maleonitrile were calculated to be $1.0\pm0.3\times10^9$, $2.4\pm0.5\times10^9$, and $3.8\pm0.7\times10^9$ M^{-1} sec^{-1} respectively. These rate constants are in agreement with the corresponding rate constants measured by laser flash photolysis[8] (see Table 1 in Chapter 1) when experimental error is taken in to account.

The rate constants for quenching triplet 2-cyclopentenone with acrylonitrile, fumaronitrile and maleonitrile are in agreement with the mechanism proposed in Scheme 71. The data indicate that reaction between acrylonitrile and 2-cyclopentenone is slower than the reaction between the 1,2-dicyanoethenes and 2-cyclopentenone. Since the triplet energies of the 1,2-dicyanoethenes are lower than the triplet energy of acrylonitrile (see above), the trend exhibited by the rate constants is consistent with an triplet energy

transfer pathway. That is, a faster rate of quenching occurs in those systems where triplet energy transfer is more favourable.

The total quantum yield of cycloadduct formation in the photocycloaddition of acrylonitrile and 2-cyclopentenone in benzene was determined at various alkene concentrations. The quantum yields determined in these studies demonstrated a much greater sensitivity to the alkene concentration compared to the quantum yield measurements for the same reaction in acetonitrile. Equation 21 relates the reciprocal of the cycloadduct quantum yield of formation ($1/\Phi_{add}$) to the reciprocal of the alkene concentration for a reaction mechanism possessing any number of biradical intermediates:

$$\frac{1}{\Phi_{add}} = \frac{1}{\Phi_{\infty}} + \frac{(k_d + k_{aq}[E])}{k_q \Phi_{\infty}} \frac{1}{[A]} \qquad (21)$$

In this equation, Φ_{∞} represents the limiting quantum yield of cycloadduct formation for the situation in which the quantum yield of triplet capture by acrylonitrile is unity. The rate constants in Equation 21 have the same meanings as in Equation 20. It is important to note that Equation 21 holds equally true for mechanisms involving triplet energy transfer (see Scheme 71) as well as mechanisms in which the reaction between the alkene and triplet enone results in biradical formation only. Therefore, the quantum yield data gathered for the photocycloaddition reaction of 2-cyclopentenone and acrylonitrile in benzene were fitted to Equation 21.

The slope and intercept parameters resulting from the plot of $1/\Phi_{add}$ versus 1/[A] for the photocycloaddition of 2-cyclopentenone and acrylonitrile in benzene (see Figure 15) have been listed in Table 24 of the results section. The intercept over slope ratio for the $1/\Phi_{add}$ versus 1/[A] plot was calculated to be 3.4 ± 0.4 M. According to Equation 21,

this intercept over slope ratio represents the same ratio of rate constants as the slope over intercept ratio for the resulting from the plots of $1/\Phi_{dimer}$ versus the alkene concentration discussed above, namely $k_q/(k_d + k_{sq}[E])$. The ratio of $k_q/(k_d + k_{sq}[E])$ determined in the plots of $1/\Phi_{dimer}$ versus [A] for the photocycloaddition of 2-cyclopentenone and acrylonitrile in acetonitrile was calculated to be 21 ± 4 M. Since the same concentration of enone was used in the reaction of 2-cyclopentenone and acrylonitrile in both acetonitrile and benzene, the ratio of $k_q/(k_d + k_{sq}[E])$ determined for each solvent can be compared. The value of this ratio of rate constants in acetonitrile is very different from the corresponding ratio determined in benzene. Evidently, quenching of triplet 2-cyclopentenone by acrylonitrile in benzene occurs much more slowly than in acetonitrile. Alternatively, the rate of triplet enone self quenching (k_{sq}) might be significantly greater in benzene than in acetonitrile. Since no flash photolysis data exists for the self quenching process of 2-cyclopentenone in benzene, it is not possible to substantiate these hypotheses. In conclusion, the reasons for the difference between the magnitudes of the k_q or k_{sq} in acetonitrile and benzene are unclear.

One of the reasons for studying the reaction of 2-cyclopentenone and acrylonitrile in benzene was so that the quantum yield data could be compared with the mechanistic investigations conducted by Weedon and co-workers on the same reaction.[12] Weedon and co-workers generated biradicals **214** and **215** by photolysis of diketones **216** and **217** respectively in benzene solution (see Scheme 72). The relative yield ratio of cyclopentenone formation to cycloadduct formation resulting from fragmentation and closure of each of the independently generated biradicals was determined. The relative yields of cycloadducts **203** and **204** that result from the photocycloaddition of 2-

Scheme 72

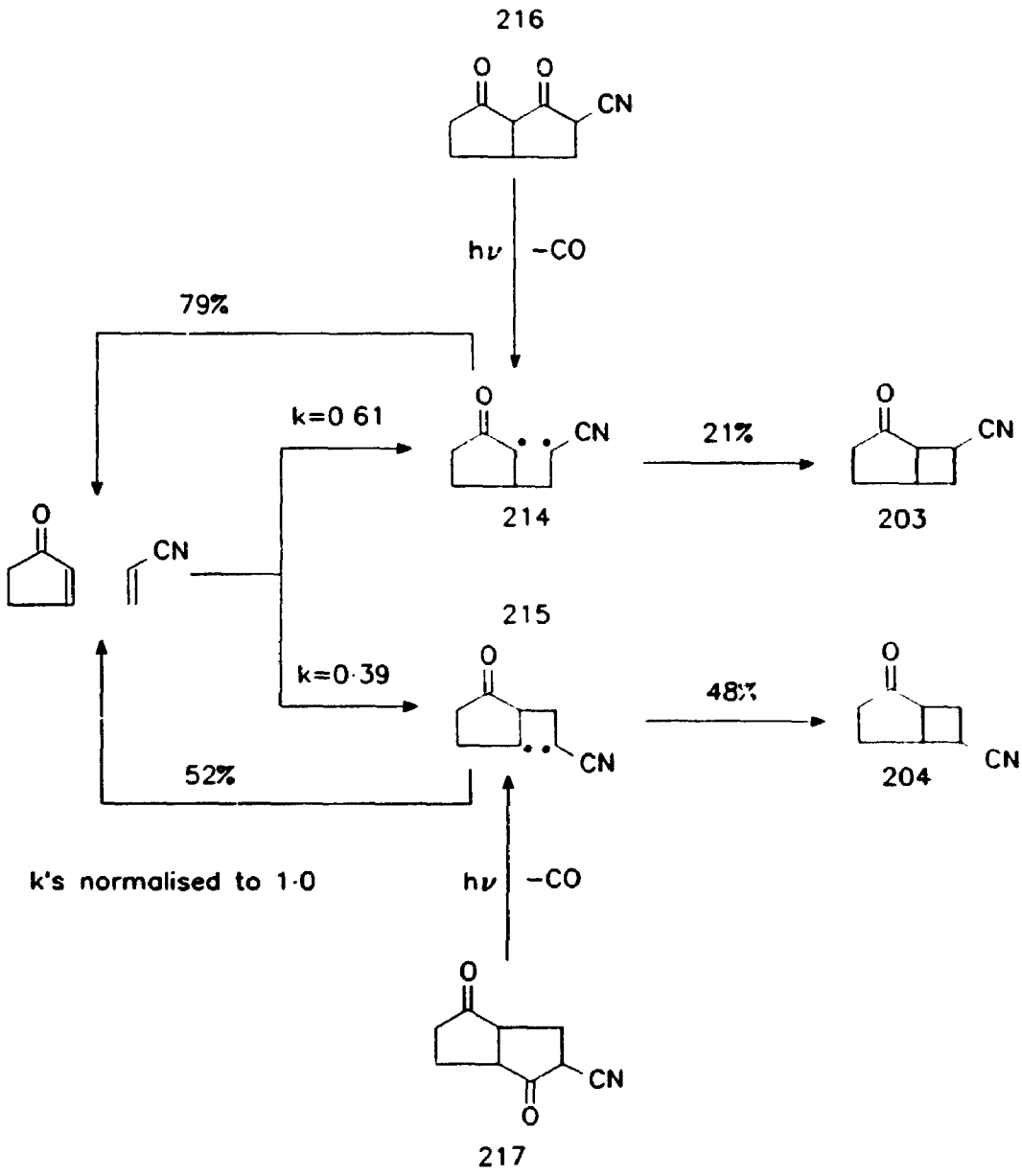

cyclopentenone and acrylonitrile were used in conjunction with the biradical closure to fragmentation ratios in order to determine the relative rates of formation of **214** and **215** in the photocycloaddition reaction. Scheme 72 contains a summary of the biradical fragmentation to closure ratios as well as the relative rates of biradical formation that

Weedon and co-workers[12] determined for **214** and **215**.[11]

Using the data summarised in Scheme 72, it is possible to calculate a theoretical maximum quantum yield of cycloadduct formation for the reaction of 2-cyclopentenone and acrylonitrile. Equation 22 defines the limiting quantum yield of cycloadduct formation for this photo-reaction in the context of the parameters summarised in Scheme 72:

$$\Phi_{add} = \alpha_{HH}\rho_{HH} + \alpha_{HT}\rho_{HT} \qquad (22)$$

In this equation, ρ_{HH} and ρ_{HT} represent the fractions of biradicals **214** and **215** that close to form cycloadducts while α_{HH} and α_{HT} represent the relative rates of formation of biradicals **214** and **215**. All of the ρ and α parameters must be normalised to unity. Therefore, the limiting quantum yield of cycloadduct formation, according to Equation 22, was calculated to be 0.32.

The limiting quantum yield of cycloadduct formation for the photocycloaddition reaction of 2-cyclopentenone and acrylonitrile in benzene that was determined in the quantum yield investigations was 0.29. This value was obtained from the reciprocal of the y-intercept resulting from the linear relationship of $1/\Phi_{add}$ versus 1/[A] described by Equation 21. The excellent agreement between this limiting quantum yield and the limiting quantum yield calculated from the data published by Weedon and co-workers indicates that biradical reversion could account for almost all of the inefficiency in the

---

[11] In this determination, Weedon and co-workers assumed that primary radical containing biradicals do not contribute significantly to the photocycloaddition reaction. Conformational equilibration of biradicals **214** and **215** was also assumed.

photocycloaddition reaction between acrylonitrile and 2-cyclopentenone. If this is so then the inefficiencies resulting from triplet enone quenching by acrylonitrile via a triplet energy transfer pathway (see Scheme 71) are unimportant in this particular cycloaddition reaction.

It is important to note that the kinetic data discussed above indicate that the rate of reaction between triplet 2-cyclopentenone and acrylonitrile might be considerably slower in benzene than in acetonitrile. The slower rate of reaction between acrylonitrile and triplet 2-cyclopentenone in benzene compared to that in acetonitrile may reflect the absence of a quenching process involving triplet energy transfer in benzene solution. The reasons why energy transfer might be slower in benzene compared to acetonitrile are far from obvious.

Attempts to trap the biradicals formed in the photocycloaddition of 2-cyclopentenone and acrylonitrile with hydrogen selenide were unsuccessful. The irradiation of benzene solutions containing 2-cyclopentenone, acrylonitrile and hydrogen selenide with Pyrex filtered light from a medium pressure mercury lamp did not result in the formation of cycloadducts or products representative of trapped biradicals. In order to determine if this apparent lack of reactivity was due to efficient quenching of the enone triplet by H_2Se, competition experiments were conducted in which solutions containing cyclopentene, acrylonitrile, 2-cyclopentenone and H_2Se were irradiated with U.V. light. Cyclopentene was included in these competition experiments because Hastings and Weedon have demonstrated that H_2Se is capable of completely trapping the biradicals formed in the cycloaddition of cyclopentene and 2-cyclopentenone.[18]

Analysis of the reaction mixtures resulting from the competition reactions

indicated that significant amounts of products **209** and **210** were formed; however, no products derived from an interaction between 2-cyclopentenone and acrylonitrile were observed. In the absence of H_2Se, these competition experiments resulted in the formation of acrylonitrile and cyclopentene derived adducts in a ratio of 1.74:1 respectively. Based on this ratio and the quantum yield of cycloadduct formation for the reaction of 2-cyclopentenone and acrylonitrile, the lack of cycloadducts in the competition experiments performed in the presence of H_2Se cannot be explained by considering reversion of untrapped biradicals. The quantity of trapped products resulting from the reaction of 2-cyclopentenone and cyclopentene indicates that some acrylonitrile derived cycloadducts should have been detected even if none of the biradicals responsible for the formation of these cycloadducts were trapped. Therefore, the complete absence of trapped biradicals or cycloadducts resulting from the reaction between 2-cyclopentenone and acrylonitrile in the competition experiments cannot be explained in terms of the mechanism proposed in Scheme 71.

For some reason H_2Se seems to quench the reaction between acrylonitrile and 2-cyclopentenone more efficiently than the reaction between cyclopentene and 2-cyclopentenone. However, the sensitisation and triplet quenching studies discussed above proved that the same enone triplet excited state is involved in both cycloaddition reactions. Therefore, the observations resulting from the attempted H_2Se trapping experiments seem to suggest that additional intermediates may be present in the 2-cyclopentenone plus acrylonitrile photocycloaddition reaction. These intermediates are apparently quenched by H_2Se. Based on the evidence available, it is difficult to speculate on the nature of such intermediates.

The mechanism proposed in Scheme 71 does not explain all of the results discussed above adequately. In particular, the results obtained from the attempted biradical trapping studies cannot be rationalised in terms of this mechanism. Therefore, a different mechanism has been proposed in Scheme 73. This new mechanism was proposed with the intent that it should explain, in a reasonable fashion, all the results for photocycloaddition reactions of cyclic enone with cyanoalkenes that have been obtained thus far.

Scheme 73

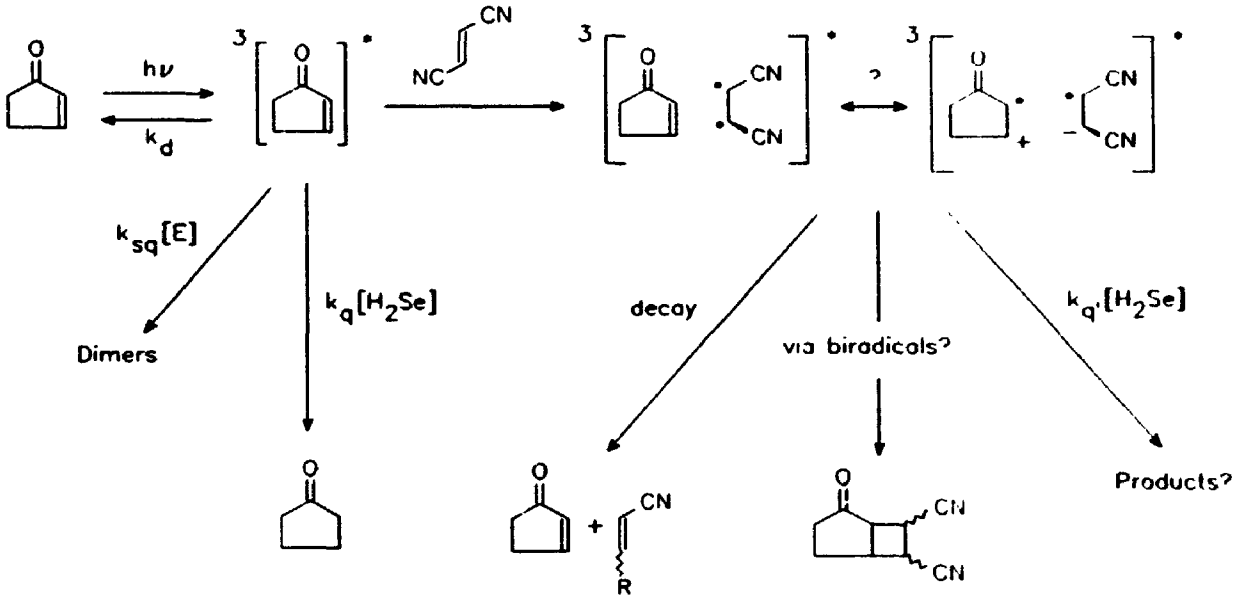

The most speculative aspect of Scheme 73 involves the triplet excited state complex that could be produced by the initial reaction between triplet excited state 2-cyclopentenone and the ground state alkene. It is reasonable to suggest that the alkene component of the triplet exciplex would have a twisted orthogonal geometry. The formation of a intermediate containing an orthogonal alkene components might explain

why identical cycloadduct product distributions are obtained for different alkene geometrical isomers.

The electron distribution of the exciplex intermediate shown in Scheme 73 may be indicative of a considerable amount of charge transfer. The pronounced electron withdrawing ability of the nitrile substituents would favour the formation of a charge transfer complex. In addition, the formation of a charge transfer complex could explain why the rate constant for triplet enone quenching in the polar solvent acetonitrile appears to be much larger than the corresponding rate constant in benzene. In order to evaluate the degree of charge transfer in the hypothesised exciplex intermediate, one would have to examine the appropriate reduction potentials of the enone and alkene closely. At this point such an examination seems a little premature given the highly speculative nature of the entire mechanism proposed in Scheme 73.

The presence of the triplet exciplex in Scheme 73 is useful in explaining the results observed in the attempted trapping studies. As discussed above, the observations made in these studies cannot be explained in terms of a mechanism in which the only quenchable intermediates consist of the triplet enone and 1,4-biradicals. However, if a triplet exciplex intermediate were formed along the photocycloaddition pathway then additional modes of H_2Se quenching can be postulated. The different modes of H_2Se induced triplet exciplex quenching are summarised as one process in Scheme 73. These modes might include pathways in which H_2Se increases the rate of intersystem crossing, or pathways in which H_2Se acts as a hydrogen or proton donor towards the triplet exciplex. Any of these quenching pathways could be used to explain why no cycloadducts or trapped biradical are formed in the photocycloaddition reactions of

cyclopentenone with cyano-substituted alkenes that are preformed in the presence of H_2Se.

6.6 Conclusions

As mentioned in the introduction, the aim of the studies presented in this Chapter was not to develop and prove a general reaction mechanism for the photocycloaddition reaction of 2-cyclopentenone and low triplet energy alkenes; rather, the aim of these studies was to define the mechanistic problems associated with this special type of enone photocycloaddition more precisely. Some of the arguments mentioned in the discussion above support a reaction mechanism in which biradical formation competes with triplet energy transfer from the enone to the alkene (see Scheme 71). On the other hand, the results of the quantum yield study involving the reaction of 2-cyclopentenone and acrylonitrile in benzene suggest that the inefficiencies of this reaction can be completely accounted for by considering reversion of the 1,4-biradicals. At least for this particular reaction, inefficiencies caused by enone triplet quenching via an energy transfer process appear to be insignificant. However, it would be very dangerous to apply this conclusion to other examples of photocycloaddition reactions in which cyclic enones react with low triplet energy alkenes. It is possible that the energy transfer reaction may be more important in some enone-alkene photocycloaddition reactions than others.

The data discussed in this chapter are also consistent with the mechanism proposed in Scheme 73. This mechanism involves the formation of a triplet excited state

complex or exciplex. The expected orthogonal geometry of the alkene component of the exciplex can be conveniently used to explain why the photocycloaddition reactions of 2-cyclopentenone and 3-methyl-2-cyclohexenone with 1,2-cyanoethene result in identical product distribution for the two different geometrical isomers of the alkene.

The mechanism which involves the triplet exciplex intermediate has the additional advantage of being able to rationalise the results obtained from the attempted biradical trapping studies. The results of these experiments indicate that H_2Se quenches the reaction between 2-cyclopentenone and acrylonitrile faster than it quenches the reaction between 2-cyclopentenone and cyclopentene. This observation is difficult to explain in terms of a reaction mechanism in which the only intermediates quenchable by H_2Se are the triplet enone and the 1,4-biradicals. If a triplet exciplex were involved in photocycloaddition reactions between cyclic enones and cyano-substituted alkene, then this intermediate could also be quenched by H_2Se. This quenching pathway might explain why H_2Se is much more efficient in quenching photocycloaddition reactions involving cyclic enones with cyano-substituted alkenes.

The results described in this chapter by no means offer any conclusive evidence which can be used to prove a particular reaction pathway for these types of photocycloaddition reactions. Clearly, the discussion above demonstrates the need for further investigation into the photocycloaddition of 2-cyclopentenone and low triplet energy alkenes.

6.7 References

1. Lavilla, J. A.; Goodman, J. L. *Chem. Phys. Lett.* **1987**, *141*, 149.

2. Schuster, D. I.; Dunn, D. A.; Heibel, G. E.; Brown, P. B.; Rao, J. M.; Woning, J.; Bonneau, R. *J. Am. Chem. Soc.* **1991**, *113*, 6245.

3. Schuster, D. I.; Heibel, G. E.; Woning, J. *Angew. Chem. Int. Ed. Engl.* **1991**, *30*, 1345.

4. Cantrell, T. S. *J. Org. Chem.* **1974**, *39*, 3063.

5. Murov, S. L. *Handbook of Photochemistry*; Marcel Dekker: New York, 1973; pp 3-22.

6. Kumar, S. M.; Rao, M. *Tetrahedron Lett.* **1990**, *46*, 5383.

7. Demuth, M. *Pure & Appl. Chem.* **1986**, *58*, 1233.

8. Schuster, D. I.; Heibel, G. E.; Brown, P. B. *J. Am. Chem. Soc.* **1988**, *110*, 8261.

9. Bonneau, R. *J. Am. Chem. Soc.* **1980**, *102*, 3816.

10. Hosaka, S.; Wakamatsu, S. *Tetrahederon Lett.* **1968**, 219.

11. (a) Eaton, P. E.; Hurt, W. S. *J. Am. Chem. Soc.* **1966**, *88*, 5038. (b) de Mayo, P.; Nicholson, A. A.; Tchir, M. F. *Ibid.* **1970**, *48*, 225. (c) Ruhlen, J. L.; Leermakers, P. A. *J. Am. Chem. Soc.* **1966**, *88*, 5671. (d) Ruhlen, J. L.; Leermakers, P. A. *J. Am. Chem. Soc.* **1967**, *89*, 4944.

12. Krug, P.; Rudolph, A.; Weedon, A. C. *Tetrahedron Lett.* **1993**, *34*, 7221.

13. Corey, E. J.; Bass, J. D.; LeMahieu, R.; Mitra, R. B. *J. Am. Chem. Soc.* **1964**, *86*, 5570.

14. Ullman, E. F.; Singh, P. *J. Am. Chem. Soc.* **1972**, *94*, 5077.

15. Sayre, R. *J. Am. Chem. Soc.* **1955**, *77*, 6689.

16. Lambkin, M.; Mittag, T. W. *J. Chem. Soc. (C)* **1966**, 2300.

17. Singh, P.; Boocock, D. G. B.; Ullman, E. F. *Tetrahedron Lett.* **1971**, 3935.

18. Hastings, D. J.; Weedon, A. C. *J. Am. Chem. Soc.* **1991**, *113*, 8525.

19. Dilling, W. L.; Tabor, T. E.; Boer, F. P.; North, P. P. *J. Am. Chem. Soc.* **1970**, *92*, 1399

20. Griesbeck, A. G.; Stadtmuller, S.; Busse, H.; Bringmann, G.; Buddrus, J. *Chem. Ber.* **1992**, *125*, 933.

21. Bunce, N. J.; LaMarre, J.; Vaish, S. P. *Photochem. Photobiol.* **1984**, *39*, 531.

22. Peet, N. P.; Cargill, R. L.; Bushey, D, F. *J. Org. Chem.* **1973**, *38*, 1218.

23. De Mayo, P.; Pete, J-P.; Tchir, M. *Can. J. Chem.* **1968**, *46*, 2535.

24. Caldwell, R. A.; Tang, W.; Schuster, D. I.; Heibel, G. E. *Photochem Photobiol.* **1991**, *53*, 159.

CHAPTER 7

EXPERIMENTAL SECTION FOR PART I

7.1 General experimental details for all chapters

Spectrophotometric grade benzene, acetonitrile, hexane, methanol and toluene were supplied by BDH Corporation and used as received. Cyclopentenone was synthesized from cyclopentene (Aldrich Chemical Company) according to the method of Mihelich and Eickhoff and was purified by distillation (56°C at 23 mm Hg).[1] This preparation is described below. The grey selenium powder and aluminum powder used in the preparation of aluminum selenide were obtained from the Aldrich Chemical Company. Silica gel (60-200 mesh) was supplied by Syn Org Chemica Alta Ltd.

The ^{1}H nmr spectra was recorded on a Varian XL200 or a Varian Gemini 200 instrument at 200 MHz or a Varian Gemini 300 at 300 MHz. The ^{13}C nmr spectra were recorded on a Varian Gemini 200 instrument at 50 MHz or a Varian XL300 instrument at 75 MHz. The lanthanide shift reagent Eu(fod)$_3$ was obtained from the Aldrich Chemical Company and was stored over $CaSO_4$ in a desiccator. Data obtained from the ^{1}H nmr spectra are reported as follows: δ (multiplicity, coupling constants, integration, assignment were appropriate). Abbreviations used are: s (singlet), d (doublet), t (triplet), q (quartet), mult. or m (multiplet), br (broad). Data obtained from ^{13}C nmr spectra are reported as follows: δ (multiplicity). The multiplicity of ^{13}C nmr signals was determined in Attatched Proton Test (APT) experiments.

Coupled gas chromatography-mass spectrometry (g.c.-m.s.) was performed using

a Varian 3400 gas chromatograph fitted with a 30m DB-5 methyl silicone capillary column which was attached to a Finnegan-MAT 8230 mass spectrometer. Ionisation was achieved by electron impact (EI) or chemical ionisation (CI) with isobutane. Mass spectrum data are listed as follows: Fragment mass (relative intensity in %); calculated exact mass (observed exact mass).

Ultraviolet absorption spectra were obtained on a Shimadzu UV-160 spectrophotometer. Infrared spectra were recorded on a Bruker IFS 32/IBM System 9000 FT-instrument.

Routine analytical g.c. was carried out using a Hewlett-Packard 5880 or a Hewlett-Packard 5890 gas chromatograph fitted with a 30 meter DB-5 methyl silicone capillary column and a flame ionization detector (FID). Most analytical g.c. separations were carried out by maintaining the column at 50°C for 5 minutes after injection and then ramping the temperature at 7 per minute to 250°C. Preparative g.c. was carried out on a Varian 1400 gas chromatograph using a 2 m Silar 5CP column (50% phenyl, 50% cyanopropyl groups on a siloxy-backbone).

Unless otherwise stated, the photochemical reactions were performed at room temperature with an 400 W Hanovia medium pressure mercury lamp which was housed in a water cooled Pyrex jacket. Photochemical reactions requiring shorter wavelength light were performed using light emitted from a Rayonet apparatus (The Southern New England Ultraviolet Co.). The Raynot was equipped with tubes that emitted more than 95% of their light at 254 nm.

7.1.1 Preparation of 2-Cyclopentenone

The method of Mihelich and Eickhoff[18] was used. A 250 mL solution of cyclopentene (50.0 g; 0.725 mol), acetic anhydride (72.75 mL; 0.757 mol), pyridine (29.0 g; 0.368 mol), tetratolylporphyrin (0.05 g), and 4-(dimethylamino)pyridine (1.798 g; 0.015 mol) in CH_2Cl_2 was added to an immersion-well reactor which was fitted with a dry-ice/acetone condenser, oxygen inlet, and a quartz water cooled lamp jacket. A 400 W Hanovia medium pressure mercury lamp fitted with a Uranium glass filter was placed in the water cooled lamp jacket and the solution was irradiated for 10 hours while a constant stream of oxygen was bubbled through the solution. After 10 hours it was determined by g.c. that 80% of the cyclopentene had been converted to cyclopentenone. The reaction mixture was washed with a saturated $NaHCO_3$ solution (5x100 mL) to remove the acetic acid by-product. The organic layer was then washed with 1N aqueous HCl (2x100 mL) followed by saturated aqueous NaCl (3x100 mL) and dried over $MgSO_4$. After removing the solvent under low vacuum at 35°C, the remaining concentrate was distilled at 56°C (23 mm Hg) to yield colourless 2-cyclopentenone (19.1 g) in 32% yield. ^1H, ^{13}C nmr and mass spectra were identical to published data.

7.2 Experimental details for Chapter 2.

7.2.1 Irradiation of 2-cyclopentenone and 1,1-difluoroethene.

A solution of cyclopentenone (1.638 g; 0.0399 mole/L) in methanol (0.50 L) was saturated at 25°C with 1,1-difluoroethene by bubbling the gas through a fine frit for

20 minutes. (In a separate experiment, the concentration of 1,1-difluoroethene in CD_3OD at saturation was determined by ^1H nmr to be 0.15 M.) The solution was irradiated at room temperature for 7 hours with water and Pyrex filtered light from a 400 W Hanovia medium pressure mercury lamp housed in a quartz water cooled jacket. The solvent was removed under reduced pressure at 50°C to yield 1.785 g of crude product. The reaction mixture was analyzed by g.c. and coupled g.c./m.s. and it was determined that the mixture contained 16% of unreacted 2-cyclopentenone, 65% of two 2-cyclopentenone dimers in a ratio of 1.9:1.0, and 18% of two enone plus alkene cycloadducts in a ratio of 2.8:1.0. The reaction mixture was separated by column chromatography in which a 3 cm x 80 cm column containing 130 g of 60-200 mesh silica gel packed in 1:1 diethyl ether:hexanes was used. The column was eluted with 0.5 L of 1:1 diethyl ether:hexanes followed by 1 L of 2:1 diethyl ether: hexanes. Three fractions were collected and analyzed by g.c: I, 0.335 g of cycloadducts **31** and **32** in a 2.8:1.0 ratio; II, 0.280 g of cyclopentenone; III, 1.17 g of two enone dimers in a 1.9:1.0 ratio. Fraction I was separated further by preparative g.c. into two fractions : IV, 0.240 g of pure **31**; and V, 0.086 g of 98% pure **32** with the 2% contaminant consisting of **31**. All fractions were isolated as colourless oils.

Characterisation of 31. ^1H nmr (300 MHz, in $CDCl_3$): δ 2.04 (dq, J=14.1 Hz, J=9.6 Hz, 1H), 2.2 to 2.7 (complex, 5H), 2.94 (dtt, J=3.3 Hz, J=10.6 Hz, J=14.4 Hz, 1H), 3.36 (m, 1H). ^{13}C nmr (300 MHz, proton decoupled ^{19}F coupled, in $CDCl_3$): δ 218.2 (d, J=4.0 Hz, C=O), 119.9 (dd, J=285 Hz, J=282 Hz, CF_2), 47.9 (dd, J=23.5 Hz, J=25.1 Hz, CH), 38.8 (t, J=25.3 Hz, CH_2), 36.3 (s, CH_2), 34.5 (dd, J=7.5 Hz, J=10.6 Hz, CH), 19.6 (dd, J=2.9 Hz, J=5.8 Hz, CH_2). ^{19}F nmr (300

MHz, ref. $CFCl_3$, in $CDCl_3$): δ -98.9 (dtt, J_{FF}=196 Hz, J_{HF}=5.7 Hz, J_{HF}=11.0 Hz), -88.4 (dddt, J_{FF}=196 Hz, J_{HF}=3.5 Hz, J_{HF}=11.0 Hz, J_{HF}=14.7 Hz). ^{13}C-^{1}H heteronuclear correlation results for clearly defined resonances (^{13}C δ; ^{1}H δ): (19.6; 2.04), (38.8; 2.94), (47.9; 3.36). Mass spectrum (EI, 70 eV): m/e(%) 146(64), 91(12), 90(15), 82(100), 55(80), 54(40); calculated M^+ for $C_7H_8OF_2$ 146.05431 (found 146.0539).

Characterisation of 32. ^{1}H nmr (300 MHz, in $CDCl_3$): δ 2.00 (dddd, J=3.5 Hz, J=1.3 Hz, J=9.0 Hz, J=13.5 Hz, 1H), 2.1 to 2.5 (complex, 3H), 2.61 (ddd, J=18.5 Hz, J=11.3 Hz, J=9.5 Hz, 1H), 2.8 to 3.1 (complex 2H), 3.23 (m, 1H). ^{13}C nmr (300 MHz, proton decoupled ^{19}F coupled, in $CDCl_3$): δ 212.2 (dd, J=3.0 Hz, J=1.5 Hz, C=O), 115.8 (dd, J=282 Hz, J=289 Hz, CF_2), 57.8 (t, J=23.3 Hz, CH), 40.3 (t, J=22.4 Hz, CH_2), 36.7 (d, J=4.0 Hz, CH_2), 27.0 (d, J=2.8 Hz, CH_2), 25.6 (dd, J=6.1 Hz, J=11 Hz, CH). ^{19}F nmr (300 MHz, ref. $CFCl_3$, in $CDCl_3$): δ -88.6 (dddt, J_{FF}=198 Hz, J_{HF}=11 Hz, J_{HF}=2.6 Hz, J_{HF}=6.4 Hz), -91.6 (d, J_{FF}=198 Hz, J_{HF} coupling results in an undetermined muliplet). ^{13}C-^{1}H heteronuclear correlation results for clearly defined resonances (^{13}C δ; ^{1}H δ): (57.8; 3.23), (36.7; 2.61), (27.0; 2.00). Mass spectrum (EI, 70 eV): m/e(%) 146(45), 91(62), 90(24), 82(100), 55(45), 54(72); calculated M^+ for $C_7H_8OF_2$ 146.05431 (found 146.0548).

7.2.2 Irradiation of 2-cyclopentenone and methyl acrylate.

A Pyrex irradiation tube was filled with a solution of 2-cyclopentenone (1.445 g; 0.0978 mole/L) and freshly distilled methyl acrylate (10.8 g; 0.679 mole/L) in 180 mL of benzene. The solution was irradiated with Pyrex filtered light from a 400 W

Hanovia medium pressure mercury lamp for 12 hours. The temperature during the irradiation was maintained at 10°C by means of a recirculating water bath. Analysis of the reaction mixture by g.c./m.s. revealed the ratio of 2-cyclopentenone: cycloadducts: enone dimers was 24:70:6. The benzene solvent was removed under reduced pressure to yield a thick white syrup. Addition of 50 mL of diethyl ether to the product resulted in the precipitation of a white polymeric material. The polymeric material was removed by filtration and washed by 5x50 mL additional portions of diethyl ether. The diethyl ether extracts were combined and concentrated under reduced pressure to yield 1.53 g of a faint yellow oil. The product was dissolved in 100 mL of benzene and flash chromatographed through 20 g of silica gel. The products were eluted with an additional 5x150 mL portions of benzene. The benzene portions where combined and concentrated under reduced pressure to yield 1.43 g of oil which was found by g.c. to contain only 2-cyclopentenone and enone plus methyl acrylate cycloadducts in the same ratio as in the crude reaction mixture. The mixture resulting after flash chromatography was separated further by column chromatography in which a 3 cm x 80 cm column containing 155 g of 60-200 mesh silica gel packed in 1:4 diethyl ether:hexanes was used. The column was eluted with a 1:5 diethyl ether: hexanes solution and the following fractions were obtained: I, 0.215 g of **34**; II, 0.259 g of **33**:**34**:**35** (12:54:34); III, 0.496 g of **34**:**35** (36:64); IV, 0.110 g of 2-cyclopentenone; V, 0.350 g of **35**:**36** (38:62). All fractions were isolated as faint yellow oils.

Purification of column fractions: Fraction II (0.118 g) was further purified by column chromatography by employing a 2.5 cm x 80 cm column containing 85 g of silica gel packed in 1:10 diethyl ether: hexanes. Two fractions, both consisting of colourless oils,

were collected after eluting the column with 1:10 diethyl ether/hexanes: IIa, 0.065 g of **34**; IIb, 0.054 g of **33**:**35** (25:75). Preparative g.c. was not useful in separating IIb further; therefore, **33** was not obtained pure. Fraction V (0.162 g) was further purified by column chromatography by employing a 2.5x80 cm column containing 100 g of silica gel packed in 1:8 diethyl ether/hexanes. Two fractions, both consisting of colourless oils, were collected after eluting the column with 1:8 diethyl ether/hexanes: Va, 0.049 g of **35**:**36** (85:15); Vb, 0.112 g of **35**:**36** (20:80). These two sub-fractions were enriched in their major components by peak trimming in preparative gas chromatography (resolved g.c. peaks were not obtained under a variety of conditions). Thus, compounds **35** and **36** were obtained in 90% and 87% purity respectively.

Characterisation of 33 in fraction IIb. ^{1}H nmr (300 MHz, in $CDCl_3$): δ 3.57 (s, CH_3O), remaining resonances unresolved due to the presence of **35**. ^{13}C nmr (300 MHz, in $CDCl_3$): δ 219.7 (C=O), 172.4 (C=O), 51.7 (OCH_3), 47.1 (CH), 37.3 (CH_2), 36.5 (CH), 32.2 (CH), 27.7 (CH_2), 26.6 (CH_2). Mass spectrum (EI, 70 eV): m/e(%) 168(4), 137(8), 136(4), 113(21), 109(18), 108(8), 87(16), 83(8), 82(100), 81(46), 67(18); calculated M^+ for $C_9H_{12}O_3$ 168.0786 (found 168.0784).

Characterisation of 34. ^{1}H nmr (300 MHz, in C_6D_6): δ 1.21 (dddd, J=2.3 Hz , J=-4.1 Hz, J=9.4 Hz, J=13.5 Hz, 1H), 1.44 (ddt, J=7.7 Hz, J=13.6 Hz, J=9.8 Hz, 1H), 1.61 (ddd, J= 5.5 Hz, J=8.9 Hz, J= 12.4 Hz, 1H), 1.89 (dddd, J=1.50 Hz, J=4.1 Hz, J=9.7 Hz, J=18.4 Hz, 1H), 2.15 (dt, J=18.6 Hz, J=9.3 Hz, 1H), 2.32 (dddd, J=2.1 Hz, J=5.5 Hz, J=9.2 Hz, J=12.5 Hz, 1H), 2.57 (brd. quintet, J=7 to 9 Hz), 2.68 to 2.82 (complex, 2H), 3.34 (s, 3H). ^{13}C nmr (300 MHz, in C_6D_6): δ 217.7 (C=O), 174.2 (C=O), 51.6 (OCH_3), 47.3 (CH), 38.3 (CH), 36.6 (CH_2), 33.1

(CH), 28.6 (CH_2), 27.2 (CH_2). ^{13}C nmr (300 MHz, in $CDCl_3$): δ 219.3 (C=O), 174.2 (C=O), 51.9 (OCH_3), 47.2 (CH), 38.1 (CH), 36.7 (CH_2), 33.0 (CH), 28.6 (CH_2), 27.2 (CH_2). ^{13}C-^1H heteronuclear correlation results for clearly defined resonances, in C_6D_6 (^{13}C δ; ^1H δ): (51.6; 3.34), (47.3; 2.68 to 2.82), (38.3; 2.68 to 2.82), (33.1; 2.57), (28.6; 2.32 and 1.61), (36.6; 2.15 and 1.89), (27.2; 1.44 and 1.21). IR (neat film, cm^{-1}): 1734 (vs, C=O), 1208, 1167, 1239, 2953, 1437, 1275, 1354. Mass spectrum (EI, 70 eV): m/e(%) 168(35), 137(5), 113(30), 109(33), 108(47), 82(18), 81(90), 80(41), 79(54), 67(48), 55(100); calculated M^+ for $C_9H_{12}O_3$ 168.0786 (found 168.0783).

Characterisation of 35. ^1H nmr (300 MHz, in C_6D_6): δ 1.25 to 1.37 (complex, 2H), 1.70 to 1.83 (m, 1H), 1.88 (dddd, J=18.8 Hz, J= 9.0 Hz, J=2.5 Hz, J=1.4 Hz, 1H), 2.03 (dt, J=18.8 Hz , J= 10.2 Hz, 1H), 2.16 to 2.26 (m, 1H), 2.36 to 2.54 (complex, 2H), 2.78 (brd. quartet, J=7 to 9 Hz, 1H), 3.30 (s, 3H). ^{13}C nmr (300 MHz, in $CDCl_3$): δ 221.5, (C=O), 174.8 (C=O), 51.9 (OCH_3), 41.7 (CH), 40.7 (CH), 40.2 (CH), 36.3 (CH_2), 27.1 (CH_2), 24.9 (CH_2). Mass spectrum (EI, 70 eV): m/e(%) 168(65), 140(20), 137(32), 136(18), 109(22), 108(38), 84(15), 82(100), 81(80), 67(40), 55(96); calculated M^+ for $C_9H_{12}O_3$ 168.0786 (found 168.0787).

Characterisation of 36. ^1H nmr (300 MHz, in $CDCl_3$): δ 1.88 (dddd, J=14.2 Hz, J=9.0 Hz, J=5.1 Hz, J=3.0 Hz, 1H), 2.0 to 2.7 (complex, 5H), 2.76 (dt, J=9.3, J=6.5, 1H), 3.21 (brd. quartet, J=7 to 9 Hz, 1H), 3.46 (dt, J=8.3 Hz, J= 9.5 Hz, 1H), 3.69 (s, 3H). ^{13}C nmr (300 MHz, in $CDCl_3$): δ 220.2 (C=O), 173.5 (C=O), 51.5 (OCH_3), 41.4 (CH), 38.4 (CH), 37.4 (CH_2), 37.0 (CH), 24.6 (CH_2), 23.6 (CH_2). ^{13}C-^1H heteronuclear correlation results for clearly defined resonances, in $CDCl_3$ (^{13}C δ; ^1H δ): (51.5; 3.69), (38.4; 3.46), (37.0; 3.21), (41.4; 2.76), (23.6; 1.88). Mass spectrum (EI,

70 eV): m/e(%) 168(1), 137(8), 136(18), 109(11), 108(8), 87(35), 82(100), 81(29), 79(14), 67(16); calculated M^+ for $C_9H_{12}O_3$ 168.0786 (found 168.0781)

7.2.3 Analytical determination of product ratios in the 2-cyclopentenone plus methyl acrylate photocycloaddition.

A solution of 2-cyclopentenone (1.493 g; 0.101 mole/L) and methyl acrylate (25.0 g; 1.61 mole/L) in 180 mL of toluene was placed in a Pyrex irradiation tube. The tube was chilled to -20°C in an $CaCl_2$/ice bath and irradiated for 8 hours with filtered light ($\lambda > 327$ nm) from a 450 watt Hanovia medium pressure mercury lamp which was surrounded by 1.5 cm of a 0.4 mole/L $SnCl_2$ in 10% HCl/H_2O filter. The temperature of the irradiation vessel was maintained at -20°C during the irradiation. The toluene was removed under reduced pressure at 65°C to yield a thick syrup. The addition of 100 mL of diethyl ether to the product resulted in the precipitation of a white polymer. The polymer was extracted with additional portions of diethyl ether until no cycloaddition products were detected in the washings. The washings were combined and concentrated under reduced pressure to yield 1.726 g of a colourless oil. A solution of 0.30 g of this oil dissolved in 1.0 g of $CDCl_3$ was analyzed by quantitative ^{13}C nmr spectroscopy (i.e. small pulse width and a delay of approximately 2 times the longest T_1 between pulses). The ratio of **33:34:35:36** was determined to be 6.5:40:35:19 (with relative error of 5%) by integrating the corresponding OCH_3 ^{13}C signal in each molecule. The highest field CH ^{13}C signal in each molecule was also integrated and these results were consistent with the product ratios listed above. The cycloadducts in $CDCl_3$ solution were irradiated for 4 hours with filtered light ($\lambda > 327$ nm) from a 450 watt Hanovia medium pressure

mercury lamp which was surrounded by 1.5 cm of a 0.4 mole/L $SnCl_2$ in 10% HCl/H_2O filter. The cycloadduct ratios, as determined by ^{13}C nmr spectroscopy were not changed after irradiation.

7.2.4 Hydride reduction of 2-cyclopentenone plus methyl acrylate photo-cycloadducts.

A methanol solution (65 mL) of a cycloadduct mixture (0.755g; 4.50 mmol) was chilled to 0°C in a ice bath. The ratio of **33**:**34**:**35**:**36** was 6.5:40:35:19. Sodium borohydride (0.200 g; 5.29 mmol) was added to the over a period of 5 minutes after which the reaction mixture was stirred for an additional 1.1 hours at 0°C. Approximately 1 g of potassium dihydrogen phosphate was added and then the reaction mixture was allowed to warm to room temperature. The mixture was diluted with water (100 mL) and extracted with 4x60 mL of CH_2Cl_2. The CH_2Cl_2 extracts were combined, washed with saturated $NaCl/H_2O$ (80 mL), dried over $MgSO_4$, and concentrated under reduced pressure to yield a colourless oil (0.717 g; 94% yield). The product mixture was analyzed by g.c and the ratio of **37**:**38**:**39**:**40**:**41** was found to be 2:3:42:34:18. The products were separated by column chromatography in which a 3 cm x 80 cm column contain 150 g of 60-200 mesh silica gel packed in 3:7 diethyl ether:hexanes was used. The column was eluted with 1 L of a 3:7 diethyl ether: hexanes solution and 1.5 L of a 4:6 diethyl ether: hexanes solution to yield the following fractions: I, 0.020 g of **37** and **38** (4:6); II. 0.041 g of **39**; III, 0.220 g of **39** and **40** (6:4); IV, 0.278 g of **39**, **40**, and **41** (1:1.2:1); V, 0.063 g of **41**. All fractions were collected as colourless oils.

Characterisation of fraction I (37 and 38). ^{1}H nmr (300 MHz, in $CDCl_3$): δ 5.15 (brd. s., exchanged in D_2O), 5.02 (dd, J=6.4 Hz, J=4.0 Hz), 4.56 (dd, J=5.5 Hz, J=3.3 Hz), 3.30 (brd. quartet, J=6 to 7 Hz), 3.09 (brd. quartet, J=5 to 7 Hz), remaining signals complex. ^{13}C nmr (300 MHz, in $CDCl_3$): δ 180.6 (C=O), 105.5 (CH), 86.0 (CH), 85.5 (CH), 47.7 (CH), 44.3 (CH), 40.8 (CH), 36.1 (CH), 36.0 (CH_2), 35.6 (CH), 34.5 (CH_2), 33.3 (CH), 32.7 (CH_2), 31.3 (CH_2), 31.2 (CH_2), 30.6 (CH_2). IR (neat film, cm^{-1}): 3510(brd), 1770(vs, C=O), 1003(s), 2934(s), 1169(s), 1046, 1088, 1204. Mass spectrum for **38** (EI, 70 eV): m/e(%) 138(20), 110(4), 109(5), 95(5), 93(7), 91(6), 84(40), 83(19), 82(14), 81(15), 79(46), 77(15), 67(42), 66(100), 55(48); calculated M^+ for $C_8H_{10}O_2$ 138.06811 (found 138.0686). Mass spectrum for **38** (CI, isobutane): m/e(%) M+1 139(100), 138(6), 113(11), 93(6), 84(16), 79(22), 67(64), 66(49). Mass spectrum for **37** (EI, 70 eV): m/e(%) 140(2), 123(1), 112(1), 111(1), 94(10), 84(4), 83(14), 79(38), 67(20), 66(100); calculated M^+ for $C_8H_{12}O_2$ 140.0837 (found 140.0840). Mass spectrum for **37** (CI, isobutane): m/e(%) M+1 141(10), 123(91), 94(15), 83(14), 79(38), 67(35), 66(100).

Characterisation of 39. ^{1}H nmr (300 MHz, in $CDCl_3$): δ 1.4 to 2.1 (complex, 5H), 2.27 (brd. s., 1H), 2.45 to 2.65 (complex, 2H), 2.84 (brd. quartet, J=6 to 7 Hz, 1H), 3.09 (dt, J=9.3 Hz, J=6.0 Hz, 1H), 3.64 (s, 3H), 4.21 (dt, J=10.2 Hz, J=6.8, 1H). ^{13}C nmr (300 MHz, in $CDCl_3$): δ 176.6 (C=O), 74.0 (CH), 51.8 (OCH_3), 45.0 (CH), 33.6 (CH), 32.7 (CH), 31.4 (CH_2), 29.3 (CH_2), 27.7 (CH_2). IR (neat film, cm^{-1}): 3428(brd), 1732(vs, C=O), 1173, 2952, 1076, 1267, 1437, 1236, 1362. Mass spectrum (EI, 70 eV): m/e(%) 170(7), 152(%), 139(18), 138(28), 127(18), 115(11), 111(15), 96(20), 87(63), 84(33), 83(71), 82(16), 81(24), 67(34), 55(100); calculated M^+ for

$C_9H_{14}O_3$ 170.09430 (found 170.0939).

Characterisation of 40 in fraction III. ^{13}C nmr (300 MHz, in $CDCl_3$): δ 176.4 (C=O), 73.9 (CH), 51.5 (OCH_3), 40.9 (CH), 40.5 (CH), 37.5 (CH), 31.3 (CH_2), 28.9 (CH_2), 18.8 (CH_2). Mass spectrum of **40** (EI, 70 eV): m/e(%) 170(2), 152(4), 139(16), 138(12), 114(13), 113(11), 109(13), 110(15), 93(23), 87(80), 84(66), 83(76), 82(27), 81(26), 67(38), 66(56), 55(100).

Characterisation of 41. ^1H nmr (300 MHz, in $CDCl_3$): δ 1.3 to 2.0 (complex, 5H), 2.36 (ddd, J=6.5 Hz, J=8.8 Hz, J=15.4 Hz, 1H), 2.39 (brd. s., 1H), 2.71 (d. of quartets, J=9.0 Hz, J=6.7 Hz, 1H), 2.90 (brd. quartet, J=7 to 9 Hz, 1H), 3.32 (dt, J=8.9 Hz, J=10.0 Hz, 1H), 3.64 (s, 3H), 4.12 (dt, J=9.6 Hz, J=6.9 Hz, 1H). ^{13}C nmr (300 MHz, in $CDCl_3$): δ 173.7 (C=O), 74.7 (CH), 51.2 (CH), 39.2 (CH), 38.1 (CH), 37.6 (CH), 32.2 (CH_2), 25.4 (CH_2), 18.6 (CH_2). IR (neat film, cm^{-1}): 1733(vs, C=O), 3420 (brd), 1170, 2950, 1075. Mass spectrum (CI, isobutane): m/e(%) M+1 171(23), 154(8), 153(80), 139(63), 110(18), 94(12), 93(20), 87(100), 84(20), 83(30), 82(26), 81(18), 67(68), 66(70).

7.2.5 Small scale reduction of 33, 34, 35 and 36 with sodium borohydride.

A solution of the pure cycloadduct or mixture of cycloadducts (0.050 g) dissolved in methanol (7 mL) was chilled to 0°C in an ice bath. Sodium borohydride (0.013 g) was added to the solution and the mixture was stirred for 1.3 hours. Potassium dihydrogen phosphate (0.1 g) was added to the reaction mixture followed by 20 mL of water. The aqueous layer was extracted with 3x30 mL of CH_2Cl_2. The combined extracts were dried over $MgSO_4$ and concentrated to 10 mL under reduced pressure. The

resulting concentrate was analyzed by g.c. and the products of the concentrate were identified by g.c. co-injection with the products isolated from the large scale reduction of the cycloadduct mixture. The following were determined: 1. A 25:75 mixture of **33**:**35** reduced to a 10:15:75 mixture of **37**:**38**:**40**; 2. Pure **34** reduced to compound **39**; 3. Compound **35** reduced to compound **40**; 4. Compound **36** reduced to compound **41**.

7.2.6 Preparation of Al_2Se_3.

Aluminum selenide was prepared according to the method of Waitkins and Sutt[2] with the following modifications. Finely ground aluminum powder (6 g; 0.222 mol) and finely ground grey selenium powder (10 g; 0.127 mol) were thoroughly mixed. Approximately 2 g of this mixture was placed in a dry crucible and ignited with a burning magnesium strip. Once ignited, additional 2 g quantities of the aluminum/selenium mixture were added to the crucible at 5 second intervals. CAUTION: THIS IS A VERY EXOTHERMIC REACTION. After the crucible had been allowed to cool, the solid Al_2Se_3 pellet was removed and ground with a mortar and pestle into a course powder. The Al_2Se_3 was stored in a desiccator until needed.

7.2.7 Irradiation of 2-cyclopentenone and 1,1-difluoroethene in the presence of H_2Se.

CAUTION: Al_2Se_3 REACTS VIOLENTLY WITH H_2O TO PRODUCE H_2Se. HYDROGEN SELENIDE IS AN EXTREMELY TOXIC GAS.

In a 100 mL two-neck round bottom flask that was fitted with a gas outlet and dropping funnel was placed 5 g of aluminum selenide. The gas outlet was attached to

a constricted pipet which was inserted into another 100 mL two-neck round bottom flask containing 50 mL of acetonitrile. After the entire system was flushed with nitrogen, 20 mL of water was added to the aluminum selenide dropwise over 20 minutes. The addition of water to the aluminum selenide was regulated so that the rate of evolution of H_2Se gas in the acetonitrile solution (solution A) was constant. Four irradiation tubes were filled with the following solutions: I. 5 mg of decane, 33 mg of 2-cyclopentenone, 10 mL of solution A; II. same as I; III. 5 mg of decane, 33 mg of 2-cyclopentenone, 5 mL of solution A, 5 mL of acetonitrile; IV. 5mg of decane, 33 mg of 2-cyclopentenone, 1.5 mL of solution A, 8.5 mL of acetonitrile. (The decane was used as a g.c internal standard). All four solutions were then chilled in a NaCl/ice bath at -10°C while 1,1-difluoroethene was bubbled into each solution through a frit. Solutions I, III, and IV were warmed to room temperature and then irradiated with Pyrex filtered light from a 450 watt Hanovia medium pressure mercury lamp for 30 minutes. Solution II was warmed to room temperature and kept dark for 30 minutes. All four solutions were analyzed by g.c. to determine the relative ratio of their components (excluding the 1,1-difluoroethene): I, 11.6% cyclopentanone, 76.0% 2-cyclopentenone, 1.7% **31**, 0.6% **32**, 10.2% of two enone dimers (1.2:1); II, only 2-cyclopentenone detected; III, 24.0% cyclopentanone, 72.1% 2-cyclopentenone, 0.5% **31**, 0.2% **32**, 3.1% of two enone dimers (1:1); IV, 27.3% cyclopentanone, 71.3% 2-cyclopentenone, 0.0% **31**, 0.0% **32**, 1.4% of two enone dimers (1:1). No evidence of trapped enone dimer biradicals or trapped enone plus alkene biradicals was detected by g.c./m.s.

a constricted pipet which was inserted into another 100 mL two-neck round bottom flask containing 50 mL of acetonitrile. After the entire system was flushed with nitrogen, 20 mL of water was added to the aluminum selenide dropwise over 20 minutes. The addition of water to the aluminum selenide was regulated so that the rate of evolution of H_2Se gas in the acetonitrile solution (solution A) was constant. Four irradiation tubes were filled with the following solutions: I. 5 mg of decane, 33 mg of 2-cyclopentenone, 10 mL of solution A; II. same as I; III. 5 mg of decane, 33 mg of 2-cyclopentenone, 5 mL of solution A, 5 mL of acetonitrile; IV. 5mg of decane, 33 mg of 2-cyclopentenone, 1.5 mL of solution A, 8.5 mL of acetonitrile. (The decane was used as a g.c internal standard). All four solutions were then chilled in a NaCl/ice bath at -10°C while 1,1-difluoroethene was bubbled into each solution through a frit. Solutions I, III, and IV were warmed to room temperature and then irradiated with Pyrex filtered light from a 450 watt Hanovia medium pressure mercury lamp for 30 minutes. Solution II was warmed to room temperature and kept dark for 30 minutes. All four solutions were analyzed by g.c. to determine the relative ratio of their components (excluding the 1,1-difluoroethene): I, 11.6% cyclopentanone, 76.0% 2-cyclopentenone, 1.7% **31**, 0.6% **32**, 10.2% of two enone dimers (1.2:1); II, only 2-cyclopentenone detected; III, 24.0% cyclopentanone, 72.1% 2-cyclopentenone, 0.5% **31**, 0.2% **32**, 3.1% of two enone dimers (1:1); IV, 27.3% cyclopentanone, 71.3% 2-cyclopentenone, 0.0% **31**, 0.0% **32**, 1.4% of two enone dimers (1:1). No evidence of trapped enone dimer biradicals or trapped enone plus alkene biradicals was detected by g.c./m.s.

7.2.8 Irradiation of 2-cyclopentenone and methyl acrylate in the presence of H_2Se.

A solution of cyclopentenone (2.132 g; 0.200 mole/L) and methyl acrylate (11.19; 1.00 mole/L) dissolved in toluene (130 mL) was chilled to -20°C in a $CaCl_2$/ice bath. The solution was saturated with H_2Se at -20°C by bubbling the gas through a constricted pipet. Hydrogen selenide was produced from the reaction of Al_2Se_3 and water (see method descibed above). The solution was irradiated with Pyrex filtered light emanating from a 400 W Hanovia medium pressure mercury lamp for 7 hours. The ratio of products **(42+43):(44+45):46** was determined to be 5:45:50 by g.c. after 1 hour of irradiation (approximately 6% of enone converted to products). After 7 hours of irradiation g.c. analysis of the solution revealed that 21% of the 2-cyclopentenone was converted to trapped products, 26% was converted to cyclopentanone, and 53% remained unreacted. The reaction mixture was concentrated under reduced pressure with heating to a volume of 5 mL. The concentrate was subjected to column chromatography in which a 3x80 cm column containing 160 g of 60-200 mesh silica gel packed in 1:4 diethyl ether: hexanes was used. The column was eluted with 1:4 diethyl ether: hexanes to yield the following fractions: I, 0.538 g of cyclopentanone (faint yellow oil); II, 0.241 g of **100** and **101** (red oil); III, 0.181 g of **102** (red oil); IV, 0.045 g of **(42+43)** approximately 80% pure with other unidentified dark reaction products (faint reddish brown oil); V, 0.419 g of 2-cyclopentenone:**(44+45):46** in the ratio 1:2:7 (yellow oil); VI, 0.807 g of 2-cyclopentenone:**(44+45):46** in the ratio 44:38:18 (yellow oil); VII, 0.776 g of 2-cyclopentenone (yellow oil).

Mass balance. Amount of cyclopentenone reclaimed in fractions: 1.174 g. Amount of cyclopentanone isolated: 0.538 g. Total amount of trapped products

(MM=170) isolated: 0.874 g. Mass of 2-cyclopentenone converted into trapped products: 0.421 g. Mass 2-cyclopentenone converted to cyclopentanone: 0.525 g. Total amount of 2-cyclopentenone reclaimed in the form of cyclopentanone, trapped products (MM=170), and 2-cyclopentenone: 2.123 g (99% recovery).

Purification of column fractions. Fraction IV was purified using preparative g.c. to yield fraction IVa which contained only **42** and **43** in a 1:1 ratio. Fraction V was purified by preparative g.c. to yield three fractions: Va, 2-cyclopentenone; Vb, **44** and **45** in a 1:1 ratio; Vc, **46** 95% pure with traces of **44** and **45**. All of these fractions were collected as colourless oils.

Characterisation of a 1:1 mixture of 42 and 43 (fraction IVa). ^{1}H nmr (300 MHz, in $CDCl_3$): δ 1.085 (d, J=7.2 Hz, 3H), 1.237 (d, J=7.3 Hz, 3H), 1.6 to 2.4 (complex, 13H), 2.54 (dddd, J=1.2 Hz, J=5.6 Hz, J=8.1 Hz, J= 12.0 Hz, 1H), 2.80 (d. of quartets, J=5.8 Hz, J=7.1 Hz, 1H), 3.03 (d. of quartets, J=4.4 Hz, J=7.3 Hz, 1H), 3.63 (s, 3H), 3.68 (s, 3H). ^{1}H nmr (300, in C_6D_6): δ 1.00 (d, J=7.2 Hz, 3H), 1.07 (d, J=7.3 Hz, 3H), 1.1 to 1.7 complex, 1.75 (ddd, J=4.5 Hz, J=8.2 Hz, J=11.2 Hz, 1H), 1.8 to 2.0 complex, 2.28 (dddd, J=1.2 Hz, J=5.8 Hz, J= 8.1 Hz, J=12.0 Hz, 1H), 2.76 (d. of quartets, J=5.8 Hz, J=7.1 Hz, 1H), 2.95 (d. of quartets, J=4.4 Hz, J=7.3 Hz, 1H), 3.24 (s, 3H), 3.38 (s, 3H). ^{13}C nmr (300 MHz, in $CDCl_3$): δ 51.7 (OCH_3, 2 isochronous signals), 51.54 (CH), 51.47 (CH), 39.1 (CH), 38.8 (CH), 38.1 (CH_2, 2 isochronous signals), 26.1 (CH_2), 25.9 (CH_2), 20.6 (CH_2), 20.5 (CH_2), 15.2 (CH_3), 13.7 (CH_3), due to the very low concentration of the sample the carbonyl peaks were not identified. IR (neat film, cm^{-1}): 1732 (vs, C=O). Mass spectrum for **42** (EI, 70 eV): m/e(%) 170(22), 139(22), 138(18), 127(14), 111(50), 110(28), 88(21), 84(33),

83(50), 74(71), 59(100); calculated M^+ for $C_9H_{14}O_3$ 170.0943 (found 170.0944). Mass spectrum for **43** (EI, 70 eV): exactly the same fragmentation as **42**, M^+ found 170.0943.

Characterisation of a 1:1 mixture of 44 and 45 (fraction Vb). ^1H nmr (300 MHz, in $CDCl_3$): δ 1.17 (d, J=6.6 Hz, 3H), 1.20 (d, J=6.6 Hz, 3H), 1.4 to 2.5 complex, 3.65 (s, 3H), 3.68 (s, 3H). ^{13}C nmr (300 MHz, in $CDCl_3$): δ 218.1 (C=O), 218.0 (C=O), 175.9 (C=O), 175.8 (C=O), 51.7 (OCH_3, two isochronous signals), 44.5 (CH), 44.4 (CH), 43.4 (CH_2), 42.7 (CH_2), 40.3 (CH), 40.0 (CH), 38.6 (CH_2), 38.5 (CH_2), 27.7 (CH_2), 27.2 (CH_2), 15.9 (CH_3), 15.1 (CH_3). Mass spectrum of **44** (EI, 70 eV): m/e(%) 170(2), 139(6), 113(11), 111(15), 97(16), 88(63), 83(100), 82(17), 69(12), 55(64); calculated M^+ for $C_9H_{14}O_3$ 170.0943 (found 170.0945). Mass spectrum for **45** (EI, 70 eV): exactly the same fragmentation as **44**, M^+ found 170.0946.

Characterisation of 46. ^1H nmr (300 MHz, in $CDCl_3$): δ 1.40 to 2.34 complex, 2.38 (t, J=7.3 Hz, 2H), 3.62 (s, 3H). ^1H nmr (300 MHz, in C_6D_6): δ 0.83 to 0.98 (m, 1H), 1.02 to 1.20 (m, 1H), 1.3 to 1.44 (m, 1H), 1.47 (ddd, J=6.7 Hz, J=7.7 Hz, J=13.5 Hz, 1H), 1.54 to 1.68 (complex, 3H), 1.84 (dddd J=18.8 Hz, J=8.7 Hz, J=2.8 Hz, J=1.4 Hz, 1H), 1.99 (ddt, J=5.4 Hz, J=13.5 Hz, J=7.6 Hz, 1H), 2.20 (t, J=7.7 Hz with second order effects, 2H), 3.34 (s, 3H). ^{13}C nmr (300 MHz, in $CDCl_3$): δ 219.9 (C=O), 173.5 (C=O), 51.4 (OCH_3), 48.2 (CH), 37.9 (CH_2), 31.9 (CH_2), 29.5 (CH_2), 25.0 (CH_2), 20.6 (CH_2). Mass spectrum (EI, 70 eV): m/e(%) 170(14), 139(42), 138(100), 111(11), 110(40), 97(19), 84(16), 83(24), 82(24), 74(20), 59(28), 55(78); calculated M^+ for $C_9H_{14}O_3$ 170.0943 (found 170.0940).

Characterisation of a 1:1 mixture of 100 and 101 (fraction II). ^1H nmr (200 MHz, in $CDCl_3$): δ 1.42 (d, J=7.2 Hz, 3H), 1.49 (d, J=7.2 Hz, 3H), 3.60 to 3.75

(two over-lapping quartets, J=7.2 Hz), 3.61 (s, 3H), 3.63 (s, 3H). ^{13}C nmr (200 MHz, in $CDCl_3$): δ 173.8 (C=O), 173.6 (C=O), 51.9 (OCH_3), 33.7 (CH), 33.4 (CH), 17.9 (CH_3), 17.2 (CH_3). Mass spectrum for **54** (EI, 70 eV): m/e(%) for ions containing ^{80}Se 254(10), 222(15), 195(10), 135(30); m/e(%) for ions containing no Se 88(90), 59(100). Mass spectrum for **55** (EI, 70 eV): exactly the same fragmentation as **54**.

Characterisation of 102 (fraction III). ^{1}H nmr (200 MHz, in $CDCl_3$): δ 1.47 (d, J=7.1 Hz, 3H), 2.65 to 3.05 complex, 3.64 (s, 3H), 3.67 (s, 3H), methine proton under methoxy signals. ^{13}C nmr (300 MHz, in $CDCl_3$): δ 174 (C=O), 172.4 (C=O), 52.1 (OCH_3), 51.7 (OCH_3), 35.0 (CH_2), 31.9 (CH), 18.2 (CH_2), 17.3 (CH_3). Mass spectrum for (EI, 70 eV): m/e(%) for ions containing ^{80}Se 254(36), 222(36), 195(14), 135(26); m/e(%) for ions containing no Se: 88(100), 59(100).

7.2.9 Synthesis of compound 47.

Bicyclo[3.3.0]octa-2,8-dione[3] (0.132 g; 0.953 mmol) was added to 50 mL of 0.50 mole/L H_2SO_4 in methanol and the reaction mixture was heated under gentle reflux for 4 hours. The mixture was allowed to cool to room temperature, diluted with 200 mL of diethyl ether, neutralised by slowly adding solid Na_2CO_3 (6 g), and then washed with water (2x100 mL). The ether extracts were washed with saturated NaCl/water (1x100 mL), dried over $MgSO_4$, and concentrated under reduced pressure to yield a yellow oil. The oil was dissolved in 1 mL of diethyl ether and this solution was added to a column (0.5 x 9.0 cm) containing 2 g of silica gel in diethyl ether. The column was eluted with 12 mL of diethyl ether. The elutant was concentrated under reduced pressure to yield pure **47** (0.130 g; 0.765 mmol; 80%) as a colourless oil.

Characterisation of 47. ^{1}H nmr (300 MHz, in $CDCL_3$): δ 1.36 to 1.50 (m, 1H), 1.64 to 1.76 complex, 1.98 to 2.34 complex, 2.28 (t, J=7.3 Hz, 2H), 3.58 (s, 3H). ^{13}C nmr (300 MHz, in $CDCl_3$): δ 218.0 (C=O), 173.3 (C=O), 51.3 (OCH_3), 44.6 (CH_2), 38.1 (CH_2), 36.4 (CH), 32.2 (CH_2), 30.4 (CH_2), 29.0 (CH_2). Mass spectrum (EI, 70 eV): m/e(%) 170(5), 152(5), 139(21), 110(6), 97(21), 96(67), 84(10), 83(100), 32(25), 74(39), 67(13); calculated M^+ for $C_9H_{14}O_3$ 170.0943 (found 170.0941).

7.3 Experimental for Chapter 3

7.3.1 General Experimental Details for Chapter 3

The 2-methylpropene (99%), 2-methylcyclopentenone (95%), and 3-methylcyclopentenone (97%) were obtained from the Aldrich Chemical Company. The two methylated enones were both distilled under reduced pressure prior to use. The 2-methylpropene was distilled into a dry ice condensor.

7.3.2 Irradiation of 2-cyclopentenone with 2-methylpropene.

A solution of cyclopentenone (2.42 g; 0.118 M) and 2-methylpropene (25 g; 1.78 M) in benzene (250 mL) was prepared. Addition of the 2-methylpropene was accomplished by condensing the alkene on a dry-ice/acetone cold finger and allowing the condensate to drip into the preweighed, stirred benzene solution. The solution was transferred to an immersion well photochemical reactor and irradiated for 3.75 hours

with a 450 W Hanovia medium pressure mercury lamp fitted with a Pyrex filter and water cooling jacket. The relative product yields for **54**, **55**, **56**, and **57** were determined by g.c. at 5% conversion of cyclopentenone to be 2.9%, 69.5%, 18.6%, 9.1% respectively. After the 3.75 hour irradiation period, g.c. analyses rrevealed that 47% of the cyclopentenone was converted to cycloadducts. The solvent was removed under reduced pressure and the remaining concentrate (3.21 g) was separated into its components by silica gel column chromatography (190g 60-200 mesh silica gel, 95:5 (v/v) hexanes:diethyl ether solvent). The following fractions were obtained and analysed by g.c.: I, 0.0503 g of **54** and **56** (2:1); II, 0.303 g of **54**, **55** and **56** (1:1:7); III, 1.23 g of **55** and **56** (7:1); IV, 0.352 g of **55** and **57** (1:1). After collecting the 4 fractions described above, the column was flushed with methanol to yield 1.28 g of cyclopentenone.

Compounds **55** and **56** were purified further by performing thin layer chromatography on fractions II and III. After TLC, compounds **55** and **56** were obtained about in 90% and 85% purity. Purification of fractions **54** and **57** was unsuccessful. Spectral data for compounds **54** and **57** were deduced by subtracting the spectra of relatively pure **55** and **56** from the spectra obtained for fractions I and IV.

Characterisation of 54. ^{1}H nmr (300 MHz, in $CDCl_3$): δ 1.65 (dt, J=1.5 Hz, J=0.75 Hz, 3H), 1.7 to 2.5 (complex), 4.65 (mult., 1H), 4.72 (mult., 1H). ^{13}C nmr (75 MHz, in $CDCl_3$): δ 220.9 (C=O), 143.4 (C), 111.6 (CH_2), 47.3 (CH), 38.0 (CH_2, 2 signals), 29.3 (CH_2), 20.5 (CH_2), 21.9 (CH_3). Mass spectrum (EI, 70 eV): m/e(%) 138(40), 123(10), 110(15), 95(30), 82(100); calculated M^+ for $C_9H_{14}O$ 138.1045 (found 138.1049).

Characterisation of 55. ^{1}H nmr (300 MHz, in $CDCl_3$): δ 0.99 (s, 3H), 1.15 (s, 3H), 1.68 (dd, J=12.5 Hz, J=5.9 Hz, 1H, assigned Hc), 1.9 to 2.1 (mult. partially overlapping Hb, 2H, assigned He), 2.09 (ddd, J=1.8 Hz, J=12.5 Hz, J=10.7 Hz, 1H, assigned Hb), 2.18 to 2.32 (mult., 1H, assigned to one proton at Hf), 2.44 to 2.75 (complex, 3H, assigned to Hd, Ha and one Hf). In a lanthanide induced chemical shift ^{1}H nmr study, Hd was shifted away from the Hf and Ha protons and was observed as a doublet, J=1.8 Hz, of quartets J=6$\pm$1 Hz. ^{13}C nmr (75 MHz, in $CDCl_3$): δ 222.6 (C=O), 44.2 (CH), 39.3 (CH), 37.5 (CH_2) 37.4 (CH_2), 35.0 (C), 31.4 (CH_3), 24.3 (CH_3), 21.9 (CH_2). Mass spectrum (EI, 70 eV): m/e(%) 138(4), 123(8), 109(2), 95(12), 83(100); calculated M^+ for $C_9H_{14}O$ 138.1045 (found 138.1048).

Characterisation of 56. ^{1}H nmr (300 MHz, in $CDCl_3$): δ 0.89 (s, 3H), 1.21 (s, 3H), 1.69 (dd, J=7.3 Hz, J=12.3 Hz, 1H, assigned Hb or Hc), 1.8 to 2.4 (complex, 5H), 2.50 (ddd, J=19 Hz, J=9.2 Hz, J=12.2 Hz, 1H, assigned to one H at Hf), 2.94 (quintet, J=7.5 Hz, 1H, assigned Hd). In a lanthanide induced chemical shift ^{1}H nmr study the following additional resonance was resolved: a doublet with J=7$\pm$1 Hz, assigned Ha. ^{13}C nmr (75 MHz, in $CDCl_3$): δ 221.6 (C=O), 55.4 (CH), 38.7 (CH_2), 37.9 (CH_2), 34.7 (C), 31.2 (CH_3), 29.9 (CH), 27.4 (CH_2), 25.1 (CH_3). Mass spectrum (EI, 70 eV): m/e(%) 138(2), 109(4), 95(2), 83(100); calculated M^+ for $C_9H_{14}O$ 138.1045 (found 138.1041).

Characterisation of 57. ^{1}H nmr (300 MHz, in $CDCl_3$): δ 1.64 (brd. s., 3H), 1.7 to 2.4 (complex), 4.61 (mult., 1H), 4.67 (mult., 1H). ^{13}C mnr (75 MHz, in $CDCl_3$): δ 219.3 (C=O), 143.5 (C), 111.5 (CH_2), 44.8 (CH_2), 43.7 (CH_2), 38.0 (CH_2), 34.7 (CH), 29.0 (CH_2), 22.2 (CH_3). Mass spectrum (EI, 70 eV): m/e(%) 138(2), 123(3),

109(3), 95(8), 83(75), 82(35), 55(100); calculated M^+ for $C_9H_{14}O$ 138.1045 (found 138.1042).

7.3.3 Irradiation of 2-methylcyclopentenone with 2-methylpropene.

A solution of 2-methylcyclopentenone (2.017 g; 0.100 M) and 2-methylpropene (19.1 g; 1.62 M) in benzene (210 mL) was prepared. The alkene was added to the solution in the same way as was described for the irradiation of cyclopentenone with 2-methylpropene. The solution was transferred to an immersion well photochemical reactor and irradiated with a 450 W Hanovia medium pressure mercury lamp which was fitted with a Pyrex filter and water cooling jacket. The reaction mixture was analysed frequently by g.c. The relative product yields determined at 3% conversion of the enone were 7.3%, 46.0%, 5.2%, 28.9%, 3.4%, and 9.3% for products **60**, **61**, **62**, **63**, **64**, and **65** respectively. Compounds **58** and **59** began to appear at later irradiation times. The growth of **58** and **59** mirrored depletion of products **60** and **61** relative to the other products. Analysis of the irradiated solution by g.c. indicated that 65% of the enone was converted to products after 20 hours. The relative product yields determined by g.c. at 65% conversion were 3.1%, 20.1%, 4.6%, 29.1%, 5.2%, 27.2%, 3.2%, and 7.5% for **58**, **59**, **60**, **61**, **62**, **63**, **64**, and **65** respectively. After 20 hours of irradiation the solvent was removed under reduced pressure to yield a yellow oil (2.78 g). The yellow oil was separated into its components by silica gel column chromatography (160g 60-200 mesh silica gel, 97:3 (v/v) hexanes:diethyl ether solvent). The following fractions were recovered and analysed by g.c.: I, 0.418 g of **58** and **59** (1:7); II, 0.463 g of **58**, **59**, **60**, **61**, **62**, **64**, **65** (1:6:5:26:4:1:4); III, 1.073 g of **60**, **61**, **62**, **63**, **64** and **65**

(2:12:2:13:1:2); IV, 0.156 g of **61**, **63**, **64**, **65** (3:18:1:1). The column was flushed with methanol in order to elute the unreacted enone (0.700 g of 2-methylcyclopentenone was recovered).

Preparative g.c. was performed on fractions I, II, III. and IV. Separation of compounds **58** and **59** in fraction I was unsuccessful. Fraction II was separated into 4 fractions (all of which were oils): IIa contained **58** and **59** (1:7); IIb contained **60**, **61** and **62** (1:7:1); IIc contained **64** and **65** (2:5); and IId also contained **64** and **65** (2:1). Fraction III was separated into 2 fractions (both of which were oils): IIIa contained **60**, **61** and **62** (3:29:1); IIIb contained **63**, **64**, and **65** (15:1:2). Fraction IV was separated into 2 fractions (both of which were oils): IVa contained **61**, **63**, **64** and **65** (1:5:1:2); IVb contained **63** with traces of **61**. Fraction IVb was used to obtain spectral data for **63**. Fraction IIIa was used to obtain nmr spectral data for **61**. The nmr spectral data for **64** and **65** were deduced from IIc and IId. Similarly, nmr spectral data were deduced for **60** and **62** from fractions IIb and IIIa by subtracting the signals due to **61**.

Characterisation of 58. ^{1}H nmr (300 MHz, in $CDCl_3$): δ 1.03 (s, 6H), 1.47 (tt, J=1.2 Hz, J=2.2 Hz, 3H), 9.74 (t, J=1.8 Hz, 1H), remaining protons obscured by 11 signals. ^{13}C nmr (75 MHz, in $CDCl_3$): δ 202.6 (HC=O), 146.0 (C), 132.9 (C), 43.2 (CH_2), 42.7 (CH_2), 40.7 (C), 24.5 (CH_3), 20.8 (CH_2), 18.9 (CH_3). Mass spectrum (EI, 70 eV): m/e(%) 152(16), 137(4), 123(10), 119(8), 110(100), 109(40), 95(80), 81(52), 67(48).

Characterisation of 59. ^{1}H nmr (300 MHz, in $CDCl_3$): δ 1.08 (s, 6H), 1.59 (quin., J=1.2 Hz, 3H), 2.00 (mult. 2H), 2.20 to 2.28 (t, J=7.5 Hz, of mult. J<1 Hz, 2H), 2.4 to 2.6 (t, J=7.5Hz, of mult. J<1 Hz, 2H), 9.75 (t, J=1.8 Hz, 1H). ^{13}C nmr

(75 MHz, in $CDCl_3$): δ 202.5 (HC=O), 145.7 (C), 133.5 (C), 45.5 (CH_2), 41.8 (CH_2), 41.3 (C), 25.4 (CH_3), 18.4 (CH_2), 14.0 (CH_3). Mass spectrum (EI, 70 eV): m/e(%) 152(42), 137(64), 119(34), 110(32), 109(66), 95(88), 93(100), 81(90), 67(94).

Characterisation of 60. ^1H nmr (200 MHz, in $CDCl_3$): δ 0.96 (s., 3H), 0.84 (s., 3H), 1.08 (s., 3H), remaining methine and methylene signals not identified due to overlapping signals of the other components of the mixture. ^{13}C nmr (75 MHz, in $CDCl_3$): δ 223.1 (C=O), 54.3 (C), 38.3 (CH), 38.1 (CH_2), 37.3 (CH_2), 35.6 (C), 26.5 (CH_3), 25.2 (CH_3), 25.0 (CH_2), 15.1 (CH_3). Mass spectrum (EI, 70 eV): m/e(%) 152(1), 137(0.8), 125(2), 123(3), 97(100), 69(15), 68(20), 67(20).

Characterisation of 61. ^1H nmr (200 MHz, in $CDCl_3$): δ 0.96 (s., 3H), 1.17 (s. 3H), 1.18 (s. 3H), 1.71 (AB with J_{AB}=12.5 Hz, $\Delta\nu_{AB}$=14.2 Hz or $\Delta\delta_{AB}$=0.071 ppm), 1.8 to 2.4 (complex, 4H), 2.59 (ddd, J=10 Hz, J=11 Hz, J=19 Hz, 1H). ^{13}C nmr (75 MHz, in $CDCl_3$): δ 223.8 (C=O), 49.9 (CH), 44.5 (CH_2), 42.6 (C), 37.1 (CH_2), 32.4 (CH_3), 31.6 (C), 24.6 (CH_3), 20.8 (CH_2), 20.5 (CH_3). Mass spectrum (EI, 70 eV): m/e(%) 152(5), 137(5), 109(5), 97(100), 69(12), 68(12), 67(12).

Characterisation 62. ^1H nmr (300 MHz, in $CDCl_3$): δ 0.97 (s., 3H), 1.64 (brd. s., 3H), methylene region complex due overlapping signals from other components of the mixture, 4.66 (brd. s., 1H), 4.80 (mult. J~1.5 Hz, 1H). ^{13}C nmr (75 MHz, in $CDCl_3$): δ 224.6 (C=O), 142.4 (C), 114.8 (CH_2), 48.4 (C), 44.6 (CH_2), 37.4 (CH_2), 35.3 (CH_2), 24.2 (CH_3), 22.7 (CH_3), 18.6 (CH_2). Mass spectrum (EI, 70 eV): m/e(%) 152(48), 137(12), 123(10), 110(5), 109(28), 96(52),97(50), 81(100), 67(18).

Characterisation of 63. ^1H nmr (300 MHz, in $CDCl_3$): δ 0.94 (d, J=6.7 Hz, 3H), 1.61 (brd. s., 3H), 1.7 to 2.3 complex, 4.61 (mult. J<1.0 Hz, 1H), 4.64 (mult.

J<1.0 Hz, 1H). ^{13}C nmr (75 MHz, in $CDCl_3$): δ 220.3 (C=O), 143.2 (C), 111.6 (CH_2), 50.0 (CH), 43.1 (CH_2), 42.3 (CH), 36.9 (CH_2), 27.0 (CH_2), 22.1 (CH_3), 12.5 (CH_3). Mass spectrum (EI, 70 eV): m/e(%) 152(1), 137(1), 123(2), 97(100), 81(25), 69(65).

Characterisation of 64. ^1H nmr (300 MHz, in $CDCl_3$): δ 0.91 (s., 9H), 5.34 (t, J=1.8 Hz, 1H), 6.12 (t, J=1.8 Hz, 1H), 1.2 to 2.6 complex. ^{13}C nmr (75 MHz, in $CDCl_3$): δ 208.3 (C=O), 146.8 (C), 120.2 (CH_2), 60.6 (CH), 36.8 (CH_2), 33.9 (C), 27.5 (CH_3), 21.7 (CH_2). Mass spectrum (EI, 70 eV): no parent ion peak, m/e(%) 137(10), 96(100), 57(90). Mass spectrum (CI, isobutane): m/e(%) 153(M+, 90), 137(30), 109(10), 97(75), 96(100), 95(35), 68(40), 67(60).

Characterisation of 65. ^1H nmr (300 MHz, in $CDCl_3$): δ 0.92 (d, J=6.6 Hz, 3H), 0.94 (d, J=6.6 Hz, 3H), 5.20 (dd, J=0.9 Hz, J=2.9 Hz, 1H), 5.98 (dd, J=0.9 Hz, J=2.6 Hz, 1H), 1.2 to 2.7 complex. ^{13}C nmr (75 MHz, in $CDCl_3$): δ 207.6 (C=O), 149.7 (C), 116.2 (CH_2), 43.6 (CH_2), 39.0 (CH), 37.2 (CH_2), 26.6 (CH_2), 25.4 (CH), 23.6 (CH_3), 21.8 (CH_3). Mass spectrum (EI, 70 eV): m/e(%) 152(2), 137(4), 110(20), 97(100), 96(30), 95(85), 81(40), 68(60), 67(40).

7.3.4 Irradiation of 3-methylcyclopentenone with 2-methylpropene.

A solution of 3-methylcyclopentenone (2.601 g) and 2-methylpropene (20 g) in benzene (270 mL) was prepared. The alkene was added to the solution in the same way as was described for the irradiation of cyclopentenone with 2-methylpropene. The solution was transferred to an immersion well photochemical reactor and irradiated with a 450W Hanovia medium pressure mercury lamp which was fitted with a Pyrex filter and

water cooling jacket. The reaction mixture was analysed frequently by g.c. The relative product yields determined at 5% conversion of the enone were 20.8%, 4.5%, 47.4%, and 27.3% for products **72**, **73**, **74**, and **75** respectively. Analysis of the irradiated solution by g.c. indicated that 69% of the enone was converted to products after 9 hours. After irradiation the solvent was removed under reduced pressure to yield a yellow oil (3.65 g). The yellow oil was separated into its components by silica gel column chromatography (160 g 60-200 mesh silica gel; 97:3 (v/v) hexanes:diethyl ether). The following fractions were recovered and analysed by g.c.: I, 0.019 g of **72** and **73** (1:4.6); II, 0.23 g of **72** and **73** (1.4:1); III, 0.39 g of **72**, **73**, **74**, and **75** (10:1.4:1.4:1), IV, 1.58 g of **72**, **74**, and **75** (1:3.5:2.2); V, 0.47 g of **74** and **75** (1.7:1); VI, 0.16 g of **74** and **75** (3:1). The column was flushed with methanol in order to elute the unreacted enone (0.78 g of 3-methylcyclopentenone was recovered).

Preparative g.c. was performed on fractions II, VI and V in order to obtain enriched samples of **72**, **73**, **75** and **74**. It was not possible to completely separate **75** from **74**. Using preparative g.c. fraction II was separated into 2 fractions: IIa contained **72** (with traces of **73**); and, IIb contained **73** (92% pure with **72** impurity). Fraction VI was separated into 2 fractions: VIa contained **74** (90% pure with a trace of **75**); and, VIb contained **74** and **75** (1:1.5). Fraction V was separated into 2 fractions: Va contained **74** and **75** (3:1); and, Vb contained **74** and **75** (1.2:1). All fractions were isolated as oils.

Characterisation 72. ^{1}H nmr (200 MHz, in $CDCl_3$): δ 0.90 (s., 3H), 1.25 (s., 3H), 1.32 (s., 3H), 1.5 to 1.8 (mult., 2H, assigned to the two Hd protons), 1.84 (ABX pattern with J_{AB}=12.5 Hz, $\Delta\nu_{AB}$=20.7 Hz, J_{AX}=0 Hz, J_{BX}=2.0 Hz, δ_A=1.89 ppm,

δ_B=1.79 ppm, B=Hb, A=Hc, X=Ha), 2.02 (brd. s., 1H, assigned Ha), 2.32 (ddt, J=18 Hz, J=8.9 Hz, J=1.9 Hz, 1H, assigned He or Hf), 2.52 (dddd, J=18 Hz, J=12 Hz, J=8.9 Hz, J=0.7 Hz, 1H, assigned He or Hf). ^{13}C nmr (50 MHz, in $CDCl_3$): δ 221.2 (C=O), 60.4 (CH), 45.1 (CH_2), 39.6 (CH_2), 36.6 (CH_2), 36.4 (C), 31.7 (CH_3), 31.6 (C), 27.9 (CH_3), 25.5 (CH_3). Mass spectrum (EI, 70 eV): m/e(%) 152(3), 137(1), 109(5), 97(100), 83(50), 67(8).

Characterisation of 73. ^{1}H nmr (300 MHz, in $CDCl_3$): δ 1.10 (d., J=6.1 Hz, 3H), 1.66 (brd. s., 3H), 1.6 to 2.5 (complex, 8H), 4.66 to 4.78 (mult., 2H). ^{13}C nmr δ (75 MHz, in $CDCl_3$): 220.9 (C=O), 143.5 (C), 112.4 (CH_2), 54.4 (CH), 37.7 (CH_2), 37.4 (CH), 37.1 (CH_2), 29.5 (CH_2), 22.3 (CH_3), 19.9 (CH_3). Mass spectrum (EI, 70 eV): m/e(%) 152(15), 137(20), 110(100), 109(30), 97(60), 96(62), 95(50), 81(50), 67(30).

Characterisation of 74 (nmr spectral data obtained from fractions Va, Vb, VI). ^{1}H nmr (300 MHz, in $CDCl_3$): δ 0.98 (s., 3H), 1.05 (s., 3H), 1.10 (s., 3H), 1.58 (ddd, J=5.6 Hz, J=10 Hz, J=14 Hz, 1H, assigned to one proton at Hd), 1.74 (dd, J=7.3 Hz, J=11.9 Hz, 1H, assigned to Hc), 2.00 (dd, J=10 Hz, J=11.9 Hz, 1H, assigned to Hb), 2.2 to 2.6 (Ha, Hc, Hf and one of Hd all overlapping; however, in the presence of $Eu(fod)_3$ the Hd proton was observed as a triplet of doublets, J=9.0 Hz, J=14 Hz). ^{13}C nmr (75 MHz, in $CDCl_3$): δ 221.6 (C=O), 48.0 (CH), 46.6 (C), 39.1 (CH_2), 37.3 (C), 35.9 (CH_2), 30.1 (CH_2), 26.5 (CH_3), 23.0 (CH_3), 21.0 (CH_3). Mass spectrum (EI, 70 eV): m/e(%) 152(very weak), 137(2), 119(1.5), 109(4), 97(100), 81(20), 67(20). Mass spectrum (CI, isobutane): m/e(%) 153(16), 137(2), 109(2), 97(100), 81(10), 67(10).

Characterisation of 75 (nmr spectral data obtained from fractions Va, Vb, VI). ^{1}H nmr (300 MHz, in $CDCl_3$): δ 1.03 (s., 3H), 1.75 (brd. s., 3H), 1.7 to 2.5 complex, 4.66 (d., J=2.3 Hz, of quart., J=0.87 Hz, 1H), 4.85 (d., J=2.3 Hz, of quart., J=1.5 Hz, 1H). ^{13}C nmr (75 MHz, in $CDCl_3$): δ 219.5 (C=O), 142.5 (C), 114.5 (CH_2), 52.5 (CH_2), 49.4 (CH_2), 39.6 (C), 36.5 (CH_2), 35.6 (CH_2), 25.2 (CH_3), 24.6 (CH_3). Mass spectrum (EI, 70 eV): m/e(%) 152(very weak), 137(2), 123(2), 109(3), 97(90), 96(30), 81(10), 69(100). Mass spectrum (CI, isobutane): m/e(%) 153(7), 137(4), 123(2), 109(4), 97(100), 81(12), 69(84).

7.3.5 Small Scale Irradiaton of 60 and 61.

Approximately 0.01 g of a mixture of **60**, **61** and **62** in a ratio of 3:29:1 was dissolved in 2 mL of benzene. To this solution was added 0.008 mg of decane (internal standard). The solution was then irradiated with the light from a 400 W Hanovia medium pressure mercury lamp fitted with a Pyrex filter and water cooling jacket. After 10 minutes of irradiation, the mixture was analysed by g.c. These analyses indicated that **58** and **59** were formed during the reaction. The ratio of **58**:**59**:**60**:**61**:**62** was 1.4:15:1.4:16:1.0 at 10 mins. After 15 minutes of irradiation the ratio of the same compounds was 2.1:20:1:9:1. The ratio of the combined g.c. peak area of compounds **58**, **59**, **60**, **61**, and **62** to the g.c. peak area of the internal stadard did not change during the 15 mintue irradiation. Therefore, it was concluded that no other products were formed. It was also concluded that compound **60** forms **58** upon photolysis and **61** forms **59**.

7.3.6 Method of Hydrogenation of Unsaturated Compounds.

An absolute ethanol solution (10 mL) containing approximately 0.01 g of 10% Pd on carbon catalyst was saturated with hydrogen gas. To this mixture, the the compound containing the alkene functionality (approximately 0.010 g) was added. Hydrogen gas was bubbled through the mixture for an additional 15 minutes during which time periodic g.c. analyses were performed in order monitor the growth of the saturated compound(s). The catalyst was removed by filtration and product analysis was accomplished by g.c. and coupled g.c.-m.s. This general method was applied to compounds **73**, **75**, **62**, **63**, **64**, and **65**. All mass balances were greater than 94%.

7.3.7 Method of Epimerization of Ketones.

The starting ketone (approximately 0.075 g) was dissolved in methanol (10 mL) containing NaOH (0.5 mol/L). The reaction mixture was gently heated under reflux for 20 minutes after which time 20ml of water was added. The mixture was extracted with diethyl ether (3x20 mL), washed with water (2x10 mL) and saturated NaCl/water (2x10ml) and dried over $MgSO_4$. The resulting ether solution was subjected to g.c. and g.c.-m.s. analysis and then concentrated under reduced pressure. This general method was applied to compounds **77**, **63**, **67**, **68**, **69**, and **70**. All mass balances were greater than 96%.

7.3.8 Epimerization and hydrogenation results for 73

Epimerization of **73** resulted in formation of a 6.9:1 mixture of **73** and **76**. Hydrogenation of this mixture resulted in a 6.8:1 mixture of **77** and **78**. Hydrogenation of **73** resulted in formation of **77**. Epimerization of **77** resulted in formation of a 6.3:1 mixture of **77** and **78**. Compound **76** mass spectrum (EI 70eV) was identical to that obtained for **73**. Compound **77** mass spectrum (EI, 70 eV): m/e(%) 154(8), 139(2), 125(5), 111(4), 97(100), 96(20), 83(10), 81(10), 69(20). Compound **78** mass spectrum (EI, 70 eV): m/e(%) 154(0.5), 123(1), 109(1), 97(100), 96(30), 81(14). 69(90).

7.3.9 Hydrogenation results for 75.

Hydrogenation of a 1.2:1 mixture of **74** and **75** resulted in the formation of a 1.2:1 mixture of **74** and **79**. Compound **79** mass spectrum (EI, 70 eV): m/e(%) 154(42), 139(10), 125(22), 111(18), 97(100), 96(70), 83(60), 69(80).

7.3.10 Hydrogenation results for 62.

Hydrogenation of a 1:7:1 mixture of **60**, **61** and **62** resulted in formation of a 1:7:1 mixture of **60**, **61** and **71**. Compound **71** mass spectrum (EI, 70 eV): parent ion not observed, m/e(%) 98(100), 83(20), 69(10). Compound **71** mass spectrum (CI, isobutane): m/e(%) 155(3), 111(2), 98(100), 83(15), 69(20).

7.3.11 Epimerization and hydrogenation results for 63.

Epimerization of **63** resulted in formation of a 12:1 mixture of **63** and **66**. Hydrogenation of this mixture resulted in a 12:1 mixture of **67** and **68**. Hydrogenation of **63** resulted in formation of **67**. Epimerization of **67** resulted in formation of a 13:1 mixture of **67** and **68**. Compound **66** mass spectrum (EI 70eV) was identical to that obtained for **63**. Compound **67** mass spectrum (EI 70eV) m/e(%) 154(50), 125(20), 111(18), 110(100), 97(55), 83(40), 69(60). Compound **68** mass spectrum (EI 70eV) was identical to that obtained for **67**.

7.3.12 Epimerization and hydrogenation results for a mixture of 64 and 65.

Hydrogenation of a 1:2.5 mixture of **64** and **65** resulted in the formation of a 2.8:1.0:1.4:3.0 mixture (g.c. ratio) of **67**, **69**, **70**, and **68** respectively. The ratio of **69** plus **70** to **67** plus **68** was determined to be 1:2.4 by g.c. Epimerization of this mixture of four compounds resulted in a mixture containing **67**, **69**, and **68** in a 12:5.5:1 ratio. The ratio of **69** to **67** plus **68** in the epimerized mixture was therefore determined to be 1:2.4. The identity of **67** and **68** was confirmed by g.c. co-injection with authentic samples obtained from the hydrogenation followed by epimerization of **63**. Compound **69** mass spectrum (EI, 70 eV): m/e(%) 154(20), 139(4), 111(4), 110(4), 98(40), 97(55), 83(28), 69(20), 57(100). Compound **70** mass spectrum (EI, 70 eV) was identical to that obtained for **69**.

Hydrogenation of a 2:1 mixture of **64** and **65** resulted in the formation of a 1:1.9:2.3:1.2 mixture of **67**, **69**, **70**, and **68** respectively. Epimerization of this mixture of four compounds resulted in a mixture containing **67**, **69**, and **68** in a 9:17:1 ratio.

7.3.13 Quantum yield measurements.

All quantum yields were determined at $\leq 6\%$ conversion of the enone using a PTI QUANTACOUNT instrument equipped with a high pressure 100 watt mercury lamp. The light flux was calibrated using an azoxybenzene actinometer.[4] The absolute amount of cycloadducts formed in each irradiation was determined by g.c. analysis using decane as an internal standard. Calibration curves were constructed for the g.c. FID detector using pure samples of cycloadducts. It was assumed that regio- and stereoisomers of the photo-cycloaddition products had the same g.c. FID response factor. The samples were degassed by three freeze-pump-thaw cycles after which the residual pressure in each cell was below 2×10^{-4} mbar. In each irradiation, benzene was the solvent and the excitation wavelength was fixed at 340 nm. The concentration of enone used in the cyclopentenone plus 2-methylpropene quantum yield determinations was 0.0401 mol/L. The concentration of enone used in the quantum yield determinations involving 2-methylcyclopentenone and 2-methylpropene was 0.0407 mol/L. The same concentration of enone was used in the quantum yield determinations involving 3-methylcyclopentenone and 2-methylpropene. The quantum yield measurements are summarised in Table 25 below.

Table 25: Quantum yields of product formation at various alkene concentrations for the photocycloaddition reactions of 2-methylpropene with each of 2-cyclopentenone, 2-methyl-2-cyclopentenone, and 3-methyl-2-cyclopentenone in benzene.

cyclopentenone (0.0401 M)		2-methylcyclopentenone (0.0407 M)		3-methylcyclopentenone (0.0407 M)	
[alkene] /M	Φ (±8%)	[alkene] /M	Φ (±12%)	[alkene] /M	Φ (±10%)
0.0803	0.0174	0.0848	0.00834	0.0800	0.0498
0.0944	0.0201	0.113	0.0122	0.115	0.0654
0.120	0.0249	0.204	0.0181	0.149	0.0800
0.171	0.0292	0.369	0.0263	0.244	0.0954
0.181	0.0337	0.725	0.0338	0.452	0.122
0.324	0.0443	1.266	0.0446	0.735	0.141
0.478	0.0609	2.525	0.0503	1.219	0.154
1.117	0.0814			2.557	0.160
1.973	0.0829				
2.401	0.0849				

7.3.14 Irradiation of 2-cyclopentenone and 2-methylpropene in the presence of H_2Se.

A solution of 2-cyclopentenone (2.05 g; 0.100 M) and 2-methylpropene (19.5 g; 1.39 M) in benzene (250 mL) was prepared. Addition of the alkene was accomplished by condensation of the alkene on a dry-ice/acetone cold finger and dissolution of the condensate in the benzene solution containing the enone. Aluminum selenide (5 g) was placed in a separate flask fitted with a gas outlet and dropping funnel. A pipet was connected to the gas outlet of the flask containing Al_2Se_3 and its tip was submerged into

the benzene solution. The benzene solution was chilled in ice water and the entire system was flushed with nitrogen. Distilled water was added to the flask containing Al_2Se_3 at an initial rate of 1 drop per 20 seconds via the dropping funnel. The hydrogen selenide gas liberated was allowed to pass through the gas outlet and bubble through the benzene solution. After the first few drops of water had been added to the Al_2Se_3 powder, the rate of addition was increased until all of the Al_2Se_3 was consumed. An aliquot of the benzene solution was analyzed by ^1H nmr spectroscopy to check the concentrations of the volatile components: $[H_2Se]=0.30$ M and [2-methylpropene] = 1.35 M. The benzene solution was placed in a quartz immersion-well reactor fitted with a water cooled lamp jacket. The solution was irradiated with a 450 W Hanovia medium pressure mercury lamp fitted with a Pyrex filter for 2 hours. Aliquots were withdrawn every 15 minutes and analyzed by g.c. The relative ratios of the recovered products were determined by g.c. at 5% conversion of cyclopentenone: **83**(0.40%), **80**(2.3%), **81**(15.3%), **54**(10.0%), **82**(7.5%), **84**(64.5%). Prolonged irradiation was not possible due to a build-up of elemental selenium on the lamp jacket. Subsequent g.c. analyses of similar irradiations carried out in the presence of a hydrocarbon standard (2-methylnonane) revealed that only 25% of the cyclopentenone was converted to trapped products under these conditions. An additional 30% of the cyclopentenone was converted to cyclopentanone while approximately 45% was left unreacted. No cyclopentanone nor products identified as trapped biradicals were observed in reaction mixtures containing cyclopentenone, 2-methylpropene, and H_2Se that were not exposed to U.V. light. Separation of the reaction mixture after removal of the benzene solvent was accomplished by silica gel column chromatography in which a stationary phase consisting 60-200 Mesh

silica gel and a mobile phase consisting to 97% hexanes and 3% diethyl ether (v/v) were employed. Chromatographic separation of the concentrate (2.53 g) resulted in the following fractions which were analyzed by g.c.: I, 0.012 g of **83** and **80** (1:1.5); II, 0.013 g of **83**, **80**, **81** (1:4:3.5); III, 0.041 g of **81** (with traces of other compounds); IV, 0.145 g of **81**, **54** and **84** (1.5:1:1.7); V, 0.554 g of **84** (with traces of **54** and **82**); VI, 0.100 g of **84** and **82** (3.5:1); VII, 0.0083 g of **84** and **82** (1:2). The nmr spectral data for **54** and **82** were deduced by subracting the spectra of the mixtures IV and VII from the spectra obtained for **81** and **84**. The nmr spectra of compound **54** obtained in the trapping reactions were identical to the spectra of the same compound isolated from the reaction mixture resulting from the photocycloaddition of 2-methylpropene and 2-cyclopentenone.

Characterisation of the mixture of 83 and 80 (1:1.5). ^{1}H nmr (200 MHz, in $CDCl_3$): δ 0.88 (d, J=6.5 Hz, 3H), 0.90 (d, J=6.5 Hz, 3H), 0.96 (singlet, 9H), 1.1 to 2.9 (complex), 6.07 (m, 2H). ^{13}C nmr (50 MHz, in $CDCl_3$): δ 220.5 (C=O), 219.7 (C=O), 133.6 (CH), 127.1 (CH), 57.9 (CH), 50.5 (CH), 42.4 (CH_2), 40.3 (CH_2), 39.9 (CH_2), 32.5 (C), 27.7 (CH_3, very intense), 26.4 (CH_2), 26.1 (CH), 23.2 (CH_3), 22.0 (CH_3), 20.2 (CH_2). Mass spectrum of **83** (EI, 70 eV): m/e(%) 140(15), 125(10), 97(10), 84(85), 78(100). Mass spectrum of **80** (EI, 70 eV): m/e(%) 138(4), 123(55), 110(12), 95(42), 82(100), 81(5). Hydrogenation of the 1:1.5 mixture of **83** and **80** resulted in a 1:1.5 mixture of **83** and **81** (see method of hydrogenation below).

Characterisation of 81. ^{1}H nmr (200 MHz, in $CDCl_3$): δ 0.87 (d, J=6.3Hz, 3H), 0.91 (d, J=6.3Hz, 3H), 1.4 to 2.4 (complex, 10H). ^{13}C nmr (50 MHz, in $CDCl_3$): δ 222.0 (C=O), 47.5 (CH), 38.9 (CH_2), 38.0 (CH_2), 30.1 (CH_2), 26.2 (CH), 23.3

(CH_3), 21.5 (CH_3), 20.8 (CH_2). Mass spectrum (EI, 70 eV) m/e(%) 140(6), 125(5) 83(5), 84(100).

Characterisation of 54 (data obtained from mixture described above). ^{1}H nmr (200 MHz, in $CDCl_3$): δ 1.65 (brd. s., 3H), 4.64 (multiplet, 1H), 4.70 (multiplet, 1H), remaining signals not identified due to overlap of **54**, **81** and **84** resonances. ^{13}C nmr (50 MHz, in $CDCl_3$): δ 220.8 (C=O), 143.3 (C), 111.5 (CH_2), 47.2 (CH), 37.9 (CH_2, 2 signals), 29.3 (CH_2), 20.5 (CH_2), (CH_3) 22.0. Mass spectrum (EI 70eV) m/e(%) 138(40), 123(10), 110(20), 95(30), 83(5), 82(100). It was also determined that **54** hydrogenates to **81**.

Characterisation of 84. ^{1}H nmr (200 MHz, in $CDCl_3$): δ 0.80 (d, J=6.6 Hz, 6H), 1.22 (t, J=6.8 Hz, 2H), 1.3 to 2.3 (complex, 8H). ^{13}C nmr (50 MHz, in $CDCl_3$): δ 219.5 (C=O), 45.2 (CH_2), 45.0 (CH_2), 38.3 (CH_2), 34.8 (CH), 29.6 (CH_2), 26.2 (CH), 22.7 (CH_3), 22.5 (CH_3). Mass spectrum (EI, 70 eV) m/e(%) 140(50), 125(16), 111(40), 96(62), 83(100).

Characterisation of 82 (data obtained from the mixture described above). ^{1}H nmr (200 MHz, in $CDCl_3$): δ 0.81 (d, J=6.6 Hz, 6H), 1.75 (sept., J=6.7 Hz, 2H), 1.99 (dd, J=6.8 Hz, J=1.4 Hz, 2H), 2.30 to 2.36 (mult., 2H), 2.48 to 2.56 (mult., 2H), 7.24 (tt., J=1.35Hz, J=2.5Hz, 1H). ^{13}C nmr (50 MHz, in $CDCl_3$): δ 209.9 (C=O), 158.3 (CH), 145.1 (C), 34.4 (CH_2), 33.8 (CH_2), 26.9 (CH), 26.3, 22.4 (CH_3). Mass spectrum (EI, 70 eV): m/e(%) 138(80), 123(60), 96(100), 95(40), 81(8), 82(8), 83(5). It was also determined that **82** hydrogenates to **81**.

7.3.15 Small scale irradiation of 2-methyl-2-cyclopentenone and 2-methylpropene in the presence of H_2Se.

A solution of 2-methylcyclopentenone (0.10 mol/L) and 2-methylpropene (2.08 mol/L) in benzene (10mL) was prepared. Addition of the alkene was accomplished by condensation of the alkene on a dry-ice/acetone cold finger and dissolution of the condensate in the benzene solution containing the enone. Hydrogen selenide gas was bubbled through this solution in exactly the same way as described above for the 2-cyclopentenone plus 2-methylpropene solution. An aliquot of the benzene solution was analyzed by ^1H nmr spectroscopy to check the concentrations of the volatile components: $[H_2Se]=0.30$ mol/L and [2-methylpropene]=2.0 mol/L. The benzene solution was placed in a Pyrex irradiation tube and irradiated with a 450 W Hanovia medium pressure mercury lamp fitted with a Pyrex filter for 3 hours. After 3 hours of irradiation only 4% of the 2-methylcyclopentenone was converted to trapped products; however, 55% of the 2-methylcyclopentenone was converted to 2-methylcyclopentanone. Prolonged irradiation was not possible due to a build-up of elemental selenium on the inside of the irradiation vessel. No 2-methylcyclopentanone nor products identified as trapped biradicals were observed in reaction mixtures containing 2-methylcyclopentenone, 2-methylpropene, and H_2Se that were not exposed to U.V. light. The following relative product yields were determined by g.c. after 3 hours of irradiation: 4.5%, 1.4%, 70.7%, 3.7%, and 19.7% for compounds **71**, **62**, **67**, **69**, and **68** respectively. The identity of these trapped products was determined by g.c. co-injections with authentic samples obtained from the reactions described above.

7.3.16 Small scale irradiation of 3-methyl-2-cyclopentenone and 2-methylpropene in the presence of H_2Se.

A solution of 2-methylcyclopentenone (0.11 mol/L) and 2-methylpropene (2.21 mol/L) in benzene (10mL) was prepared. Hydrogen selenide gas was bubbled through this solution in exactly the same way as described above for the 2-cyclopentenone plus 2-methylpropene solution. An aliquot of the benzene solution was analyzed by ^1H nmr spectroscopy to check the concentrations of the volatile components: $[H_2Se]=0.32$ mol/L and [2-methylpropene]=1.9 mol/L. The benzene solution was placed in a Pyrex irradiation tube and irradiated with a 450 W Hanovia medium pressure mercury lamp fitted with a Pyrex filter for 1 hour. After 1 hour of irradiation only 5% of the 3-methylcyclopentenone was converted to trapped products; however, 28% of the 3-methylcyclopentenone was converted to 3-methylcyclopentanone. Prolonged irradiation was not possible due to a build-up of elemental selenium on the inside of the irradiation vessel. No 3-methylcyclopentanone nor products identified as trapped biradicals was observed in reaction mixtures containing 3-methylcyclopentenone, 2-methylpropene, and H_2Se that were not exposed to U.V. light. The following relative product yields were determined by G.C after 1 hour of irradiation: 13.5%, 5.6%, 5.5%, 70.5%, and 4.9% for compounds **77**, **73**, **78**, **79**, and **76** respectively. The identity of these trapped products was determined by g.c. co-injections with authentic samples obtained from the reactions described above, and comparison of the mass spectra using g.c.-m.s.

7.4 Experimental details for Chapter 4.

7.4.1 General experimental details for Chapter 4.

The *trans*-2-butene (99%) and *cis*-2-butene (97%) were obtained from the Aldrich Chemical Company and the Phillips Petroleum Company and were used as received. The major impurity present in the *cis*-2-butene (2.5%) was shown to be *trans*-2-butene by g.c. co-injection with an authentic sample of *trans*-2-butene. It was determined that the small amount of *trans*-2-butene present in the *cis*-2-butene was insignificant in the kinetic analyses.

7.4.2 Irradiation of 2-cyclopentenone and *cis* or *trans*-2-butene

Liquid *cis*-2-butene (21 g; 1.5 mol/L) was added to a (250 mL) solution of cyclopentenone (2.05 g; 0.10 mol/L) in benzene. This addition was accomplished by condensing the butene on a dry-ice/acetone cold finger and allowing the condensate to drip into the stirred solution of cyclopentenone in benzene. The solution was added to an immersion well photochemical reactor and irradiated for four hours with light eminating from a 400 watt Hanovia medium pressure mercury lamp fitted with a Pyrex filter and water cooling jacket. Analysis of the reaction mixture by g.c. indicated that 82% of the cyclopentenone had been converted to cycloadducts. The solvent was removed under reduced pressure and the components of the remaining concentrate (3.25 g) were separated by silica-gel column chromatography in which a mobile phase consisting of 95:5 (v/v) hexanes:ether and a stationary phase consisting of 130g of 60-200 mesh silica-gel were used. The following fractions were collected and analyzed by

g.c.: I, 0.160 g of **114a** and **114d** (8:92); II, 0.140 g of **114a** and **114d** (55:45); III, 0.151 g of **114a**, **114b**, and **114d** (60:10:30); IV, 1.21 g of **114a**, **114b**, and **114d** (72:15:13); V, 1.18 g of **114a**, **114b**, and **114c** (5:90:5). The relative yields of the cycloadducts **114a**, **114b**, **114c**, and **114d** were determined by g.c. at 5% conversion of cyclopentenone. For addition of *cis*-2-butene the product ratios were 42.6%, 43.5%, 2.2%, and 11.7% respectively. For addition of *trans*-2-butene the product ratios were 50.2%, 28.5%, 2.1%, and 19.2% respectively.

Characterisation of 114a (fraction IV). ^{1}H nmr (in C_6D_6): δ 0.75 (d, J=7.2Hz, 3H, Me2), 0.88 (d, J=7.2Hz, 3H, Me1), 1.2 to 2.4 (complex, 8H). The following ^{1}H nmr resonances (300 MHz, in $CDCl_3$) were ressolved in the presence of $Eu(fod)_3$: (quin. of d., J=7.2 Hz, J=3.8 Hz, 1H, Hb), (quartet, J=6.8Hz, 1H, Hd), (sextet, J=7 Hz, Hc). ^{1}H nmr (300 MHz, in $CDCl_3$) decoupling results in the presence of $Eu(fod)_3$: Hb (quintet, J=7.2Hz, of d, J=3.8Hz) was decoupled to give a doublet (J=7.2Hz) of doublets (J=3.8Hz) by high power irradiation of Me1; Hd (quartet, J=6.8Hz) was unaffected by high power irradiation of Hb, Me1, or Me2; high power irradiation of Hc collapsed Hb to a quintet (J=7 Hz) and collapsed Hd to a triplet (J=7 Hz). ^{13}C nmr (75 MHz, in $CDCl_3$): δ 14.9 (CH_3), 15.8 (CH_3), 26.5 (CH_2), 34.1 (CH), 35.7 (CH), 37.5 (CH_2), 41.3 (CH), 50.6 (CH), 222.8 (C=O). Mass spectrum (EI, 70 eV): m/e(%) 138(20), 123(15), 109(15), 95(15), 83(22), 82(22), 81(30), 69(100); calculated M^+ for $C_9H_{14}O$ 138.1045 (found 138.1050).

Characterisation of 114b (fraction V). ^{1}H nmr (200 MHz, in C_6D_6): δ 0.66 (d, J=7.0 Hz, 3H, Me2), 0.94 (d, J=6.9 Hz, 3H, Me1), 1.2 to 2.4 (complex, 8H). ^{1}H nmr (200 MHz, in $CDCl_3$): δ 0.97 (d, J=7.0 Hz, 3H), 1.13 (d, J=6.8 Hz, 3H), 2.81

(quart. of d., J=7.2Hz, J=3.6Hz, 1H, Hd), 1.8 to 2.7 (complex, 7H). The following ^{1}H nmr resonances (300 MHz, in $CDCl_3$) were ressolved in the presence of Eu(fod)$_3$: (sextet, J=7 Hz, 1H, Hb), (quartet of d., J=7.2 Hz, J=3.6 Hz, 1H, Hd). ^{1}H nmr (300 MHz, in $CDCl_3$) decoupling results in the presence of Eu(fod)$_3$: Hb (sextet, J=7.4 Hz, 1H) was collapsed to a triplet (J=7.4 Hz) by high power irradiation of Me1 ; Hd (quartet, J=7.2 Hz, of d, J=3.6 Hz, 1H) was unaffected by high power irradiation of Me1, Me2, or Hb; high power irradiation of the group of resonances (3H) with the largest change in chemical shift in the presence of Eu(fod)$_3$ collapsed Hb to a quintet (J=7 Hz), and collapsed Hd to a triplet (J=7 Hz) of doublets (J=4 Hz). ^{13}C nmr (75 MHz, in $CDCl_3$): δ 15.1 (CH_3), 20.6 (CH_2), 20.8 (CH_3), 34.2 (CH), 38.2 (CH), 38.6 (CH_2), 41.3 (CH), 50.8 (CH), 221.5 (C=O). Mass spectrum (EI, 70 eV): m/e(%) 138(25), 123(18), 109(19), 95(15), 83(25), 82(25), 81(40), 69(100); calculated M^+ for $C_9H_{14}O$ 138.1045 (found 138.1048).

Characterisation of 114c (not isolated). Mass spectrum (EI, 70 eV): m/e(%) 138(5), 123(10), 109(12), 95(5), 83(45), 82(20), 81(25), 69(100).

Characterisation of 114d (fraction I). ^{1}H nmr (200 MHz,in C_6D_6): δ 0.82 (d, J=7.0 Hz, 3H), 0.85 (d, J=7.0 Hz, 3H), 1.2 to 1.5 (complex, 3H, He and Hc), 1.78 (ddq, J=9.9 Hz, J=8.6 Hz, J=7.0 Hz, Hb), 1.85 to 2.1 (complex, 3H, Hf and Hd), 2.32 (d, J=9.9 Hz, of d, J=6.7 Hz, Ha). The following ^{1}H nmr resonances (300 MHz, in $CDCl_3$) were ressolved in the presence of Eu(fod)$_3$: (quartet of d., J=6.7 Hz, J=1.5 Hz, Hd). ^{1}H nmr (300 MHz, in $CDCl_3$) decoupling results in the presence of Eu(fod)$_3$: Hb was collapsed to a doublet (J=10 Hz) of doublets (J=9 Hz) by high power irradiation of the methyl signal exhibiting the largest change in chemical shift in the presence of

$Eu(fod)_3$; Ha was collapsed to a doublet (J=6.7 Hz) by high power irradiation of Hb; Hd (quartet of d., J=6.7 Hz, J=1.5 Hz) was collapsed to a doublet (J=1.5 Hz) of triplets (J=6.7 Hz) by high power irradiation of Ha. ^{13}C nmr (75 MHz, in $CDCl_3$): δ 15.9 (CH_3), 20.1 (CH_3), 26.9 (CH_2), 36.8 (CH), 38.5 (CH_2), 41.50 (CH), 41.55 (CH), 46.5 (CH), 222.3 (C=O). Mass spectrum (EI, 70 eV): m/e(%) 138(10), 123(10), 109(10), 95(12), 83(58), 82(25), 81(30), 69(100); calculated M^+ for $C_9H_{14}O$ 138.1045 (found 138.1041).

7.4.3 Reduction of 114a, 114b, and 114d.

The procedure of Yamamura and Hirata[5] was used to reduce the ketone functionality of **114a**, **114b**, and **114d** to a methylene group. The following procedure was applied to samples of **114d**, **114a**, and **114b**. Approximately 0.050 g of each cycloadduct or mixture of cycloadducts was added to 20ml of diethyl ether saturated with hydrogen chloride at 0°C. Active zinc powder (2.0 g, see preparation method below) was added slowly to the stirred solution over a 20 minute interval, and then the temperature was gradually raised to room temperature. The reaction mixture was stirred for 2 hours and then poured on to 100 mL of ice water. The aqueous solution was neutralized with sodium carbonate, and extracted with ether. The ether layer was washed with saturated aqueous NaCl, dried over $MgSO_4$ and concentrated under reduced pressure. The homogeneity of the resulting product was determined by g.c. Product yields ranged from 80% to 85%.

Compound **118** was the major product (>90% of the reaction mixture) obtained from the reduction of compounds **114b** and **114d** in fractions V and I, respectively: ^1H

nmr (200 MHz, in $CDCl_3$): δ 0.79 (d, J=7.2Hz, 3H), 0.98 (d, J=7.2Hz, 3H), 1.2 to 2.0 (complex, 8H), 2.15 (m, 1H), 2.55 (m, 1H). Mass spectrum (EI, 70 eV): m/e(%) 124(8), 109(5), 95(28), 68(100), 67(40).

Reduction of the 75:15:13 mixture of **114a**, **114b**, and **114d** resulted in a mixture of **118** and **119** in a 20:80 ratio (ratio determined by g.c.). This mixture was used to determine the following for **119**: ^{1}H nmr δ 0.92 (d, 7.1Hz, 2 CH_3), 2.15 (m, 2H), 1.1 to 2.1 (complex, 8H). Mass spectrum of **119** was identica' to that of **118**.

7.4.4 Preparation of active zinc powder.

Commercial Zinc dust (Aldrich) was washed with 5% aqueous HCl for 5 minutes, after which subsequent washings with water, ethanol, acetone and ether were carried out. The powder was dried at 90°C for 20 minutes and used immediately.

7.4.5 Preparation of 115.

2-cyclopentenone (1.234 g; 0.150 mol/L) and 2-butyne (5.15 g; 0.952 mol/L) were dissolved in benzene (100 mL). The solution was placed in a Pyrex irradiation tube and irradiated with light from a 450 watt Hanovia medium pressure mercury lamp that was filtered through 1.5 cm of 0.4 mol/L $SnCl_2$ in 10% HCl/H_2O solution ($\lambda > 327$ nm). After 6 hours of irradiation the solution was analysed by g.c. and the ratio of 2-cyclopentenone:**116**:**115**:enone dimers was found to be 23:2.7:55:19. The two enone dimers were found in a ratio of 84:16. The benzene solvent and 2-butyne were removed under reduced pressure to yield a faint yellow oil which was subjected to further separation. The crude mixture was separated into its components using column

chromatography in which 3 x 70 cm column containing 120 g of 60-200 mesh silica gel packed in 9:1 hexanes/diethyl ether was used. The column was eluted with 0.8 L of 9:1 hexanes/diethyl ether and 1.2 L of 1:1 hexanes/diethyl ether to yield the following fractions: I, 0.050 g of **116**; II, 0.940 g of **115**; III, 0.395 g of 2-cyclopentenone; IV, 0.318 g of two enone dimers.

Characterisation of 115. ^{1}H nmr (300 MHz, in $CDCl_3$): δ 1.45 (brd. s., 3H), 1.52 (brd. s., 3H), 1.6 to 1.8 (complex, 2H), 1 95 (ddt, J=18 Hz, J=8.4 Hz, J=1.4 Hz, 1H), 2.60 (dddd, J=18 Hz, J=11.7 Hz, J=9.4 Hz, J=1.3 Hz, 1H), 2.80 (mult., 1H), 2.99 (mult., 1H). ^{13}C nmr (75 MHz, in $CDCl_3$): δ 11.7 (2 CH_3), 20.4 (CH_2), 34.3 (CH_2), 42.8 (CH), 54.1 (CH), 136.7 (C), 142.7 (C), 216.7 (C=O). IR (neat film, cm^{-1}): 1725 (C=O, vs), 1685 (C=C, vs). Mass spectrum (EI, 70 eV): m/e(%) 136(40), 121(18), 108(20), 93(100), 91(51), 79(44), 77(54), 65(15); calculated M^+ for $C_9H_{12}O$ 136.0888 (found 136.0891).

Characterisation of 116. ^{1}H nmr (300 MHz, in $CDCl_3$): δ 1.17 (s, 3H), 1.54 (t, J=1.8 Hz), 1.7 to 1.9 (complex, 2H), 2.13 (ddd, J=18 Hz, J=1.9 Hz, J=7.8 Hz, 1H), 2.90 (ddd, J=18 Hz, J=9.7 Hz, J=11.4 Hz, 1H), 5.87 (quart., J=1.8 Hz, 1H). ^{13}C nmr (75 MHz, in $CDCl_3$): δ 12.4 (CH_3), 12.8 (CH_3), 21.1 (CH_2), 35.1 (CH_2), 47.8 (CH), 65.9 (C), 131.9 (CH), 150.1 (C), 219.1 (C=O). Mass spectrum (EI, 70 eV): m/e(%) 136(44), 121(25), 108(28), 93(100), 91(50), 79(37), 77(50); calculated M^+ for $C_9H_{12}O$ 136.0888 (found 136.0877).

Characterisation of enone dimers. A solution containing 2-cyclopentenone (0.2 mol/L) in benzene was irradiated with light from a 450 watt Hanovia medium pressure mercury lamp that was filtered through 1.5 cm of 0.4 mol/L $SnCl_2$ in 10%

HCl/H_2O. The retention times of the two dimers resulting from this reaction were identical to the retention times of the products identified as dimers in fraction IV described above.

7.4.6 Hydrogenation of 115.

A catalyst consisting of 10% Pd on a carbon support (0.060 g) was added to absolute ethanol (50 mL). The catalyst was saturated with H_2 by bubbling H_2 gas through the mixture for 15 minutes. Compound **115** (0.226 g; 1.66 mmol) was added to the reaction flask while the bubbling of H_2 through the solution continued for an additional 45 minutes. The catalyst was removed by gravity filtration and the solvent was removed under reduced pressure to yield a colourless oil (0.215 g; 1.56 mmol; 94%). Analysis of this oil by g.c. indicated that two products were present in a 93:7 ratio. The major component of this mixture was identical to the minor product (i.e. compound **114c**) observed in the cycloaddition reaction between 2-cyclopentenone and each of the 2-butenes, according to g.c. co-injection and mass spectrum fragmentation pattern. The minor component of the hydrogenation reaction mixture was identical to the cycloadduct denoted **114a**. The 93:7 mixture of **114c** and **114a** was used to characterise compound **114c**.

Characteriastion of 114c. ^{1}H nmr (200 MHz, in $CDCl_3$): δ 0.77 (d, J=7.4 Hz, 3H), 0.87 (d, J=7.4 Hz, 3H), 1.7 to 3.0 (complex, 8H). The following ^{1}H nmr resonances (300 MHz, in $CDCl_3$) were ressolved in the presence of $Eu(fod)_3$: (t, J=9 Hz, H_a), (quart. of t., J=7 Hz, J=9 Hz, H_b), (quart. of t., J=7 Hz, J=9 Hz, H_c), (quart. of d., J=9 Hz, J=2.2 Hz, H_d). ^{1}H nmr (300 MHz, in $CDCl_3$) decoupling results in the

presence of $Eu(fod)_3$: Irraiation of Me1 collapses H_b to a triplet (J=9 Hz); irradiation of Me2 collapses H_c to a triplet (J=9 Hz); irradiation of H_a collapses H_d to triplet (J=9 Hz) of doublets (J=2.2 Hz) and collapses H_b to a quartet (J=7 Hz) of doublets (J=2.2 Hz); irradiation of H_d collapses H_a to a doublet (J=9 Hz) and collapses H_c to a doublet (J=9 Hz) of quartets (J=7 Hz). ^{13}C nmr (75 MHz, in $CDCl_3$): δ 10.5 (CH_3), 11.3 (CH_3), 21.6 (CH_2), 32.3 (CH), 32.7 (CH), 35.9 (CH), 40.2 (CH_2), 47.9 (CH), 222.3 (C=O). Mass spectrum (EI, 70 eV): m/e(%) 138(5), 123(10), 109(12), 95(5), 83(45), 82(20), 81(25), 69(100); calculated M^+ for $C_9H_{14}O$ 138.1045 (found 138.1049).

7.4.7 Hydrogen - deuterium exchange for compound 114d.

A solution of sodium methoxide (0.5 mol/L) in CH_3OD was prepared by dissolving sodium metal in CH_3OD. Compound **114d** (0.030 g) was added to 6 mL of this solution. The solution was stirred magnetically for 25 minutes after which time the solution was diluted with D_2O (10 mL) and extracted with diethyl ether (2 x 30 mL). The ether extracts were combined, washed with saturated NaCl/water (1 x 20 mL), dried over $MgSO_4$, and concentrated under reduced pressure to yield 0.026 g of product **119**.

Characterisation of 119. ^1H nmr (300 MHz, in $CDCl_3$): δ 0.91 (d, J=7.0 Hz, 3H), 1.12 (d, J=7.0 Hz, 3H), 1.6 to 2.0 (complex, 3H, He and Hc), 2.12 (ddq, J=9.9 Hz, J=8.6 Hz, J=7.0 Hz, Hb), 2.45 (dq, J=1.4 Hz, J=6.5 Hz, Hd), 2.63 (d, J=9.9 Hz, of d, J=6.5 Hz, Ha).

7.4.8 Quantum yield measurements.

All quantum yields were determined at ≤4% conversion of 2-cyclopentenone using a PTI QUANTACOUNT apparatus fitted with a high pressure 100 W mercury lamp. The light flux was calibrated using an azoxybenzene actinometer.[4] The absolute amount of cycloadducts formed in each irradiation was determined by g.c. analysis using 2-methylnonane as an internal standard. Calibration curves were constructed for the g.c. FID detector using pure samples of cycloadducts. It was assumed that regio- and stereochemical cycloadduct isomers had the same g.c. FID response factor. The samples were degassed by three freeze-pump-thaw cycles after which the residual pressure in each cell was below 1.5×10^{-4} mbar. In each irradiation, benzene was the solvent and the excitation wavelength was fixed at 340nm (5nm bandwidth). The concentration of enone used in the 2-cyclopentenone plus 2-butene quantum yield determinations was 0.0278M.

7.4.9 Irradiation of 2-cyclopentenone and *cis*- or *trans*-2-butene in the presence of H_2Se.

A 250 mL solution of cyclopentenone (2.05 g; 0.10 mol/L) and *cis* or *trans*-2-butene (21 g; 1.5 mol/L) in benzene was prepared. Addition of the butene was accomplished by first condensing the butene on a dry-ice/acetone cold finger and then dissolving the condensate in the benzene solution. In a separate flask, fitted with a gas outlet and dropping funnel, 5g of Al_2Se_3 was placed. A pipet was connected to the gas outlet of the flask containing Al_2Se_3 with Tygon tubing and then the pipet was submerged in the benzene solution. The benzene solution was chilled in ice water and the entire

system was flushed with nitrogen. Distilled water was added to the flask containing Al_2Se_3 at an initial rate of 1 drop per 20 seconds via the dropping funnel. Hydrogen selinide gas was allowed to pass through the gas outlet and bubble through the benzene solution. CAUTION: H_2Se IS EXTREMELY TOXIC. After the first several drops of water had been added to the Al_2Se_3 powder, the rate of addition was increased until all the Al_2Se_3 was consumed. An aliquot of the benzene solution was analyzed by ^1H nmr spectroscopy to check the concentrations of the volatile components: H_2Se (0.35 mol/L), butene (1.5 mol/L). The benzene solution was placed in a quartz immersion-well reactor fitted with a water cooled lamp jacket. The solution was irradiated with a 450 watt Hanovia medium pressure mercury lamp fitted with a Pyrex filter for 2 hours. Aliquots were withdrawn every 15 minutes and analyzed by g.c. Prolonged irradiation was not possible due to a build-up of elemental selenium on the lamp jacket. Subsequent g.c. analyses of similar irradiations carried out in the presence of a hydrocarbon standard (2-methylnonane) revealed that only 25% of the cyclopentenone was converted to products under these conditions. Comparison of the g.c. analyses of the irradiated solution with analyses of aliquots withdrawn before the light source was turned on allowed for identification of the ultra-violet light initiated reaction products. According to relative g.c. peak areas, 60% of the products produced were light initiated and 40% (3 products) were a result of "dark reactions".

After the benzene solvent was removed under reduced pressure, the components of the remaining concentrate (2.60 g) were separated by silica gel column chromatography in which a mobile phase consisting of 95% hexanes and 5% diethyl ether (v/v) and a stationary phase of 120 g of 60-200 Mesh silica gel were employed. The

following fractions resulting from *trans*-2-butene addition to cyclopentenone were collected and analyzed by g.c. (all fractions obtained as oils): I, 0.002 g of **120** and **124** (2:1); II, 0.007 g of **120** and **124** (1:3); III, 0.005 g of **121** and **125** (2:1); IV, 0.007 g of **121** and **125** (1:3.5); V, 0.029 g of **122** and **126** (6:1); VI, 0.120 g of **122** and **126** (1:1.5); VII, 0.031 g of **122** and **126** (1:7); VIII, 0.260 g **127** and **128** (compounds not resolved by g.c.); IX, 0.051 g **123**, **127** and **128** with a ratio of **123**:(**127** + **128**) equal to 2.5:1. Products **120** to **128** were identified as the light initiated products of the reaction. The 3 dark reaction products (all of which were determined to contain selenium by coupled g.c-m.s.) decomposed on the silica gel and thus none were isolated. Enriched samples of **122**, **126** and **123** were obtained by performing silica gel thin layer chromatography on the fractions V, VII and IX respectively. In this thin layer chromatography, a solvent consisting of 3% diethyl ether in 97% hexanes (v/v) was employed. Separation of **127** and **128** as well as the other two mixtures was not possible by this method.

The relative ratios of the nine light initiated products were determined by g.c. at 5% conversion of the cyclopentenone: for *cis*-2-butene addition the ratios were **120**(2.3%), **121**(2.0%), **122**(13.2%), **123**(10.3%), **124**(2.1%), **125**(2.0%), **126**(12.6%), **127**+**128**(55.4%); for *trans*-2-butene addition the ratios were **120**(1.4%), **121**(1.2%), **122**(9.1%), **123**(10.2%), **124**(2.4%), **125**(2.4%), **126**(13.7%), **127**+**128**(59.6%). The relative ratio of **127** to **128** was determined by integration of the two methyl triplet ^{1}H nmr resonances in the nmr spectra (recorded in the presence of shift reagent) of the mixture of **127** and **128**: For *cis*-2-butene addition the ratio of **127**:**128** was 1.0:1.0 and for *trans*-2-butene addition the ratio of **127**:**128** was either 1:3.97 or 3.97:1 (**127** and **128**

were not distinguished).

Characterisation of the mixtures of 120 and 124 (see fractions I and II). ^{1}H nmr (200 MHz, in $CDCl_3$): δ 0.74 (d, J=6.8 Hz, methyl assigned to **124**), 0.85 (t, J=7.3 Hz, methyl assigned to **120**), 0.93 (t, J=7.3 Hz, methyl assigned to **124**), 0.97 (d, J=6.9 Hz, methyl assigned to **120**), 1.1 to 1.5 (in the presence of Eu(fod)$_3$ this region disperses to allow identification of 2 quintets in a 1:3 area ratio, J=7.1 Hz for each), 1.8 to 2.0 (complex), 2.7 to 2.9 (complex), 6.0 to 6.2 (complex). The partially overlapping methyl resonances were dispersed in ^{1}H nmr spectra of the mixture recorded in the presence of various concentrations of lanthanide shift reagent. ^{13}C nmr (50 MHz, in $CDCl_3$) for compound **120**: δ 132.7 (CH), 128.9 (CH), 58.6 (CH), 44.5 (CH_2), 37.3 (CH), 27.1 (CH_2), 18.1 (CH_3), 12.9 (CH_3), sample too dilute to see carbonyl resonance. Mass spectrum (EI, 70 eV): (identical for **120** and **124**) m/e (%) 138(82), 110(20), 95(24), 82(100), 81(60). Precise mass for **120**: calculated M^+ for $C_9H_{14}O$ 138.1045 (found 138.1054). Precise mass for **124**: calculated M^+ for $C_9H_{14}O$ 138.1045 (found 138.1058).

Characterisation of a 1:3.5 mixture of 121 and 125. ^{1}H nmr (200 MHz, in $CDCl_3$): δ 0.94 (d, J=7.0 Hz methyl assigned to **125**), 1.10 (d, J=7.0 Hz, methyl assigned to **121**), 1.1 to 2.8 (complex), 4.9 to 5.06 (complex), 5.52 to 5.88 (complex). ^{13}C nmr (50 MHz, in $CDCl_3$): δ 220.0 (C=O), 220.8 (C=O), 142.0 (CH), 140.0 (CH), 54.0 (CH), 53.4 (CH), 36.6 (CH), 36.3 (CH), 114.8 (CH_2), 113.4 (CH_2), 39.1 (CH_2), 39.0 (CH_2), 25.1 (CH_2), 24.7 (CH_2), 20.65 (CH_2), 20.60 (CH_2), 17.8 (CH_3), 15.1 (CH_3). Mass spectrum (EI, 70 eV): (identical for **121** and **125**) m/e (%) 138(34), 123(20), 110(80), 95(38), 84(100), 83(30). Precise mass for **121**: calculated M^+ for $C_9H_{14}O$

138.1045 (found 138.1051). Precise mass for **125**: calculated M^+ for $C_9H_{14}O$ 138.1045 (found 138.1059).

Characterisation of 122. ^1H nmr (200 MHz, in $CDCl_3$): δ 0.86 (t,J=7.2 Hz, 3H), 0.96 (d, J=6.8 Hz, 3H), 1.0 to 2.4 (complex, 10H). ^{13}C nmr (200 MHz, in $CDCl_3$): δ 221.1 (C=0), 54.6 (CH), 34.2 (CH), 39.2 (CH_2), 25.9 (CH_2), 25.3 (CH_2), 20.6 (CH_2), 17.4 (CH_3), 12.0 (CH_3). Mass spectrum (EI, 70 eV): m/e (%) 140(6), 84(100), 83(28); calculated M^+ for $C_9H_{16}O$ 140.12012 (found 140.1197).

Characterisation of 126. ^1H nmr (200 MHz, in $CDCl_3$): δ 0.76 (d, J=6.8 Hz, 3H), 0.90 (t, J=7.2 Hz, 3H), 1.0 to 2.4 (complex, 10H). ^{13}C nmr (50 MHz, in $CDCl_3$): δ 221.6 (C=0), 53.1 (CH), 33.5 (CH), 39.2 (CH_2), 28.0 (CH_2), 23.5 (CH_2), 20.6 (CH_2), 15.1 (CH_3), 11.8 (CH_3). Mass spectrum (EI, 70 eV): m/e (%) 140(6), 84(100), 83(25); calculated M^+ for $C_9H_{16}O$ 140.12012 (found 140.1208).

Characterisation of 123 (from the mixture). ^1H nmr (200 MHz, in $CDCl_3$): δ 0.83 (t, J=7.3 Hz, 3H), 1.06 (d, J=6.9 Hz, 3H), 1.2 to 2.6 (complex, 7H), 7.26 (t, J=2.5 Hz, of d, J=0.8 Hz, 1H). ^{13}C nmr (50 MHz, in $CDCl_3$): δ 210.7 (C=0), 131.0 (C), 157.7 (CH), 31.6 (CH), 35.5 (CH_2), 28.7 (CH_2), 26.8 (CH_2), 19.3 (CH_3), 12.1 (CH_3). Mass spectrum (EI, 70 eV): m/e (%) 138(83), 123(78), 110(66), 109(85), 96(85), 95(46), 82(10), 81(100); calculated M^+ for $C_9H_{14}O$ 138.1045 (found 138.1040).

Characterisation of the mixture of 127 and 128. ^1H nmr (200 MHz, in $CDCl_3$): δ 0.82 to 0.96 (in the presence of $Eu(fod)_3$ this region disperses to allow identification of 2 methyl triplets, J=7.3 Hz each, and 2 methyl doublets, J=6.8Hz each), 1.00 to 2.45 (complex). ^{13}C nmr (50 MHz, in $CDCl_3$): δ 220.0 (C=0), 220.1

(C=0), 42.8 (CH), 42.7 (CH), 39.8 (CH), 39.6 (CH), 43.9 (CH_2), 43.3 (CH_2), 39.1 (CH_2), 39.0 (CH_2), 27.8 (CH_2, 2 resonances overlapping), 27.5 (CH_2), 26.8 (CH_2), 16.9 (CH_3), 16.1 (CH_3), 11.[illegible] (CH_3, 2 resonances overlapping). Mass spectrum of mixture (EI, 70 eV): m/e (%) 140(35), 84(27), 83(100); calculated M^+ for $C_9H_{16}O$ 140.12012 (found 140.1194).

7.4.10 Preparation of E- and Z-2-sec-butylidenecyclopentanones (130 and 129).

A 1000 mL flask was charged with freshly distilled cyclopentanone (42 g; 0.50 mol), freshly distilled 2-butanone (144 g; 2.0 mol), 1 N aqueous sodium hydroxide (300 mL), and enough ethanol to make the reaction mixture homogeneous. After the mixture was stirred at room temperature for 24 hours, the reaction mixture was neutralized with 6 mol/L aqueous HCl. The organic fraction was separated and the remaining aqueous fraction extracted with ether (3x120 mL). The combined organic fractions were washed with saturated NaCl (2x100 mL), dried over $MgSO_4$, and concentrated at reduced pressure. The concentrate was analyzed by g.c. and was found to contain 3 products in the ratio 1:1:4.5 (uncalibrated g.c. ratios). Distillation of the concentrate at 101-105 (25 mm Hg) through a 20cm vigreaux gave 5.2 g (7.5%) of a 1:1:0.1 mixture of E-2-sec-butylidenecyclopentanone **(130)**, Z-2-sec-butylidene-cyclopentanone **(129)** and 2-cyclopentylidenecyclopentanone respectively. Further separation of this distillate was accomplished by preparative thin layer silica gel chromatography using a mobile phase consisting of 90% hexanes and 10% diethyl ether (v/v). Compounds **130** and **129** were obtained 90% pure with the 10% impurity consisting of the other geometrical isomer. The minor component of the distillate mixture was isolated as a pure compound and its

^1H and ^{13}C nmr and mass spectra confirmed the assignment of 2-cyclopentylidenecyclopentanone to this compound.

Characterisation of 130. ^1H nmr (200 MHz, in C_6D_6): δ 0.769 (t, J=7.6 Hz, 3H), 1.37 (quin., J=7.2 Hz, 2H), 1.76 (quart., J=7.6 Hz, 2H, assigned He), 2.03 (t, J=7.4 Hz, 2H), 2.16 (multiplicity determined in LIS spectrum: brd. t., J=7.2 Hz, 2H), 2.26 (t, J=2.0 Hz, 3H, assigned Hd). Mass spectrum (EI, 70 eV): m/e(%) 138(100), 123(50), 110(20), 109(35), 95(30), 82(30), 81(46), 67(60).

Characterisation of 129. ^1H nmr (200 MHz, in C_6D_6): δ 1.02 (t, J=7.6 Hz, 3H), 1.37 (quin., J=7.2 Hz, 2H), 1.44 (t, J=1.5 Hz, 3H, assigned Hd), 2.03 (t, J=7.4 Hz, 2H), 2.12 (multiplicity determined in ^1H nmr spectrum obtained in the presence of $Eu(fod)_3$, brd. t., J=7.2 Hz, 2H), 2.80 (quart. of t., J=7.5 Hz, J=1.2 Hz, 2H assigned He). Mass spectrum (EI, 70 eV): m/e(%) 138(100), 123(45), 110(20), 109(35), 95(32), 82(32), 81(45), 67(60).

7.4.11 Hydrogenation of unsaturated compounds.

The alkene (approximately 0.010 g) was dissolved in ether (10 mL) to which approximately 5 mg of 10% Pd on carbon catalyst was added. Hydrogen gas was bubbled through the solution for 20 minutes during which time periodic additions of ether were made in order to keep the mixture volume at 10ml. The catalyst was removed by filtration and the solvent was removed under reduced pressure to yield the hydrogenation products in better than 95% yield. Product analysis was accomplished by g.c. and g.c./m.s. Identification of each hydrogenation product was determined by g.c. co-injection with samples of the corresponding saturated compound. The following

transformations were observed upon hydogenation: a 1:3 mixture of **120** and **124** hydrogenates to a 1:3 mixture of **122** and **126**; a 1:3.5 mixture of **121** and **125** hydrogenates to a 1:3.5 mixture of **122** and **126**; **123** hydrogenates to a 1:1 mixture of **122** and **126**; **129** hydrogenates to **122**; and, **130** hydrogenates to **126**.

7.4.12 Base catalysed isomerism of compounds 120 and 124.

A 1:3 mixture of **120** and **124** (0.0081 g) was dissolved in 2 mL of a methanol solution containing 0.15 mol/L sodium methoxide. The solution was stirred magnetically for 20 minutes after which time the solution was diluted with 5 mL of water and extracted with dichloromethane (5 x 10 mL). The dichloromethane extracts were combined, dried over $MgSO_4$, and concentrated under reduced pressure to yield 0.0074 g of product. The product was analysed by g.c./m.s. It was found that the product contained no trace of **120** or **124**; rather, only compound **123** was observed. The identity of **123** was confirmed by g.c. co-injection with a sample of this compound isolated from the 2-cyclopentenone plus *trans*-2-butene plus H_2Se reaction mixture.

7.4.13 Synthesis of 127 and 128 by conjugate addition to 2-cyclopentenone.

Magnesium metal (2.442 g; 0.101 mol) and anhydrous diethyl ether were placed in a 100 mL 3-neck flask fitted with a reflux condensor, dropping funnel, nitrogen inlet and a rubber septum. To this mixture, 2-bromobutane (13.703 g; 0.100 mol) was added over a 30 minute period under an atmosphere of nitrogen. The concentration of the Grignard was calculated to be 2.0 M. In a separate 2-neck flask, a solution of $ZnCl_2$•TMEDA (1.684 g; 6.67mmol) in dry THF (30 mL) at 0°C was prepared under

nitrogen. To this solution, 10 mL of the Grignard solution (20 mmol of 2-butane manesium bromide) was added via a 10 mL syringe immediately followed by 0.546 g (6.66 mmol) of 2-cyclopentenone. The reaction mixture was stirred for an additional 30 minutes at 0°C. The solution was poured onto 30 mL of saturated aqueous NH_4Cl and then 30 mL of diethyl ether was added. The ether layer was separated, washed with saturated NH_4Cl/H_2O (2x30 mL) followed by saturated NaCl (2x30 mL), and dried over $MgSO_4$. The solvent was removed under reduced pressure to yield 0.777 g of a pale yellow oil. This oil was loaded onto a flash chromatography column containing 80 g of silica gel and eluted with a 18:1 mixture of hexanes and diethyl ether to yield 0.489 g (52% based on 2-cyclopentenone) of a mixture of diastereomers **127** and **128**. The mixture was identified as a single peak by g.c. (DB-5 30 m column).

Characterisation of the reaction mixture. ^1H nmr (300 MHz, in $CDCl_3$): δ 0.83 to 0.95 (in the presence of $Eu(fod)_3$ this region disperse to allow identification of 2 methyl triplets, J=7.3 Hz, and 2 methyl doublets, J=6.9 Hz), 1.0 to 2.4 (complex). ^{13}C nmr (300 MHz, in $CDCl_3$): δ 11.1 (CH_3, 2 resonances), 16.1 (CH_3), 17.0 (CH_3), 26.8 (CH_2), 27.5 (CH_2), 27.8 (CH_2, 2 resonances), 39.0 (CH_2), 39.1 (CH_2), 39.6 (CH), 39.8 (CH), 42.8 (CH), 43.3 (CH_2), 43.9 (CH_2). Mass spectrum (EI, 70 eV): m/e(%) 140(M+, 35), 84(27), 83(100); calculated M^+ for $C_9H_{16}O$ 140.12012 (found 140.1196).

7.4.14 Attempted cyclobutane ring opening of 114c with trimethylsilyl iodide.

A solution of **114c** (0.107 g; 0.777 mmol), decane (0.030g; internal standard) and NaI (1.372 g; 9.15 mmol) in 10 mL dry acetonitrile (dried by distillation over CaH_2) was prepared was added to a 3-neck flask that was fitted with a rubber septum and a

nitrogen inlet. The apparatus was flushed with dry nitrogen and then freshly distilled trimethylsilyl chloride (1.2 mL; 9.5 mmol) was added via a syringe. A milky white precipitate immediately formed upon addition of the trimethylsilyl chloride. The reaction mixture was refluxed for 70 hours during which time the reaction mixture was frequently analysed by coupled g.c.-m.s. These analyses indicated that less than 5% of the starting material reacted, and that no products exhibiting a mass representative of the desired product were formed. The reaction mixture was not worked up.

7.4.15 Photolysis of compound 114c

A solution of **114c** (0.300 g; 2.17 mmol; 0.108 M) in acetonitrile (20 mL) was irradiated with Pyrex filtered light from a 400 W Hanovia medium pressure mercury lamp for 2 hours. The solvent was removed under reduced pressure to yield 0.292 g of a pale yellow oil. The crude product mixture was loaded onto a column containing 160 g of silica gel and eluted with a 20:1 mixture of hexanes and diethyl ether. The following fractions were collected: I, 0.038 g of **114c**; and II, 0.244 g (81% yield) of **136**.

Characterisation of 136. ^{1}H nmr (300 MHz, in $CDCl_3$): δ 0.91 (d, J=6.6 Hz, 3H, assigned to CH_3), 0.93 (d, J=6.6 Hz, 3H, assigned to CH_3), 2.12 to 2.35 (complex, 2H), 2.51 (dt, J=1.7 Hz, J= 7.5 Hz, 2H), 2.65 to 2.78 (complex, 2H), 5.68 (s, 1H, assigned to vinylic CH), 9.73 (t, J=1.7 Hz, 1H, assigned to HC=O). ^{13}C nmr (75 MHz, in $CDCl_3$): δ 13.0 (CH_3), 14.5 (CH_3), 21.3 (CH_2), 37.1 (CH), 40.54 (CH), 40.57 (CH_2), 131.8 (CH), 151.5 (C), 202.2 (HC=O). Mass spectrum (EI, 70 eV): m/e(%)

138(M+, 47), 109(12), 96(76), 95(20), 80(100), 78(87), 67(57); calculated M^+ for $C_9H_{14}O$ 138.1045 (found 138.1044).

7.5 Experimental details for Chapter 5

7.5.1 Preparation of t-butyl selenol.

The following adaptation of the methods reported by Gaufrès et al[6] and Arnold et al[7] was used to prepare t-butyl selenol. To a solution of t-butyl chloride (4.087 g; 44.4 mmol) in anhydrous diethyl ether (70 mL) was added finely ground magnesium turnings (1.07 g; 44 mmol). The solution was heated with a heat-gun until a cloudy white precipitate began to form. An exothermic reaction commenced and the solution was allowed to reflux under its own heat for 1 hour. At this point, the reaction flask was fitted with a nitrogen inlet and flushed with dry nitrogen gas. Powdered grey selenium (1.90 g; 24 mmol) was added slowly over 30 min with vigorous stirring under nitrogen to the t-butylmagnesium chloride. After an additional 30 min of stirring, diethyl ether (50 mL) was added and the solution was left to stand under a nitrogen atmosphere for 12 hours. The solution was chilled in an ice bath and ice-cold water (30 mL) was added followed by sulphuric acid (75 mL; 2.5 M) which was added slowly over a 2 hour period under nitrogen. After the ether layer was separated, the aqueous layer extracted with diethyl ether (2 x 50 mL) and all of the ether extracts were combined and dried over sodium sulphate. The diethyl ether was removed by fractional distillation using a 50 cm fractionating column was used. The desired product, t-butyl selenol, was fractionally

distilled from the residue using the same column at 75-78°C (760 mm Hg) and collected under nitrogen. The crude product was redistilled through a 60 cm spinning band column at 77-78°C (lit.[6] Bp_{760}= 78.5°C to yield 0.92 g (15% based on t-butyl chloride). The product was stored under nitrogen for 1 day before being used in the biradical trapping experiment. The product was found to contain approximately 2 to 4% diethyl ether and approximately 3% di-t-butyl diselenide by coupled g.c.-m.s. analysis. Mass spectrum (CI, isobutane): m/e(%, Se isotope) 140(3.9, ^{82}Se), 139(1.0, ^{81}Se), 138(21, ^{80}Se), 136(10, ^{79}Se), 135(3.4 ^{78}Se), 134(3.8, ^{77}Se), 57(100). ^{13}C nmr (75 MHz, $CDCl_3$): δ 39.1 (quaternary), 36.0 (CH_3). Lit.[8] ^{13}C nmr (in $CDCl_3$): δ 39.3, 36.0.

7.5.2 Oxidation of t-butyl selenol to di-t-butyl diselenide.

In order to confirm the identity of the di-t-butyl diselenide contaminant in the prepared sample of t-butyl selenol, deliberate air oxidation of t-butyl selenol was performed. A stream of moist air was bubbled through a solution containing a small amount of t-butyl selenol (approximately 10 mg) dissolved in diethyl ether (2 mL). The disappearance of t-butyl-selenol was monitored by g.c. An increase in concentration of the impurity initially present in the t-butyl-selenol was also detected by g.c. The impurity was identified as di-t-butyl diselenide by coupled g.c.-m.s. evidence. Mass spectrum of di-t-butyl diselenide (CI, isobutane): m/e(%) 273(1.5), 271(1.4), 269(0.8), 217(1.5), 215(1.5), 213 (0.9), 138(2), 136(1.3), 57(100), 56(55).

7.5.3 Irradiation of 2-cyclopentenone and *trans*-2-butene in the presence of t-butyl selenol.

A solution containing t-butyl selenol (0.505 g; 3.69 mmol; 0.37 M), 2-cyclopentenone (0.066 g; 0.80 mmol; 0.08 M) and *trans*-2-butene (0.842 g; 15.0 mmol; 1.5 M) in benzene (10 mL) was prepared under nitrogen. Part of this solution (5 mL) was irradiated with Pyrex filtered light from a 400 W Hanovia medium pressure mercury lamp for 30 min and then analyzed by g.c. and coupled g.c.-m.s. The remaining solution (5 mL) was kept dark for 1 hour and then analyzed by g.c. The irradiated solution was found to contain trapped biradical products **121**:**122**:**123**:**125**:**126**:(**127**+**128**) in the ratio 2:8:15:4:15:56, cycloadducts **114a**:**114b**:**114d** in the ratio 50:30:20, and a large amount of unidentified dark reaction products. The ratio of the combined yield of cycloadducts to the combined yield of trapped products was 1:3. The identity of the trapped products and the cycloadducts was confirmed by g.c. co-injection of the samples of these compounds with those obtained in the experiments described in the Experimental Section for Chapter 4.

7.5.4 Preparation of Benzeneselenol.[9]

Ground magnesium turnings (3.76 g; 0.155 mol) were placed in a 3-neck round bottom flask containing anhydrous diethyl ether (170 mL). To this mixture, freshly distilled bromobenzene (24.27 g; 0.155 mol) was added via a dropping funnel over a 30 minute period. In order to initiate the reaction it was necessary to heat the reaction with a heat-gun until the ether began to boil. After stirring the reaction mixture for an

additional 1.5 hours, the dropping funnel was replaced with an addition flask containing powdered grey selenium (12.25 g; 0.155 mol) and the system was flushed with dry nitrogen. The ether solution was heated to bring about gentle refluxing and then the selenium was added over a 1 hour period. The reaction mixture was cooled to room temperature and stirred for additional an 30 minutes, after which time the reaction flask was placed in an ice bath and the addition flask replaced with a dropping funnel. Ice-cold water (100 mL) was added over 30 minutes followed by ice-cold HCl/H_2O (100 mL; 6 M) which was also added over 30 minutes. The ether layer was separated and the aqueous layer extracted with 3 x 60 mL additional portions of ether. The ether extracts were combined and dried over sodium sulphate. The diethyl ether was removed by distillation at atmospheric pressure and then the residue was distilled under reduced pressure (25 mm Hg) at 84 to 86°C (Lit.[9] Bp. = 86°C/25 mm Hg) to yield the desired product (8.21 g; 0.0522 mol) in 34% yield. The benzeneselenol was stored under nitrogen.

7.5.5 Irradiation of 2-cyclopentenone and *trans*-2-butene in the presence of benzeneselenol.

A solution containing benzeneselenol (0.779 g; 4.96 mmol; 0.50 M), 2-cyclopentenone (0.068 g; 0.83 mmol; 0.083 M) and *trans*-2-butene (0.850 g; 15.2 mmol; 1.5 M) in benzene (10 mL) was prepared under nitrogen. Part of this solution (5 mL) was irradiated with pyrex filtered light from a 400 W Hanovia medium pressure mercury lamp for 45 min and then analyzed by g.c. and coupled g.c.-m.s. The remaining solution

(5 mL) was kept dark for 1 hour and then analyzed by g.c. Both reaction mixtures contained a large number of new products according to g.c. analysis. Neither reaction mixture contained any trace of products representative of trapped biradicals nor any trace of cycloadducts. The absence of trapped products and cycloadducts was confirmed by g.c. co-injection of the reaction mixtures with authentic samples of products.

7.5.6 Preparation of 1-pyrroline N-oxide (185).

The following adaptation of the method reported by Murahashi and co-workers[10] was used to prepare 1-pyrroline N-oxide. To a 250 mL 3-neck round bottom flask equipped with a dropping funnel, magnetic stirring bar and nitrogen inlet, $Na_2WO_4 \bullet 2H_2O$[5] (2.65 g; 8.00 mmol) was added. After flushing the reaction flask with nitrogen, water (40 mL) followed by freshly distilled pyrrolidine (14.22 g; 200 mmol) were added via the dropping funnel. The flask was cooled to -10°C with an ice bath and H_2O_2/H_2O (45 mL of 30% solution; 440 mmol) was added over 45 minutes. The solution was warmed to room temperature and stirred for an additional 3 hours. The solution was chilled in an ice bath, solid $NaHSO_3$ (2 g) was added, and the resulting mixture stirred for another 30 minutes. The solution was then saturated with NaCl (25 g) and extracted with 5 x 100 mL portions of CH_2Cl_2. The CH_2Cl_2 extracts were combined, dried over $MgSO_4$ and concentrated under reduced pressure to yield a yellow oil which was immediately subjected to column chromatography. A 2.5 cm x 70 cm column containing 170 g of silica gel packed in 9:1 (v/v) ethyl acetate and methanol was

---

[5]The $Na_2WO_4 \bullet 2H_2O$ was recrystallised from boiling water and dried under vacuum at 40°C prior to use.

loaded with a chloroform solution of the crude product and then eluted with 1 L of a 20:1 mixture of chloroform and methanol followed by 1 L of a 8:2 mixture of the same solvent. Fractions were collected in 100 mL volumes and analyzed by TLC. The desired product was contained in fractions 14 to 30. These fractions were combined and concentrated under reduced vacuum to yield 3.56 g of product (21% yield). IR (neat film): 2950, 1593 (C=N, s), 1450, 1355, 1225, 1170, 1063, 1043. ^{1}H nmr (300 MHz, in $CDCl_3$): δ 6.78 (tt, J=2.6 Hz, J=2.0 Hz, 1H, assigned H_2), 3.84 (quart. t., J=2.0 Hz, J=8.0 Hz, 2H, assigned H_5), 2.61 (quart. t., J=2.5 Hz, J=7.9 Hz, 1H, assigned H_3), 2.13 (mult., 2H, assigned H_4). ^{13}C nmr (75 MHz, in $CDCl_3$): δ 135.1 (CH, assigned C_5), 61.8 (CH_2, assigned C_2), 28.4 (CH_2), 18.8 (CH_2). Mass spectrum (70 eV): m/e(%) 85(M+, 100), 69(10), 55(50), 41(40).

7.5.7 Irradiation of 2-cyclopentenone, cyclopentene and 1-pyrroline N-oxide in methanol.

A solution containing 2-cyclopentenone (0.036 g; 0.22 M), cyclopentene (0.221 g; 1.62 M), decane (0.0041 g; internal standard) and 1-pyrroline N-oxide (0.304 g; 1.79 M) in methanol (2.0 mL) was prepared and then immediately chilled in a dry ice/acetone cooling bath. A second solution containing 2-cyclopentenone (0.033 g; 0.20 M), decane (0.0050 g; internal standard) and cyclopentene (0.164; 1.20 M) in methanol (5,0 mL) was also prepared. Equal amounts of these two solutions (1.0 mL) were placed in separate irradiation tubes located in an irradiation dewar contained a dry ice/acetone cooling solution. The contents of the irradiation tubes were irradiated with acetone

filtered light from a 400 W Hanovia medium pressure mercury lamp for 30 minutes and then analyzed by g.c. The remaining portion of the solution containing the 1-pyrroline N-oxide was kept dark in a dry ice/acetone cooling bath for 50 minutes and then analyzed by g.c. The g.c. analyses of the two irradiated solutions indicated that amount of cycloadducts formed in each solution was the same. In addition to cycloadduct formation, the irradiated solutions contained products that were also observed in the dark reaction containing 2-cyclopentenone, cyclopentene and 1-pyrroline N-oxide. These products were thermal 1,3-dipolar addition products formed as a result of ground state reaction between the 1-pyrroline N-oxide and 2-cyclopentenone or cyclopentene.

7.5.8 Irradiation of 2-cyclopentenone, ethyl vinyl ether and 1-pyrroline N-oxide in methanol.

A solution containing 2-cyclopentenone (0.053 g; 0.13 M), ethyl vinyl ether (0.366 g; 1.02 M), decane (0.0061 g; internal standard) and 1-pyrroline N-oxide (0.310 g; 0.73 M) in methanol (5.0 mL) was prepared and then immediately chilled in a dry ice/acetone cooling bath. A second solution containing 2-cyclopentenone (0.055 g; 0.13 M), decane (0.0049 g; internal standard) and ethyl vinyl ether (0.380; 1.05 M) in methanol (5.0 mL) was also prepared. Equal amounts of these two solutions (2.0 mL) were placed in separate irradiation tubes located in an irradiation dewar contained a dry ice/acetone cooling solution. The contents of the irradiation tubes were irradiated with acetone filtered light from a 400 W Hanovia medium pressure mercury lamp for 45 minutes and then analyzed by g.c. The remaining portion of the solution containing the

1-pyrroline N-oxide was kept dark in a dry ice/acetone cooling bath for 50 minutes and then analyzed by g.c. The g.c. analyses of the two irradiated solutions indicated that the relative product ratios of the four cycloadducts formed in each solution were identical and that the total amount of cycloadducts formed in each solution was also the same. In addition to cycloadduct formation, thermal 1,3-dipolar addition products, formed as a result of ground state reaction between the 1-pyrroline N-oxide and 2-cyclopentenone or cyclopentene, were also detected in the irradiated solutions. These products were detected in the dark reaction mixture.

7.5.9 Irradiation of 1-hexene, 2-cyclopentenone and butanethiol in benzene.

A solution containing 2-cyclopentenone (0.090 g; 0.110 M), isobutene (0.956 g; 1.7 M), and butanethiol (0.455; 0.505 M) in benzene (10 mL) was irradiated with Pyrex filtered light from a 400 W Hanovia medium pressure mercury lamp for 1 hour. The contents of the reaction were analyzed g.c. and coupled g.c.-m.s. Compounds **54**, **57**, **55** and **56** were found to be present in the reaction mixture in the ratio 3:9:70:18. The identity of the products was confirmed comparing the g.c. retention times of the compounds observed in this irradiation with the retention times of the products observed the irradiation of 2-cyclopentenone and isobutene in benzene described in the experimental section for Chapter 3. Both reactions resulted in identical product distributions.

7.5.10 Irradiation of 1-hexene and 2-cyclopentenone in liquid SO_2.

2-Cyclopentenone (0.184 g; 2.24 mmol) and 1-hexene (1.265 g; 15.0 mmol) were placed in a Pyrex irradiation tube which was fitted with a gas inlet. The irradiation tube was flushed with dry nitrogen and chilled in a low temperature quartz irradiation Dewar with a dry ice/acetonitrile slurry. With the gas inlet was connected to a sulphur dioxide gas cylinder, liquid SO_2 was condensed in the irradiation tube until a total volume of 15 mL was achieved. The concentrations of 2-cyclopentenone and 1-hexene were calculated as 0.15 M and 1.0 M respectively. The solution was irradiated through an acetone filter with light from a 400 W Hanovia medium pressure mercury lamp for 2 hours at the dry ice/acetonitrile cooling bath temperature. The solution was allowed to warm to room temperature while a stream of nitrogen gas bubbled through the solution. After evaporation of the SO_2, a white solid polymeric material remained in the irradiation tube. The contents of the tube were dissolved in CH_2Cl_2 and this solution was washed with a saturated $NaHCO_3/H_2O$ (3x100 mL) followed by saturated $NaCl/H_2O$ (2x100 mL). The CH_2Cl_2 layer was dried over $MgSO_4$ and concentrated under reduced pressure to yield 1.30 g of white polymeric solid. A g.c. analysis of the product only revealed peaks corresponding to the starting materials. The starting materials were removed from the product under high vacuum at 40°C and the resulting solid was characterised. IR ($CDCl_3$ film): 1308 (S=O, s), 1133 (S=O, s). ^{1}H nmr (300 MHz, in $CDCl_3$): δ 0.91 (brd. t., J=7.1 Hz, 3H, assigned CH_3), 1.3 to 1.6 (brd., 4H), 1.8 to 2.2 (brd. 2H), 3.2 to 4.0 (brd., 3H). ^{13}C nmr (75 MHz, in $CDCl_3$): δ 57 (brd. CH), 49 (brd. CH_2), 28 (brd. CH_2), 22.4 (CH_2), 13.2 (CH_3). Mass spectrum (CI, negative ion): m/e(%) 591(2), 443(8), 295(22), 147(100).

7.6 Experimental details for Chapter 6

7.6.1 Preparation of 2,3-dimethyl-2,3-dinitrobutane (206)

This compound was synthesised according to the method of Sayre[11]. A stirred solution of 2-nitropropane (44.5 g; 0.500 mol) in 6 M $NaOH/H_2O$ (85 mL) was cooled in an ice water bath. To this solution, bromine (40 g; 0.25 mol) was added dropwise over a 2 hour period. Ethanol (165 mL) was added and the resulting homogeneous solution was refluxed for 3 hours. The yellow solution was poured onto an ice water slurry (500 mL) and the crystalline product was removed from this mixture by filtration. The pale yellow solid was dried under vacuum (1-2 mm Hg) for 4 hours to yield 24.1 g (0.137 mol) of 2,3-dimethyl-2,3-dinitrobutane in 55% yield. Mp=210-212°C (lit.[11] mp=211-212°C). ^1H nmr (200 MHz, in $CDCl_3$): δ 1.71 (s). ^{13}C nmr (50 MHz; in $CDCl_3$): δ 22.8 (CH_3), 91.4 (C).

7.6.2 Preparation of NN'-dihydroxy-2,3-diamino-2,3-dimethylbutane (207)

This compound was prepared according to the method of Lamchen and Mittag.[12] A solution containing 2,3-dimethyl-2,3-dinitrobutane (17.5 g; 0.0993 mol) and ammonium chloride (10 g) in 50% (v/v) aqueous ethanol (200 mL) was chilled in an ice bath. To this mixture, powdered zinc (40 g) was added over a period of 3 hours. The slurry was stirred for an additional 3.5 hours at room temperature. The mixture was filtered and the zinc oxide residue was washed with 3 x 60 mL portions of water. The filtrate was concentrated under reduced pressure with heating to yield a thick brown oil. The oil was mixed with 50 g of K_2CO_3 and then this mixture was extracted with

chloroform (300 mL) in a Soxhlet continuous extractor for 4.5 hours. The chloroform solution was dried over $MgSO_4$ and concentrated under reduced pressure to yield a light brown oil (5.80 g). Due to the fact that NN'-dihydroxy-2,3-diamino-2,3-dimethylbutane undergoes spontaneous decomposition at room temperature[13], the entire crude product was used directly in the next step (see below).

7.6.3 Preparation of 3,3,4,4-tetramethyl-1,2-diazetine 1,2-dioxide (205)

The crude N,N'-dihydroxy-2,3-diamino-2,3-dimethylbutane(5.80 g; 0.0391) was suspended in 200 mL of water. To this suspension, bromine (12.5 g; 0.0782 mol) was added slowly with stirring. The colour of the mixture turned from light purple to a green and finally to brown during the course of the bromine addition. The aqueous solution was extracted with 5 x 100 mL portions of chloroform. The combined chloroform extracts were dried over $MgSO_4$ and concentrated under reduced pressure to yield light brown crystals. The crude product was recrystallised thrice from methanol to yield white crystalline 3,3,4,4-tetramethyl-1,2-diazetine 1,2-dioxide (1.85 g; 0.0128 mol; 13% based on 2,3-dimethyl-2,3-dinitrobutane). Mp=185-188°C decomposes (lit.[14] mp=190-192°C decomposes). IR (film in $CHCl_3$): 1555 (vs, N-O). UV (in CH_3CN): λ_{max}=255 nm (ϵ=9700). ^1H nmr (200 MHz, in $CDCl_3$): δ 1.60 (s). ^{13}C nmr (50 MHz, in $CDCl_3$): δ 19.1 (CH_3), 80.6 (C). Mass spectrum (EI, 70 eV): m/e(%) 144(M+, 1.5), 114(14), 84(65), 69(100); calculated M^+ for $C_6H_{12}N_2O_2$ 144.0899 (found 144.0901).

7.6.4 Photocycloaddition of 2-cyclopentenone and fumaronitrile in acetonitrile.

2-Cyclopentenone (0.994 g; 12.1 mmol; 0.110 M) and fumaronitrile (5.322 g; 68.2 mmol; 0.620 M) were dissolved in acetonitrile (110 mL). The solution was placed in a Pyrex irradiation tube which was located in a water bath (T = 18°C) and irradiated with light from a 400 W Hanovia medium pressure mercury lamp for 45 hours. The reaction mixture was analyzed by g.c. at 2 to 4 hour intervals throughout the irradiation. The solvent was removed under reduced pressure to yield 6.311 g of a orange-brown oil. This oil was dissolved in acetonitrile, pre-absorbed onto 15 g of silica gel and placed on a flash column containing 80 g of silica gel. The column was eluted with the following solvent mixtures: 8x200 mL fractions consisting of 2:3 diethyl ether:hexanes; 3x300 mL fractions consisting of 7:3 diethyl ether:hexanes; 3x400 mL fractions consisting of diethyl ether; one 500 mL fraction consisting of 1:4 acetonitrile:diethyl ether; and one 400 mL fraction consisting of 2:3 acetonitrile:diethyl ether.

Fractions 1 to 3 were combined and concentrated under reduced pressure to yield 2.43 g of fumaronitrile. Fractions 4 to 7 were combined and concentrated under reduced pressure to yield 2.57 g of a mixture of 2-cyclopentenone (CP) and maleonitrile. Fractions 8 and 9 were combined and concentrated under reduced pressure to yield 0.450 g of a pale yellow oil **212a** and two enone dimers. Fractions 10 to 12 were combined and concentrated under reduced pressure to yield 0.478 g of a brown oil containing ~ 2:3 mixture of **212b** and **212c**. Fractions 15 and 16 were combined and concentrated under reduced pressure to yield 0.372 g of a dark brown oil consisting of **212d**.

The fraction containing 2-cyclopentenone and maleonitrile was separated into a fraction consisting of pure maleonitrile (2.35 g) and a fraction containing 2-

cyclopentenone (0.211 g) by column chromatography on silica gel. The fraction containing **212a** and two enone dimers was separated by column chromatography into two fractions: one fraction which contained pure **212a** (0.250 g of a colourless oil; 13% yield based on CP) and the other contained a mixture of the two enone dimers (0.194 g of a colourless oil; 9.6% yield based on CP). The faction containing a mixture of **212b** and **212c** was separated into two fractions consisting of pure **212b** (0.165 g of a colourless oil; 8.5% yield based on CP) and pure **212c** (0.307 g of a colourless oil; 16% yield based on CP) by column chromatography in which 100 g of silica eluted by 1:1 hexanes:diethyl ether was used. Impure **212d** was subjected to more flash chromatography in which a column containing 60 g of silica was eluted with 1:4 ethyl acetate and hexanes. Compound **212d** was recovered as a yellow solid and recrystallised from ethyl acetate/hexanes to yield 0.355 g (18% yield based on CP) of a pure white solid (mp=148-151°C).

Characterisation of 212a. ^{1}H nmr (300 MHz, in DMSO-d_6): δ 2.0 to 2.7 (complex, 4H) 3.05 to 3.25 (complex, 2H, assigned Ha and Hd), 4.28 (mult., 2H, assigned Hb and Hc). ^{13}C nmr (300 MHz, in DMSO-d_6): δ 22.8 (CH_2), 25.3 (CH), 28.0 (CH), 34.6 (CH), 37.5 (CH_2), 45.5 (CH), 117.8 (C≡N), 118.6 (C≡N), 214.6 (C=O). Mass spectrum (CI, isobutane): m/e(%) 161(M+1, 100), 82(18), 78(12). Precise mass determination: 160.06340 (observed), 160.0637 (calculated).

Characterisation of 212b. ^{1}H nmr (300MHz, in DMSO-d_6): 1.90 to 2.16 (complex, 2H, assigned He), 2.37 (dddd, J=19 Hz, J= 8.1 Hz, J=3.0 Hz, J=1.7 Hz, 1H, assigned Hf), 2.72 (dt, J=19 Hz, J=10 Hz, 1H, assigned Hf), 2.94 (brd. t., J=9 Hz, 1H, assigned Ha), 3.32 (brd. quart., J=7±1 Hz, 1H, assigned Hd), 4.04 (dd,

J=9.5 Hz, J=7.? Hz, 1H, assigned Hc), 4.26 (t, J=9.5 Hz, 1H, Hb). ^{13}C nmr (75 MHz, in DMSO-d_6): δ 24.4 (CH), 25.3 (CH_2), 27.4 (CH), 36.1 (CH_2), 40.1 (CH), 44.2 (CH), 116.6 (C≡N), 119.2 (C≡N), 215.6 (C=O). Mass spectrum (CI, isobutane): m/e(%) 161(M+1, 100), 82(34), 78(24). Precise mass determination: 160.0633 (observed), 160.0637 (calculated).

Characterisation of 212c. ^{1}H nmr (300 MHz, in DMSO-d_6): δ 1.9 to 2.2 (complex, 2H, assigned He), 2.32 (dddd, J=19 Hz, J= 8.8 Hz, J=4.6 Hz, J= 1.5 Hz, 1H, assigned Hf), 2.63 (dt, J=19 Hz, J=9.3 Hz, 1H, assigned Hf), 3.08 (dd, J=8 Hz, J=4.0 Hz, 1H, assigned Ha), 3.43 (quart. of d., J=7±1 Hz, J=2.4 Hz, 1H, assigned Hd), 3.81 (dd, J=9.3 Hz, J=4.0 Hz, 1H, assigned Hb), 3.91 (dd, J=9.3 Hz, J=6.1 Hz, 1H, assigned Hc). ^{13}C nmr (75 MHz, in DMSO-d_6): δ 25.2 (CH_2), 26.4 (CH), 28.4 (CH), 35.9 (CH_2), 39.3 (CH), 44.9 (CH), 118.4 (C≡N), 118.7 (C≡N), 215.5 (C=O). Mass spectrum (CI, isobutane): m/e(%) 161(M+1, 100), 82(25), 78(17). Precise mass determination: 160.0639 (observed), 160.0637 (calculated).

Characterisation of 212d. ^{1}H nmr (300 MHz, in DMSO-d_6): δ 1.78 (mult., 1H, assigned He), 2.01 (mult., 1H), 2.22 to 2.32 (complex, 2H), 2.81 (brd. t., J=9±1 Hz, 1H, assigned Ha), 3.02 (brd. quart., J=9±1 Hz, 1H, assigned Hd), 4.00 (mult., 2H, assigned Hb and Hc). ^{1}H nmr (300 MHz, in C_6D_6): δ 1.04 (dddd, J=14.8 Hz, J=10.7 Hz, J=9.9 Hz, J=8.7 Hz, 1H, assigned He), 1.54 to 1.86 (complex, 4H, assigned Hf, He, Ha, and Hd), 2.19 (dt, J=1.2 Hz, J=9.5 Hz, 1H, assigned Hc), 2.25 (t, J=9.3 Hz, 1H, assigned Hb), 2.49 (dt, J=19 Hz, J=10 Hz, 1H, assigned Hf). An ^{1}H nmr shift reagent study was carried out in benzene using Eu(fod)$_3$ in order to elucidate the coupling constants to unresolved resonances (see results). ^{13}C nmr (75 MHz, in

DMSO-d_6): δ 23.9 (CH_2), 25.0 (CH), 28.7 (CH), 35.1 (CH), 37.1 (CH_2), 44.6 (CH), 116.4 (C≡N), 117.5 (C≡N), 215.7 (C=O). Mass spectrum (CI, isobutane): m/e(%) 161(M+1, 100), 82(28), 78(19). Precise mass determination: 160.0634 (observed), 160.0637 (calculated).

7.6.5 Preparation of dimers of 2-cyclopentenone.

The preparation of 2-cyclopentenone dimers was carried out in order to obtain a sample for g.c. calibration purposes. Therefore, a solution of 2-cyclopentenone (1.019 g; 12.4 mmol; 0.827 M) in acetonitrile (15 mL) was prepared. This solution was irradiated with acetone filtered light (λ>330 nm) from a 400 W Hanovia medium pressure mercury lamp for 6.5 hours. A g.c. analysis of the reaction mixture indicated that 82% of the 2-cyclopentenone was converted to two dimers which were formed in a 1:1 ratio. The solvent was removed under reduced pressure and the concentrate was subjected to flash chromatography. A flash column containing 80 g of silica gel was eluted with the following mixtures of diethyl ether and hexanes: 500 mL of a 1:4 mixture; 750 mL of a 3:7 mixture; and, 1 L of a 2:3 mixture. The dimers were collected as the column was eluted with the 2:3 mixture of diethyl ether and hexanes. The chromatographic solvent was removed and 0.810 g (4.94 mmol; 80% yield) of white crystalline material was recovered. This solid was composed of the two 2-cyclopentenone dimers in a 1:1 ratio. Since these dimers have previously been identified[15], a full characterisation was not performed; however, the following spectral properties were observed for the 1:1 mixture of dimers. ^{13}C nmr (300 MHz, in $CDCl_3$): δ 27.2 (CH_2), 27.9 (CH_2), 35.5 (CH_2), 36.0 (CH_2), 37.1 (CH), 40.0 (CH), 44.8 (CH),

49.3 (CH), 218.3 (C=O), 219.5 (C=O). Mass spectrum of both dimers was identical (EI, 70 eV): m/e(%) 164(M+, 100), 136(9), 122(10), 108(10), 94(15), 82(40), 81(80), 54(40).

7.6.6 Synthesis of maleonitrile by isomerisation of fumaronitrile.

A solution of fumaronitrile (3.859 g; 0.0494 mol; 0.330 M) and acetophenone (0.905 g; 7.53 mmol; 0.0502 M) in acetonitrile (150 mL) was placed in a Pyrex irradiation tube located in a water bath (T=14°C). The solution was irradiated with light from a 400 W Hanovia medium pressure mercury lamp for 44 hours. The progress of the reaction was monitored by g.c. at regular 4 hour intervals. The steady state ratio of fumaronitrile to maleonitrile was determined by g.c. to be 1.07:1. The solvent was removed under reduced pressure and the concentrate (4.76 g) was loaded on to a column consisting of 310 g of silica gel packed in a 1:1 solution of diethyl ether and hexanes. The column was eluted with 0.8 L of a 1:1 mixture of diethyl ether and hexanes and a fraction consisting of acetophenone and fumaronitrile was collected. The column was then eluted with 1.1 L of diethyl ether and a fraction containing pure maleonitrile was collected. The mixture of fumaronitrile and acetophenone could have been recycled and used to generated more maleonitrile; however, since we were not concerned with maximizing the yield of maleonitrile, this was not done. The fraction containing maleonitrile was concentrated under reduced pressure to reveal a pale yellow solid. This crude product was recrystallised twice from a diethyl ether/hexanes mixture to yield white crystalline maleonitrile (1.85 g; 48% yield; mp= 31-32°C). ^{1}H nmr (200 MHz,

in DMSO-d_6): δ 6.86 (s). ^{13}C nmr (300 MHz, in DMSO-d_3): δ 119.7 (CH), 114.8 (C≡N). Precise mass determination: 78.02168 (observed), 78.02180 (calculated).

7.6.8 Irradiation of 2-cyclopentenone and acrylonitrile in the presence of H_2Se.

A solution containing 2-cyclopentenone (0.210 g; 2.56 mmol; 0.102 M) and acrylonitrile (1.33 g; 25.1 mmol; 1.00 M) in benzene (25.0 mL) was saturated with gaseous H_2Se at room at 10°C ([H_2Se]=0.35±0.05 M). A 10 mL portion of this solution was transferred to a Pyrex irradiation tube and another 10 mL portion was transferred to a flask which was placed in the dark. The contents of the irradiation tube were irradiated with light from a 400 W Hanovia medium pressure mercury lamp for 2 hours. The progress of the dark reaction and the light reaction were monitored frequently by g.c. A coupled g.c.-m.s. analysis of the reaction mixture that was exposed to light revealed that no products representative of trapped biradicals nor any cycloadducts were formed. The only products that were formed in the reaction mixture exposed to light were also formed in the reaction mixture that was kept dark.

7.6.7 Quantum yield determinations for the 2-cyclopentenone plus cyano-alkene photocycloaddition reactions

Fumaronitrile (supplier: Aldrich) and maleonitrile (prepared according to the method described above) were both purified by recrystallisation from hexanes/diethyl ether immediately prior to use. Acrylonitrile (supplier: BDH) and 2-cyclopentenone (prepared according to the method described above) were both distilled immediately prior to use. The concentration of 2-cyclopentenone used in all of the quantum yield

determinations involving cyano-substituted alkenes was 0.0940 M. All of the quantum yields were determined at less than 6% conversion of the reagent (enone or alkene) present in the lowest concentration. A PTI QUANTACOUNT apparatus fitted with a high pressure 100 W mercury lamp and a monochromater (set at 340 nm for all determinations) was used to determine the number of photons absorbed by each sample. The light flux was calibrated using an azoxybenzene actinometer.[4] All samples were degassed by three freeze-pump-thaw cycles after which the residual pressure in the cell was below 1.5×10^{-4} mbar.

The absolute amount of cycloadducts or 2-cyclopentenone dimers formed in each irradiation was determined by g.c. using heptadecane (fumaronitrile and maleonitrile systems) or decane (acrylonitrile systems) as an internal standard. The relative response of the flame ionisation detector to each cycloadduct, the 2-cyclopentenone dimers, and the internal standards was determined by constructing calibration curves using pure samples of each material.[88] It was assumed that regio- and stereoisomeric cycloadducts had the same relative response to the g.c. detector. Each quantum yield of product formation was calculated according to the formula Φ=(moles of product formed)/(Einstiens of light absorbed).

Table 22 (see Chapter 5) summarises the quantum yields of cycloadduct formation that were measured for the photocycloaddition reactions involving 2-cyclopentenone and each of acrylonitrile, fumaronitrile and maleonitrile in acetonitrile. Table 26 (see below) summarises the quantum yields of enone dimer formation that were

---

[88]A pure sample of a acrylonitrile plus 2-cyclopentenone cycloadduct was graciously supplied by Mr. P. Krug of the Weedon group.

determined for the same reactions. Table 27 (see below) summarises the quantum yields of cycloadduct formation that were measured for the photocycloaddition of 2-cyclopentenone with acrylonitrile in benzene.

Table 26: Quantum yields of enone dimer formation for the photocycloaddition reaction of 2-cyclopentenone (0.0940 M) with acrylonitrile, fumaronitrile, and maleonitrile in acetonitrile.

acrylonitrile		fumaronitrile		maleonitrile	
[alkene] M	Φ_{dimers}	[alkene] M	Φ_{dimers}	[alkene] M	Φ_{dimers}
0.0269	0.22±0.03	0.0289	0.12±0.02	0.0394	0.062±0.008
0.0497	0.16±0.02	0.0501	0.079±0.008	0.102	0.035±0.004
0.0665	0.14±0.02	0.0991	0.047±0.005	0.206	0.011±0.002
0.110	0.11±0.03	0.203	0.025±0.003	0.415	0.007±0.001
0.199	0.053±0.006	0.501	0.092±0.009	0.823	0.004±0.001
0.502	0.020±0.003	1.00	0.043±0.005		
1.00	0.011±0.002				

Table 27: Quantum yields of cycloadduct formation for the photocycloaddition reaction of 2-cyclopentenone (0.0940 M) with acrylonitrile in benzene.

acrylonitrile concentration (M)	$\Phi_{adducts}$
0.0253	0.021±0.003
0.0371	0.029±0.004
0.0822	0.066±0.007
0.114	0.089±0.009
0.185	0.12±0.01
0.269	0.15±.02
0.581	0.20±0.02
0.993	0.22±0.02
2.001	0.24±0.03
4.028	0.29±0.03

7.7 References

1. Mihelich, E. D.; Eickhoff, D. J. *J. Org. Chem.* **1983**, *48*, 4135.

2. Watkins, G.R.; Shutt, R., In *Inorganic Syntheses*; Fernelius, W.C. Ed.; New York, 1946, Vol. II; p. 184.

3. Bicyclo[3.3.0]octa-2,8-dione was generously donated by Andreas Rudolph. The compound was prepared according to the method of Duthaler and Maienfisch: see Duthaler, R.O.; Maienfisch, P. *Helv. Chim. Acta*, **1984**, *67*, 856.

4. Bunce, N. J.; LaMarre, J.; Vaish, S. P. *Photochem. Photobiol.* **1984**, *39*, 531.

5. (a) Yamamura, S.; Hirata, Y. *J. Chem. Soc. (C)* **1968**, 2887. (b) Toda, M.; Hirata, Y. *Chem. Comm.* **1969**, 919.

6. Gaufrès, R.; Perez, A.; Bribes, J. L. *Bull Soc. Chim. Fr.* **1971**, 2898.

7. Arnold, A. P.; Canty, A. J. *Inorg. Chim. Acta* **1981**, *55*, 171.

8. Anderson, J. A.; Odom, J. D. *Organometallics* **1988**, *7*, 267.

9. Foster, D. G. In *Organic Syntheses*; J. Wiley, New York, 1955, Coll. Vol. III, p.771.

10. Murahashi, S. I.; Mitsui, H.; Shiota, T.; Tsuda, T.; Watanabe, S. *J. Org. Chem.* **1990**, *55*, 1736.

11. Sayre, R. *J. Am. Chem. Soc.* **1955**, *77*, 6689.

12. Lamchen, M.; Mittag, T. W. *J. Chem. Soc. (C)* **1966**, 2300.

13. Sundholm, F.; Luckhurst, G. R. *Tetrahedron Lett.* **1971**, 675.

14. Singh, P.; Boocock, D. G. B.; Ullman, E. F. *Tetrahedron Lett.* **1971**, 3935.

15. (a) Eaton, P. E. *J. Am. Chem. Soc.* **1962**, *84*, 2344. (b) Eaton, P. E.; Hurt, W. S. *ibid.* **1966**, *88*, 5038. (c) Wagner, P. J.; Bucheck, D. J. *J. Am. Chem. Soc.* **1969**, *91*, 5090.

PART II

PHOTOCHEMICAL REACTIONS IN SUPERCRITICAL FLUIDS

CHAPTER 1

PHOTOFRIES REACTIONS IN SUPERCRITICAL CARBON DIOXIDE

1.1 Introduction to Supercritical Fluids (SCFs)

1.1.1 General properties of SCFs

The supercritical phase is defined by the critical temperature (T_c) of a fluid. Above this temperature, the fluid remains as a homogeneous medium with no phase boundary being present regardless of what pressure is applied to the system.[1] Therefore, the critical temperature denotes the last point on a fluid's vapour pressure curve, above which the pressure on a fluid can be varied without inducing a gas-liquid phase separation. The critical pressure (P_c) of a fluid denotes the last pressure point on the fluid's vapour pressure curve.

The phase diagram for carbon dioxide presented in Figure 16 can be used to illustrate the definitions of the critical pressure and temperature.[2] Starting at the lowest temperature indicated in this figure, the sublimation line rises monotonically to the triple point which defines the temperature and pressure at which all three phases, gas, liquid, and solid, are present. From the triple point (T_t=216.58 K, P_t=5.180 bar),[2] two curves, the melting curve and the saturation vapour pressure curve, rise monotonically. These two curves break the phase diagram into three areas corresponding to the gas, liquid, and solid states. The saturation vapour pressure curve defines the gas-liquid equilibrium phase boundary. This curve ends at the critical pressure and temperature

(T_c=304.21 K, P_c=73.825 bar)[2] indicating that the point defined by this temperature marks the highest temperature at which more than one phase of carbon dioxide can be observed. Table 28 contains a list of the critical temperatures and pressures of the more commonly used supercritical fluids.

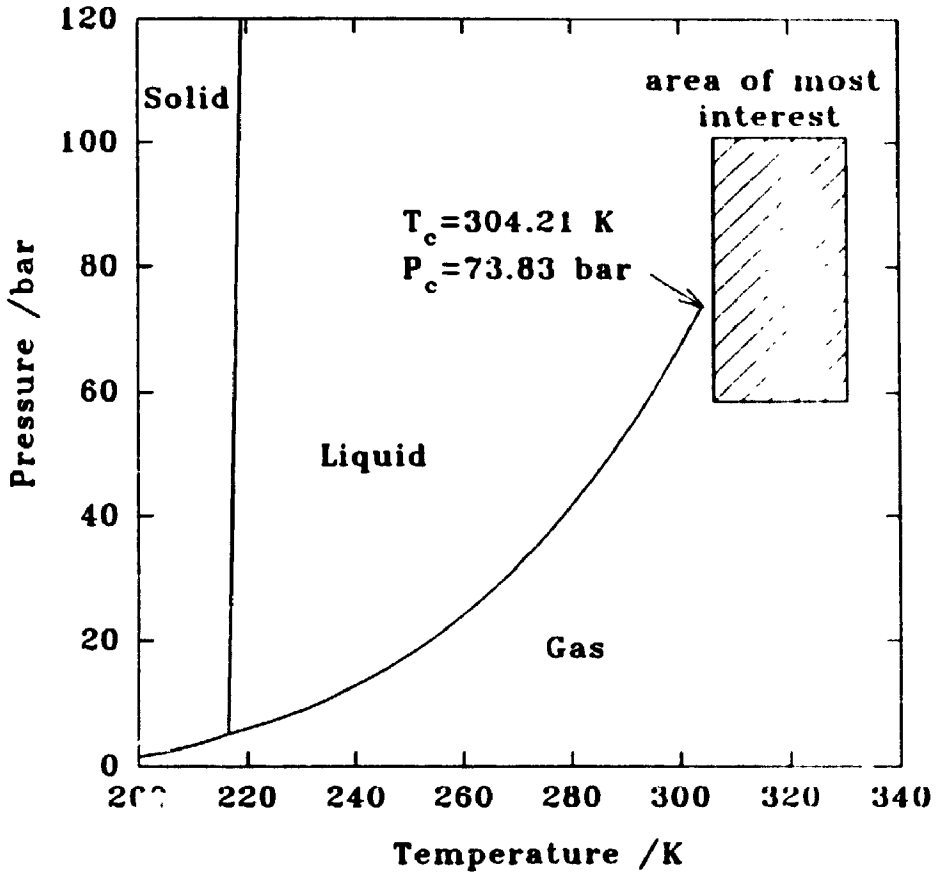

Figure 16: Phase diagram for pure carbon dioxide.

Supercritical fluids are attractive solvents because they offer a means to achieve solvating properties which have gas- or liquid-like characteristics by simply changing the pressure on the system. Moreover, changes in the solvation properties can be induced without causing a phase change to occur. Therefore, a supercritical fluid can be used as

a continuously adjustable medium in which to carry out thermal reactions[3] or chromatographic separations.[4] Small pressure changes can be applied to supercritical fluid solution in order to effect significant changes in the density, viscosity, diffusivity, and dielectric constant of the medium. Table 29 below illustrates how supercritical fluids exhibit properties which are intermediate between those exhibited by gases and liquids.

Table 28: The critical properties of some common fluids.[2,5]

Compound	T_c, K	P_c, bar	ρ_c, g/cm^3
CH_3-CH_3	305.4	48.8	0.229
H_2C=CH-CH_3	365.1	46.0	
CO_2	304.21	73.83	0.466
N_2O	309.6	72.7	0.45
H_2O	647.3	218.3	
CHF_3	298.8	48.4	0.107
NH_3	405.6	112.8	0.24

T_c, P_c and ρ_c represent the temperature, pressure and density, respectively, at the critical point of the fluid.

Table 29: Comparison of the properties of Gases, Liquids and Supercritical Fluids (SCF).[6]

	Gas	SCF	Liquid
Density (g/cm^3)	10^{-3}	0.1-1	1
Diffusion Coeff. (cm^2/s)	10^{-1}	10^{-3}-10^{-4}	$< 10^{-5}$
Bimolecular k_d (L/mol·s)	10^{14}	10^{11}-10^{12}	10^{10}
Viscosity (g/cm·s)	10^{-4}	10^{-3}-10^{-4}	10^{-2}

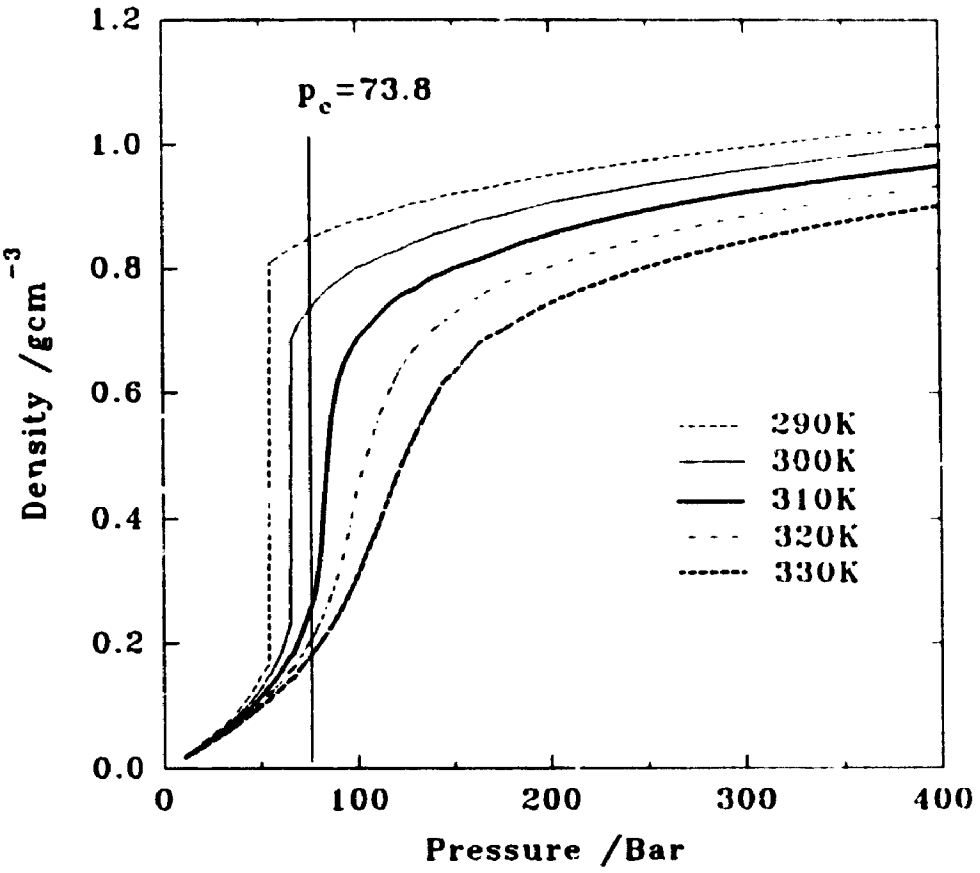

Figure 17: The pressure dependence of the density of pure carbon dioxide at constant temperature.

The pressure dependence exhibited by the density of carbon dioxide along sub-critical isotherms (T=290 K and 300 K) and supercritical isotherms (T=310 K, 320 K, 330 K) is illustrated in Figure 17.[2] The sub-critical isotherms plotted in this figure show discontinuities at the saturation vapour pressure. The gas phase and liquid phase exist in equilibrium at this pressure; therefore, two densities, a liquid density and a gas density, are measurable at this point. Above the critical pressure, the density isotherms are continuous functions which have a single density value at each pressure. The isothermal density-pressure functions in the supercritical region demonstrate that changes in the bulk density of carbon dioxide are most sensitive to pressure variations near the

critical temperature. The increased sensitivity of bulk density to pressure in the critical region is reflected in other properties of carbon dioxide. The diffusion coefficient, dielectric constant, and viscosity all exhibit a pronounced pressure dependence near the critical point. Therefore, when using supercritical carbon dioxide as a reaction solvent one might expect that the most interesting region for study is the region just above the critical point. This region is indicated by the hatched box in Figure 16.

The amount of data published in the literature on reactions carried out in supercritical fluid solvents in rather limited. In fact, almost all of the studies involving an examination of reaction mechanisms in supercritical fluid solvents have been published since the mid-1980's. Most of the investigations in which thermal reactions were studied involve an examination of the effect of pressure on the reaction rate constant. Diels-Alder reactions seem to have attracted the most attention in this regard[7,8,9]; however, the decomposition of α-chlorobenzyl methyl ether[10] and the tautomerisation reaction between 2-hydroxy-pyridine and 2-pyridone[11] have also been studied. On the other hand, some photochemical reactions have also been investigated in supercritical fluids. Examples of photochemical reactions studied in supercritical fluids include the photodimerisation of 2-cyclohexenones[12,13], the photofragmentation of dibenzylketones[14], the photodissociation of iodine[15], the photoisomerisation of diphenylbutadiene[16], the triplet-triplet annihilation process for benzophenone[17], and the dimerisation of excited state singlet pyrene.[18,19] In addition to these photochemical reactions, the literature also contains several examples of investigations involving the study of solvatochromic shifts in the absorbance spectra of solute molecules dissolved in supercritical fluids.[20,21] These particular studies were performed in order to examine

the unique solvation properties of supercritical fluids. The remainder of this introduction will focus in more detail on some of the literature examples mentioned above and explain how the properties of supercritical fluids can be manipulated in order to control reaction rates and product distributions.

The variety of ways in which supercritical fluids affect reaction rates and product distributions can be divided into the following categories: 1. Changes in diffusion rates; 2. Pressure effects on the reaction rate constant; and, 3. Changes in the local solvent density around a solute molecule. Through control of the pressure and temperature of the supercritical fluid solvent, each of these factors can be manipulated so that the outcome of a reaction is modified relative to the outcome in liquid solvents. Examples of reactions which demonstrate effects of these three factors in supercritical fluids are discussed below.

1.1.2 Diffusion rates in SCFs.

The bimolecular rate constant, k_{diff}, for a diffusion controlled reaction, according to Einstein-Smoluchowski diffusion theory, is given by the Stokes-Einstein equation:

$$k_{diff}(M^{-1}s^{-1}) = \frac{8000RT}{0.3\eta} \qquad (23)$$

where R is the gas constant (J $mol^{-1}K^{-1}$), T is the temperature (K), and η is the fluid viscosity (poise).[22] The viscosity of supercritical fluid solutions at various pressures and temperatures can be used to calculate the maximum rate for a diffusion controlled process using this equation. Chateauneuf and co-workers[17] used this equation and the viscosity

data available for carbon dioxide[23] to calculate k_{diff} at different pressures and temperatures near the critical point. Their calculations revealed that at T=35°C k_{diff} increases from $1.3x10^{11}$ L $mol^{-1}sec^{-1}$ to $3.5x10^{11}$ L $mol^{-1}sec^{-1}$ when the supercritical carbon dioxide pressure is decreased from 85 to 70 bar. These calculated rate constants for the diffusion are consistent with the values obtained from measured diffusion (D) coefficients for naphthalene in supercritical carbon dioxide.[24]

Chateauneuf and co-workers also used flash photolysis techniques to measure rate constants for the triplet-triplet annihilation (TTA) process of triplet benzophenone and the self-termination reaction of the benzyl radical ($PhC\bullet H_2$). These reactions were chosen for investigation by Chateauneuf and co-workers because the TTA process of benzophenone[25] and the self-termination of the benzyl radical[26] have both been shown to occur at diffusion controlled rates in condensed liquid solution. In supercritical CO_2,[17] ethane,[17] and CHF_3[27] the rates of these two process, when corrected by the appropriate statistical spin factor, were found to be very similar to the diffusion controlled rates calculated according to the Stokes-Einstein equation. These results indicated that the diffusion limiting reaction rate constant in supercritical fluid solvents is at least an order of magnitude greater than that in liquid solvents. Thus rate constants can be manipulated in supercritical fluid solutions by pressure perturbations in order to control diffusion limited reactions.

1.1.3 Pressure effects on reaction rate constants in SCFs

Pressure is a thermodynamic state property and its effect on the reaction rate constant can be explained in terms of transition state theory.[28] In transition state theory,

the reactant molecules (A and B) are in equilibrium with the transition state ($TS^{\ddagger}$) from which the products are formed directly. The pressure effect on a bimolecular reaction, within the context of transition state theory, depends on the change in molar volume that occurs upon formation of the $TS^{\ddagger}$ from the reactants. That is,

$$RT\frac{\partial(\ln k_{rxn})}{\partial P} = -\Delta V^{\ddagger} - RTk_T \qquad (24)$$

where k_{rxn} is the bimolecular rate constant, $\Delta V^{\ddagger} = V_{ts}-V_A-V_B$ (V_i is a partial molar volume), and k_T is the isothermal compressibility. In liquid solutions, partial molar volumes are usually small (5 to 10 cm^3mol^{-1}); however in supercritical solutions, very large and negative partial molar volumes are not uncommon (vidi infra). Therefore, in supercritical fluids the effect of pressure on the rate of reactions can be large.

There are a few thermal reactions which have been studied in supercritical fluids in order to investigate pressure effects. One of the first studies to find a dramatic pressure effect involved an investigation of the Diels Alder reaction of isoprene and maleic anhydride in supercritical carbon dioxide.[7] In this study, Paulaitis and Alexander observed a two-fold increase in the rate constant at 35°C over a 10 bar increase in pressure near the critical point. This observation indicates that the activation volume for the reaction must be negative and relatively large.

There have been additional investigations of Diels-Alder reactions in supercritical carbon dioxide using infra-red spectroscopy.[8,9] In this work, Ikushima and co-workers examined the catalyzed reaction of isoprene and maleic anhydride[8] and the uncatalyzed

reaction of isoprene with methyl acrylate.[9] The rate of each reaction was found to increase with increasing pressure. In the case of the former reaction, an activation volume of approximately -800 cm^3mol^{-1} was calculated. In addition to the pressure effects on the reaction rate constants, dramatic changes in the product ratios were also observed for each reaction near the critical point of the supercritical solvent. It was suggested by Ikushima and co-workers that strong interactions between the solvent and transition state, caused by an aggregation of solvent molecules around the transition state, might favour the formation of some isomers over others. The concept of increased local solvent densities around solute molecules in supercritical fluids is address in section 1.1.4 below.

In another study involving the investigation of pressure effects on reaction rate constants, Johnston and Haynes[10] examined the decomposition of α-chlorobenzyl methyl ether in supercritical 1,1-difloroethane. In this study, a seven-fold decrease in the rate constant for the decomposition reaction as the pressure was dropped by 14 bar near the critical point. This latter change in the reaction rate constant corresponds to an activation volume of -6000 cm^3mol^{-1} which is one of the lowest activation volumes measured for a reaction carried out in a supercritical fluid.

In general, pressure effects on the rate constants of reactions carried out in the supercritical phase are difficult to predict, or even rationalise once they have been observed. In order to make such predictions, one must have knowledge of the characteristics of the transition state as well as knowledge of the partial molar volumes of the reacting molecule(s). Obviously, in many cases the characteristics of the transition state are not well understood. On the other hand, it is also very difficult to accurately

calculate the partial molar volumes of solute molecules in the highly compressible region near the critical point of a supercritical fluid. Since the partial molar volumes of reactant molecules make up the activation volume for a reaction, a lack of information regarding these properties means that it is very difficult to make an accurate prediction of the effect of pressure on the reaction rate constant.

1.1.4 Local density fluctuations in SCFs

In recent years, a lot of attention has been directed towards the phenomenon of increased local density around solute molecules in supercritical fluids. In terms of photochemical reactions and photophysical studies, this phenomenon is probably the most studied and yet least understood aspect of supercritical fluids.

There is a number of theoretical studies which suggest that the environment around a solute molecule is continuously enriched with solvent relative to the bulk solution near the critical point of a supercritical fluid.[29,30,31] A crude model which may be used to conceptualize this phenomenon is shown in Figure 18. This figure illustrates how the solvation sphere around a solute molecule is dramatically enhanced near the critical point. However, it is important to note that theoretical studies indicate that these "solvent clusters" do not have a finite structure; rather, they are dynamic in nature. The studies conducted by Petsche and Debenedetti[30] suggest that the solvent clusters lose their identity after a few picoseconds. At present, there is very little theoretical information available which would allow one to development of a more comprehensive model that describes these local density fluctuation in more detail.

The concept of "solvent clustering" about solute molecules dissolved in

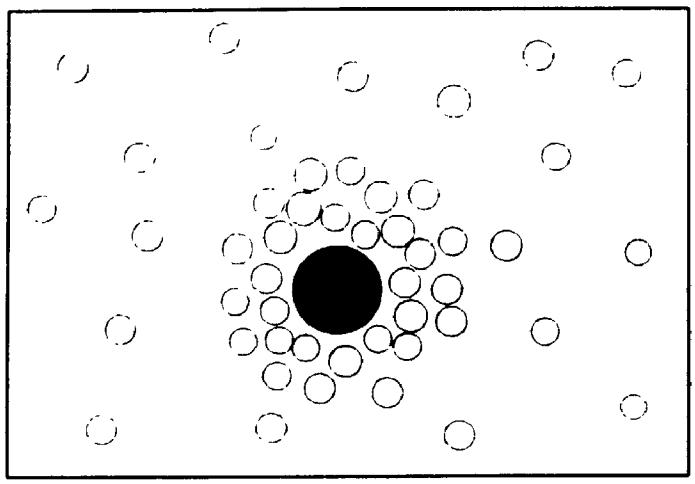

Figure 18: Pictorial representation of solvent clustering around a solute molecule in a supercritical fluid just above the critical point.

supercritical fluids was first postulated in order to explain the very large and negative partial molar volumes that are observed for solutes dissolved in supercritical fluids at infinite dilution.[32,33] Eckert and co-workers[32,33] measured the partial molar volume at infinite dilution for solutions of naphthalene, camphor, or tetrabromomethane dissolved in supercritical CO_2 and ethene. The partial molar volume of naphthalene dissolved in supercritical carbon dioxide at 35.2°C is quite insensitive to pressure above 110 bar and remains relatively constant at approximately 50 to 100 cm^3mol^{-1}. However, the partial molar volume for this solute drops rapidly as the pressure is reduced near the critical point. Upon decreasing the pressure from 105 to 80 bar, the observed partial molar volume of naphthalene decreases from -120 to -8000 cm^3mol^{-1} for this system. A large negative partial molar volume for a solute in solution means that addition of a very small amount of the solute to a large amount of solvent results in a significant decrease in the total volume of the system relative to the sum of the volumes of the solute and solvent

before mixing. One interpretation of large negative solute partial volumes is that the solute causes local disturbances in the three dimensional structure of the fluid solvent so that areas of local density enrichment develop.

The majority of the early investigations of solvent cluster formation in supercritical fluids involved the use of steady-state solvatochromic absorbance measurements of well known chromophores.[20,21] In these experiments, local densities were recovered by comparing the observed spectral shifts of the dissolved tracer at different bulk solvent densities with that expected for a homogeneous polarizable fluid. Evidence for solvent clustering was obtained from these experiments when local densities were compared with the expected values based on the linear McRae continuum model.[14] It was found that the local solvent densities recovered from this treatment were much larger than the bulk density of the solution.

Steady state fluorescence spectroscopy has also been used to investigate the effects of clustering in supercritical fluids on twisted intramolecular charge transfer excited state formation. Johnston, Fox, and co-workers[35,36] investigated the solute-solvent interactions of p-(dimethylamino)benzonitrile and ethyl p-(dimethylamino)benzoate in mixtures of supercritical CHF_3 and CO_2 using fluorescence spectroscopy. In these investigations the relative contributions of the twisted intramolecular charge transfer (TICT) state and the locally excited singlet state (LE) to the fluorescence emission spectrum were determined at various bulk solven densities. In addition, an Onsager field treatment was applied to the bathochromic and hipochromic spectral shifts of the TICT fluorescence spectrum at different solvent densities. The results of these investigations indicated that the local solvent density around molecules in the TICT state

is greater than the bulk solvent density in density regions just above the critical point of the supercritical fluid.

Scheme 74

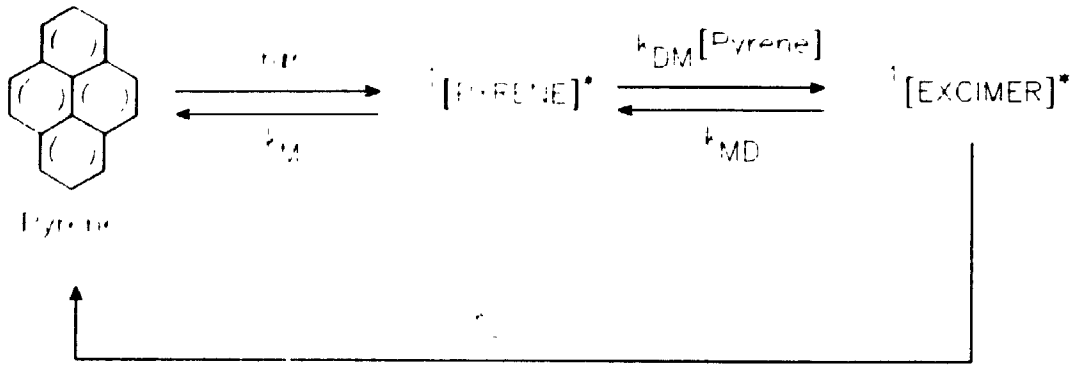

The unique fluorescence characteristics of pyrene emission have also been studied in supercritical fluids. Pyrene, which exists as a monomer in the ground state, is known to form a singlet excited state dimer (excimer) in solutions of relatively high concentration (millimolar range or higher).[37] This dimer exists in equilibrium with the singlet excited monomer. Scheme 74 summarises the photophysics of the singlet excited state pyrene monomer as well as those of the excimer.

Brennecke and co-workers[18] have reported a study of the steady state fluorescence spectra of the pyrene monomer and excimer in supercritical CO_2, ethene, and CHF_3. In this investigation, it was found that excimer formation starts to occur in the low micromolar concentration range which is much lower than the concentration required to observe excimer emission in condensed liquid solution. Also, the intensity of excimer emission relative to monomer emission increased as the bulk density of the supercritical solvent decreased and approached the critical density. These observations were explained

in terms of increased pyrene-pyrene interactions near the critical point.

Bright and co-workers[19] studied the pyrene system using time resolved techniques and were therefore able to measure rate constants for decay of the monomer (k_M), decay of the excimer (k_D), formation of the excimer from the monomer (k_{DM}), and formation of the monomer from the excimer (k_{MD}) in supercritical fluids. In the case of supercritical CO_2, the variation with pressure of the rate constant k_{DM} followed the same trend as the calculated maximum rate constant for diffusion. The rate constant k_M changed little as the pressure was varied; on the other hand, the rate constants k_{MD} and k_D decreased substantially (three and seven fold respectively) as the pressure was decreased by less than 5 bar near the critical point. These data were interpreted in the context of a solvent clustering model in which the pyrene excimer is effectively shielded from radiative decay by the increased local density of solvent molecules around the excimer. The data also excluded the possibility of an increased rate of eximer formation due to pre-association of ground state pyrene molecules in a solvent cluster since the rate of formation of the excimer was shown to be diffusion controlled.

There is a very limited number of examples in the literature in which the phenomenon of solvent clustering in the near-critical region has been shown to influence photochemical reactions directly. In the few examples that do seem to show a manifestation of local solvent density enrichment, the evidence in support of mechanistic perturbations that are brought about by solvent clustering is either weak or indirect at best. For example, the pressure dependence of the quantum yield of product formation in the photodimerisation of 2-cyclohexenone (see Scheme 75) was investigated by Combes *et al* in supercritical carbon dioxide.[12] In this study, it was found that the

relative quantum yield of 2-cyclohexenone dimer formation increased sharply as the pressure was decreased near the critical point. This increase in quantum yield was attributed to an increase in the rate at which encounters between triplet enone and ground state enone occur. An increase in solute-solute interactions facilitated by clustering in the near-critical region was proposed as a reasonable explanation for the apparent increase in rate. The head-to-head dimer to head-to-tail dimer (HH/HT) ratio also increased sharply near the critical point. This increase in the HH/HT ratio was attributed to an increase in the polarity of the local environment around the triplet excited enone caused by solvent clustering. This explanation is consistent with the liquid phase investigations of the photodimerisation reaction in which the HH/HT ratio increases with increasing solvent polarity.

Scheme 75

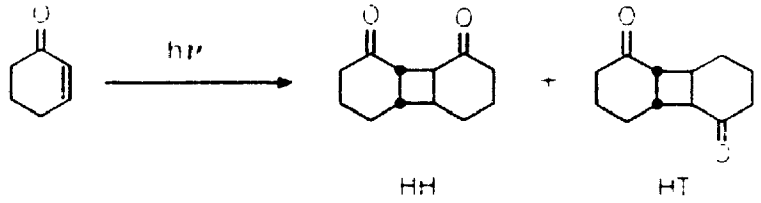

Scheme 76

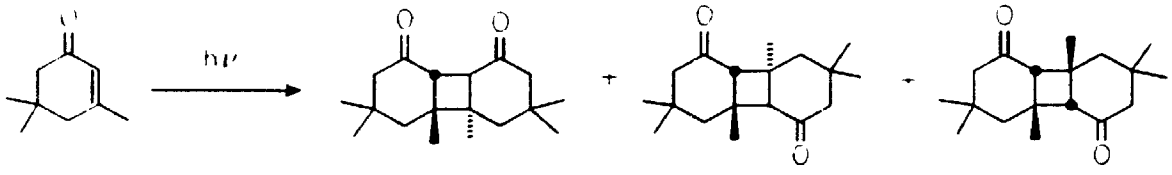

In a similar study, Fox, Johnston and co-workers[13] observed pressure dependent variations in the product distribution obtained from the photo-dimerisation of isophorone (see Scheme 76) in supercritical carbon dioxide and CHF_3. The changes in the product ratios observed in these experiments were interpreted in terms of the need for reorganisation of solvent molecules in the solvation sphere around an excited enone and ground state enone encounter pair. The solvent molecule reorganisation required for the formation of certain configurations of the encounter pair was considered to be less than that required for other configurations, and so, on the basis of entropy arguments, the formation of certain stereoisomers were considered to be more favourable. However, in both of these studies of the photodimerisation of cyclic enones,[12,13] the concepts of 1,4-biradical formation, reversion and closure (see Part I of this Thesis) were not explicitly considered. By ignoring the mechanistic implications of medium-induced variations in the rates of all of these processes, the authors of these studies also ignored many other possible explanations for their observations.

So far, the only example of a supercritical phase photochemical reaction that appears to provide direct evidence *against* the formation of solvent clusters in the near-critical region of a supercritical fluid is the photofragmentation reaction of unsymmetrically substituted dibenzyl ketones.[14] This reaction was investigated by Fox, Johnston, and co-workers who studied the photolysis of 1-(4-methylphenyl)-3-phenyl-2-propanone in supercritical carbon dioxide at various pressures. It was observed that the benzyl radical recombination products formed after fragmentation and decarbonylation represented the statistical distribution expected for an out-of-cage reaction (see Scheme 77). The 1:2:1 statistical distribution was observed at all pressures, even in the

Scheme 77

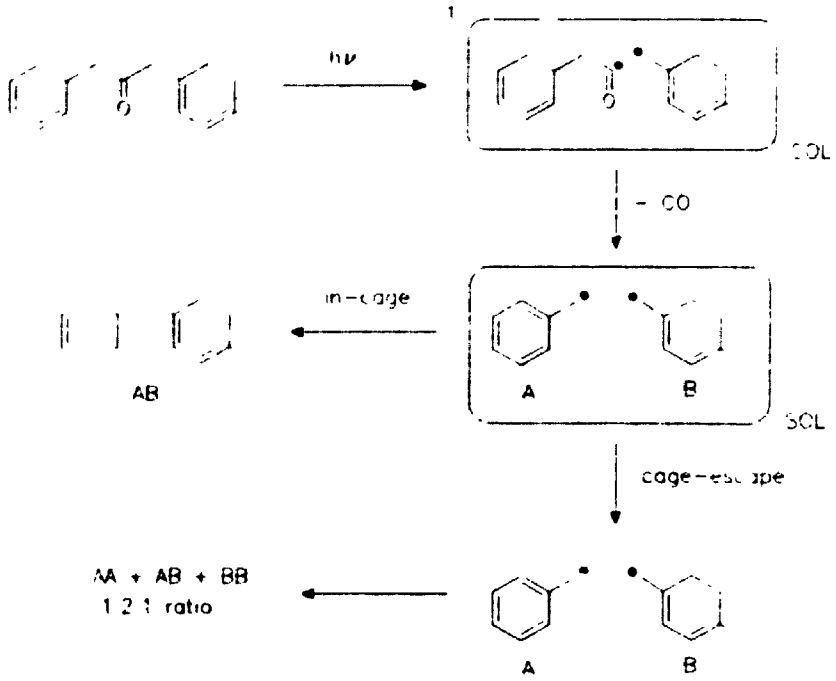

near critical region. These data indicate that an enhanced cage effect is not present at the critical point and the authors argue that this is evidence against the existence of solvent clusters. However, the time scale over which this reaction occurs could be much longer than the dynamic lifetime of solvent clusters. The rate constant for the decarbonylation step in the photolysis of 1,3-diphenylacetone in supercritical carbon dioxide solutions at 35°C was measured by Roberts and co-workers[17] and found to be between 1.8×10^7 and 2.5×10^7 sec^{-1} for the pressure region of 78 to 105 bar. Therefore, the results published by Fox, Johnston and co-workers[14] do not explicitly exclud the formation of solvent clusters in the near-critical region; rather, these data indicate that lifetime of the solvent cluster, if it exists, must be shorter than approximately 10 to 50 nanoseconds.

1.2 Initial goals of the investigations into SCF phase photochemical reactions

In 1992, it was decided that the Weedon research group would enter the field of supercritical fluid phase photochemistry given the relatively small amount of work published in the area at that time and the high potential for exploiting some of the advantageous, but little understood, properties of supercritical fluid solvents. The initial task when the work in supercritical phase photochemistry began was to identify a photochemical system which could be used to exploit one or more of the potential advantages supercritical fluids offer over traditional solvents. Specifically, a photochemical reaction which is sensitive to changes in solvent polarity, solvent viscosity and density, or dependent on the limiting rate of diffusion was required in order to study the special properties exhibited by supercritical fluids. It was also required that the changes induced in the photochemical reaction by applying perturbations to the reaction solvent should be observable in the product distribution of the reaction. The latter condition was imposed because of equipment limitations.

In the first experiments, the only way of characterising any solvent induced effects on a particular photochemical system was to monitor any changes in the relative yields of the reaction products by analytical methods such as nmr spectroscopy or coupled gas chromatography-mass spectrometry. No equipment for measuring changes in quantum yields, transient lifetimes, or variations in absorbance or emission spectra was adapted and coupled with the supercritical fluid photochemical reactor. It was decided that the initial goal of the project would be to find a quantifiable change in a photochemical reaction in a supercritical fluid solvent, and thereby learn about the particular design and operational aspects of a supercritical fluid photochemical reactor. Modification and

adaptation of specialised photophysical equipment for use in monitoring supercritical phase photochemical reactions spectroscopically was left for future investigations.

1.3 Design of the Supercritical Fluid Photochemical Reactor

The supercritical fluid photochemical reactor was designed to operate at pressures up to 400 bar (5800 psi) and at temperatures between ambient and 70°C. The general design of the system is presented in Figure 19. The system can be divided into four major components: the fluid supply component, the recirculation pump, the sampling system and the optical cell. The design details of each of these components are given in the experimental section. The function of each component as it applies to the general operation of the reactor system is described below.

The fluid supply cylinders shown in Figure 19 supply carbon dioxide to the apparatus through a heat exchanger or a chiller. The function of the chiller is to ensure that carbon dioxide is in the liquid phase and not the gaseous phase when it enters the pump. Fluid exiting the heat exchanger encounters a check valve, a particulate filter, and then the pump. From the pump the system plumbing leads to a vent valve, through which the system can be evacuated, and then to a rupture disc. The rupture disc acts as a safety device. Above a pressure of 424 bar this disc was designed to fracture and thereby release the pressurised contents of the system. Initially, a second safety device, a variable pressure relief valve, was also connected to the system; however, this device was later removed from the system because it was suspected that soft buna-N rubber seals in this device were contaminating the system. After the rupture disc, the system leads to a 2-position 6-port sampling valve. This valve operates in the same way as an

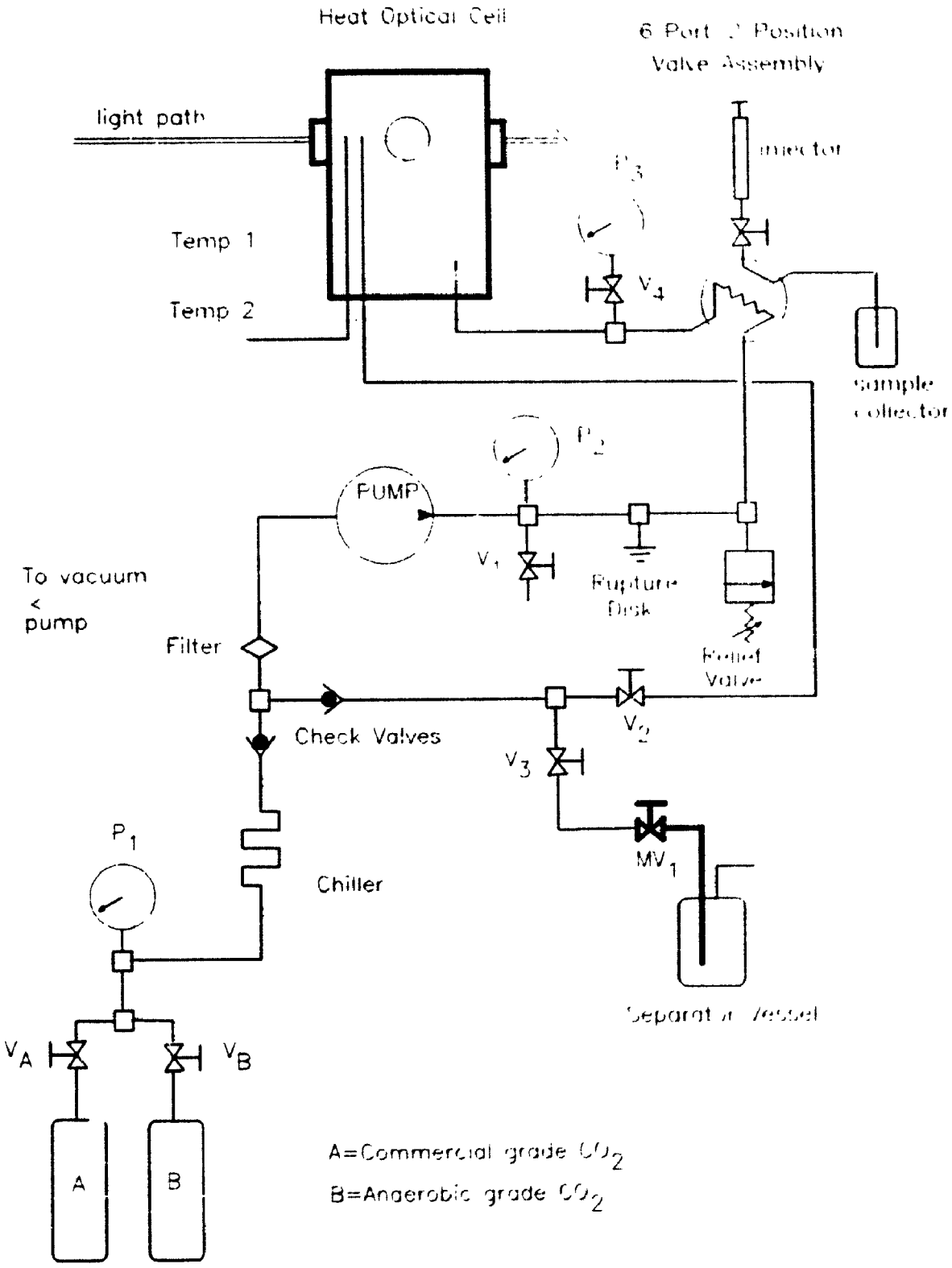

Figure 19: Schematic of the Supercritical Fluid Photochemical Reactor.

HPLC injection valve, with the minor difference being that in this particular application the valve was used both to inject material into the system as well as to take samples out of the system. The sampling and injection procedures are described in the experimental section.

The optical cell is located in the fluid flow just after the sampling valve. The temperature of the optical cell is controlled by a heating band wrapped around the outside of the cell. The contents of the optical cell were irradiated through quartz windows. The high pressure optical cell is described in detail in the experimental section. The fluid flow leaving the optical cell is controlled by a shut-off valve which is labelled V_2 in Figure 19. In order to charge the system with carbon dioxide, this valve is closed so that the pump can pressurise the contents of the system with fluid drawn out of the supply cylinders. Once the desired pressure is reached, V_2 is opened and the contents of the system enter a recirculation cycle.

The pressure in different parts of the system is measured with three pressure gauges. The gauge labelled P_1 in Figure 19 measures the pressure inside each of the supply cylinders. When the supply cylinders are full, this pressure is typically 57 bar. The pressure inside the recirculation loop is measured by pressure gauges P_2 and P_3. The accuracy and specifications of these gauges are described in the experimental section.

Depressurisation of the system is accomplished by opening the shut-off valve labelled V_3 and letting the contents of the system bleed past the micrometering valve labelled MV_1. The purpose of the metering valve is to facilitate a controlled pressure release from the system by offering a variable flow restriction. The micrometering valve is heated because of the Joule-Thompson cooling effect caused by the pressure drop

across the valve. Valve MV_1 and the downstream tubing are emboldened to indicate that these components are surrounded by heating tape.

1.4 Results and Discussion

1.4.1 Preliminary experiments

The first photochemical reaction to be investigated in supercritical carbon dioxide was the Photo-Fries reaction of phenyl esters. The photochemical reaction of phenyl esters in condensed liquid solution results in the formation of products similar to the those formed in ground state Fries rearrangements (see Scheme 78).[18] In addition to the rearrangement products, the Photo-Fries reaction of these compounds is also accompanied by the formation of significant amounts of phenol.

Scheme 78

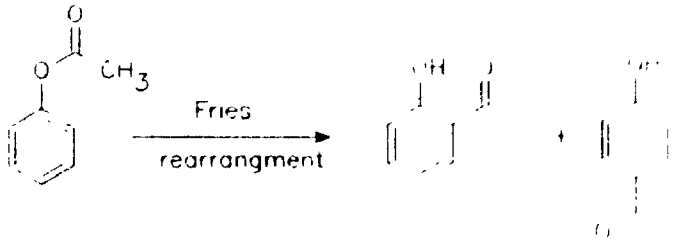

The mechanism by which the Photo-Fries rearrangement of phenyl esters proceeds has been well studied since Anderson and Reese[38a] first observed the reaction in 1960. It is now generally accepted that the reaction is non-concerted and proceeds by O-acyl bond homolysis, followed by recombination of the resulting radical pair. The involvement of the phenoxyl radical in the Photo-Fries rearrangement of phenyl acetate mechanism has been confirmed by the detection of this radical as well as a transient

cyclohexadienone in flash spectroscopy experiments.[39] The excited state responsible for the formation of the rearrangement products observed in the irradiation of phenyl acetate was identified as a singlet since various triplet sensitisers and quenchers have no effect on the rearrangement.[39,40] Other studies also indicate that the formation of the [1,3] rearrangement product (i.e. the *ortho* product) occurs from the $S_1(n,\pi^*)$ state.[41]

Scheme 79

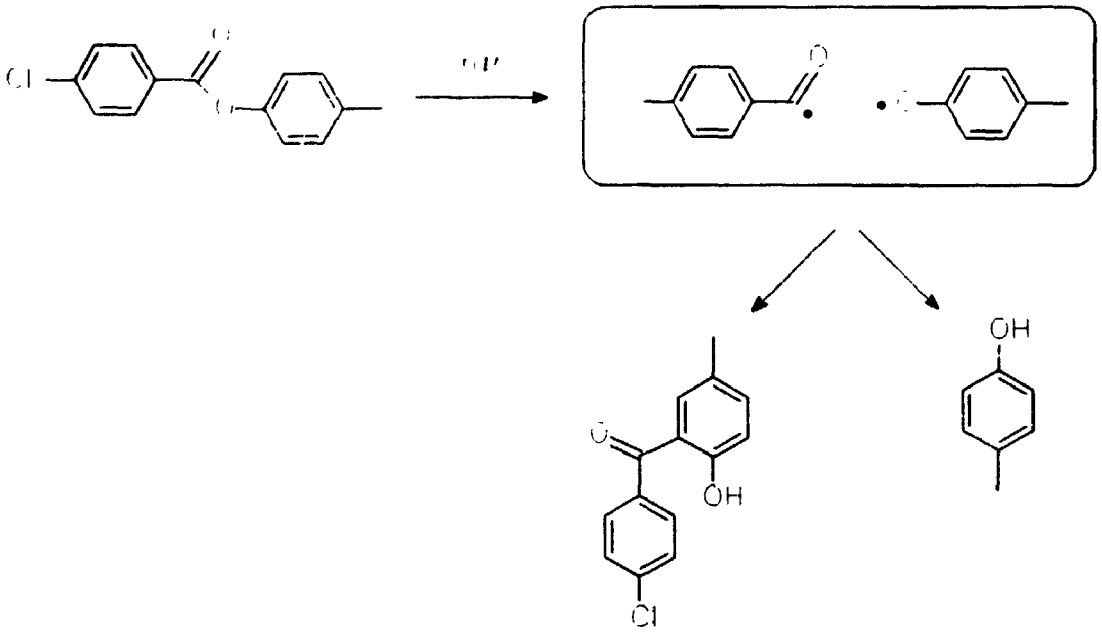

The involvement of a singlet radical pair in the Photo-Fries rearrangement of 4-methylphenyl 4-chlorobenzoate to 2-[4-chlorobenzoyl]-4-methylphenol was confirmed in Chemically Induced Dynamic Nuclear Polarisation (CIDNP) experiments.[42] This reaction is shown in Scheme 79. From the net polarisation measurements, and from the ESR parameters for each of the 4-chlorobenzoyl and 4-methylphenoxyl radicals, it was deduced that a singlet radical pair must be responsible for the observed CIDNP in the photolysis of this compound. Based on this result, it is very probable that the singlet

radical pair is formed by direct homolytic cleavage of the singlet excited state. In addition to the rearrangement product, photolysis of 4-methylphenyl 4-chlorobenzoate also results in the formation of a small amount of 4-methylphenol.

Scheme 80

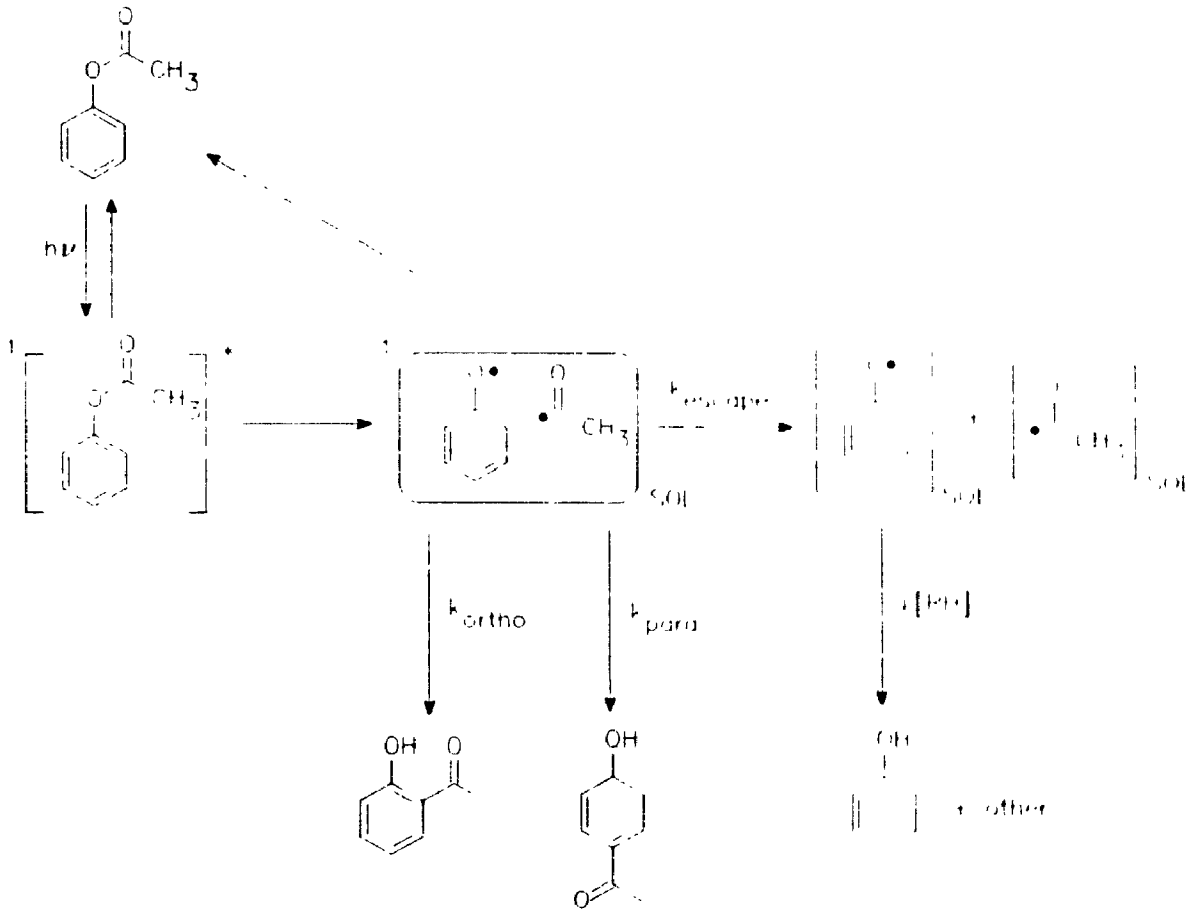

A general mechanism for the Photo-Fries rearrangement of phenyl acetate which is consistent with all of the experimental results described above is presented in Scheme 80. This scheme illustrates the involvement of the singlet excited state in the O-acyl homolysis of the starting material and the radical pair that results from this homolysis. The formation of phenol occurs when the singlet radical pair diffuses out of

the solvent cage and abstracts a hydrogen from an appropriate hydrogen donor which could be either the solvent or the phenyl ester starting material.

The Photo-Fries reaction of phenyl esters was chosen for investigation in supercritical carbon dioxide solution for the following reasons. First, the ratio of the yield of the 4-phenyl substituted rearrangement product to the yield of the 2-phenyl substituted rearrangement product is known to be sensitive to solvent and therefore could be used to probe how the solvent properties of a supercritical fluid change with pressure. Secondly, the relative amount of phenol which results from the radical pair escaping the solvent cage is also sensitive to the reaction environment. For example, in a solid polyethylene matrix phenols were not observed after irradiation of substituted phenyl benzoates.[43] At the other viscosity extreme, in the gas phase, phenol was the major product when phenyl acetate was irradiated.[44] In another study, the quantum yield of phenol formation from the photolysis of phenyl acetate decreased from 0.09 in 2-propanol (viscosity = 1.73 cP) to 0.02 in Carbowax 600 (viscosity = 109 cP) for the photolysis of phenyl acetate while the ratio of the quantum yield of formation of 2-acetylphenol to the quantum yield of formation of 4-acetylphenol changed from 1.4 in ethanol to 6 in hexane.[45]

These medium induced changes in the product distribution obtained from the Photo-Fries reaction of phenyl esters have been interpreted in terms of the strength of the solvent cage that holds the singlet radical pair together after homolytic cleavage of the singlet excited state. Therefore, it was postulated that the viscosity changes that can be effected by varying the pressure on a supercritical fluid at a constant temperature could be used to alter the product distribution resulting from the Photo-Fries reaction of

phenyl esters.

The first phenyl ester that was studied in supercritical carbon dioxide was 4-methylphenyl acetate. This compound was chosen as a test compound because the substitution at the 4-position was expected to produce a very simple product distribution consisting of 4-methylphenol and 2-acetyl-4-methyl-phenol (see Scheme 81). However, when a 4.07×10^{-3} M solution of this compound was irradiated in the supercritical carbon dioxide at 100 bar and 40°C with a 100 watt high pressure mercury lamp for 10 hours, no 4-methylphenol or rearrangement product were observed. In a separate experiment, a 4.15×10^{-3} M solution of 4-methylphenyl acetate in methanol was added to the supercritical fluid reactor at atmospheric pressure and 40°C. This methanol solution was irradiated with the same 100 watt high pressure mercury lamp for 10 hours and the reaction mixture analyzed by g.c.; this indicated that less than 3% of the starting material was converted to products. The very low conversion observed in the methanol solution as well as the lack of reactivity observed in the supercritical carbon dioxide solution using the same lamp set-up was probably due to the fact that the spectral output of the lamp in the region where phenyl ester absorbs light was very low.

Scheme 81

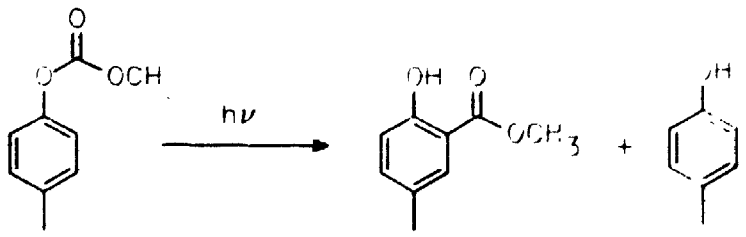

The output of the 100 watt high pressure mercury lamp below 290 nm is less than 4% of its total output and the λ_{max} for 4-methylphenyl acetate occurs at 266 nm (ϵ=500) with very little light being absorbed above 275 nm. Normally, this would not be a problem since the photochemistry could be carried out in a Rayonet photochemical reactor which uses low pressure mercury lamps that emit more than 99% of their light at 254 nm. However, these are large unfocussable light sources, and thus the design and size of the windows in the pressure cell of the supercritical reactor made the use of the Rayonet impractical. Since no focusable short wavelength light source was available for use in conjunction with the supercritical fluid photochemical reactor, the Photo-Fries rearrangement of an alternative compound with a longer wavelength absorption band was investigated.

The next compound to be investigated was N-ethoxycarbonylindole (ECI). This compound has an appropriate absorption spectrum for irradiation with a 100 watt high pressure mercury lamp since it absorbs out to 300 nm. The Photo-Fries rearrangement of this compound, which is shown in Scheme 82, has already been investigated in different solvents and the rearrangement products have been characterised.[46] The products resulting from the Photo-Fries rearrangement of ECI correspond to the 3-, 4- and 6-ethoxycarbonyl substituted indoles with the 3-substituted indole being the major product.[46] In a preliminary investigation, a 2.05×10^{-3} molar solution of ECI in supercritical carbon dioxide at 95 bar and 40°C was irradiated with light from the 100 watt high pressure mercury lamp for 10 hours. The reaction mixture was analyzed by g.c. and it was determined that less than 0.5% of the starting material was converted to Fries-rearrangement products. In a separate experiment, the supercritical fluid reactor

was filled with a 1.98×10^{-3} molar solution of ECI in methanol (atmospheric pressure, 40°C) and irradiated with the 100 watt high pressure mercury lamp for 10 hours. A g.c./m.s. analysis of the reaction mixture indicated that approximately 15% of the ECI starting material was converted to rearrangement products and indole.

Scheme 82

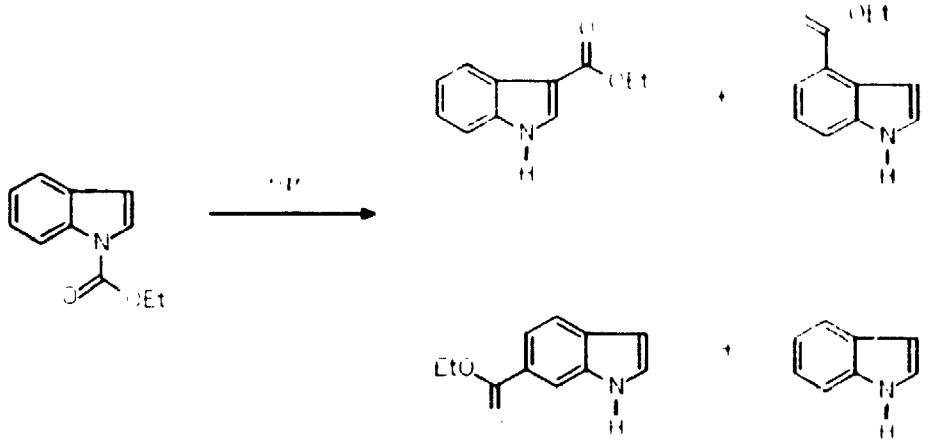

The lack of photochemical reactivity observed for the supercritical carbon dioxide solution containing ECI indicates that the quantum efficiency of the Photo-Fries rearrangement in the supercritical fluid is much lower than it is in methanol. This suggests that the supercritical fluid is acting as a non-polar medium since Oldroyd and Weedon[46] demonstrated that the Photo-Fries quantum yield for ECI in methanol is larger than it is in hexane. In order to generate any significant amount of rearrangement product in the supercritical phase Photo-Fries reaction of ECI, very long irradiation periods would be required. This was not practical with the apparatus available since maintaining a constant pressure in the supercritical fluid reactor for more than 24 hours with the recirculation pump running was very difficult. The extended wear on the pump

shaft seal during long reaction times made the elimination of leaks impossible. Therefore, we began to search for other compounds which might exhibit a much higher quantum yield of Photo-Fries product formation in supercritical carbon dioxide. This search lead to an investigation of Photo-Fries reaction of 1-naphthyl acetate in supercritical carbon dioxide which is described below.

1.4.2 Photo-Fries reaction of 1-naphthyl acetate in supercritical carbon dioxide

The products obtained from the Photo-Fries rearrangement of 1-naphthyl acetate in ethanol solution have been characterised by Ohto et al.[47] The rearrangement in this solvent results in the formation of 2-acetyl-1-naphthol, 4-acetyl-1-naphthol and 1-naphthol in a 1:0.65:0.44 ratio. Crouse et al.[48] have also studied the products resulting from the Photo-Fries rearrangement of 1-naphthyl acetate as well as other substituted naphthyl acetates for the purpose of developing a new synthetic route to 2-acylnaphthoqinones.

The external magnetic field effects on the Photo-Fries rearrangement of 1-naphthyl acetate were studied in different solvents by Nakagaki et al.[49] In these mechanistic studies, Nakagaki and coworkers were able to observe the transient absorption spectrum of the 1-naphthoxyl radical when 1-naphthyl acetate was subjected to laser flash photolysis. The presence of this transient was taken to mean that irradiation of 1-naphthyl acetate results in the homolytic cleavage of the C-O bond, and that a radical pair consisting of the 1-naphthoxyl radical and the acetyl radical exists as a precursor to the formation of the rearrangement products. The in-cage radical pair was assigned as a singlet pair based on the fact that the presence of an external magnetic field resulted in increasing the yield of the in-cage products resulting from the radical

pair.[49,50] This conclusion is supported by a comment in a review by Bellus[51] that high energy triplet sensitisers do not sensitise the photorearrangement of 1-naphthyl acetate thus implying that the radical pair is produced from the singlet excited singlet state of the ester. A mechanism for the Photo-Fries reaction of 1-naphthyl acetate which takes into consideration all of the mechanistic details described above is presented in Scheme 83.

Scheme 83

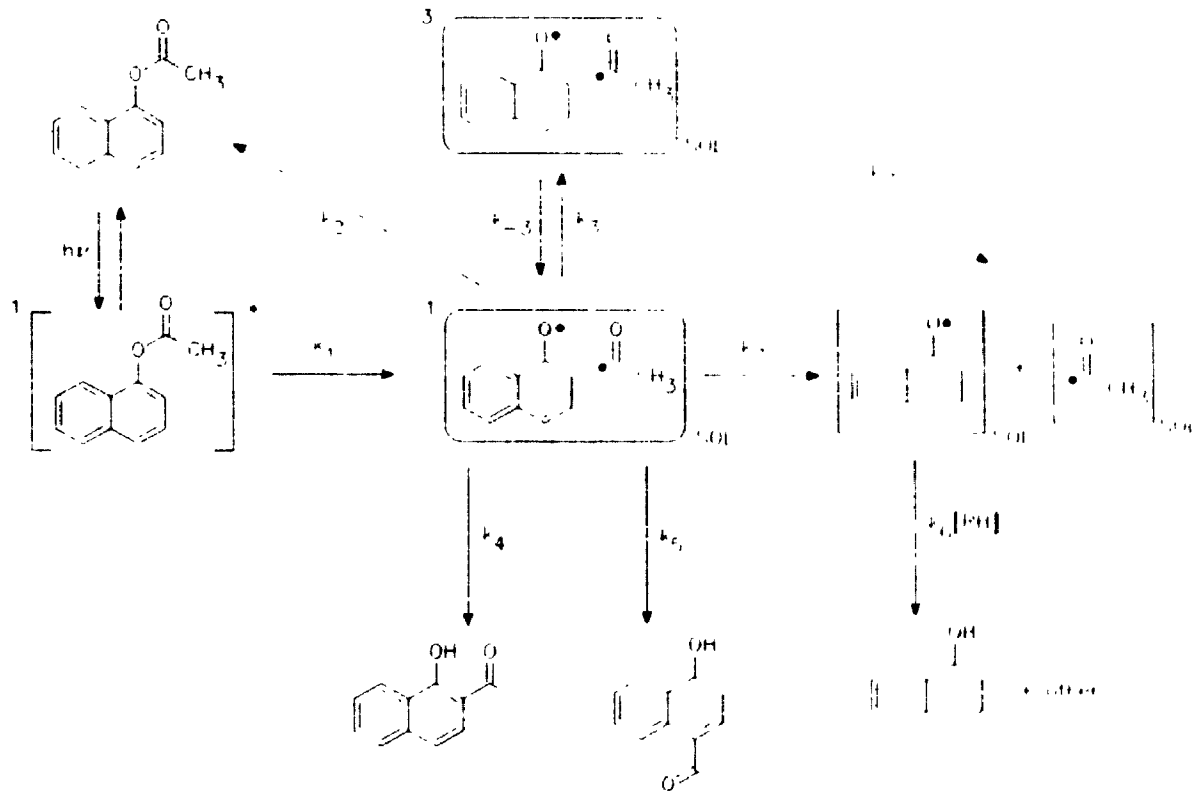

The initial experiments in the investigation of the supercritical phase photolysis of 1-naphthyl acetate involved determining whether the quantum yield of product formation was sufficiently large for the 100 watt high pressure mercury lamp to induce the formation of a significant amount of product in a practical amount of time. The total quantum yield of formation of 2-acetyl-1-naphthol, 4-acetyl-1-naphthol and 1-naphthol

in supercritical carbon dioxide at 92 bar and 40°C was measured relative to the total quantum yield of product formation in methanol. This was accomplished by using a light splitter to irradiate simultaneously an actinometer solution containing 1.81×10^{-3} M 1-naphthyl acetate in methanol and a supercritical carbon dioxide solution containing 1.80×10^{-3} M of 1-naphthyl acetate and 0.0141 M of isopropanol. The 2-propanol was added as a hydrogen source to trap radicals escaping the initial radical pair. The relative amount of light reaching each of the solutions was determined for the same optical geometry in separate experiments. It was found that the ratio of the quantum yield of product formation for the irradiation of 1-naphthyl acetate in supercritical carbon dioxide solution to that in methanol solution was 0.031 ± 0.009. Even though this relative quantum yield is rather low, enough product could be formed in the photolysis of 1-naphthyl acetate in supercritical carbon dioxide during 3 hour irradiation periods using the 100 watt high pressure mercury lamp for accurate product analysis to be conducted.

The relative chemical yields of 2-acetyl-1-naphthol, 4-acetyl-1-naphthol, and 1-naphthol formed in the photolysis of supercritical carbon dioxide solutions containing 1.80×10^{-3} M 1-naphthyl acetate and 0.0734 M 2-propanol were measured at different pressures and temperatures. All of the photolyses involved irradiating the supercritical phase solutions for 3 hours with the 100 W high pressure mercury lamp. Typically, the amount of starting material converted to products in these reactions was between 7% and 12%. Variations in the light flux of the lamp over the time period required to complete each set of experiments made it impossible to accurately determine relative quantum yields by comparing the amount of starting material converted under different reaction conditions. However, triplicate experiments were carried out at each temperature and

pressure and so accurate product ratios were determined by g.c. analysis. In these analyses the relative response of the flame ionisation detector to each photolysis product was calibrated. The identity of each photolysis product was confirmed by g.c. co-injection with authentic samples.

The concentration of 1-naphthyl acetate in solution was measured at each temperature and pressure by sampling the fluid flow into the cell while the recirculation pump was running. The concentration of 1-naphthyl acetate in these samples was determined by U.V. analysis (see experimental section for details) and it was concluded that the concentration of 1-naphthyl acetate in solution was 1.80×10^{-3} M for each temperature and pressure investigated. This confirmed that all of the experiments were carried out at 1-naphthyl acetate concentrations below the saturation concentration. The vapour-liquid equilibrium data presented by Radosz[52] and by Yonker et al.[51] indicate that all of the 2-propanol (concentration = 0.0734 M) was dissolved in the supercritical carbon dioxide in the experiments carried out at 47°C and between 75 and 345 bar. The absence of a phase boundary in the experiments carried out at 27°C and 35°C also indicated that all of the 2-propanol was dissolved in carbon dioxide under the pressures used in these experiments.

The results obtained by measuring the ratio of the combined relative yield of 2-acetyl-1-naphthol and 4-acetyl-1-naphthol to the relative yield of 1-naphthol (Φ_{fries}/Φ_{naph}) at various pressures and three different temperatures (27, 35 and 47°C) are summarised in Table 30. It is important to note that the data obtained at the sub-critical temperature of 27°C corresponds to the photolysis of 1-naphthyl-acetate in liquid carbon dioxide. The data listed in Table 30 are also plotted in Figure 20. This most obvious feature of the

supercritical carbon dioxide to behave like traditional liquid solvents which exhibit a decreased solvent cage-effect as the solvent density and viscosity are lowered. The variation in the relative yield of 1-naphthol with pressure seems to occur only in the supercritical phase since the data obtained in liquid carbon dioxide at the sub-critical temperature of 27°C do not exhibit any significant dependence on pressure.

Table 30: Variation in the ratio of the relative yield of Photo-Fries products to the relative yield of 1-naphthol (Φ_{fries}/Φ_{naph}) for the photolysis of 1-naphthyl acetate in supercritical CO_2 at different pressures and temperatures.

T=27°C		T=35°C		T=47°C	
P (bar)[a]	$\frac{\Phi_{fries}}{\Phi_{naph}}$	P (bar)[a]	$\frac{\Phi_{fries}}{\Phi_{naph}}$	P (bar)[a]	$\frac{\Phi_{fries}}{\Phi_{naph}}$
72	4.0±0.2	59	3.8±0.2	75	4.9±0.3
79	4.3±0.2	65	4.3±0.2	79	6.1±0.4
86	4.3±0.2	70	8.1±0.5	81	10.8±0.6
103	4.1±0.2	73	9.0±0.5	86	12.9±0.6
138	4.3±0.2	76	12.3±0.6	88	13.3±0.7
345	4.0±0.2	80	7.3±0.4	91	8.1±0.5
		86	4.0±0.2	95	4.6±0.2
		95	3.8±0.2	103	3.8±0.2
		105	4.0±0.2	138	4.0±0.2
		141	3.8±0.2	345	3.8±0.2
		345	3.9±0.2		

[a] The error associated with each pressure is ±1 bar.

The data summarized in Figure 20 can be rationalised in the context of solvent clustering near the critical point. As discussed above in the introduction to this chapter,

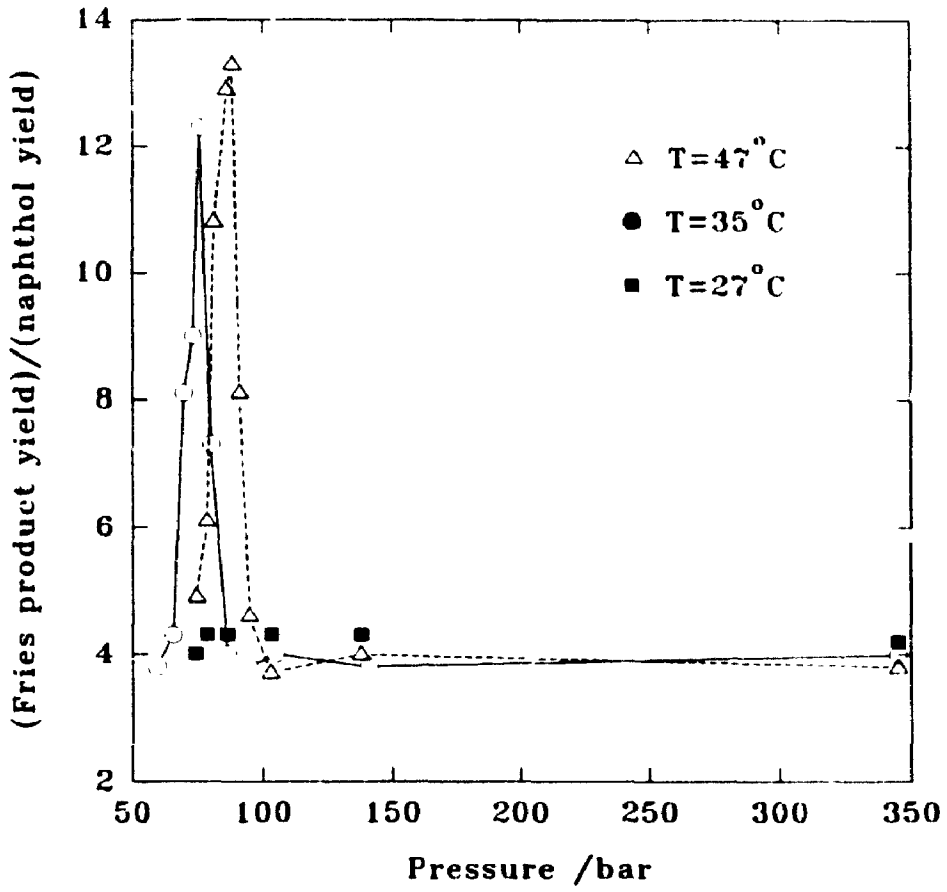

Figure 20: Pressure dependence of the ratio of the Fries-rearrangement product yield to the 1-naphthol yield for the photolysis of 1-naphthyl acetate in CO_2 at 27°C, 35°C and 47°C.

curves plotted in Figure 20 is the dramatic decrease in the yield of 1-naphthol relative to the combined yield of the Photo-Fries rearrangement products at pressures close to the critical pressure of pure carbon dioxide (73.8 bar) when the temperature is above the critical temperature. In terms of the process shown in the mechanism presented in Scheme 83, this observation indicates that the fraction of the radical pairs which escape the "solvent cage" decreases relative to the fraction of radical pairs which combine to form the *ortho* and *para* rearrangement products at pressures close to the critical point. Therefore, at lower supercritical carbon dioxide bulk densities, the solvent cage has apparently increased in strength. This observation is difficult to rationalise if one expects

supercritical carbon dioxide to behave like traditional liquid solvents which exhibit a decreased solvent cage-effect as the solvent density and viscosity are lowered. The variation in the relative yield of 1-naphthol with pressure seems to occur only in the supercritical phase since the data obtained in liquid carbon dioxide at the sub-critical temperature of 27°C do not exhibit any significant dependence on pressure.

Table 30: Variation in the ratio of the relative yield of Photo-Fries products to the relative yield of 1-naphthol (Φ_{frics}/Φ_{naph}) for the photolysis of 1-naphthyl acetate in supercritical CO_2 at different pressures and temperatures.

T=27°C		T=35°C		T=47°C	
P (bar)[a]	$\frac{\Phi_{frics}}{\Phi_{naph}}$	P (bar)[a]	$\frac{\Phi_{frics}}{\Phi_{naph}}$	P (bar)[a]	$\frac{\Phi_{frics}}{\Phi_{naph}}$
72	4.0±0.2	59	3.8±0.2	75	4.9±0.3
79	4.3±0.2	65	4.3±0.2	79	6.1±0.4
86	4.3±0.2	70	8.1±0.5	81	10.8±0.6
103	4.1±0.2	73	9.0±0.5	86	12.9±0.6
138	4.3±0.2	76	12.3±0.6	88	13.3±0.7
345	4.0±0.2	80	7.3±0.4	91	8.1±0.5
		86	4.0±0.2	95	4.6±0.2
		95	3.8±0.2	103	3.8±0.2
		105	4.0±0.2	138	4.0±0.2
		141	3.8±0.2	345	3.8±0.2
		345	3.9±0.2		

[a] The error associated with each pressure is ±1 bar.

The data summarized in Figure 20 can be rationalised in the context of solvent clustering near the critical point. As discussed above in the introduction to this chapter,

the possibility of a solvent clustering phenomenon in supercritical fluids near the critical point is a current area of theoretical and physical interest in the literature. However, the direct effect of such a phenomenon on the product distribution formed from a chemical reaction carried out in the supercritical phase has never been observed before. If solvent clustering around 1-naphthyl acetate solute molecules were occurring in supercritical carbon dioxide at pressures close to the critical point then this would explain the apparent decrease in the yield of the so-called "cage-escape" product 1-naphthol since the clustering would serve to provide local cages around solute molecules.

One of the observations reported in the literature which provides evidence for the presence of solvent clusters around solute molecules in supercritical solvents near the critical point is the finding that the partial molar volume of solutes at infinite dilution are very large, in the negative sense, near the critical point. The partial molar volume of naphthalene in supercritical carbon dioxide, measured by Eckert and co-workers, is one example of these observations.[33] The significance of this observation is discussed in the introduction to this chapter. Since the solvent-solute interactions for the naphthalene-CO_2 system are expected to be similar to the interactions in the 1-naphthyl acetate-CO_2 system, the data presented in Figure 20 were compared with data from the work of Eckert and co-workers. The purpose of this comparison was to determine if the pressure and temperature at which the partial molar volume becomes large and negative corresponds to the same pressure and temperature at which the relative yield of 1-naphthol decreases dramatically.

Figure 21 contains plots of the ratio (Φ_{frics}/Φ_{naph}) and a plot of the partial molar volume of naphthalene at infinite dilution along the same pressure axis for the

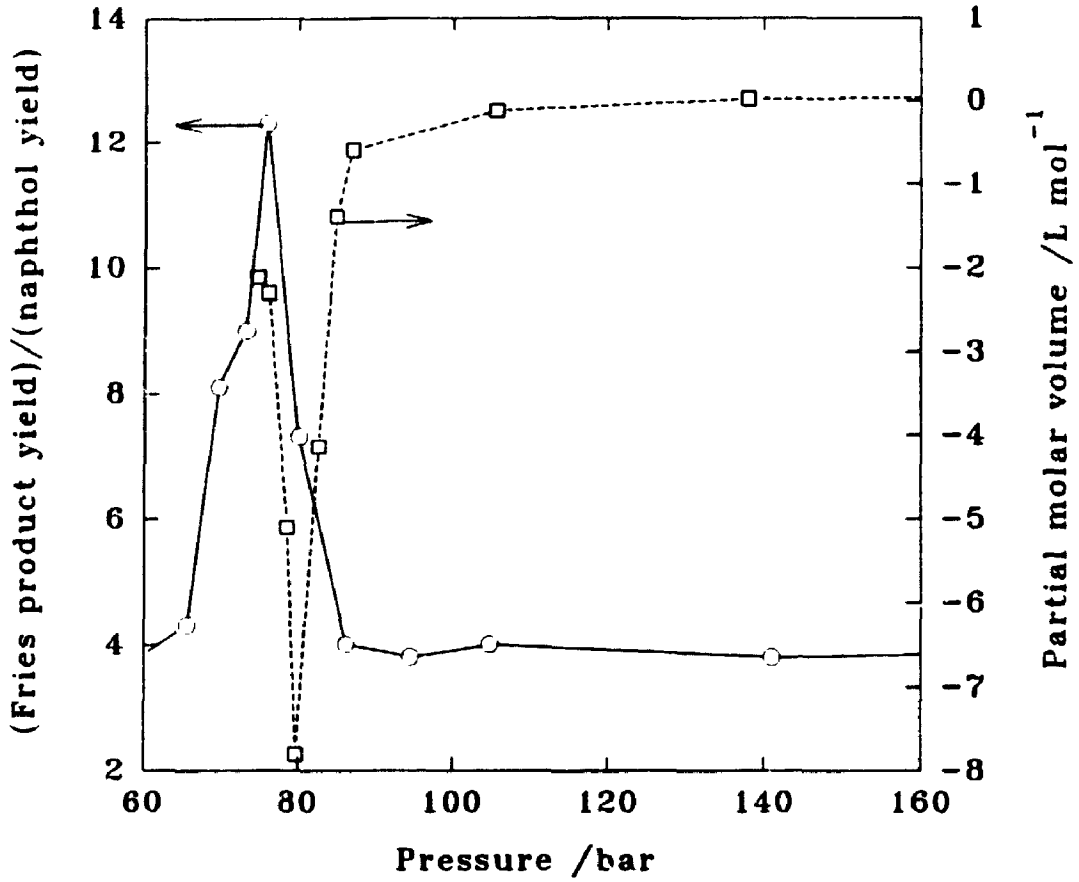

Figure 21: Comparison of the pressure dependence of the Φ_{fries}/Φ_{naph} ratio at 35°C with the pressure dependence of the partial molar volume of naphthalene in supercritical CO_2 at 35°C.

temperature of 35°C. Figure 22 contains plots of the same quantities for the case where the Photo-Fries data were obtained at 47°C and the partial molar volume data were measured at 45°C. The similarity of the trends exhibited by the partial molar volume versus pressure curve and the product yield ratio versus pressure curve for each temperature is remarkable. In the pressure region where partial molar volume of naphthalene measured at infinite dilution reaches a minimum, the relative yield of 1-naphthol also reaches a minimum. The comparison of these two different types of data suggests that the effect of solvent clustering around the solute molecules in supercritical CO_2 reaches a maximum between 70 and 85 bar at 35°C, and between 80 and 100 bar

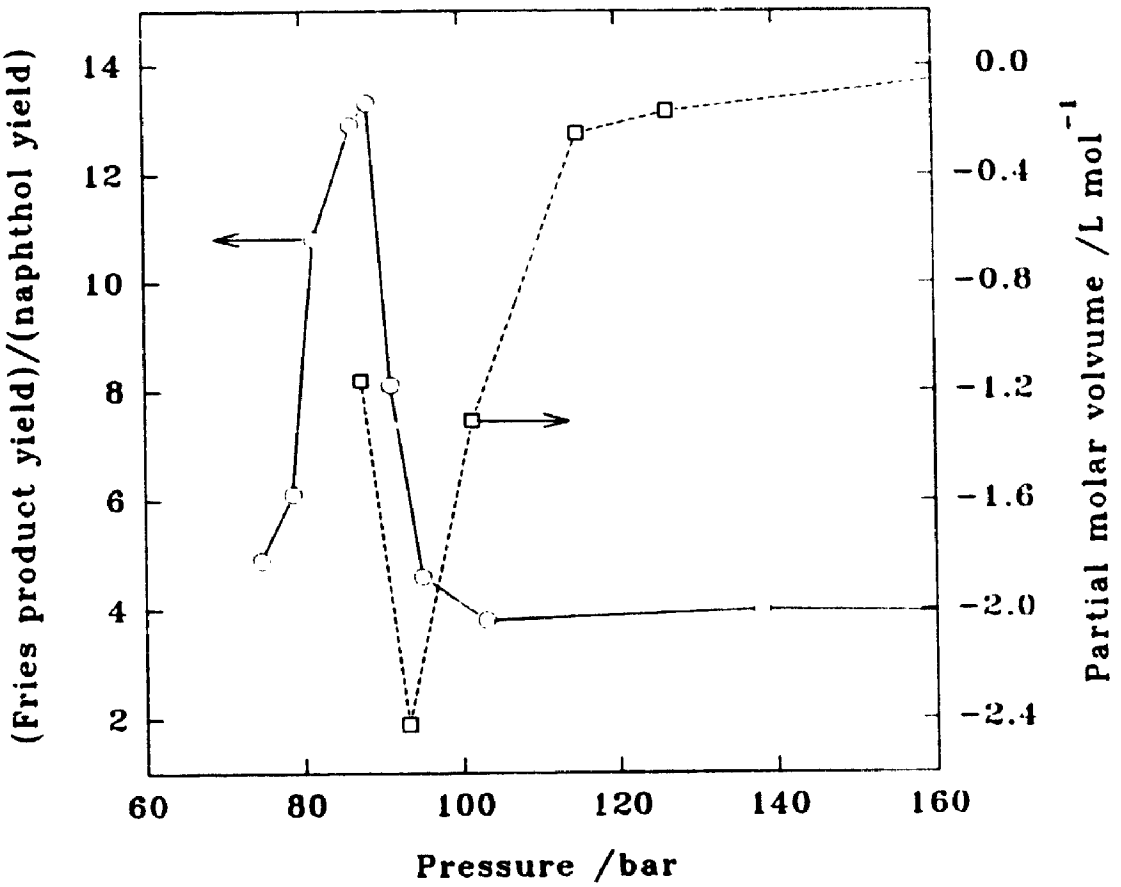

Figure 22: Comparison of the pressure dependence of the (Φ_{fries}/Φ_{naph}) ratio at 47°C with the pressure dependence of the partial molar volume of naphthalene in supercitical CO_2 at 45°C.

at 47°C.

A problem with the thermodynamic data presented by Eckert and co-workers[33] is that it does not provide any information about the lifetime of the solvent clusters that seem to form at pressures close to the critical point. Obviously, the lifetime of these clusters is very important if one attempts to modify the path of a particular reaction by carrying out the reaction in a supercritical fluid near its critical point. If the rate of the particular mechanistic step being investigated is much longer than the dynamic lifetime of the solvent clusters, then the formation or lack of formation of the solvent clusters may have a minimal effect on the course of the reaction. In this case, the reaction

pathway should be influenced by the bulk properties of the solvent and not by local perturbations in solvent density. If one accepts the involvment of solvent clusters in the Photo-Fries reaction of 1-naphthyl acetate as described above, then one must also postulate that the lifetime of the singlet radical pair formed by the homolytic cleavage of the ester C-O bond is comparable to, or shorter than, the lifetime of the solvent clusters around the solute molecules. Evidence exists that supports this: Nakagaki and co-workers[49] in their investigation of the Photo-Fries reaction of 1-naphthyl acetate in external magnetic fields determined that the rate constant for decay of the singlet radical pair is $4x10^{10}$ sec^{-1} in acetonitrile which corresponds to a lifetime of 25 ps. This relatively short lifetime is of same order of magnitude as the theoretical solvent cluster lifetime of a few picoseconds calculated by Petsche and Debenedetti.[30]

Formation of the 1-naphthol product must occur by hydrogen abstraction by the 1-naphthoxyl radical from an appropriate hydrogen atom donor. In the supercritical fluid phase experiments described above, 2-propanol was added to the reaction mixtures to act as a hydrogen atom donor. It is conceivable that not all of the 1-naphthoxyl radicals which escape the radical pair are intercepted by the hydrogen donor. If this occurred then some cage-escape radicals might combine to form other products; for example, 1-naphthoxyl radicals that escape the solvent cage might dimerise to form several different types of radical combination products.[54] However, coupled g.c./m.s. analysis of reaction mixture resulting from the photolysis of 1-naphthyl acetate in supercritical carbon dioxide near the critical pressure indicated no trace of naphthoxyl radical dimerisation products.

In order to investigate whether or not all of the 1-naphthoxyl radicals were

intercepted by the 2-propanol added to the reaction mixture, experiments were carried out in which the concentration of 2-propanol in the high pressure cell was varied. These experiments were difficult to conduct since the addition of a solute such as 2-propanol to a supercritical fluid solution in which the number of moles of solvent, system volume, and temperature are held constant results in a substantial pressure decrease for the system in the region of the critical point. This is presumably due to the large negative partial molar volume of 2-propanol in this region. Since it was demonstrated that the yield of 1-naphthol is very sensitive to pressure changes near the critical point, the perturbation induced by adding more 2-propanol to the Photo-Fries reaction mixture was difficult to interpret. Therefore, it was decided that the experiments in which the concentration of 2-propanol inside the high pressure cell was varied should be carried out at a pressure where the relative yield of 1-naphthol produced in the Photo-Fries reaction is relatively insensitive to pressure variations.

The effect of varying the concentration of 2-propanol on the relative yield of 1-naphthol was studied at a pressure of 110 bar and a temperature of 40°C. In these experiments, the concentration of 2-propanol in the supercritical fluid solution was varied by injecting known volumes of the alcohol into the system by means of the sample injection valve. The ratio of the combined yield of the Photo-Fries products to the yield of 1-naphthol was measured after each photolysis of 1-naphthyl acetate in which a different concentration of 2-propanol was present in the supercritical solution. This ratio is plotted against the concentration of 2-propanol in the Figure 23. The figure demonstrates that the relative yield of 1-naphthol is insensitive to the concentration of 2-propanol for the concentration range examined. Therefore, it was concluded that all of

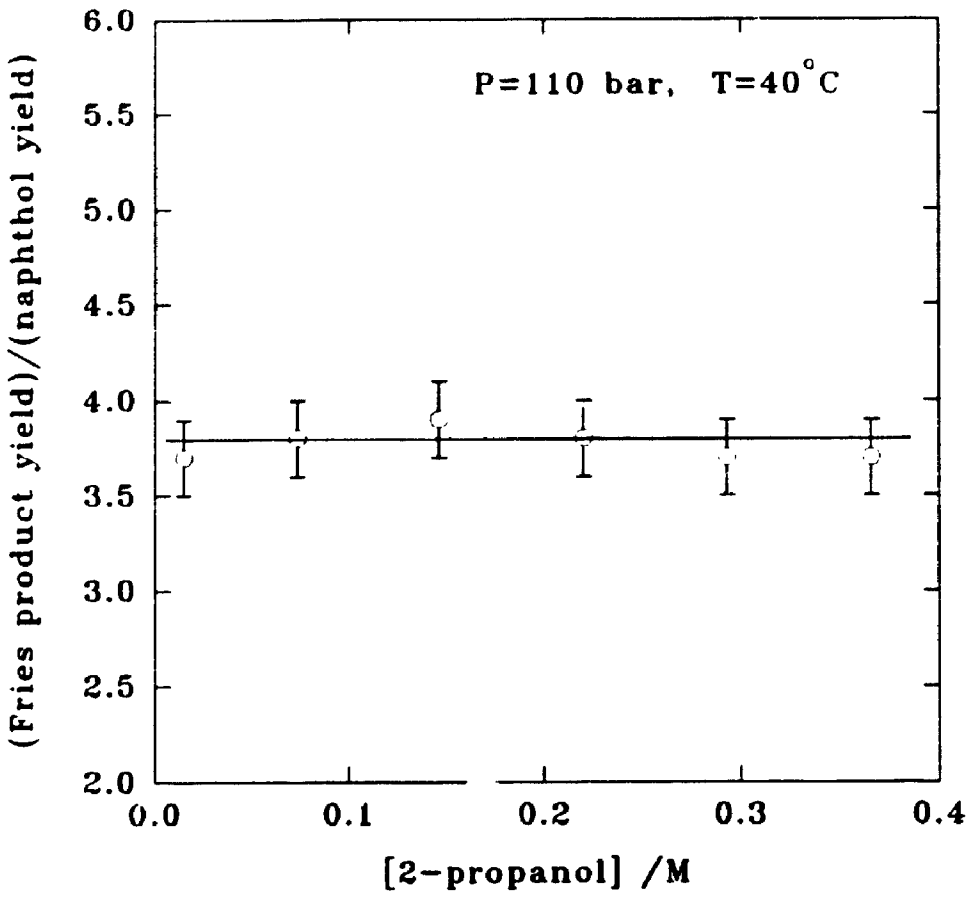

Figure 23: The dependence of the ratio of Fries-rearrangement product yield to the yield of 1-naphthol (Φ_{fries}/Φ_{naph}) on the concentration of 2-propanol.

the 1-naphthoxy radicals were intercepted by 2-propanol and reduced to 1-naphthol.

The ratio of the relative yields of 2-acetyl-1-naphthol and 4-acetyl-1-naphthol was also determined at different pressures and temperatures. These data are summarised in Table 31 and plotted in Figure 24. The most notable feature present in each curve plotted in Figure 24 is the sharp decrease in the *ortho/para* ratio near the critical pressure of carbon dioxide. In the case of the data gathered along the 47°C isotherm, the *ortho/para* ratio dropped from 2.28 to 0.98 over a pressure drop of less than 10 bar near the critical pressure. The *ortho/para* ratio observed for the photolysis of 1-naphthyl acetate in sub-critical liquid carbon dioxide did not exhibit any significant variation as

the pressure was changed indicating that the phenomenon responsible for the variation in the relative product yields was confined to the supercritical phase.

Table 31: Variation in the ratio of the relative yield of 2-acetyl-1-naphthol to the relative yield of 4-acetyl-1-naphthol for the photolysis of 1-naphthyl acetate in supercritical CO_2 at different pressures and temperatures.

T=27°C		T=35°C		T=47°C	
P (bar)[a]	$\frac{\Phi_{ortho}}{\Phi_{para}}$	P (bar)[a]	$\frac{\Phi_{ortho}}{\Phi_{para}}$	P (bar)[a]	$\frac{\Phi_{ortho}}{\Phi_{para}}$
72	2.6±0.1	59	1.55±0.08	75	1.24±0.06
79	2.8±0.1	65	1.53±0.08	79	1.05±0.05
86	2.7±0.1	70	1.54±0.08	81	1.04±0.05
103	2.8±0.1	73	1.43±0.07	86	0.98±0.04
138	2.7±0.1	76	1.42±0.08	88	1.45±0.06
345	2.6±0.1	80	2.52±0.14	91	1.97±0.10
		86	2.49±0.14	95	2.28±0.14
		95	2.43±0.13	103	2.04±0.12
		105	2.40±0.13	138	1.76±0.10
		141	2.21±0.12	345	1.82±0.10
		345	2.20±0.12		

[a] The error associated with each pressure is ±1 bar.

The odd π-electron spin densities at each atom in the 1-naphthoxyl radical have been calculated using SCF MO methods.[47] These calculations indicate that the odd π-electron density at the oxygen atom in the 1-naphthoxyl radical is 0.098 and the densities at the *ortho* and *para* position are 0.139 and 0.221 respectively. The greater odd π-electron density at the *para* position relative to the *ortho* position suggests that formation

of 4-acetyl-1-naphthol from the singlet radical pair generated in the photolysis of 1-naphthyl acetate should be favoured over formation of 2-acetyl-1-naphthol. This, however, is not observed in liquid solutions. The data presented in Table 32 demonstrates that the major Photo-Fries rearrangement product is always 2-acetyl-1-naphthol in liquid solvents. The preference for the *ortho* product has been explain by Ohto[47] and Crouse[48] as being due to the fact that the *ortho* site is closer to the acetyl radical when the radical pair is initially formed. Formation of the *para* isomer requires that the acetyl radical move a greater distance within the solvent cage.

Table 32: Relative product yields for the photolysis of 1-naphthyl acetate in different organic solvents.

Solvent	Temp (°C)	Press. (Bar)	2-acetyl-1-naphthol	4-acetyl-1-naphthol	1-naphthol
Methanol	25	atm	1	0.43	0.21
Acetonitrile	25	atm	1	0.45	0.12
Benzene	25	atm	1	0.24	0.12
Benzene	47	97	1	0.20	0.13
Toluene	25	atm	1	0.25	0.12

The dramatic increase in the yield of 4-acetyl-1-naphthol relative to the yield of 2-acetyl-1-naphthol near the critical pressure of carbon dioxide in supercritical phase photolyses of 1-naphthyl acetate can be partially explained in the context of the solvent cluster model discussed above. It was suggested above that the presence of solvent clusters near the critical point enhance the apparent strength of the cage around the

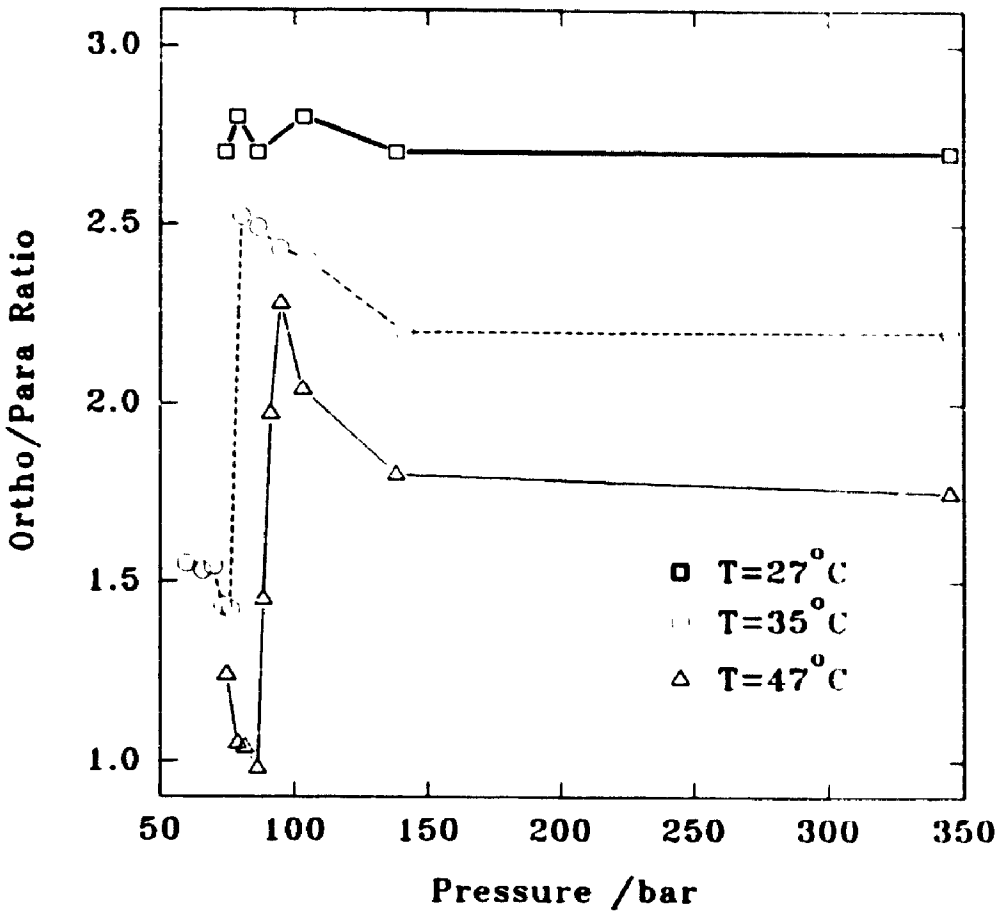

Figure 24: The pressure dependence of the ratio of the yield of 2-acetyl-1-naphthol to the yield of 4-acetyl-1-naphthol for the photolysis of 1-naphthyl acetate in CO_2 at 27°C, 35°C and 47°C.

singlet radical pair. If this is true then the decrease in the *ortho/para* ratio near the critical point may be due to an increase in the fraction of acetyl radicals that are able to reach the *para* position of the 1-naphthoxyl radical before the radical pair diffuses apart. That is to say, perhaps the presence of solvent clusters near the critical point increases the lifetime of the radical pair so that the *para* position of the naphthoxyl radical becomes more accessible to acetyl radical. However, this explanation does not explain the small, but significant, increase in the *ortho/para* ratio just above the near-critical region. It is very probable that more than one effect causes the variations in the *ortho/para* ratio. For example, changes in the bulk polarity of the supercritical solution that accompany bulk

density changes at different pressures may also have a significant effect on the *ortho/para* ratio. Therefore, it is difficult to make any concrete conclusions regarding the trends exhibited by the functions plotted in Figure 24.

1.5 Conclusions for the 1-Naphthyl Acetate Work

The ultra-violet light irradiation of 1-naphthyl acetate in solutions of supercritical carbon dioxide results in the formation of 1-naphthol, 2-acetyl-1-naphthol, and 4-acetyl-1-naphthol. The quantum yield of product formation in this reaction was found to be approximately 30 times lower than the quantum yield of product formation for the same reaction in methanol. The decrease of the quantum yield in supercritical carbon dioxide solutions might be due to an increase in the rate of intersystem crossing to the triplet excited state of 1-naphthyl acetate.

The relative ratios of the products obtained from the supercritical phase Photo-Fries reaction of 1-naphthyl acetate were very sensitive to pressure in the near-critical region. A decrease in the relative yield of 1-naphthol accompanied a reduction in pressure just above the critical pressure of CO_2. This decrease was interpreted in terms of a decrease in the relative amount of naphthoxyl radicals which were able to escape the solvent cage. The pressure at which the largest decrease in the relative yield of 1-naphthol was observed corresponded to the same pressure at which the partial molar volume of naphthalene in supercritical carbon dioxide reaches a minimum. The coincidence of the minimum in the partial molar volume pressure dependent isotherm with the minimum in the relative yield of the cage-escape product, 1-naphthol, is consistent with the idea that solvent clustering in supercritical CO_2 near the critical point

has a dramatic effect on the Photo-Fries reaction of 1-naphthyl acetate. The observed decrease in the relative yield of the cage-escape product in the Photo-fries reaction of 1-naphthyl acetate is the first evidence of a direct effect of supercritical phase solvent clustering on the products of a photochemical reaction.

The *ortho/para* ratio of the two Fries-rearrangement products identified in the supercritical phase photolysis of 1-naphthyl acetate was also measured. It was found that the *ortho/para* ratio rises slightly then drops significantly as the critical point is approached from high pressure regions of the phase diagram. This decrease can be explained in terms of increased solvent clustering. It was postulated that the increased strength of the solvent cage in the near-critical region results in an increased in the number of acyl radicals that are able to reach the 4-position of the 1-naphthoxyl radical before the cage collapses. It is important to remember that the dipoles of 2-acetyl-1-naphthol and 4-acetyl-1-naphthol are substantially different; therefore, the variation of the *ortho/para* with pressure may also be a result of the changes in the solvent dielectric strength that accompany variations in solvent density. Possibly the sharp change in the *ortho/para* ratio in the near-critical region is also due to dramatic changes in the local dielectric strength around the singlet radical that are brought about by solvent clustering. In conclusion, it is difficult to say whether the pressure induced changes observed for the *ortho/para* ratio in the near-critical region are a result of an increase in the dynamic lifetime of the solvent cage, or whether these changes are a result of some other property of supercritical fluids which undergoes a pronounced change near the critical point.

1.6 References

1. Reid, R. C.; Prausnitz, J. M.; Poling, B. E. *The Properties of Gases and Liquids*; 4th ed; McGraw-Hill: New York, NY, 1987.

2. Angus, S., Armstrong, B., de Reuck, K., Eds. *International Thermodynamic Tables of the Fluid State: Carbon Dioxide*; Pergamon Press: Oxford, 1976.

3. For reviews of thermal reactions that have been carried out in supercitical fluids see: (a) Brennecke, J. F. In *Supercritical Fluid Engineering Science: Fundamentals and Applications*; Kiran, E., Brennecke, J. F., Eds.; ACS Symposium Series 514; American Chemical Society: Washington, DC, 1993, Chapter 1. (b) Bright, F. V.; McNally, M. E. P. In *Supercitical Fluid Technology: Theoretical and Applied Approaches to Analytical Chemistry*; Bright, F. V., McNally, M. E. P., Eds.; ACS Symposium Series 488; American Chemical Society: Washington, DC, 1992, Chapter 1. (c) Bruno, T. J.; Ely, J. F. *Supercritical Fluid Technology: reviews in Modern Theory and Applications*; CRC Press: Boca Raton, FL, 1991.

4. For examples of supercritical fluid in chromatography and extraction technology see: (a) Klesper, E. *Agnew. Chem. Int. Ed. Engl.* **1978**, *17*, 738. (b) Novotny, M. V.; Springston, S. R.; Peaden, P. A.; Fjeldsted, J. C.; Lee, M. L. *Anal. Chem.* **1981**, *53*, 407A. (c) *Supercritical Fluid Chromatography*; Smith, R. M. Ed.; Royal Society of Chemistry Monograph; Royal Society of Chemistry: London, UK, 1988. (d) Smith, R. D.; Wright, B. W.; Yonker, C. R. *Anal. Chem.* **1988**, *60*, 1323A. (e) McHugh, M. A.; Krukonis, V. J. *Supercritical Fluid Extraction: Principles and Practices*; Butterworths: Stoneham, MA, 1986.

5. *CRC Handbook of Chemistry and Physics*; 68th ed.; CRC Press, Boca Raton, FL, 1987, F-65.

6. van Wasen, U.; Swaid, I.; Schneider, G. M. *Agnew. Chem. Int. Ed. Engl.* **1980**, *19*, 575.

7. Paulaitis, M. E.; Alexander, G. C. *Pure and Appl. Chem.* **1987**, *59*, 61.

8. Ikushima, Y.; Saito, N.; Arai, M. *Bull. Chem. Soc. Jpn.* **1991**, *61*, 282.

9. Ikushima, Y.; Saito, N.; Arai, M. *J. Phys. Chem.* **1992**, *96*, 2293.

10. Johnston, K. P.; Haynes, C. *AIChE J.* **1987**, *33*, 2017.

11. Peck, D. G.; Mehta, A. J.; Johnston, K. P. *J. Phys. Chem.* **1989**, *93*, 4297.

12. Combes, J. R.; Johnston, K. P.; O'Shea, K. E.; Fox, M. A. In *Supercritical Fluid Technology: Theoretical and Applied Approaches to Analytical Chemistry*; Bright, F. V., McNally, M. E. P., Eds.; ACS Symposium Series 488: American Chemical Society; Washington, DC, 1992, chapter 3.

13. Hrnjez, B. J.; Mehta, A. J.; Fox, M. A.; Johnston, K. P. *J. Am. Chem. Soc.* **1989**, *111*, 2662.

14. O'Shea K. E.; Combes, J. R.; Fox, M. A.; Johnston, K. P. *Photochem. and Photobiol.* **1991**, *54*, 571.

15. Otto, B.; Schroeder, J.; Troe, J. *J. Chem. Phys.* **1984**, *81*, 202.

16. Gehrke, Ch.; Schroeder, J.; Schwarzer, D.; Troe, J.; Vob, F. *J. Chem. Phys.* **1990**, *92*, 4805.

17. Roberts, C. B.; Zhang, J.; Brennecke, J. F.; Chateauneuf, J. E. *J. Phys. Chem.* **1993**, *97*, 5618.

18. Brennecke, J. F.; Tomasko, D. L.; Eckert, C. A. *J. Phys. Chem.* **1990**, *94*, 7692.

19. (a) Zagrobelny, J.; Bright, F. V. *J. Am. Chem Soc.* **1992**, *114*, 7821. (b) Zagrobelny, J.; Bright, F. V. *J. Am. Chem Soc.* **1993**, *115*, 701. (c) Zagrobelny, J.; Betts, T. A.; Bright, F. V. *J. Am. Chem Soc.* **1992**, *114*, 5249.

20. (a) Yonker, C. R.; Frye, S. L.; Kalkwarf, D. R.; Smith, R. D. *J. Phys. Chem.* **1986**, *90*, 3022. (b) Yonker, C. R.; Smith, R. D. *J. Phys. Chem.* **1988**, *92*, 235.

21. (a) Kim, S.; Johnston, K. P. *AIChE J.* **1987**, *33*, 1603. (b) Kim, S.; Johnston, K. P. *Ind. Eng. Chem. Res.* **1987**, *26*, 1206.

22. Barrow, G. M. *Physical Chemistry*; 4th ed.; McGraw-Hill: New York, 1979, Chapter 19.

23. (a) Iwasaki, H.; Takahshi, M. *J. Chem. Phys.* **1981**, *74*, 1930. (b) Kennedy, J. T.; Thodos, G. *AIChE J.* **1961**, *7*, 625.

24. Imotev, M. B.; Tsekhanskaya, Yu. V. *Russ. J. Phys. Chem.* **1964**, *38*, 485.

25. (a) Brown, R. E.; Singer, L. A.; Parks, J. H. *J. Am. Chem. Soc.* **1972**, *94*, 8584. (b) Fang, T. S.; Fukuda, R.; Brown, R. E.; Singer, L. A. *J. Phys. Chem.* **1978**, *82*, 246. (c) Yekta, A.; Turro, N. J. *Mol. Photochem.* **1972**, *3*, 307.

26. Lehni, M.; Schuh, H.; Fisher, H. *Int. J. Chem. Kinet.* **1979**, *11*, 705.

27. Roberts, C. B.; Zhang, J.; Chateauneuf, J. E.; Brennecke, J. F. *J. Am. Chem. Soc.* **1993**, *115*, 9576.

28. Evans, M. G.; Polanyi, M. *Trans. Faraday Soc.* **1935**, *31*, 875.

29. Petsche, I. B.; Debenedetti, P. G. *J. Phys. Chem.* **1991**, *95*, 386 and references cited therein.

30. Petsche, I. B.; Debenedetti, P. G. *J. Chem. Phys.* **1989**, *91*, 7075.

31. Pfund, D. M.; Lee, L. L.; Cochran, H. D. *J. Chem. Phys.* **1991**, *94*, 3107.

32. Eckert, C. A.; Ziger, D. H.; Johnston, K. P.; Ellison, T. K. *Fluid Ph. Equil.* **1983**, *14*, 167.

33. Eckert, C. A.; Ziger, D. H.; Johnston, K. P.; Kim, S. *J. Phys. Chem.* **1986**, *90*, 2738.

34. (a) Bayliss, N. S.; McRae, E. G. *J. Phys. Chem.* **1954**, *58*, 1002. (b) McRae, E. G. *J. Phys. Chem.* **1957**, *61*, 562.

35. (a) Hrnjez, B. J.; Yazdi, P. T.; Fox, M. A.; Johnston, K. P. *J. Am. Chem. Soc.* **1989**, *111*, 1915. (b) Sun, Y-P.; Bennett, G.; Johnston, K. P.; Fox, M. A. *J. Phys. Chem.* **1992**, *96*, 10001.

36. Sun, Y-P.; Fox, M. A.; Johnston, K. P. *J. Am. Chem. Soc.* **1992**, *114*, 1187.

37. Birks, J. B. *Photophysics of Aromatic Molecules*; Wiley-Interscience: New York, 1970.

38. (a) Anderson, J. C.; Reese, C. B. *Proc. Chem. Soc. (London)* **1960**, 217. (b) Anderson, J. C.; Reese, C. B. *J. Chem. Soc.* **1963**, 1781. (c) Kobsa H. *J. Org. Chem.* **1962**, *27*, 2293. (d) Finnegan R. A.; Hagen, A. W. *Tetrahedron Lett.* **1963**, 369. (e) Elad, D. *ibid.* **1963**, 873. (f) Elad, D.; Rao, D. V.; Stenberg, V. I. *J. Org. Chem.* **1965**, *30*, 3252.

39. Kalmus, C. E.; Hercules, D. M. *J. Am. Chem. Soc.* **1974**, *96*, 449.

40. Shizuka, H.; Toshifumi, M. *Bull. Chem. Soc. Jpn.* **1969**, *42*, 1831.

41. Sander, M. R.; Hedaya, E.; Trecker, D. J. *J. Am. Chem. Soc.* **1968**, *90*, 7249.

42. (a) Adam, W.; de Sanabia, J. A.; Fischer, H. *J. Org. Chem.* **1973**, *38*, 2571. (b) *Chem. Comm.* **1974**, 289.

43. Coppinger, G. M.; Bell, E. R. *J. Phys. Chem.* **1966**, *70*, 3479.

44. Meyer, J. W.; Hammond, G. S. *J. Am. Chem. Soc.* **1970**, *92*, 2189.

45. Humphrey, J. S.; Roller, R. S. *Mol. Photochem.* **1971**, *3*, 35.

46. Oldroyd, D. L.; Weedon, A. C. *J. Photochem. Photobiol. A: Chem.* **1991**, *57*, 207.

47. Ohto, Y.;Shizuka, H.; Sekiguchi, S.; Matsui, K. *Bull. Chem. Soc. Jpn.* **1974**, *47*, 1209.

48. Crouse, D. J.; Hurlbut, S. L.; Wheeler, D. M. S. *J. Org. Chem.* **1981**, *46*, 374.

49. Nakagaki, R.; Hiramatsu, M.; Watanabe, T.; Tanimoto, Y.; Nagakura, S. *J. Phys. Chem.* **1985**, *89*, 3222.

50. Sakaguchi, Y.; Hayashi, H.; Nagakura, S. *Bull. Chem. Soc. Jpn.* **1980**, *53*, 39.

51. Bellus, D. *Adv. Photochem.* **1971**, *8*, 109.

52. Radosz, M. *J. Chem. Eng. Data.* **1986**, *31*, 43.

53. Yonker, C. R.; Smith, R. D. *J. Phys. Chem.* **1988**, *92*, 2374.

54. In the Photo-Fries rearrangement of bis(4-tert-butylphenyl) carbonate, Horspool and Pauson reported the isolation of 5,5'-di-tert-butyl-2,2'-dihydroxybiphenyl in trace amounts. It was postulated that this product is the result of dimerisation of the 4-tert-butylphenoxyl radical which is formed in the Photo-Fries reaction. See Horspool, W. H.; Pauson, P. L. *J. Chem Soc.* **1965**, 5162.

CHAPTER 2

EXPERIMENTAL

2.1 Construction of the Supercritical Fluid Photochemical Reactor

The supercritical fluid photochemical reactor was an adaptation of an Autoclave Supercritical Fluid Extraction Screening System which is commercially available from Autoclave Engineers Group, Erie, Pennsylvania, USA.[1] The main modifications of this commercially extractor involved the design and construction of a high pressure optical cell and the addition of an analytical sampling and injection system. The principal design parameters of the supercritical fluid photochemical reactor include a maximum operating pressure of 400 bar, a total recirculated fluid volume of 89.0±0.5 mL, a maximum operating temperature of 70°C controlled to within 1°C, and the possibility of irradiating the contents of the optical cell at wavelength between 250nm and 700nm. A schematic of the lay out of the Supercritical Fluid Photochemical Reactor is located in Figure 19.

The optical cell assembly consisted of a capped, thick walled cylinder machined from 316 stainless steel. The wall of the cylinder was equipped with four quartz windows mounted in retaining glands which were screwed into the main cell body at 90° angles in the same plane. The commercial grade quartz windows (supplied by Emersil International) were 0.875" diameter discs polished to a uniform thickness of 0.5000". The diameter of each window visible from outside of the optical cell was 0.50". All soft mounting seals in the window assembly were made of teflon. The portion of the retaining gland which supports the quartz located outside of the cell was threaded so that a brass plug could be screwed into the retaining gland. The purpose of this brass plug

was to isolate the quartz window and act as a safety feature in case of window failure when pressure testing the cell. Each time the windows were removed from the cell for cleaning and inspection purposes and then remounted, all four of the brass plugs were screwed into the retaining glands before the optical cell was pressure tested to 380 bar. After pressure testing the windows, the brass plugs were removed so that light could be focused into the cell.

The temperature of the optical cell was controlled by a 600 Watt 120 Volt heating band. The current going to heating band was controlled by means of a Eurotherm Model 808 digital controller. The temperature inside the optical cell was monitored by a Eurotherm Model 842 digital process monitor which was connected to a Type J thermocouple encased in a 0.062" 304 stainless steel sheath. This thermocouple protruded into the cell to a depth just below the plane in which the windows were mounted and was secured by a compression type fitting. The temperature inside the cell could be maintained to within 1°C.

The pump that was used to both pressurise the optical cell with carbon dioxide and recirculate the contents of the cell during a reaction was a MiniPump Model 396 (supplied by LDC Analytical). The head of the pump was fitted with a heat exchanger through which ethylene glycol was passed. The temperature of the cooling fluid was lowered to 0°C by a constant temperature bath when the pump was being used to pressurise the system with carbon dioxide. When the pump was begin used to recirculate the contents of the cell throughout the system, the pump head temperature was heated to the cell temperature by means of the heat exchanger.

The pressure inside the system was measured by two pressure gauges. One of

these pressure gauges (P_2) was an Autoclave Model P-0482 Duragauge capable of measuring pressures up to 690 bar with an accuracy of 10 bar. The other pressure gauge (P_1) was an Autoclave Model P-0480 Duragauge capable of measuring pressures up to 207 bar with an accuracy of 1 bar. The latter gauge was connected to the system via a shut-off valve so that it could be isolated from the system during higher pressure experiments.

Sample removal from the system as well as sample injection into the system involved the use of a 6-port 2-position HPLC type valve (supplied by Valco Valves). The size of the sample loop connected to the valve was changeable. During liquid sample injection, the valve was operated in exactly the same way as it would be in an HPLC application. During the sample removal procedure the sample loop was connected to the optical cell and material in the cell was recirculated through the loop by means of the pump. The position of the valve was then rotated so that the loop was connected to two exit ports. The one of the exit ports was plugged with a removable nut and the other was connected to a small 2.5 mL 316 stainless steel separator vessel capable of withstanding pressures up to 150 bar. The separator was filled with a small volume of solvent (1 mL) through which the contents of the loop were discharge as soon as the position of the valve was changed. The pressure inside the separator vessel was slowly released by gradually loosening the plug in the other exit port of the sample valve. The separator vessel was then opened and the solution was removed quantitatively by washing the separator vessel with 3 small portions of solvent. The solution and all of the washings were transferred to a volumetric flask, diluted to a known volume and then analyzed.

The light source employed during the experiments carried out in supercritical CO_2 consisted of a water cooled 100 Watt high pressure mercury vapour lamp. The light from this lamp was columnated with a parabolic reflector and then passed through a water filter. In some experiments a quartz light splitter was placed in the beam so that the relative light flux reaching the optical cell could be determined. The path length inside the optical cell was 3.2 cm.

2.2 Synthesis of 1-naphthyl acetate

Acetyl chloride (6.26 g; 0.0797mol) was added dropwise over a period of 20 minutes to an ice-cooled solution of 1-naphthol (11.46 g; 0.0796 mol) and pyridine (12.64 g; 0.160 mol) in dichloromethane (150 mL). The solution was then warmed to room temperature and stirred for an additional 2 hrs after which time the reaction mixture was poured onto a slurry of ice and 10% HCl/water. The CH_2Cl_2 layer was separated and the aqueous layer extracted with 2x100 mL portions of CH_2Cl_2. The combined CH_2Cl_2 extracts were washed with 10% Na_2CO_3 (200 mL), saturated brine (2x200 mL), dried with $MgSO_4$ and concentrated under reduced pressure to yield a light brown oil (7.75 g). The product was adsorbed onto silica gel (10 g) and flash chromatographed using an additional 60 g of silica gel and a mobile phase consisting of 1:1 diethyl ether:hexanes. The solvent was removed under reduced pressure to reveal a white crystalline solid which was recrystallised twice from cyclohexane to yield the desired product (7.55 g; 0.0405 mol; 51%): mp 47-48°C (lit.[2] 48-49°C); IR ($CHCl_3$) υ_{max} 1760 cm^{-1}; ^1H nmr (200 MHz, in $CDCl_3$) δ 2.3 (s, 3H), 7.0-7.9 (m, 7H).

2.3 Synthesis of 2-acetyl-1-naphthol and 4-acetyl-1-naphthol

To a solution of 1-naphthol (3.033; 0.0210 mol; purified by flash chromatography on silica gel prior to use) in nitrobenzene (15 mL), was added aluminum trichloride (2.809 g; 0.0210 mol). Acetyl chloride (1.656 g: 0.0210 mol) was then added dropwise over a time period of 15 minutes. The solution was heated to 45°C and magnetically stirred for 3 hrs. The reaction mixture was poured onto 5% HCl/water (100 mL) chilled to 0°C and extracted with CH_2Cl_2 (3x150 mL). The CH_2Cl_2 extracts were washed with saturated brine and concentrated under reduced pressure to yield a brown oil. The nitrobenzene was removed from this brown oil by steam distillation and the crude product extracted with CH_2Cl_2 (3x100 mL). The combined extracts were washed with saturated brine, dried over $MgSO_4$ and concentrated under reduced pressure to yield a light brown oil (2.590 g). The crude product was subjected to flash chromatography in which 40 g of silica gel were used. The column was first eluted with 500 mL of a 2:3 mixture (v/v) of benzene and hexanes (fraction I) and then with 400 mL of a 4:1 mixture (v/v) of benzene and diethyl ether (fraction II). The solvent was removed from fraction I to reveal a yellow solid which was recrystallised from cyclohexane to yield 2-acetyl-1-naphthol (1.092 g; 5.86 mmol; 28%). The solvent was removed from fraction II to reveal a pale green solid which was recrystallised from benzene-ethanol to yield 4-acetyl-1-naphthol (1.359 g; 7.30 mmol; 35%).

Characterisation of 2-acetyl-1-naphthol. Mp 99-100°C (lit.[3] 100-101°C). ^{1}H nmr (200 MHz, in DMSO-d_6): δ 2.67 (s, 3H, CH_3), 7.35 (d, J=9 Hz, 1H), 7.55 (ddd, J=1.4 Hz, J=6.9 Hz, J=8.3 Hz, 1H), 7.68 (ddd, J=1.4 Hz, J=6.9 Hz, J=8.3 Hz, 1H), 7.78 (d, J=9 Hz, 1H), 7.86 (brd. d., J=8.2 Hz, 1H), 8.29 (m, 1H), 14.05 (s, 1H, aromatic

OH). ^{13}C nmr (75 MHz, in DMSO-d_6): δ 205.4 (C=O), 161.0 (C), 136.9 (C), 130.2 (CH), 127.6 (CH), 126.1 (CH), 125.7 (CH), 124.2 (C), 123.6 (CH), 118.3 (CH), 113.1 (C), 27.0 (CH_3). Precise mass determination: 186.0679 (found), 186.0681 (calc.).

Characterisation of 4-acetyl-1-naphthol. Mp 202-205°C (lit.[4] 204-206°C). ^1H nmr (200 MHz, in DMSO-d_6): δ 2.62 (s, 3H, CH_3), 6.93 (d, J=8.1 Hz, 1H), 7.55 (m, 2H), 8.13 (d, J=8.1 Hz, 1H), 8.25 (brd. d., J=8 Hz, 1H), 9.01 (brd. d., J=8 Hz, 1H), 11.18 (s, 1H, aromatic OH). ^{13}C nmr (75 MHz, in DMSO-d_6): δ 199.1 (C=O), 158.0 (C), 133.6 (CH), 132.1 (C), 128.4 (CH), 125.8 (CH), 125.1 (CH), 124.69 (C), 124.64 (C), 122.3 (CH), 106.7 (CH), 29.1 (CH_3). Precise mass determination: 186.0683 (found), 186.0681 (calc.).

2.4 Typical Irradiation of 1-Naphthol Acetate in Supercritical Carbon Dioxide

The temperature of the optical cell component of the supercritical fluid photochemical reactor was set and then allowed to reach equilibrium over a 20 hr. period. The main access port to the optical cell assembly was removed and 0.0300±0.0002 g of 1-naphthol acetate was added to the cell. The cell was then sealed and evacuated until the pressure inside the system was less then 10^{-2} mbar at which point the vent valve (V_1) was closed and the system charged with anaerobic grade carbon dioxide to tank pressure (59 bar). Addition of known amount of 2-propanol to the system via the sample injection valve was accomplished at this point by using a sample loop of known volume. After addition of the 2-propanol, the system was pressurised to the desired pressure by closing valve V_2, turning on the chiller system, and opening the pump flow controller to the maximum flow setting. Once the desired pressure was

achieved, valve V_2 was opened and the contents of the system were recirculated back through the pump head. The chiller was turned off and the heater was engaged so that the pump head was heated to the same temperature as the optical cell. Recirculation of the system contents through the pump for 2 hours was conducted in order to ensured thermal equilibration. The contents of the optical cell were then irradiated with the 100 watt high pressure mercury lamp for 3 hours while the pump continued to recirculate the contents of the system at a flow rate of 460 mL/hr.

At the end of the irradiation period, the pump was turned off and the system was depressurised by opening valve V_3 and allowing the contents of the system to empty into the separator vessel which was filled with 200 mL of acetone. The flow through the separator vessel was regulated by the heated micrometering valve MV_1. After the pressure inside the system was reduced to atmospheric pressure, the optical cell was opened and acetone was added until the entire system was filled. The system was then pressurised to 100 bar with commercial grade carbon dioxide and recirculated for 15 minutes. The system was depressurised through the empty separator vessel in which all of the acetone wash was collected. This wash cycle was repeated with four additional system volumes of acetone. All acetone washings were combined, dried over $MgSO_4$ and concentrated under reduced pressure to 2 mL. After a g.c. analysis was carried out on the concentrate, the last traces of acetone were removed under high vacuum and the resulting residue was weighed in order to establish a mass balance. All mass balances measured for the experiments carried out in the supercritical fluid photochemical reactor indicate that greater than 99% of the starting material mass was reclaimed. Traces of acetone were removed from the supercritical fluid reactor by washing the system with

methanol and then evacuating the system to a pressure less than 10^{-2} mbar before the next experiment.

2.5 Determination of 1-Naphthyl Acetate Concentration in Supercritical CO_2

The system was charged with 1-naphthyl acetate (0.0300 g) and anaerobic grade carbon dioxide in exactly the same way as described above. After allowing the system to reach equilibrium at the set pressure and temperature for 2 hours, the system was sampled through the 0.500 mL sample loop using the sampling procedure described in the experimental section titled "Construction of the Supercritical Fluid Photochemical Reactor." The 0.500 mL samples removed from the reactor were diluted in methanol to a volume of 10.0 mL. For each temperature and pressure, three aliquots were removed from the high pressure system at 20 minute intervals. The system was mixed at a flow rate of 460 mL/hr by the recirculating pump during the 20 minute intervals. The U.V. absorbance of each of these aliquots were measured in 1.00 cm x 1.00 cm cells at 280 nm relative to pure methanol. The concentration of 1-naphthyl acetate in the reactor was then determined by comparing these absorbances to a linear calibration curve constructed by measuring the U.V. absorbance at 280 nm for six methanol solutions containing known concentrations of 1-naphthyl acetate (see Figure 25). A total system volume of 89 mL for the supercritical fluid photochemical reactor was used when calculating the concentration of 1-naphthyl acetate in the reactor. For each temperature and pressure studied, the concentration of 1-naphthyl acetate determined from the U.V. analysis of the three aliquots was the same as that calculated from the mass of 1-naphthyl acetate added to the optical cell (1.81×10^{-3} M) within 3% error.

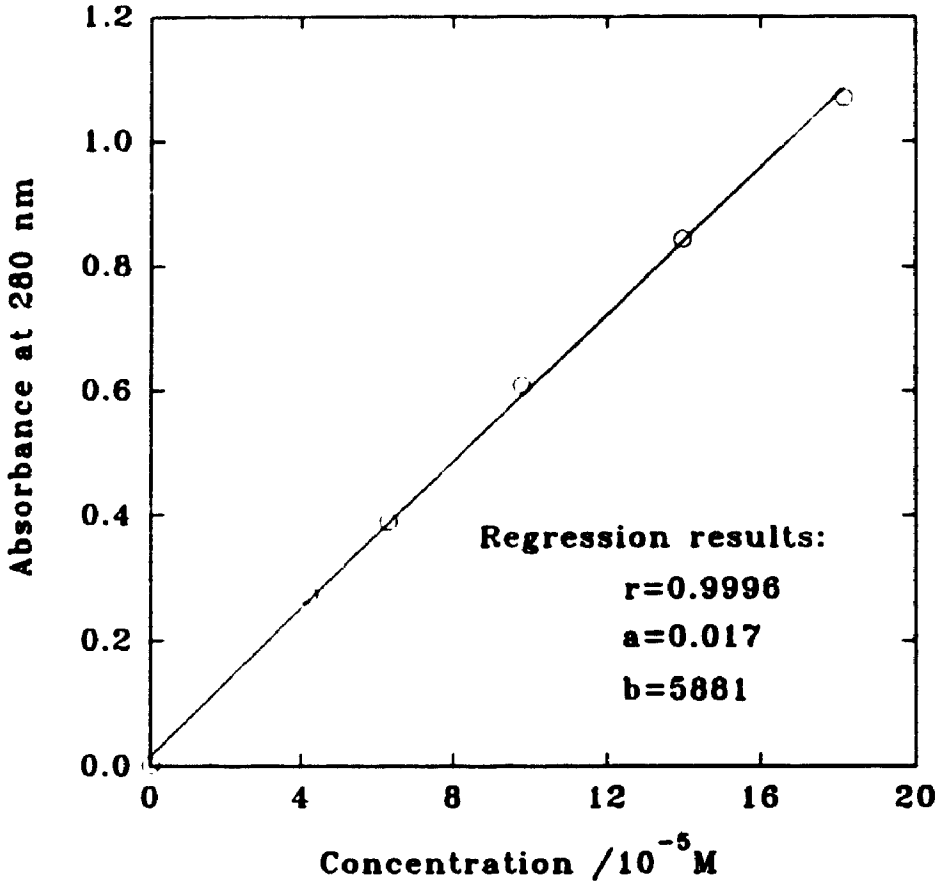

Figure 25: Calibration curve for determining the concentration of 1-naphthyl acetate in methanol. (Cell path length = 1.00 cm)

2.6 Photo-Fries Relative Quantum Yields in Supercritical CO_2 and Methanol

For these experiments a light splitter, which consisted of a quartz plate, was placed in the light path at approximately a 45° angle just in front of the optical cell window. The relative amount of light entering the high pressure optical cell compared to amount of light reflected by the splitter was determined in the following way. The high pressure optical cell was disconnected from the rest of the supercritical fluid photochemical reactor and filled with a methanol solution (85.0 mL) containing 1-naphthyl acetate (0.0121 M) and pentadecane (0.14 g/L). In a separate 3.00 cm long

quartz cell mounted beside the splitter at 90° to the optical cell window was placed a methanol solution (26.5 mL) containing the same concentrations of 1-naphthyl acetate and pentadecane. The 100 watt high pressure mercury lamp was turned on and the production of 2-acetyl-naphthol in the high pressure optical cell and the quartz cell was determined by g.c. The concentration of 1-naphthyl acetate in the quartz cell and the high pressure cell was chosen so that all of the light entering each of these cells was absorbed. Therefore, the amount of light entering the high pressure cell (I_C) relative to the amount of light entering the quartz cell (I_A) was calculated according to the following equation:

$$\frac{I_A}{I_C} = \frac{V_A \cdot \left(\frac{P}{S}\right)_A}{V_C \cdot \left(\frac{P}{S}\right)_C} \qquad (25)$$

where (P/S) is the ratio of the area of the 2-acetyl-1-naphthol g.c. peak to the area of the petadecane standard g.c. peak, V_A is the volume of the methanol solution in the quartz cell, and V_C is the volume of the methanol solution in the high pressure cell. The ratio of I_A/I_C was determined in three separate experiments and an average value of 0.30 ± 0.05 was calculated.

The I_A/I_C value was used in conjunction with the quartz cell to determine the quantum yield of Photo-Fries product formation for 1-naphthyl acetate in supercritical carbon dioxide solution relative to methanol solution. In this experiment, the high pressure optical cell was loaded with 0.0300 g of naphthyl acetate, evacuated, and then charged with anaerobic grade carbon dioxide to a pressure of 92 bar at 40°C according

to the procedure described above. This translates into a concentration of 1.81×10^{-3} M of 1-naphthyl acetate in the high pressure system. Then, the 0.100 mL sample loop was used to inject a 2-propanol solution containing pentadecane (25.1 g/L) into the high pressure system. The concentration of the pentadecane standard in the high pressure cell was calculated as 28.2 mg/L. The system was recirculated at a flow rate of 460 mL/hr for 2 hours after which time the 100 Watt high pressure mercury lamp was used to irradiate the contents of the optical cell for an additional 10.2 hours. During the time in which the cell was being irradiated, several 25.0 mL aliquots of a methanol solution containing 1-naphthyl acetate (1.81×10^{-3} M) and pentadecane (45.2 mg/L) were irradiated for exactly 50 minutes each in the actinometer cell mounted beside the light splitter. The total combined amount of 1-naphthol, 2-acetyl-1-naphthol, and 4-acetyl-naphthol formed in the actinometer cell during each 50 minute irradiation was determined by g.c. and was found to be constant, within 15% error, for the total 10.2 hour period. The average ratio of the combined product g.c. peak area to the standard's peak area was found to be 1.45 ± 0.20 for six aliquots.

After the 10.2 hour period the high pressure system was depressurised through acetone and then washed with 5 system volumes of acetone according to the procedure described above. The acetone fractions were combined, dried over $MgSO_4$, and concentrated under reduced pressure to a volume of 5 mL. This concentrate was analyzed by g.c. and the combined amount of 1-naphthol, 2-acetyl-1-naphthol, and 4-acetyl-naphthol formed in the supercritical carbon dioxide determined. The average ratio of the combined product g.c. peak area to the standard's peak area was found to be 0.83 for the reaction carried out in supercritical carbon dioxide. Using the g.c. peak area

ratios, the concentration of pentadecane in each reaction mixture, the I_A/I_C value listed above, and fact that 12.2 x 50 minute irradiation periods elapsed during the supercritical phase reaction, the ratio of the quantum yield of product formation for the irradiation of 1-naphthyl acetate in supercritical carbon dioxide solution to that in methanol solution was found to be 0.031 ± 0.009.

7.7 References for Part II Experimental

1. Autoclave SCF Reactor Vessel Serial No. 92220239-1.
2. Chattaway, F. D. *J. Chem. Soc.* **1931**, 2495.
3. Joshi, G. G.; Shah, N. M. *J. Indian Chem. Soc.* **1952**, *29*, 225.
4. Matsui, K.; Motoi, M. *Bull. Chem. Soc. Jpn.* **1973**, *46*, 565.